# CHEMICAL INVESTIGATIONS OF THE ALKALOIDS FROM THE PLANTS OF THE FAMILY ELAEOCARPACEAE

**Peter L. Katavic, BSc (Hons)**

**School of Science/Natural Product Discovery (NPD)**
**Faculty of Science, Griffith University**


**Submitted in fulfillment of the requirements of the degree of Doctor of Philosophy**

**December, 2005**

# Abstract

A phytochemical survey to detect alkaloids was performed on extracts of 339 discrete plants parts from a total of 77 species from five genera of Elaeocarpaceae, including 30 species from Queensland, 38 from PNG, and nine from China. An alkaloid detecting reagent, bismuth (III) tetraiodide (Dragendorff's reagent) was used in a preliminary test for alkaloids, with positive ESIMS used to confirm the presence of alkaloids. A total of 35 extracts of various plant parts produced positive results with Dragendorff's reagent. Positive ESIMS detected alkaloids in only 13 of these extracts. Bismuth (III) tetraiodide was demonstrated to produce false positive results with the new non-alkaloidal poly-oxygenated compounds **112** and **113**, which were purified from the extract of *Sloanea tieghemii*. Two new alkaloid producing species, *Elaeocarpus habbeniensis*, and *E. fuscoides* were detected from the survey. These species were chemically investigated for the first time. Two other previously investigated species, *E. grandis* and *Peripentadenia mearsii,* were also studied.

A total of 16 alkaloids, 11 of which are new, were purified from the extracts of these four species. The novel pyrrolidine alkaloids habbenine (**114**) and peripentonine (**123**), were isolated from the leaves of *E. habbeniensis* and *Peripentadenia mearsii*, respectively. Both of these compounds were purified as inseparable mixtures of diastereomers. The new pyrrolidine alkaloid mearsamine 1 (**124**), and the novel amino alkaloid mearsamine 2 (**125**), were also purified from the leaves of *P. mearsii.* The known pyrrolidine alkaloid peripentadenine (**81**), was purified from the bark of *P. mearsii*. Peripentonine (**123**) was reduced to peripentadenine (**81**) upon reaction with Pd/C.

Four aromatic indolizidine alkaloids were isolated from the extract of the leaves of *E. fuscoides*. One new compound, elaeocarpenine (**122**), was isolated from this New Guinean plant. Three known *Elaeocarpus* alkaloids, isoelaeocarpicine (**62**), elaeocarpine (**60**) and isoelaeocarpine (**61**) were also purified from *E. fuscoides*. Elaeocarpenine (**122**) was demonstrated to produce the epimeric compounds elaeocarpine and isoelaeocarpine via reaction with ammonia.

The chemical investigation of the Queensland plant *E. grandis* by two separate purification procedures was performed. An SCX/C18 isolation protocol was used to purify the new indolizidine alkaloids grandisine C (**127**), D (**126**), and E (**128**), in conjunction with the known tetracyclic indolizidine isoelaeocarpiline (**63**). The second purification of *E. grandis* was achieved with the use of ammonia in an acid/base partitioning protocol. Grandisine F (**129**) and G (**130**), and compounds **131a** and **b** were purified by this procedure, as were **63**, **126** and **127**. Grandisine F and G were proposed to be ammonia adducts of grandisine D (**126**). Compound **131a** and **b** were isolated as a mixture of diastereomers. The reduction of grandisine D (**126**) with Pd/C yielded a mixture of isoelaeocarpine (**61**) and elaeocarpine (**60**), whereas the reduction of isoelaeocarpiline (**63**) produced isoelaeocarpine (**61**).

All of the alkaloids isolated from the Elaeocarpaceae, except grandisine E (**128**) and **131a** and **b**, were evaluated for binding affinity against the human δ opioid receptor. Every compound except mearsamine 2 (**125**) possessed a binding affinity of less than 100 $\mu$M. The most active compounds were grandisine F (**129**), D (**126**), C (**127**), elaeocarpenine (**122**), isoelaeocarpine (**61**), isoelaeocarpiline (**63**) and peripentadenine (**81**). The $IC_{50}$ values for these compounds were 1.55, 1.65, 14.6, 2.74, 13.6, 9.86 and 11.4 $\mu$M, respectively. The SAR of the active compounds was compared. These observations indicated that the indolizidine alkaloids were more active than the pyrrolidine alkaloids, and a phenol or ketone at position C-12 of the indolizidine alkaloids produced better binding affinity. All of these alkaloids, except **129**, were proposed to interact with two of the three binding domains of the δ opioid receptor. Grandisine F (**129**) was proposed to have a different mode of action than the other alkaloids in the series.

Synthetic modifications to isoelaeocarpine (**61**) and peripentadenine (**81**) were investigated in an attempt to incorporate an extra aromatic group into these molecules. An extra aromatic group was proposed to provide increased binding affinity to the δ opioid receptor by interaction with the third binding domain of the receptor. Two different aromatic amines were successfully attached to peripentadenine (**81**) by a

reductive amination reaction using $NaBH(OAc)_3$ and a titanium catalyst. The reductive amination of the ketone in isoelaecarpine (**61**) with various amines and $NaBH(OAc)_3$ or $NaBH_4$ proved unsuccessful.

# Declaration

"This work has not previously been submitted for a degree or diploma in any university. To the best of my knowledge and belief, the thesis contains no material previously published or written by another person except where due reference is made in the thesis itself"

_____ _____

Name Date

# Acknowledgments

First of all, I would like to thank my supervisors, A. R. Carroll and D. A. Venables, for their patience and guidance during this PhD experience. My skills as a scientist have definitely matured under the supervision of Tony and Debra, and for that I am most grateful.

I am also most grateful for receiving financial assistance from the Australian Research Council for an Australian Postgraduate Award, and from AstraZeneca for an industry funded scholarship, which allowed me to pursue my research full-time.

I wish to thank the following people for help with the project: Greg Pierens for advice and help with NMR experiments, Greg Fechner and Matthew Crampton for assistance with δ opioid screening, Paul Baron and Jennifer Mitchell for acquiring high resolution mass spectra, Leanne Towerzey and Carolyn Tranter for computer related issues, Justin Ripper for invaluable discussions on synthetic chemistry, and Marc Campitelli for advice on molecular modeling.

I would like to extend thanks to my friends and colleagues Fredrik Lindahl, Rohan Davis, Declan McKeveney, Carla Rosell and Brendan Wilkinson for many scientific and non-scientific conversations.

I could not have achieved what I have without the love and support of my mum, for being there and having faith in me.

## Table of Contents

# Abbreviations

| | |
|---|---|
| FT | fourier transform |
| MHz | Megahertz |
| HPLC | high pressure liquid chromatography |
| MPLC | medium pressure liquid chromatography |
| RP | reverse phase |
| UV | ultra violet |
| IR | infra red |
| $[\alpha]_D$ | specific rotation |
| LRESIMS | low resolution electrospray mass spectrum |
| HRESIMS | high resolution electrospray mass spectrum |
| MS | mass spectrum |
| SAR | structure activity relationships |
| PDA | photo diode array |
| 2D | two dimensional |
| NMR | nuclear magnetic resonance |
| COSY | correlation spectroscopy |
| HSQC | heteronuclear single quantum coherence |
| HMBC | heteronuclear multiple bond correlations |
| ROESY | rotating frame Overhauser effect spectroscopy |
| $^{2,3}J_{CH}$ | 2 or 3 bond hydrogen to carbon correlation |
| s | singlet |
| d | doublet |
| t | triplet |
| m | multiplet |
| br | broad |
| d2 | incremental delay |
| DMSO | dimethylsulfoxide |
| DCM | dichloromethane or methylene chloride |
| DCE | 1,2-dichloroethane |
| EtOH | ethanol |
| MeOH | methanol |
| $CDCl_3$ | deuterated chloroform |
| $d_6$-DMSO | deuterated dimethylsulfoxide |
| $CD_2Cl_2$ | deuterated dichloromethane |
| $CD_3OD$ | deuterated methanol |
| $CD_3CN$ | deuterated acetonitrile |
| TFA | trifluoroacetic acid |
| TOF | time of flight |
| AcOH | acetic acid |
| $H_2SO_4$ | sulfuric acid |
| $NH_3$ | ammonia |
| KOH | potassium hydroxide |
| NaCl | sodium chloride |

| | |
|---|---|
| $NaBH(OAc)_3$ | sodium triacetoxyborohydride |
| $NaBH_4$ | sodium borohydride |
| CSIRO | Commonwealth Scientific and Industrial Research Organisation |
| PNG | Papua New Guinea |
| NZ | New Zealand |
| aq. | aqueous |
| conc. | concentrated |
| C18 | octadecyl bonded silica |
| SCX | strong cation exchange |
| MW | molecular weight |
| Da. | Daltons |
| HTS | high throughput screening |
| CNS | central nervous system |
| NSAIDs | nonsteroidal anti-inflammatory drugs |
| L | leaves |
| Se | seeds |
| St | stem |
| B | bark |
| HW | heartwood |
| M | mix of plant parts (leaves, stem and bark) |
| R | roots |
| F | flower |
| Fr | fruit |
| KI | potassium iodide |
| $BiI_4^-$ | bismuth (III) tetraiodide |
| CRC | concentration response curve |
| ppm | parts per million |
| $n_H$ | hill slope |
| μ | mu opioid receptor |
| κ | kappa opioid receptor |
| δ | delta opioid receptor or chemical shift |
| BSA | bovine serum albumin |
| PEI | polyethyl enimine |
| $MgCl_2$ | magnesium chloride |
| $Ti(O^iPr)_4$ | titanium (IV) isopropyloxide |
| μCi | micro curie |
| *m/z* | mass-ion ratio ($z = 1$) |
| SPE | solid phase extraction |
| PAG | polyamide gel |
| $t_R$ | retention time |
| Pd/C | palladium on activated carbon (10% w/w) |
| DDQ | dichlorodicyanobenzoquinone |
| rt | room temperature |
| $IC_{50}$ | concentration of a compound required to inhibit 50% of the receptor population |

# List of Figures

# List of Tables

# List of Schemes

# List of publications arising from this thesis

1**. Indolizidine alkaloids from *Elaeocarpus fuscoides.***

Katavic, P. L., Venables, D. A., Rali, T., Carroll, A. R., in prep., *J Nat Prod*.

2. **Habbenine A and B, New Pyrrolidine Alkaloids with Human δ-Opioid Receptor Binding Affinity from the Leaves of *Elaeocarpus habbeniensis*.**

Katavic, P. L., Venables, D. A., Rali, T., Carroll, A. R., in prep., *J Nat Prod*.

3. **Grandisines C-G, Novel Indolizidine Alkaloids from the Australian Rainforest Tree, *Elaeocarpus grandis.***

Katavic, P. L., Venables, D. A., Carroll, A. R., in prep., *J Org Chem*.

# CHAPTER 1 – Introduction

## 1.1 The Significance of Medicines, Toxins and Hallucinogens from Nature

Organisms such as bacteria and plants are known to naturally produce organic molecules as a means of chemical defense.[1-3] The chemical interactions of these molecules play a crucial role in the survival of such organisms. Records dating back to the 3rd millennium BC[1, 4-6] emphasize the importance of the diverse chemistry of nature to human civilization. Extracts from plants have been used as active constituents of potions, teas, poultices and poisons.[7] The poisonous constituents of certain plants have been employed in hunting practices, suicides and assassinations.[1, 7, 8] Plant derived hallucinogens became the essential ingredients for many ceremonies and rituals, particularly in witchcraft.[4, 7] The use of plants as traditional medicines has proven to be one of their most important functions.[1, 7, 8]

Medicinal remedies of natural origin were first described in tablets from ancient Greece, Egypt, Babylonia and Mesopotamia. All of these cultures used preparations derived from opium poppies for the treatment of pain.[1, 4] Hemp cultivated in China and India found particular use as a hallucinogen. Descriptions of witchcraft practiced during the Middle Ages in Europe frequently noted the use of hallucinogenic constituents of mandrake and belladonna.[4] The widespread use of natural hallucinogens also included psychoactive mushrooms in Siberia, and cacti containing hallucinogenic constituents in the cultures of South and Central America.[4] Toxic plant constituents were employed as poisons for arrows in Africa and South America.[7] Preparations of specified plants were also used in the embalming practices of the ancient Sumerian, Akkadian and Egyptian cultures.[1] Analysis of the remains of Egyptian mummies have yielded traces of commonly abused drugs such as hashish and nicotine.[9] In China, documentation of medicinal plants was made by the Emperor Shen Nung in 3000 BC.[6, 7] The common use of natural remedies in

India led to the development of the Ayurvedic system of medicine, which has been recognized since 1000 BC.[6, 7, 10] The *Ebers Papyrus* chronicled the numerous plant extracts of medical value in the ancient world,[1, 7, 10] Scholars such as Hippocrates (460 – 377 BC), Dioscorides (AD 40 – 80) and Galen (AD 130 – 210) also noted the medicinal potential of plants.[1, 6] The findings of Dioscorides were detailed in the work "*De Materia Medica*", which highlighted the medicinal value of up to 600 plants.[1] The Persian pharmacist and physician Avicenna was considered a key figure in the preservation of ancient medicinal practices during the 8th century AD.[6] Monasteries in Europe during the Middle Ages were responsible for the accumulation of knowledge of traditional medicines.[6] From the recorded knowledge of several ancient civilizations, the value of the chemistry of nature, in the form of extracts and their effects on the human body, is undoubtedly an important aspect of history.

The Swiss physician Paracelsus (1493 – 1541)[11] was the first scholar to question the use of plant extracts as medicines.[11, 12] In 1524, Paracelsus wrote the "*Archidoxa Arcanum",*[12] which described the need to isolate the active constituents of traditional medicines.[11, 12] However, it wasn't until the end of the 18th century that the first pharmacologically active compound was isolated from a plant extract. This compound was the analgesic morphine (**1**), isolated by Sertürner in 1803 from the opium poppy.[1, 6] The purification of many other pharmacologically significant molecules followed during the next century.[13] Much of this pioneering chemistry was performed by Pelletier and Caventou.[11] The results of these chemical investigations included the isolation of the toxin strychnine (**2**) in 1817 from a poisonous plant used in hunting, and the isolation of the antimalarial compound quinine (**3**) from Jesuit's Bark in 1820.[1, 6] Further work led to the purification of caffeine (**4**) in 1820, nicotine (**5**) in 1828, atropine (**6**) in 1833, and cocaine (**7**) in 1855.[1] *Erythroxylon coca* is the plant which produces the tropane alkaloid cocaine, a notoriously abused drug. The coca plant was also noted to produce other alkaloids with reduced potency that were used in the flavouring of Coca-Cola.[14] Advancements in science in the 19th century resulted in the purification of many constituents of plant extracts and hence the concept of natural products chemistry was born.[15, 16]

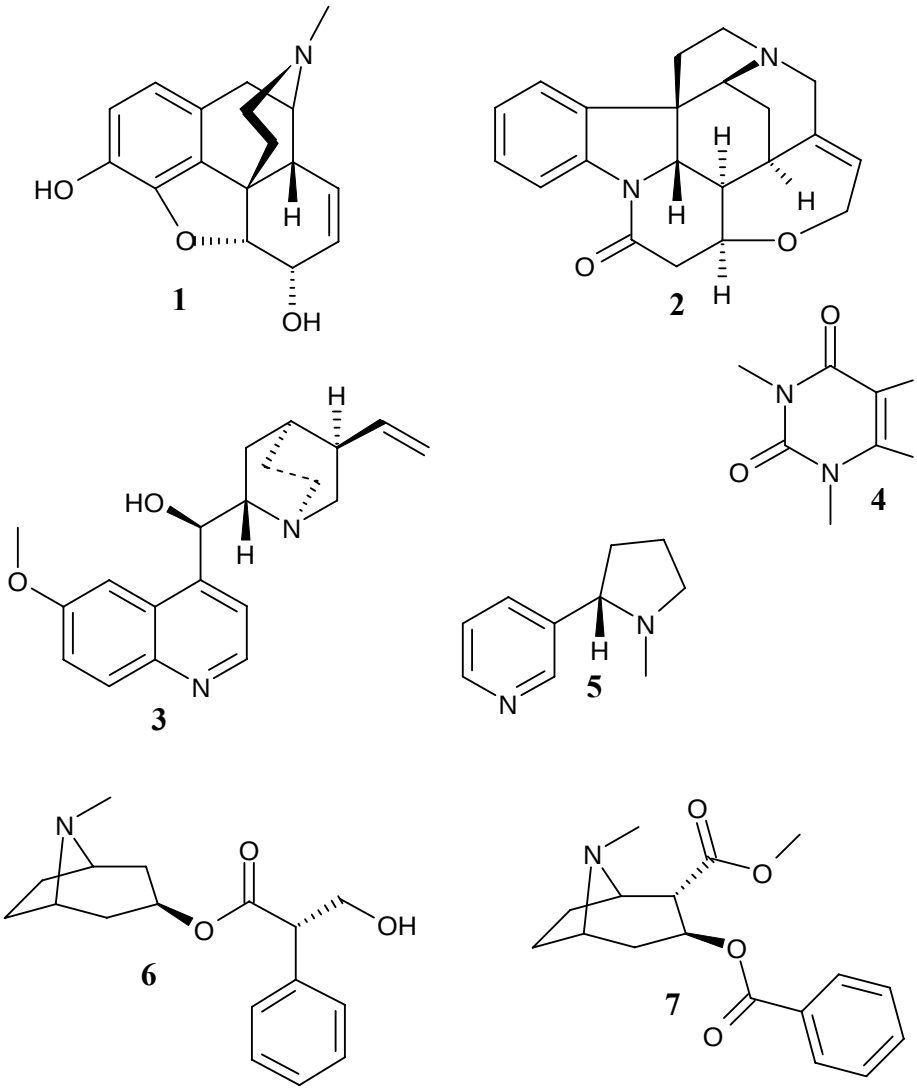


Discovery of the pharmacological properties of certain plants in ancient cultures was undoubtedly achieved by experimentation. The intrigue into nature's pharmacology and experimentation with flora appears to not be restricted to early humankind. Observations of wild chimpanzees plagued with severe diarrhea show the selection and consumption of plants that produce antimicrobial thiophenes.[17] Birds have also been observed to construct their nests with leaves containing high concentrations of tannins.[17] The growth of pathogens such as bacteria and fungi may be inhibited by the antimicrobial properties of tannins. Insects too have exploited the pharmacological properties of plants. A study of the unique behaviour of the bright red moth *Cosmosoma myrodora,* revealed the accumulation of pyrrolizidine alkaloids in the abdomen of the male moth.[18, 19] The source

of the alkaloids was found to be secretions of the plant *Eupatorium capillifolium* (Asteraceae). Intermedine (**8**) is an example of one of these pyrrolizidine alkaloids. The male moth was found to transfer some of its alkaloid content to its preferred female mate.[18, 19] The pyrrolizidine alkaloids were discovered to be crucial for protection against spiders. An amazing observation followed during an experiment with the orb-weaving spider, *Nephila clavipes*. The spider released any alkaloid-rich moths trapped in it's web,[18, 19] presumably to prevent its young from ingesting the poisonous alkaloids. Any moths that did not contain the alkaloids were promptly devoured.[18, 19] Other studies have also shown the absorption of pyrrolizidine alkaloids from species belonging to the plant families Asteraceae and Borginaceae by the *Longitarsus* flea beetles.[20] Bio-accumulation of alkaloids by arthropods has been observed in several studies.[21-26] These alkaloids have also been implicated as defensive agents[21, 23, 24] and as precursors for pheromone biosynthesis.[22, 26] Hydroxydanaidal (**9**) is an example of a pheromone produced by the moth *Creatonotos transiens,* from a pyrrolizidine precursor.[26] Exploitation of the chemistry of nature has been a common element observed across a wide range of organisms and can be considered as a systematic mechanism of survival.

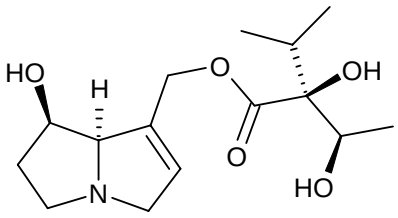


**8**

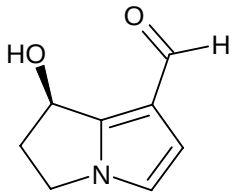


**9**

The significance of traditional medicines is still evident today with approximately 60 - 80% of the world's population reliant on these medicines for treatment of various diseases.[3, 6, 27, 28] The people of developing countries are most dependent on natural remedies, as approximately one billion people live in extreme poverty.[29] The importance of nature's medicines to humankind, both in ancient times and the present, is therefore unparalleled.

## 1.2 Alkaloids

In 1818, the term alkaloid became the accepted nomenclature for the alkaline constituents of plants.[11] As defined by Pelletier, alkaloids

> are cyclic nitrogen containing secondary metabolites[15] where the nitrogen atom is derived directly from an amino acid,[30] excluding simple amines and acyclic derivatives of ammonia,[15] which are of limited distribution in living organisms.[7] The nitrogen atom must be in a negative oxidation state, excluding nitro and nitroso compounds.[15] Basic character of an alkaloid is not a prerequisite, allowing quaternary amino and neutral amino compounds such as amides as well as *N*-oxides to be classified as alkaloids.[7]

Alkaloids constitute one of the most diverse structure classes of secondary metabolites, showing a great variety in structure type. Alkaloids are biosynthesized by many unique metabolic pathways and display a broad spectrum of pharmacological activities.[7] Secondary metabolites are defined as molecules produced in small amounts[31] by metabolic pathways which are unique to an organism,[31] where enzymatic and genetic evidence exists for these pathways.[32] Other naturally synthesized molecules, such as carbohydrates and proteins, are regarded as primary metabolites.[32] The structural diversity of alkaloids can be seen from a comparison between the simple plant toxin coniine (**10**) and batrachotoxin (**11**), a complex neurotoxin isolated from a Colombian frog.[15] The importance of alkaloids is exemplified by the observation that approximately 60% of drugs from plant origin are alkaloids.[3]

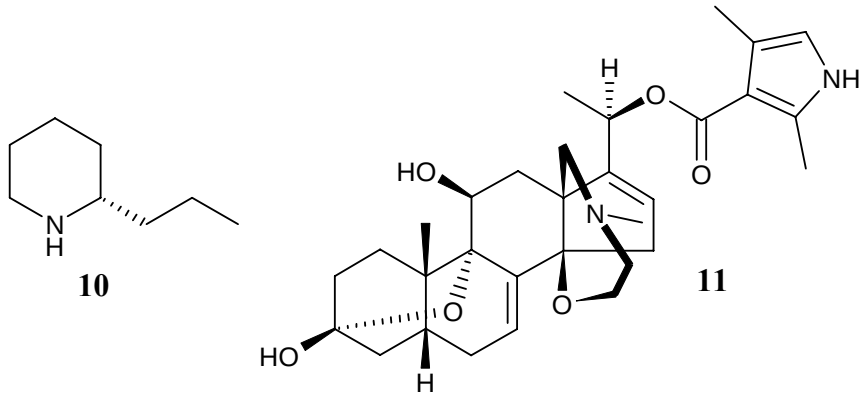


**10** **11**

The huge variation in the structures of alkaloids and the diverse range of organisms which produce them will not be encompassed here. A general overview of the main structure classes of alkaloids will be highlighted. Plants are the principal source of alkaloids, however alkaloids have been encountered in fungi, marine organisms, insects, micro-organisms and mammals.[1, 7, 15] The main structure types of alkaloids are shown in Figure 1. Alkaloids have been classified into a total of 27 structural types, with 22 of these types found in higher plants.[33]

The structures presented in Figure 1 account for a great percentage of alkaloids encountered in nature. However, alkaloids such as batrachotoxin (**11**), ephedrine (**12**), aconitine (**15**) and the ergot alkaloids (**24**, **25**), do not belong to any of these structure classes. Ephedrine (**12**) can be termed an amino alkaloid, where the nitrogen atom is not part of a heterocycle or ring system.[1] Batrachotoxin (**11**) is a member of the steroidal alkaloids. Both of these alkaloids are products of transamination reactions,[1, 34] where a nitrogen atom is attached to a non-nitrogenous substrate. In ephedrine, the amino acid phenylalanine contributes the benzene ring, the side chain carbons come from pyruvic acid and a nitrogen atom is added by a transamination reaction. Most alkaloids of this type are small, structurally simple molecules. Steroidal alkaloids are biosynthetically derived from the steroid nucleus (**13**) and a subsequent transamination reaction. The source of nitrogen for transamination reactions is an amino acid or other nitrogen containing metabolites. Coniine (**10**) is biosynthesized via a transamination of an oxidized product of octanoic acid. The source of the amino group is L-alanine.[34]

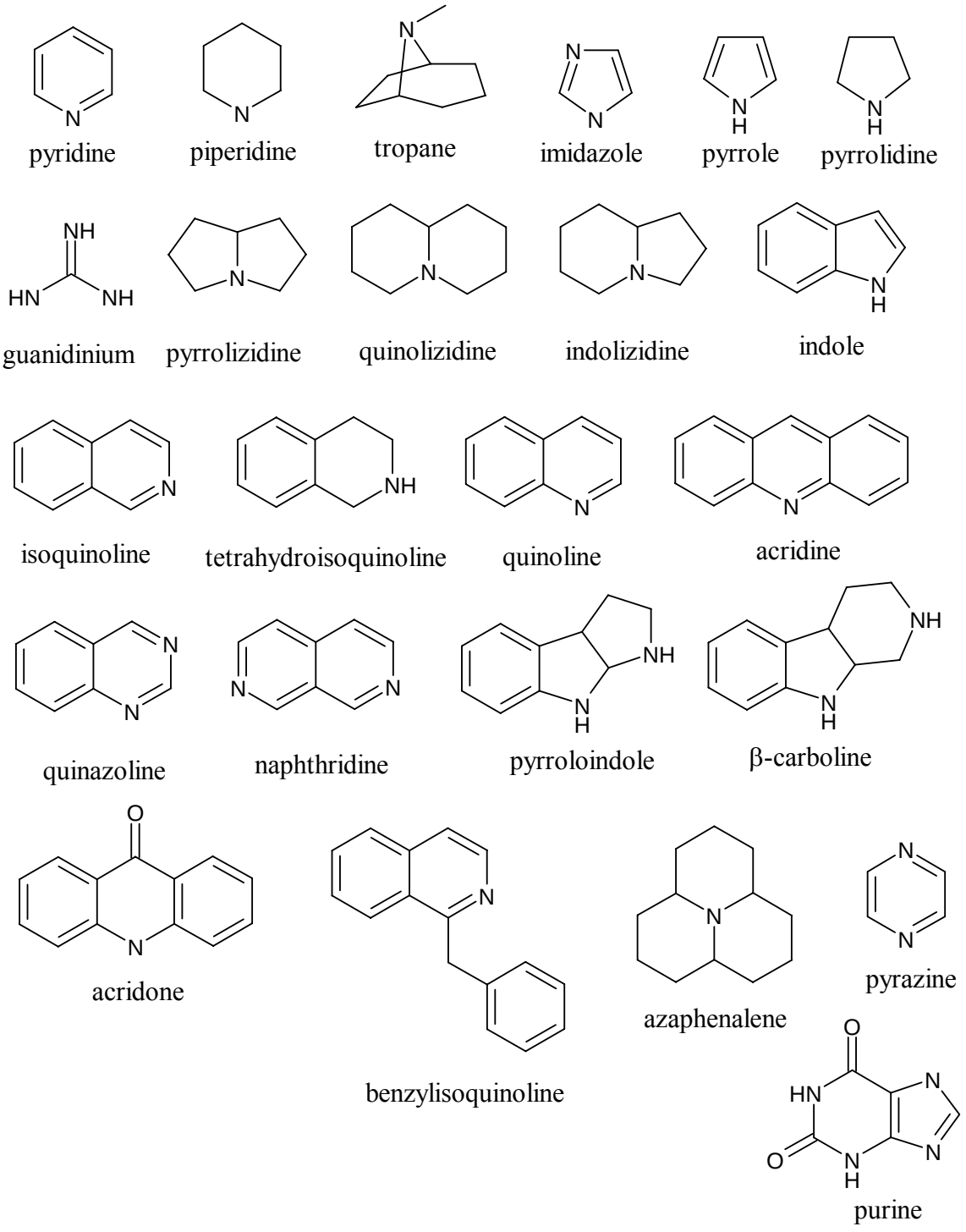


**Figure 1.** The main alkaloid structure classes encountered in nature.

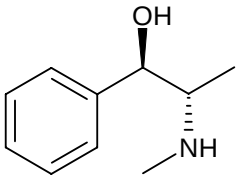


**12**

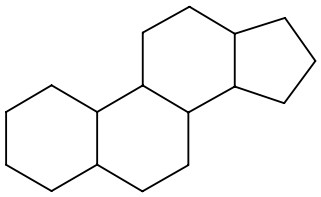

**13**

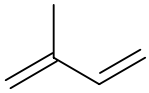

**14**

Similarly, transamination of terpenoid skeletons has been known to occur.[34] Terpenoids are biosynthesized from five-carbon isoprene units (**14**), and are one of the most widely encountered groups of natural products.[35] Structures can vary immensely in the number of isoprene units incorporated. Commonly encountered terpenoid skeletons include the 15-carbon sesquiterpenes, 20-carbon diterpenes and 30-carbon triterpenes.[34, 35] Aconitine (**15**) is an example of a terpenoid alkaloid. In the case of aconitine, transamination of the terpenoid skeleton occurs by the incorporation of 2-aminoethanol.[34] Many steroidal and terpenoid alkaloids are structurally complex and are often toxic.[1, 34] This is underlined by the lethal doses of batrachotoxin (**11**) and aconitine (**15**), 40 ng in mice and 3 – 6 mg in man, respectively.[1]

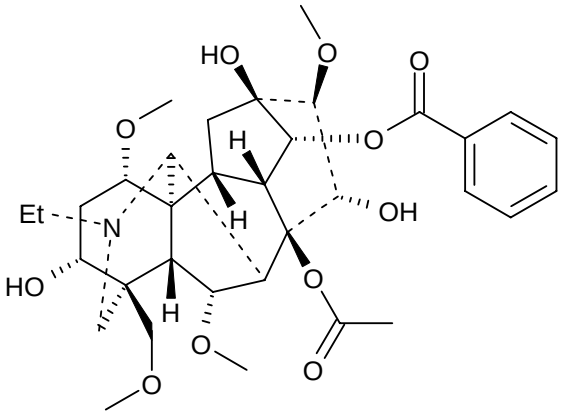


**15**

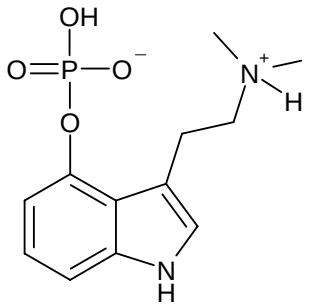


**16**

Indole alkaloids comprise one of the most chemically intriguing classes of alkaloids. This group of alkaloids can be divided into two main sub-classes, the simple and terpenoid indole alkaloids.[1, 34] Tryptamine, the biogenetic source of the indole ring system, can be incorporated into psilocybin (**16**), a simple indole alkaloid. Terpenoid indole alkaloids are a large group of approximately 3000 natural products. These alkaloids are generally limited to a select group of plant families.[34] Indole alkaloids are biosynthesized via the

coupling of tryptamine with a 10-carbon monoterpene derivative.[1, 34] The ergot alkaloids (**24, 25**) are examples of terpenoid indole alkaloids. Dimeric terpenoid indole alkaloids, of which vinblastine (**36**) is an example, are also encountered.

Another important class of alkaloids are the bisbenzylisoquinolines, which are dimers of tetrahydrobenzylisoquinolines connected by one to three ether linkages.[1] More than 270 of these alkaloids are known, with many of them pharmacologically active agents such as skeletal muscle relaxants, antihypertensives, antimalarials and cytotoxins. The most famous example of a bisbenzylisoquinoline alkaloid is tubocurarine (**17**). This compound has been used as the dart poison curare by South American tribes.[1]

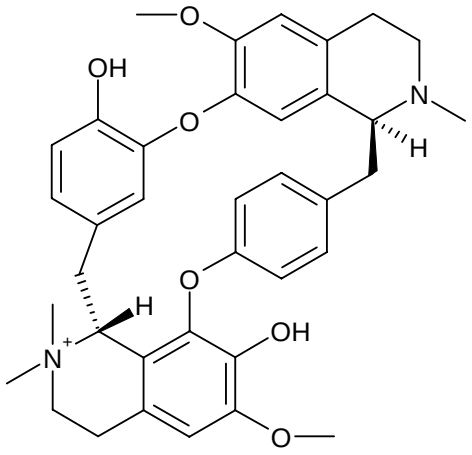


**17**

An estimated 40% of all plant families contain at least one species that produces alkaloids.[15] Many alkaloids have a bitter taste, such as strychnine (**2**) and quinine (**3**), and it has been speculated that alkaloids serve as insect feeding deterrents.[1, 7] It has also been proposed that alkaloids serves as chemical attractants, pigments, fragrances and even provide UV protection.[7] Claims have been made that alkaloids are simply elaborate mechanisms for the storage of nitrogen, although this seems improbable.[1] Evidence exists to support the role of alkaloids as protection against micro-organisms in plants.[1] The presence of alkaloids in plants may also encompass multiple functions, such as antibacterial and anti-feedant roles.[7]

Toxic alkaloids are also important for chemical protection against predation for animals such as amphibians. Examples of these toxins include batrachotoxin (**11**), samandarine (**18**) located in the skin of salamanders, and bufotenine (**19**) which is produced by toads.[15]

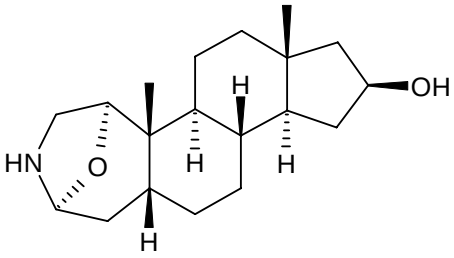


**18**

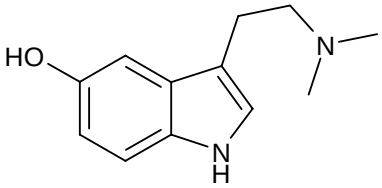


**19**

Alkaloidal secondary metabolites produced by mammals are extremely uncommon.[15] When mammalian alkaloids are encountered, they are generally not considered as protective agents. Being mobile, mammals can adequately protect themselves by physical means. Examples of mammalian alkaloids include the territorial markers (-)-castoramine (**20**) from the Canadian beaver and muscopyridine (**21**) from the musk deer.[15] The scent gland of the Canadian beaver has proven to be an interesting source of alkaloids. A total of 14 have been identified, more than half of which are quinolizidines. Also included in this group are an indolizidine alkaloid, a pyridine alkaloid and several pyrazine alkaloids.[36]

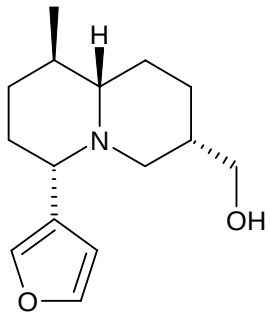


**20**

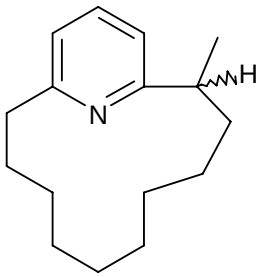


**21**

Examples of alkaloids produced by marine organisms include the potent neurotoxic guanidinium alkaloids tetrodotoxin (**22**) and saxitoxin (**23**).[1, 15] Tetrodotoxin is a sodium channel blocker that is biosynthesized by the puffer fish or "fugu".[15, 37] In Egypt, the use of this compound as a poison has been recorded since 2500 BC.[37] Saxitoxin is produced by a dinoflagellate.[1, 15]

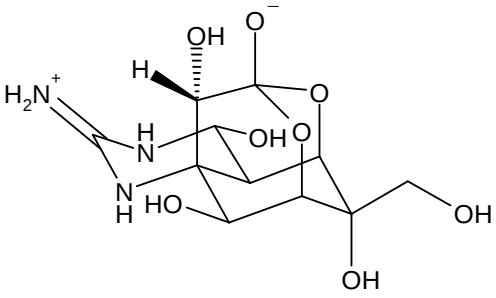


**22**

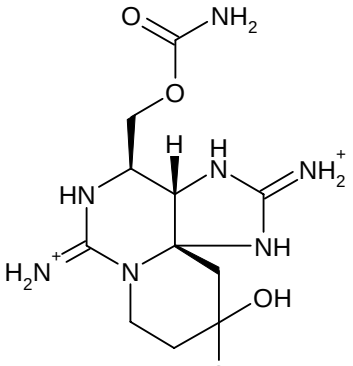


**23**

Some of the most famous alkaloids of fungal origin are the terpenoid indole ergot alkaloids from the fungus *Claviceps purpurea*.[1] More than 50 ergot alkaloids are known, including chanoclavine I (**24**) and D-lysergic acid (**25**).[15] Lysergic acid diethylamide (**26**) (LSD), a potent hallucinogen, is a semisynthetic derivative of **25**. During the Middle Ages ergot alkaloids present in rye bread contaminated with *C. purpurea* were responsible for poisonings. The ergot alkaloids produced by this fungus resulted in a condition known as "St. Anthony's Fire" which caused a sensation of burning in the limbs.

Insects have also provided some unique alkaloids to the natural product domain. The ladybird beetle of the Coccinellidae family has been the focus of chemical investigations for more than 30 years.[38-40] This research has culminated in the purification of novel azaphenalene alkaloids from several species of beetle. Examples of these compounds include hippodamine (**27**) and its *N*-oxide convergine (**28**),[38] along with more complex compounds such as the dimeric azaphenalene psylloborine A (**29**)[39] and the unusual heptocyclic chilocorine D (**30**).[40] These alkaloids have also been implicated in chemical protection roles.

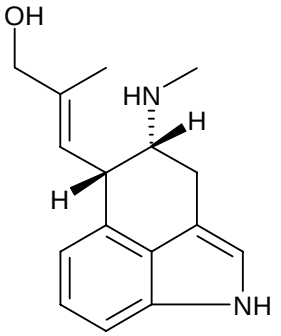


**24**

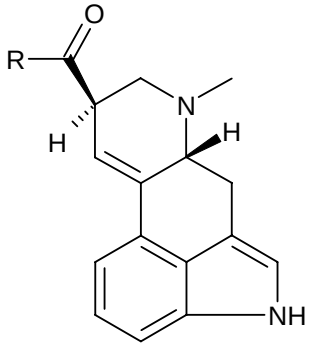


R = OH **25**
R = $NEt_2$ **26**

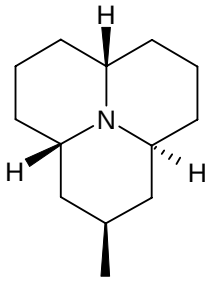


**27**

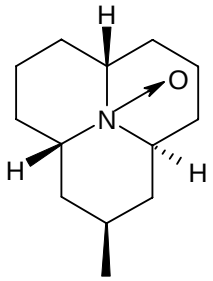


**28**

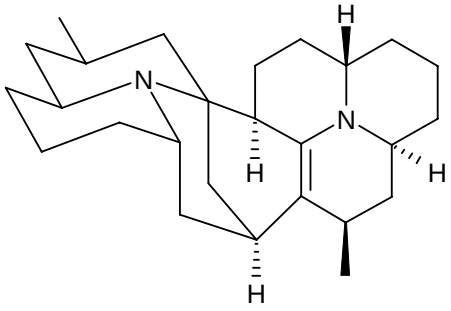


**29**

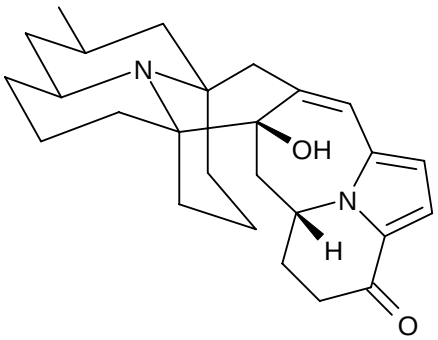


**30**

## 1.3 Natural Products and the Pharmaceutical Industry

The biological response of drugs occurs from binding with human proteins such as receptors or enzymes. The active components of traditional medicines have been altered and re-altered biosynthetically to allow them to successfully bind to human proteins in what has been termed as "evolutionary molecular modeling".[37] Receptors and enzymes can either be stimulated or obstructed by binding of a bioactive natural product. Subsequent stimulation or obstruction of mammalian proteins may be hazardous. Design and bio-production of such compounds is therefore beneficial to the organisms that produce them.[37] This infers that a poisonous natural product synthesized by an organism in high concentrations may serve as a valuable drug in low concentrations.[37]

As in ancient times, natural products still have a great impact on our lives. The value of natural products to the pharmaceutical industry has been enormous, with many modern drugs owing their origin to natural products.[1, 2, 41, 42-43] Of the 25 best selling pharmaceuticals in 1991, over half were of natural origin, which financially equated to sales of US$12 billion.[44] Similar trends were observed in 1998[45] and 1999.[41] The revenue gained from natural product based drugs in 1999 grew to US$16 billion.[41] Examples of these drugs include the cholesterol lowering agent lovastatin[41] (**31**), which was isolated from the fungi *Monascus rubber* and *Aspergillus terreus,*[46] and the angiotensin converting enzyme inhibitor captopril[41] (**32**), which is a synthetic derivative of the C-terminal proline groups of a nonapeptide isolated from the venom of the South American pit viper *Bothrops jararaca*.[46] However, the number of natural products based drugs has steadily reduced into the new millennium. Fifteen of the top 35 pharmaceuticals sold worldwide in 2000 were natural product derived. This number decreased to 10 out of 35 in 2001 and 2002.[47]

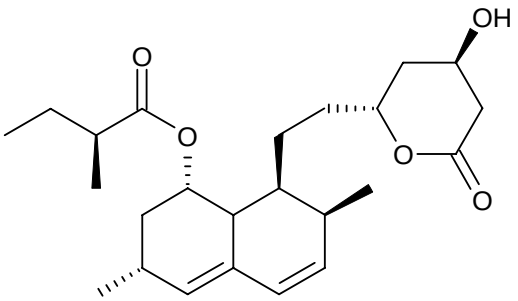


**31**

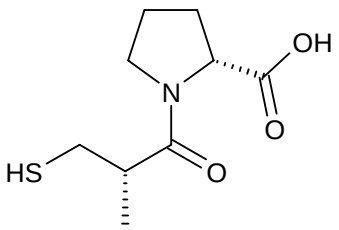


**32**

The history of the pharmaceutical industry is intricately entwined with natural products. The pharmaceutical industry began in Japan in 1637, with the selling of herbal remedies under the name of "Takeda".[48] Development of pharmaceuticals took hold in the United States in the 1800's, with a focus on the production of the analgesic alkaloid morphine (**1**).[48] It wasn't until the late 1880's that aspirin, the first synthetic drug based on a natural product, entered the market.[6, 48] In 1928, the discovery by Fleming of the antibiotic properties of the fungal natural product penicillin G (**33**) heralded the beginnings of the next phase in the maturation of the pharmaceutical industry.[47, 48] Later, the fungus *Penicillium chrysogenum* was found to produce 3000 times more penicillin than the original fungus studied by Fleming.[49] Mass production of this fungus during World War II resulted in profound improvements in the health of soldiers and civilians.[2, 13, 49] The 20 years following WWII were deemed the "Golden Age of Antibiotics",[6] and saw the manufacture of a plethora of new antibacterial and antifungal agents.[2] The major impact of antibiotics on human health can be seen in an increase of the average human lifespan by almost 30 years.[50]

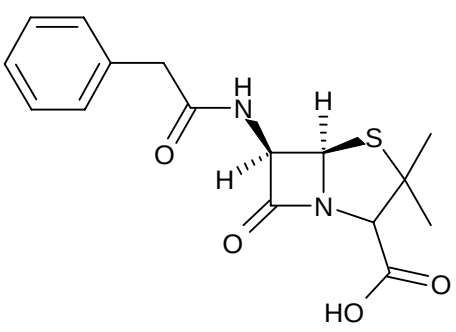


**33**

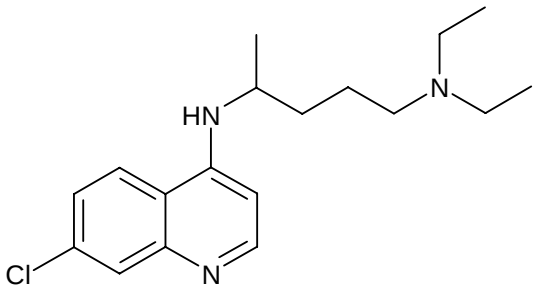


**34**

Many drugs derived from natural products are semi-synthetic derivatives. Such compounds are produced from a bioactive natural product by synthetic chemistry while retaining the core structure of the natural product. The primary goal of semi-synthesis is to improve the potency and pharmacological properties of the natural product.[7, 12] Examples of semi-synthetic derivatives[46, 51] include chloroquine (**34**), derived from the natural product quinine (**3**),[46] the anticancer drug vindesine (**35**) which is based on the natural product vinblastine (**36**),[46] the antifungal agent with a novel mode of action GM237354 (**37**) prepared by Glaxo-Wellcome from its natural product precursor sordarin (**38**),[46, 51] and two derivatives of camptothecin (**39**), the anticancer drugs topotecan (**40**) and irinotecan (**41**).[46] Camptothecin was originally isolated from the Chinese tree *Camptotheca acuminata* and was in advanced clinical trials during the 1970's, however severe bladder toxicity prevented any further development.[6]

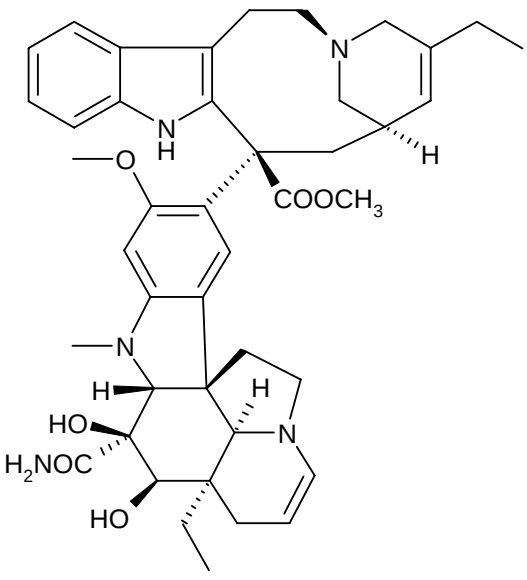


**35**

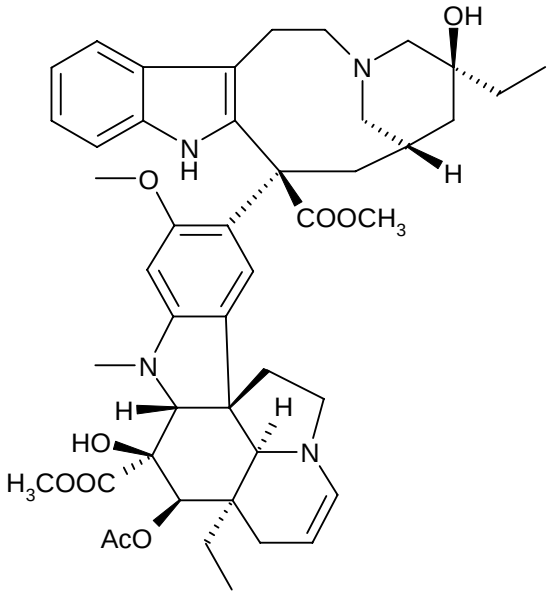


**36**

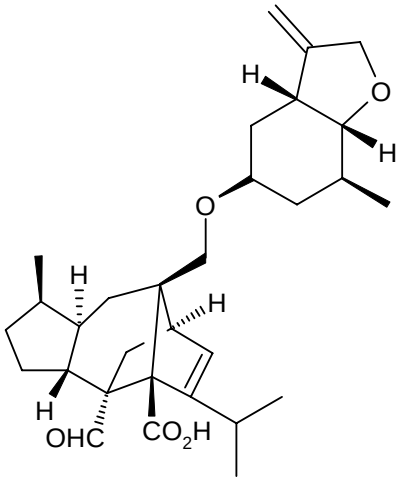


**37**

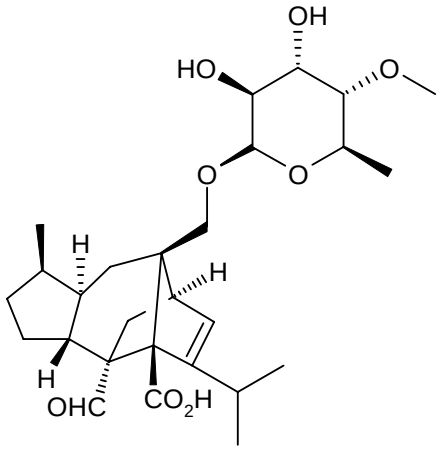


**38**

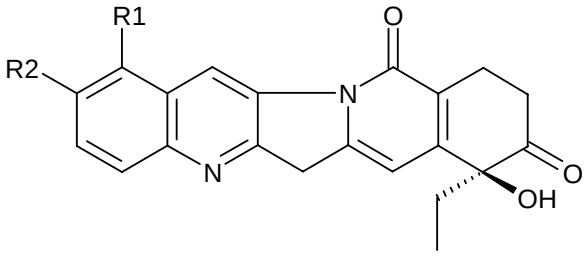


$R_1 = R_2 = H$ **39**

$R_1 = CH_2NMe_2$, $R_2 = OH$ **40**

$R_1 = Et$, $R_2 =$ 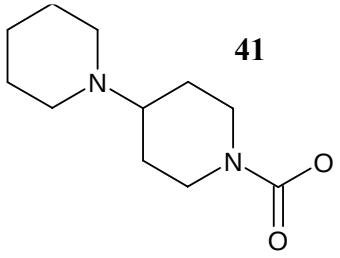 **41**



With the proven track record of natural products as medicines, assumptions may be made that natural products will forever remain entrenched in the process of developing new drugs.[47] However, the dominance of natural products in drug discovery has reduced dramatically within the last 20 years.[47, 52] Currently, the pharmaceutical industry utilizes techniques such as combinatorial chemistry combined with HTS,[1, 42, 45] computational molecular modeling[42, 51] and molecular biology[45] as avenues for drug discovery. Since the mid 1990's, many of the largest pharmaceutical companies have excluded natural products from their drug discovery programs.[2, 47, 53, 54] Several major drug companies, Abbott, Bristol Myers Squibb, Eli Lilly, and GlaxoSmithKline, no longer invest in natural products research as reported in 2002.[53] This information seems extraordinary when the revenue gained from natural product based drugs manufactured by many of these

companies surpasses US$1 billion per year.[53] So why has this industry turned its back on natural products?

The characteristic ability of combinatorial chemistry to rapidly synthesize millions of structural analogues based around a conserved core structure has proven to be an attractive feature.[54] Extraction, purification and structure elucidation of bioactive natural products has been labeled as laborious and time consuming.[53] The benefit of combinatorial chemistry and HTS is that they are automated techniques, allowing for the express processing of data.[2] The collection of samples from nature has also been impeded by changes to legislation, which has meant long waiting times for collection permits to be granted.[53] Many natural products are often seen as containing non-drug like features such as structural complexity, complex stereochemistry, and an excess of hydroxyl groups and carbonyls.[2] This has made natural products unattractive molecules to manipulate synthetically.

However, natural products have been the most dependable supply of drug leads.[41] The impressive structural diversity of natural products provides outstanding prospects for discovering low molecular weight compounds possessing activity against a broad spectrum of biological targets.[41] Arguments provided by Harvey showed that standard combinatorial chemistry does not offer this.[41] Further arguments suggest libraries of compounds generated by combinatorial synthesis are not expected to include complex structures.[1] This has been demonstrated in the structural analysis of natural products and marketed drugs. The results show natural products contribute ring systems that are not integrated into any marketed drugs,[55] and 40% of the ring systems found in the Dictionary of Natural Products are missing from synthetic libraries.[41, 56] The unique positions of heteroatoms and the range of functional groups found in natural products offer distinct advantages.[42] Also, the presence of more rings,[42] chiral centres,[42] and $sp^3$-hybridized bridgehead atoms[45, 56] emphasize the structural diversity of natural products. Bioactive natural products, particularly those from traditional medicines, are often intrinsically drug-like, allowing better uptake and metabolism by the body.[41] This is extremely useful in the decrease of development costs and time.[41] In contrast, studies

show that fully synthetic drugs are often more potent, however exhibit more side effects and development costs are higher when compared with natural product derived drugs.[57] Progress towards chiral drugs creates more opportunities for natural products as they are typically enantiomeric.[2]

Two separate analyses of marketed drugs were performed by Newman, Cragg and Snader in 1997[52] and 2003.[54] The 1997 analysis included drugs prescribed from 1983 to 1994, while the 2003 analysis included drugs from 1981 to 2002. These surveys provide an insight into the comparison of fully synthetic and natural product based drugs. New disease areas were included in the 2003 study, due to the increase in biological targets arising from the human genome project.[54] These findings can be summarized as follows. Natural product based drugs were found to be dominant in therapeutic areas such as antibacterial, antihypertensive, antiviral, anticancer, muscle relaxant, immunostimulant, immunosuppressant, anticoagulant, bronchodilator, antiglaucoma and Alzheimer's and Parkinson's diseases. Fully synthetic drugs dominated therapeutic areas including analgesic, anaesthetic, antianginal, antiarrhythmic, antihistamine, anti-inflammatory, anxiolytic, hypnotic, diuretic, antifungal and antiepileptic. Included in the natural product based drug group were pure natural products, semi-synthetic derivatives, synthetic molecules based on a bioactive natural product pharmacophore, and drugs "designed from knowledge gained from natural products".[54] Fully synthetic drugs were defined as purely synthetic molecules without any prior knowledge of a natural product precursor. Of a total of 766 drugs, excluding peptide based drugs and vaccines, 40 were natural products, 209 were semi-synthetic derivatives of natural products, 289 were fully synthetic drugs, and 238 synthetic drugs based on a natural product pharmacophore or information gained from a natural product.[54] Conclusions can be made that natural products consistently provide more drugs and drug leads than their synthetic counterparts.[54] In support of these findings, approved drugs from 2001 and 2002 show little difference from their lead structures.[58] Therefore, HTS and combinatorial synthesis have not had a major impact on the discovery and development of new drugs.[58] However, purely synthetic drugs should not be dismissed as they can be used to compliment drugs derived from natural sources.

An alarming aspect of the loss of interest in natural products research by the pharmaceutical industry is the implications for treatment of multi drug resistant bacteria and tumours, where natural product based drugs have dominated these therapeutic areas.[43, 49, 51-53] New drugs are also required to combat crippling CNS disorders such as Alzheimer's and Parkinson's disease. Natural products may be a valuable resource in the treatment of these diseases[13] when considering natural product based acetylcholinesterase inhibitors huperzine A (**42**) and galanthamine (**43**).[51] Huperzine (**42**), isolated from the club moss *Huperzia serrata,* is clinically available for memory enhancement[33] while galanthamine (**43**), from plants of the genus *Ungernia* (Amaryllidaceae), was approved in 2002 as a drug for the treatment of Alzheimer's disease.[47, 59]

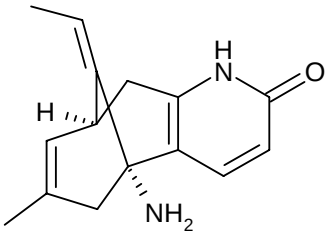


**42**

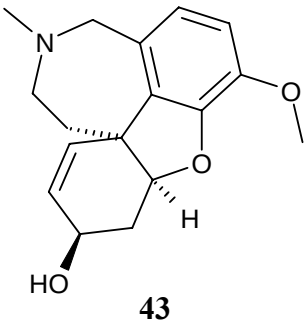


**43**

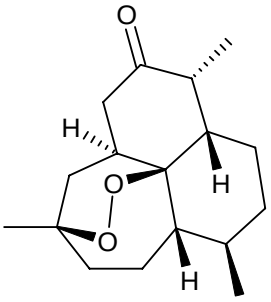


**44**

The domination of antibacterials by natural products is due to structural complexity, one of the main factors absent from a synthetic compound library. An example is the antibiotic Synercid, developed by Rhone-Poulenc Rorer which contains the complex structures quinupristin and dalfopristin. This drug is prescribed for treatment against a variety of antibiotic resistant strains of bacteria.[6, 51] Another noteworthy medicinal agent from nature with unique structural features is artemisinin (**44**). This compound was the active constituent of an ancient Chinese remedy for malaria named Quinghaosu.[6] Artemisinin, isolated from the plant *Artemisia annua*,[6] contains an unusual endoperoxide group that distinguishes it from other antimalarial drugs. Artemether was a clinically available synthetic derivative of artemisinin (**44**) and was included on the WHO list of essential medicines.[51] The serious threat of malaria to human health was confirmed in

1996 when it was reported as the cause of between 1.5 to 2.7 million deaths annually, with 500 million new cases occurring worldwide each year.[13]

A final example of the rich and diverse chemistry of nature as a vital source of drug leads is epibatidine (**45**). Isolated from the skin of an Ecuadorean frog,[60] this unique alkaloid acts at nicotinic acetylcholine receptors, resulting in a potent analgesic effect. The severe adverse side effects of epibatidine (**45**) prevented its further development. However, its discovery stimulated research efforts at Abbott Laboratories to unearth an epibatidine analogue, ABT-594 (**46**), which was undergoing preclinical trials in 2002.[6, 51]

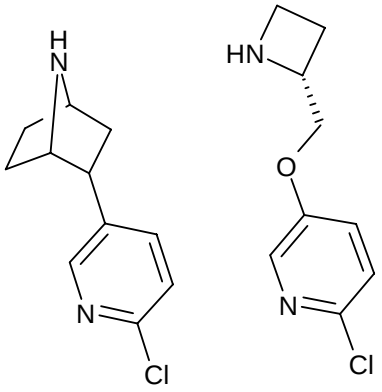


**45** **46**

Strong evidence exists for the vital role of natural products as an avenue for drug discovery. Currently, there is a lack of innovative drugs being developed.[45] The number of new approved drugs has reduced by more than 50% in a five year period. In 1996, 53 new drugs were approved in comparison to 24 in 2001.[53] This finding is linked to the exclusion of natural products research from drug discovery programs.[45, 53] The state of innovative research from the pharmaceutical industry was outlined by Angell, who showed that of a total of 415 drugs approved between 1998 and 2002, only 14% were new and innovative drugs.[61] A staggering 77% of these drugs were labeled as "me-too drugs" which are slight modifications of existing drugs as a means to extend the length of exclusive patented marketing rights and were deemed to be "no better than drugs already on the market to treat the same condition".[61] Therefore, there is a desperate need for major pharmaceutical manufacturers to re-consider natural products research.

Considering the high costs and lengthy timelines associated with drug development and research, the estimated time of one to four months[53] to isolate and characterize a bioactive natural product seems insignificant.

Plant natural products, in particular alkaloids,[33] are vital to drug discovery.[62] Higher plants are well known as producers of chemically complex and biologically active secondary metabolites.[14, 43] At least 25% of all prescription drugs in use today contain active substances which were originally isolated from plants,[3, 5, 6] and 75% of these drugs were derived from ethnobotanical approaches (traditional medicines).[3, 6, 10, 52, 53] Plants can be regarded as a prime source of bioactive molecules and yet only approximately 10% of the estimated 250 000 plants species worldwide have been tested for some sort of biological activity.[3, 5, 8, 41, 63, 64] Many plant secondary metabolites are regarded as genus- or species-specific, and many excellent drug leads may remain undiscovered.[5, 8] Of the total plant species in the world, an estimated 35 000 to 70 000 are used in traditional medicine worldwide, with China and India having strong traditions in the use of herbal remedies.[29]

Among the list of plant-based drugs produced commercially by synthesis[8] are caffeine (**4**), ephedrine (**12**), emetine (**47**) for the treatment of severe amoebiasis,[17] the smooth muscle relaxant papaverine (**48**), theobromine (**49**) for the treatment of asthma and as a diuretic,[17] and $\Delta^9$-tetrahydrocannabinol (**50**) which is used to reduce nausea associated with chemotherapy.[64] Further examples of pharmaceuticals derived from plants include pilocarpine (**51**), from the Brazilian species of *Pilocarpus jaborandi* (Rutaceae) which is used in the treatment of glaucoma, reserpine (**52**), an antihypertensive and psychotropic agent from *Rauwolfia serpentina* (Apocynaceae), and paclitaxel (**53**), from the Pacific yew tree *Taxus brevifolia*.[14, 62] In 2000 alone, the marketing of taxol as an anticancer drug provided revenues exceeding US$1.5 billion for Bristol Myers Squibb.[53]

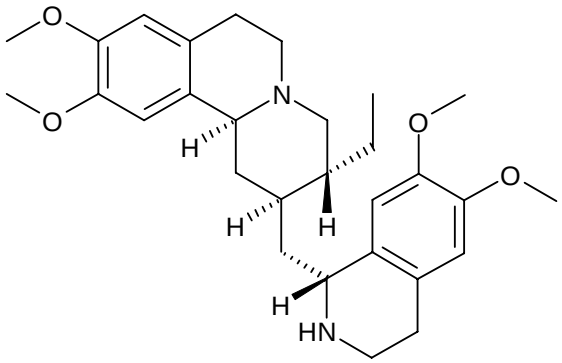

**47**

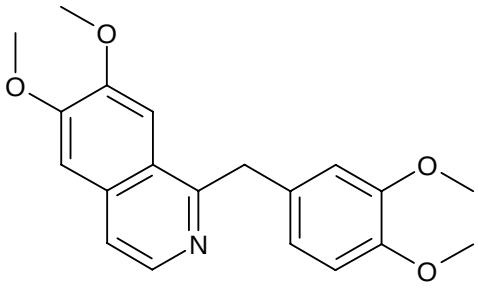

**48**

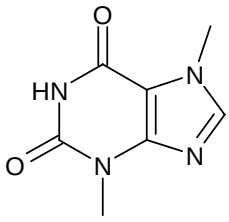

**49**

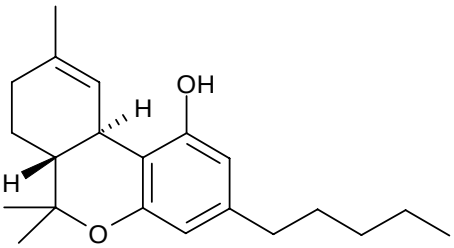

**50**

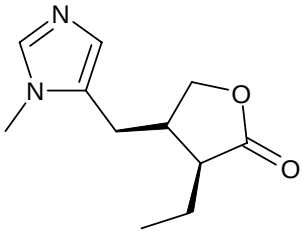

**51**

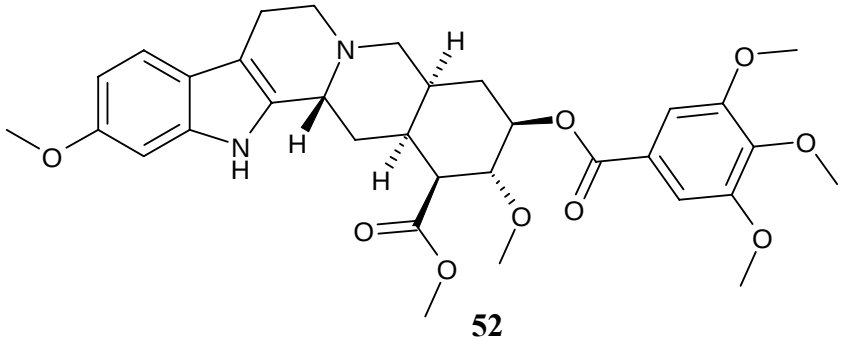

**52**

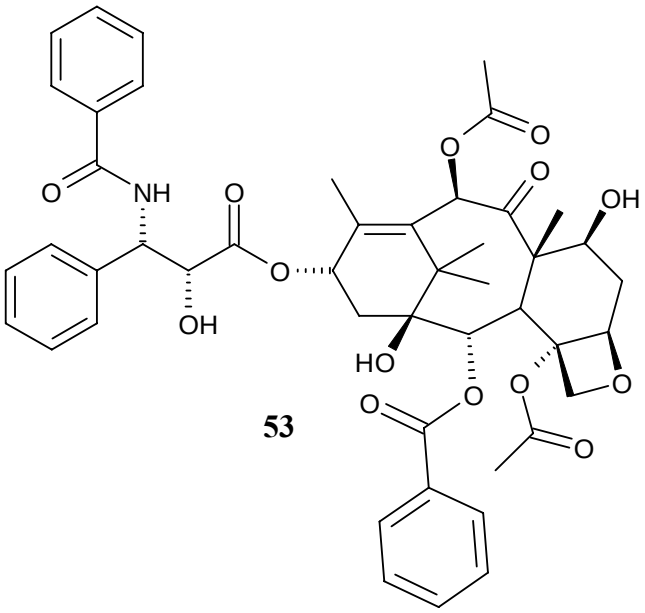

**53**

It has been estimated in 2000 that only 5000 plant alkaloids of a total of 21 120 had been evaluated for biological activity in at least one bioassay based on published data.[33, 53] Therefore, 76% of the total number of alkaloids have not been evaluated in a single bioassay. As such, plant alkaloids may well prove to be a productive avenue for new drugs.

## 1.4 The Family Elaeocarpaceae

### *1.4.1 Distribution*

Queensland contains a unique range of plants in the family Elaeocarpaceae, comprising 40 species from five genera, *Aceratium, Dubouzetia, Elaeocarpus, Peripentadenia* and *Sloanea.*[65] The largest group of Queensland Elaecarpaceae belong to the genus *Elaeocarpus* with 27 species. The genera *Aceratium* and *Sloanea* each contain five species, there are two species of *Peripentadenia* and one species of *Dubouzetia.*[65] Species

from the genera *Elaeocarpus* and *Sloanea* can be found from north Queensland to northern New South Wales, whereas species from the genera *Aceratium, Dubouzetia,* and *Peripentadenia* are found exclusively in north Queensland.[65]

The Elaeocarpaceae are found in the Australia-Pacific region (PNG and NZ), Asia including India and China, and Central and South America. Species from the genus *Sloanea* are mainly found along the equator.[66] An estimated 400 species of Elaeocarpaceae from ten genera exist worldwide.[33]

### *1.4.2 Previous Chemical Investigations of the Family Elaeocarpaceae*

Previous chemical studies of plants of the family Elaeocarpaceae have focused on species of the genus *Aristotelia* from southern Australia, New Zealand and Chile. Several species from the genus *Elaeocarpus* from PNG and one species from India have been studied. Two species from Queensland have been chemically investigated, *Peripentadenia mearsii* and *Elaeocarpus grandis*. These investigations have yielded an intriguing array of alkaloids.

In an elegant review of alkaloid producing plant species,[33] the family Elaeocarpaceae was listed as a significant alkaloid producing family. A total of 78 alkaloids were isolated from 14 species of Elaeocarpaceae belonging to a total of three genera.[33] Most of these alkaloids were isolated from the genus *Aristotelia*. In a total of 186 alkaloid producing plant families, the Elaeocarpaceae was ranked in 42$^{nd}$ position on the basis of the number of alkaloids isolated.[33]

### *1.4.3 Previous Chemical Investigations of Species from the Genus* Aristotelia

Chemical studies of several species from the genus *Aristotelia* from temperate regions of NZ, South America and southern Australia have shown the genus to be a plentiful source of indole alkaloids.[67] Over 50 terpenoid indole alkaloids have been isolated, many of which are unique to this genus. The abundant variety of *Aristotelia* terpenoid indole alkaloids can be highlighted by the compounds purified from *A. peduncularis.* This Tasmanian plant has yielded seven alkaloids, of which peduncularine (**54**), aristoteline (**55**), aristoserratine (**56**), sorelline (**57**) and tasmanine (**58**) are examples.[67]

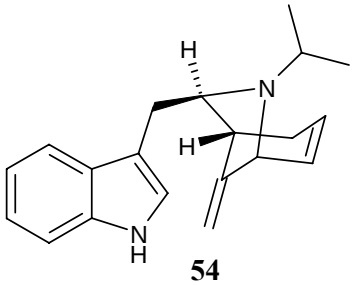

**54**

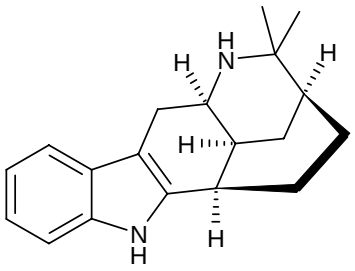

**55**

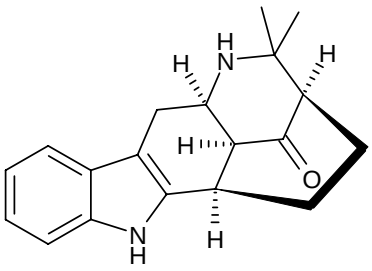

**56**

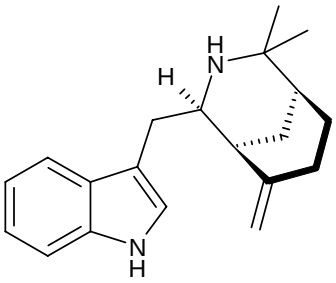

**57**

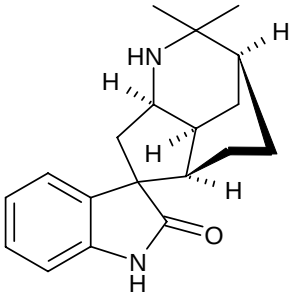

**58**

### *1.4.4 Previous Chemical Investigations of Species from the Genus* Elaeocarpus

Previous chemical studies of *Elaeocarpus* species from PNG, India and Australia have yielded mainly indolizidine alkaloids.[67-69] A total of 20 alkaloids have been isolated from

seven species of *Elaeocarpus*, five of which are from PNG, including *E. polydactylus, E. densiflorus, E. dolichostylis, E. kaniensis*, and *E. sphaericus*. A total of 17 indolizidine alkaloids have been isolated from these species. One pyrrolidine-β-carboline alkaloid, elaeocarpidine (**59**), was isolated from *E. polydactylus, E. densiflorus*[70, 71] and *E. dolichostylis*.[72] The aromatic indolizidine alkaloids (±)-elaeocarpine (**60**), (±)-isoelaeocarpine (**61**), and (+)-isoelaeocarpicine (**62**) have also been isolated from *E. polydactylus.*[73, 74] Elaeocarpidine (**59**) was isolated as the only alkaloid from *E. densiflorus*[70] *(E. archiboldianus*).[71]

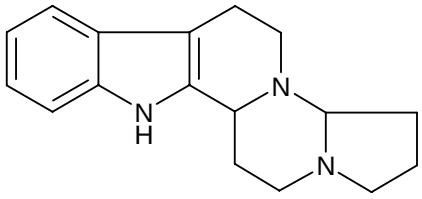


**59**

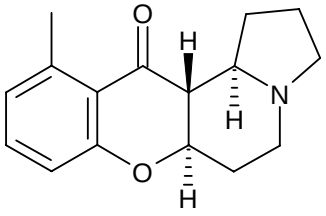


**60**

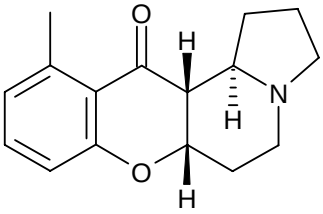


**61**

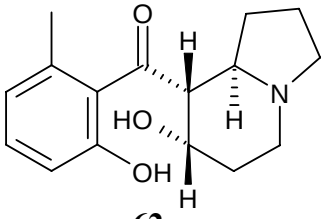


**62**

A series of non-aromatic indolizidine alkaloids have been isolated from *E. sphaericus*[75, 76] and *E. dolichostylis.*[72, 77] This group comprises eight stereoisomers, which vary about the stereochemistries of the elaeocarpiline core structure. Seven alkaloids including (-)-isoelaeocarpiline (**63**), (+)-elaeocarpiline (**64**), (+)-epiisoelaeocarpiline (**65**), (-)-epielaeocarpiline (**66**), (+)-epialloelaeocarpiline (**67**), (-)-alloelaeocarpiline (**68**) and (+)-pseudoepi-isoelaeocarpiline (**69**) have been isolated from *E. sphaericus*. [75, 76] The absolute configurations of all these compounds were determined by synthetic studies.[76] (+)-15,16-Dihydroelaeocarpine (**70**) and (-)-15,16-dihydroisoelaeocarpine (**71**) were isolated from *E. dolichostylis* and possessed undefined stereochemistry of the methyl group.[72] However, chemical degradation studies of these compounds allowed them to be

identified as (+)-elaeocarpiline (**64**) and (-)-isoelaeocarpiline (**63**), respectively.[77] Traces of elaeocarpine (**60**) and isoelaeocarpine (**61**) in *E. dolichostylis*[72] were also reported.

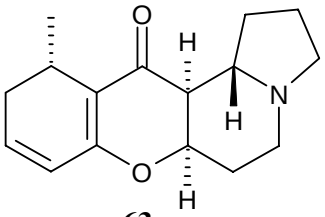


**63**

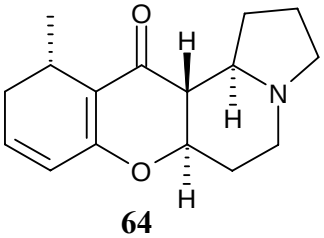


**64**

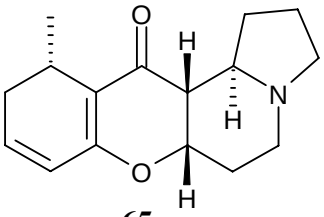


**65**

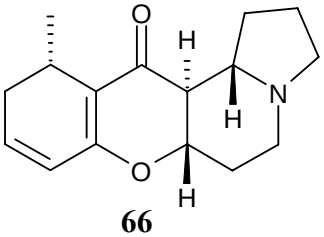


**66**

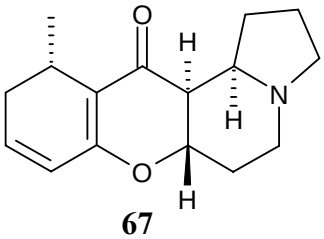


**67**

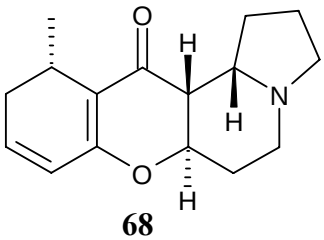


**68**

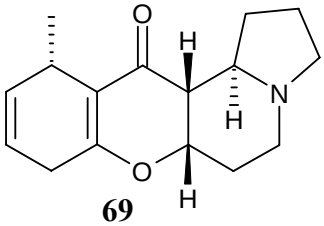


**69**

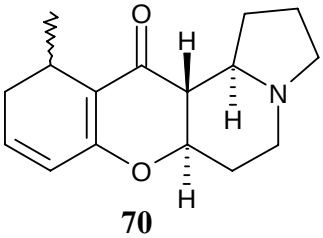


**70**

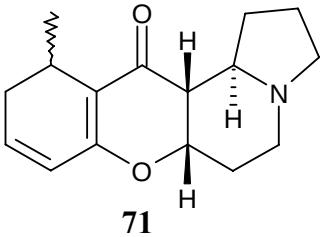


**71**

Rudrakine (**72**) is another example of a non-aromatic indolizidine alkaloid, which was isolated from the Indian species *E. ganitrus*.[68] This species name was later shown to be synonymous with *E. sphaericus*.[78, 79] This compound is different from its Papua New Guinean counterparts in that it possesses a hydroxyl group at $C_{14}$. However, the structure of this compound is tentative, as the position of the hydroxyl is based on biogenetic and MS evidence.[68] No attempts to assign the stereochemistry of rudrakine (**72**) were reported.

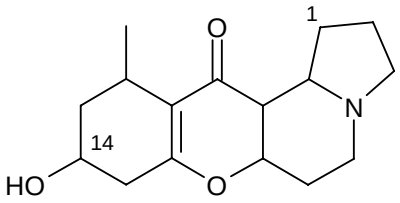


**72**

In a recent report, the presence of alkaloids in the Queensland plant *E. grandis* was demonstrated.[69] This was the first reported isolation of alkaloids from an Australian species of *Elaeocarpus*. The novel indolizidine alkaloids grandisine A (**73**) and B (**74**), as well as isoelaeocarpiline (**63**), were isolated from this plant. Grandisine B (**74**) is the only alkaloid known to possess an indolizidine-isoquinuclidinone bi-functionality.[69] Only isoelaeocarpiline (**63**) was isolated in this study. No other stereoisomers (**64** – **69**) encountered in the extraction of *E. sphaericus* and *E. dolichostylis* were purified from *E. grandis*.

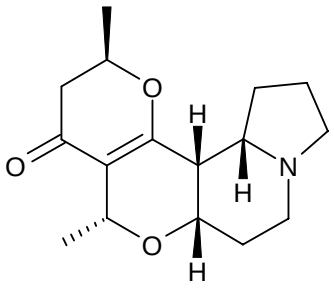


**73**

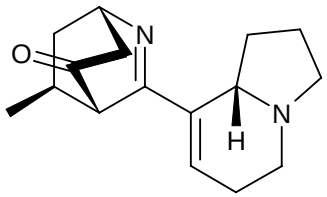


**74**

The New Guinean species *E. kaniensis* was reported to produce a different series of indolizidine alkaloids. These compounds comprised a total of six 12-carbon compounds.[80] These include the elaeokanine series A (**75**), B (**76**), C (**77**), D (**78**), E (**79**), and elaeokanidine A (**80**). All of the other *Elaeocarpus* indolizidine alkaloids are 16 carbon compounds.

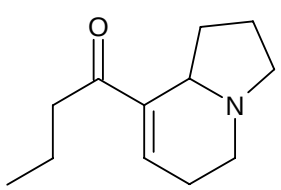


**75**

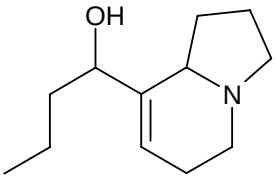


**76**

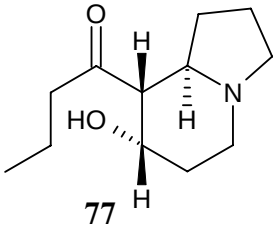


**77**

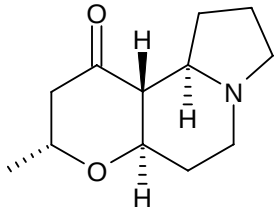


**78**

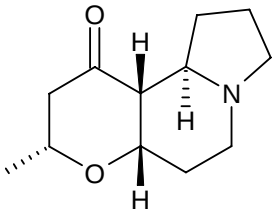


**79**

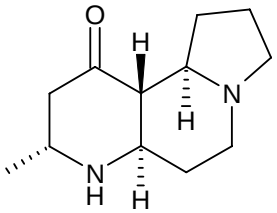


**80**

The relative stereochemistry of elaeokanine C (**77**) was determined and bears the same configuration as seen in isoelaeocarpicine (**62**). The stereochemistry of the proton α to the nitrogen in elaeokanine A (**75**) is the same as in elaeokanine C (**77**). A dehydration reaction of elaeokanine C (**77**) produced **75**. Subsequently, the dehydration of elaeokanine B (**76**) with $NaBH_4$ also produced **75**. The conserved stereochemistry of this position throughout the *E. kaniensis* indolizidine alkaloid series would therefore be consistent with the proposed biosynthesis.[80] Only the relative configurations of elaeokanine D (**78**) and E (**79**) were determined. Two further compounds, which are stereoisomers of elaeokanidine A (**80**), were reported to have been isolated, however their structures were not elucidated unambiguously.[80]

The same biosynthetic pathway is proposed for all of the *Elaeocarpus* indolizidine alkaloids mentioned above. The biosynthesis of these alkaloids as proposed by Johns *et al.* begins with the condensation of a 12-carbon polyketide chain and a 3,4-dihydropyrrole moiety.[77] The polyketide chain can be biosynthesized from six acetyl-CoA units joined in a head-to-tail fashion as depicted in Figure 2.[34] In plants, polyketide synthesis is regarded as a primary metabolic pathway.[81] Acetyl-CoA can be created from pyruvic acid, which in turn is formed from the glycolysis of carbohydrates.[81] Johns *et al.* surmised that the non-protein amino acid[34] ornithine is the precursor of the

dihydropyrrole heterocycle.[77] The biogenesis of this heterocycle from ornithine is shown in Figure 3.

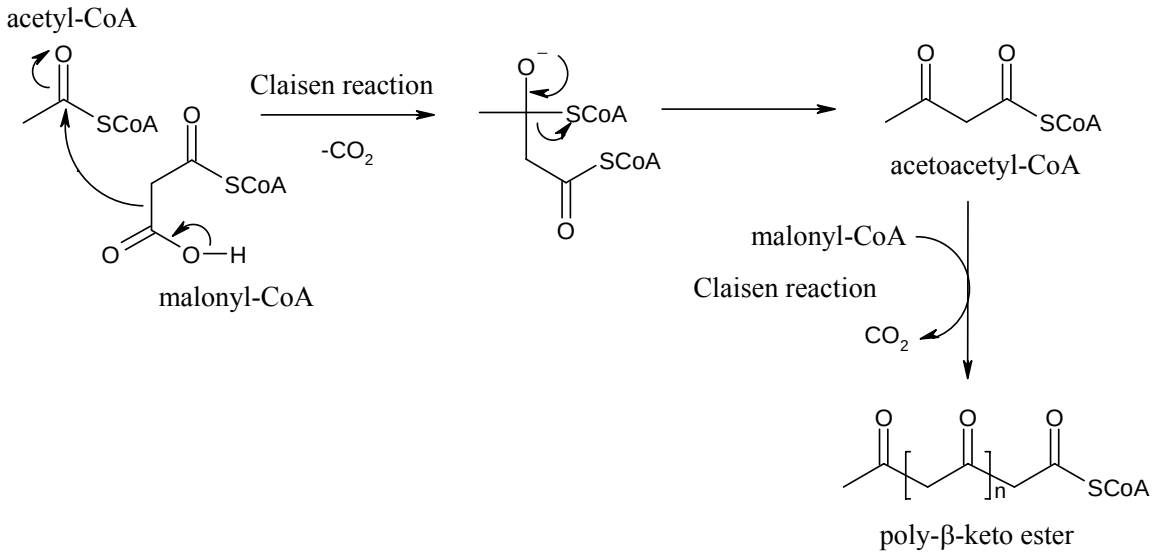


**Figure 2**. Overview of polyketide biosynthesis by sequential Claisen reactions.[34]

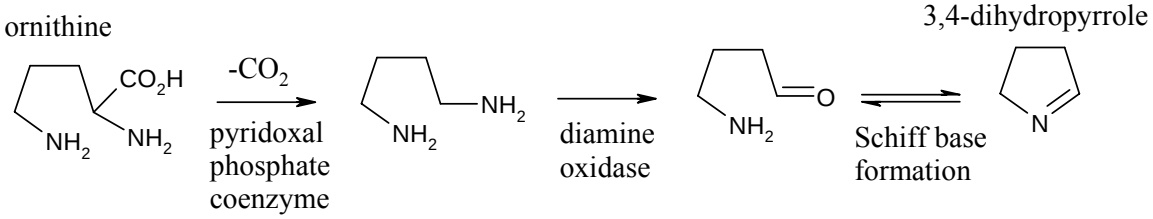


**Figure 3**. The formation of dihydropyrrole from ornithine.[34]

The condensation of the $C_{12}$ polyketide and dihydropyrrole proposed by Johns *et al.*[77] is shown in Figure 4. This pathway accounts for the formation of the $C_{16}$ indolizidine alkaloids isolated from the PNG species of *Elaeocarpus*, with the exception of *E. kaniensis*. The $C_{12}$ indolizidine alkaloids isolated from *E. kaniensis* were proposed to be biogenetically derived from a $C_8$ polyketide as depicted in Figure 5.[80]

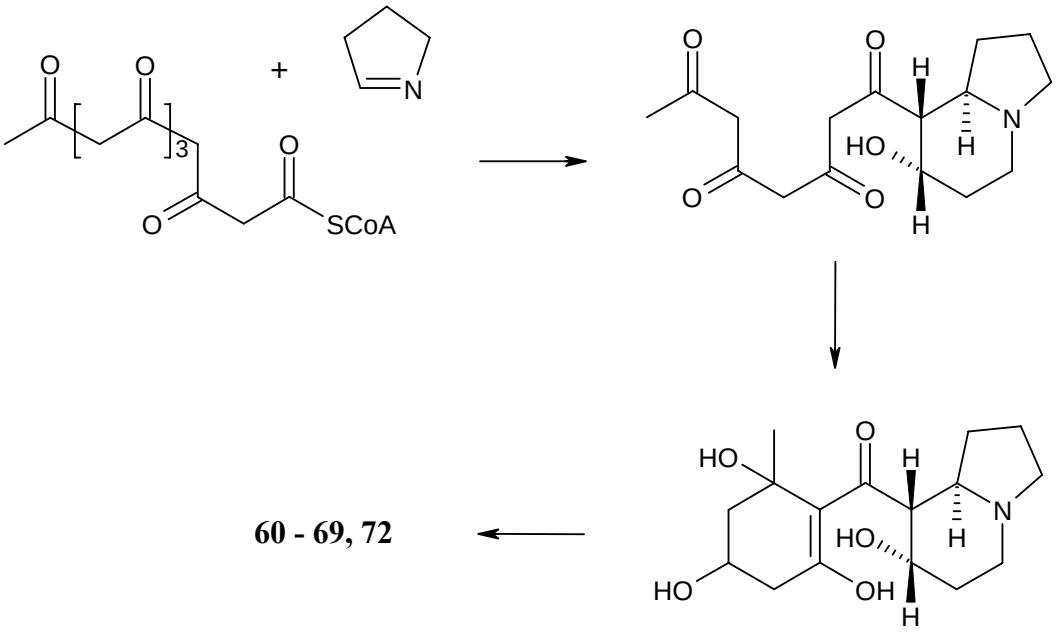


**Figure 4.** The Johns *et al.* proposed biosynthesis of the $C_{16}$ *Elaeocarpus* indolizidine alkaloids.[77]

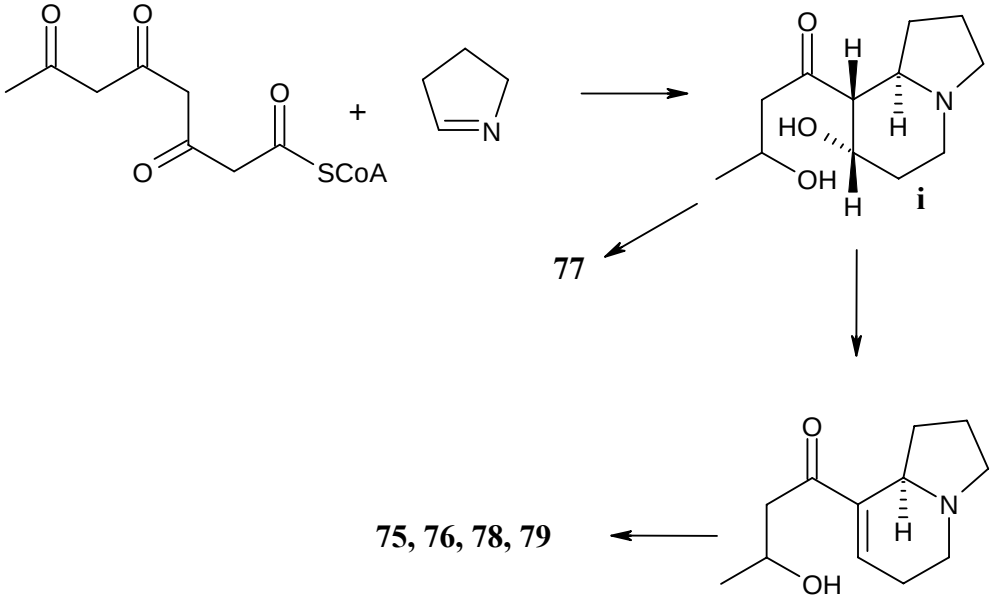


**Figure 5.** The Johns *et al.* proposed biosynthesis of the $C_{12}$ *E. kaniensis* indolizidine alkaloids.[80]

A biosynthetic pathway for elaeocarpidine (**59**) was also proposed.[70] A tryptamine unit combined with a three carbon chain derived from acetate, was postulated to be linked to a dihydropyrrole moiety as shown in Figure 6.

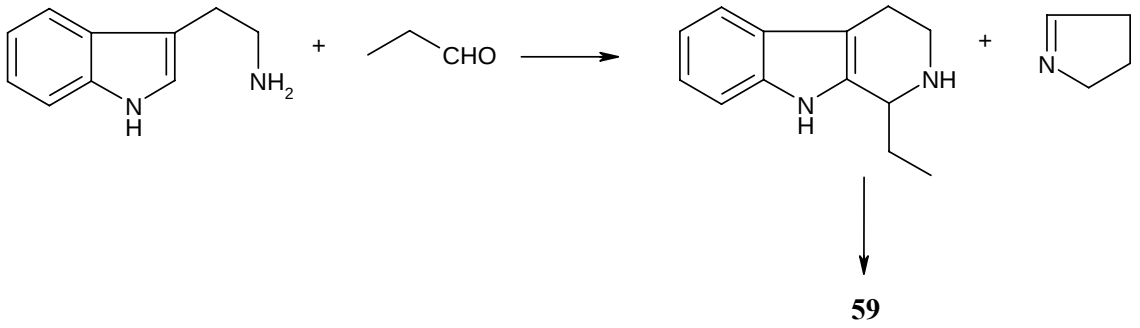


**Figure 6.** The proposed biogenesis of elaeocarpidine (**59**) from tryptamine, dihydropyrrole and a three carbon chain derived from acetate.[70]

The biogenesis of the *E. grandis* group of indolizidine alkaloids, grandisine A (**73**) and B (**74**), has been proposed by Carroll *et al*.[69] This can be regarded as an extension of the polyketide-dihydropyrrole condensation pathway originally proposed by Johns *et al*. This pathway is shown in Figure 7.[69] The polyketide condensation leads to the formation of a common precursor, from which grandisine A (**73**), B (**74**) and isoelaeocarpiline (**63**) were generated. A precursor of grandisine B was deemed to be produced by a Michael-type addition of ammonia to an α,β-unsaturated ketone of (**i**) in Figure 7. A subsequent intramolecular cyclization prompted by an approach of the primary amine on the ketone in (**ii**) resulted in the formation of grandisine B (**74**). A proposed tautomerisation of the ketone in (**i**) to its enol form, allowed the subsequent cyclization by nucleophilic addition, resulting in the formation of isoelaeocarpiline (**63**). It was surmised that (**iii**), the precursor of (**i**), undergoes a retroaldol reaction to yield the tetra-keto precursor of grandisine A (**73**). A further reduction of this precursor was proposed to produce two alcohols shown in (**iv**). Nucleophilic addition of the alcohols to the ketone and the double bond resulted in the cyclization to produce grandisine A (**73**).

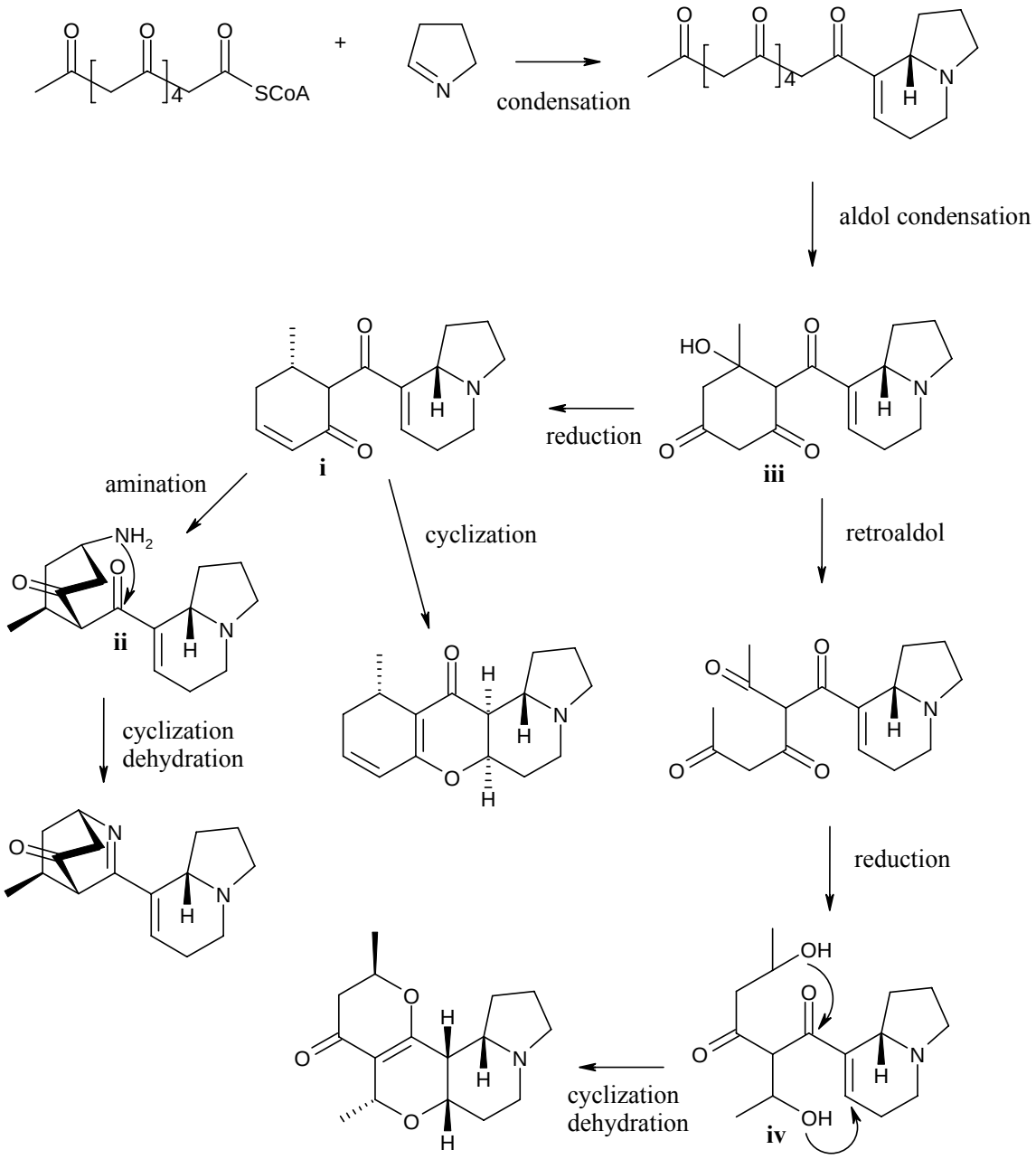


**Figure 7.** The biosynthesis of grandisine A (**73**), B (**74**) and isoelaeocarpiline (**63**) isolated from *E. grandis* as proposed by Carroll *et al*.[69]

As all of the *Elaeocarpus* alkaloids are proposed to originate by the same polyketide condensation, the configurations of $H_7$, $H_8$ and $H_{16}$ should be consistent throughout the indolizidine alkaloid series, shown in A of Figure 8. Variations in the stereochemistry of $H_9$ may be observed during formation of the tetracyclic *Elaeocarpus* indolizidine compounds. These compounds are proposed to be formed in the same manner as isoelaeocarpiline (**63**) from (**i**) in Figure 7. Cyclization results from an axial or equatorial addition of an oxygen nucleophile to a double bond as shown in Figure 9. This is evident in the report of rapid interconversion of elaeocarpine (**60**) and isoelaeocarpine (**61**) (Figure 10). Treatment of either compound with potassium hydroxide readily produces a 1:1 mixture of **60** and **61**.[73]

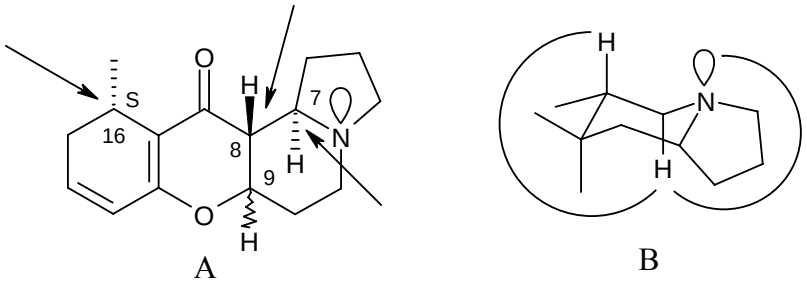


**Figure 8.** The depiction in A of the stereochemistries that should be conserved for the tetracyclic indolizidine alkaloids, marked with arrows. B shows a representation of the *trans*-diaxial configuration of the protons $H_7$ and $H_8$, and $H_7$ and the lone pair of electrons.

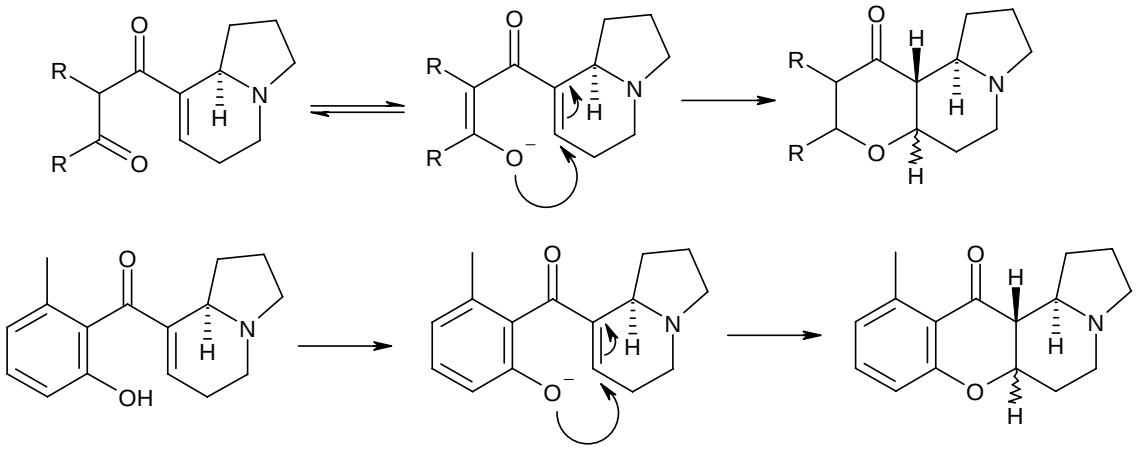

**Figure 9.** The proposed formation of the tetracyclic and tricyclic *Elaeocarpus* alkaloids by nucleophilic addition of oxygen.

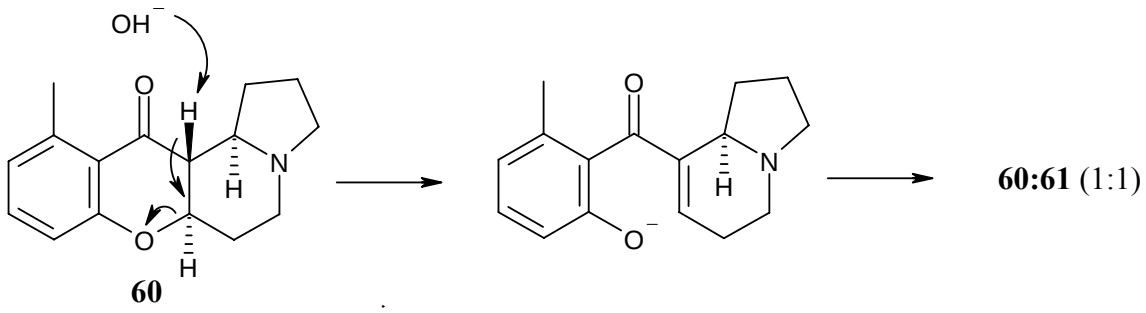


**Figure 10.** The interconversion of elaeocarpine (**60**) and isoelaeocarpine (**61**) under basic conditions.

Only the relative stereochemistries of the aromatic and *E. kaniensis* indolizidine alkaloids have been determined. Consistent *trans*-diaxial relationships are observed between the protons $H_7$ and $H_8$ of these alkaloids. The same *trans-trans* configuration was suggested to occur between the lone pair of electrons of the nitrogen and $H_7$.[73, 80] A representation of the *trans*-diaxial relationships of these protons and the lone pair is shown in B of Figure 8.

The complex mixture of isomers encountered from *E. sphaericus* (**63**–**69**) suggests the formation of an equilibrated mixture during extraction. Figure 11 shows the absolute stereochemistry of enantiomers isolated from this plant. One common feature of these compounds is an *S* configuration at $H_{16}$. This is consistent with the proposed model of conserved stereochemistry illustrated in A of Figure 8.

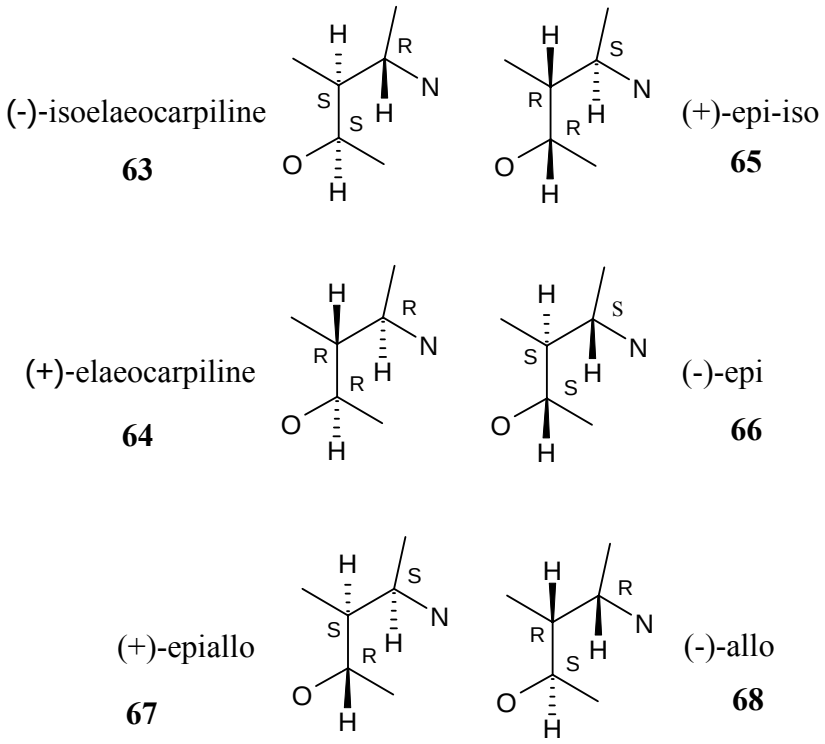


**Figure 11.** Representation of the elaeocarpiline enantiomers isolated from *E. sphaericus*.

The compounds (+)-epialloelaeocarpiline (**67**) and (-)-alloelaeocarpiline (**68**) show a *cis* arrangement for the protons $H_7$ and $H_8$. This is the opposite of the *trans* arrangement seen with all the previous *Elaeocarpus* alkaloids. An enolization of the ketone and conformational change of the six membered ring bearing the nitrogen was proposed to result in the formation of the *cis* configuration.[76]

Only the relative configuration has been reported for the alkaloids grandisine A (**73**) and B (**74**) and isoelaeocarpiline (**63**), isolated from *E. grandis*.[69] The same *cis* arrangement of $H_7$ and $H_8$ is suggested.

### *1.4.5 Previous Chemical Investigations of Species from the Genus* **Peripentadenia**

*Peripentadenia mearsii* represents the only species from this genus to be investigated chemically.[67] The novel pyrrolidine alkaloid peripentadenine (**81**)[82] is the major alkaloid isolated from this plant. This compound contains an *N*-propylhexanamide group. Four minor alkaloids purified from *P. mearsii* include dinorperipentadenine (**82**), peripentamine (**83**), anhydroperipentamine (**84**),[83] and the unusual isoquinuclidinone alkaloid mearsine (**85**).[84] The *Peripentadenia* alkaloids have been of interest to synthetic chemists, with the synthesis of **81** and **82** reported.[85]

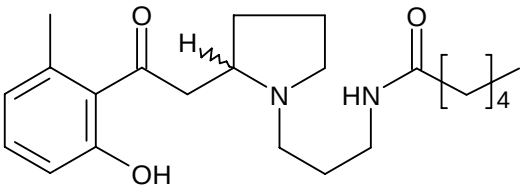


**81**

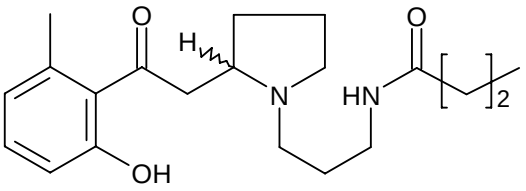


**82**

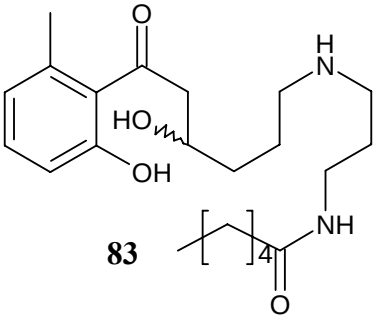


**83**

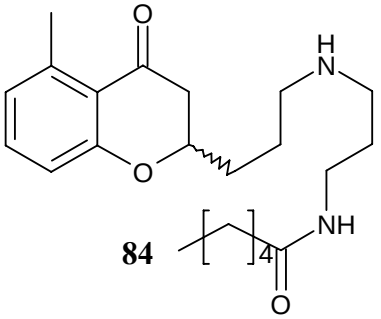


**84**

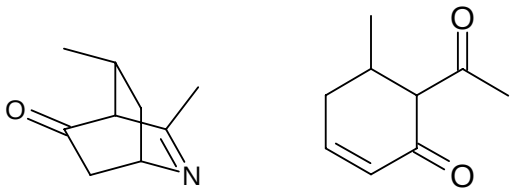

**85** **86**

The relative or absolute configurations of **81**-**85** remain undefined. Furthermore, no proposed biogenetic pathway has been hypothesized for these alkaloids. However, these molecules possess striking structural similarities to the *Elaeocarpus* alkaloids. In the structures of peripentadenine (**81**) and dinorperipentadenine (**82**), a five membered nitrogen heterocycle is linked by a keto group to a methylphenolic moiety. This methylketophenol has been previously encountered in isoelaeocarpicine (**62**). This observation suggests the biosynthesis of the *Peripentadenia* alkaloids may be related to the proposed formation of the *Elaeocarpus* alkaloids. The pyrrolidine moiety of **81** and **82** may therefore be formed from ornithine. Peripentamine (**83**) and anhydroperipentamine (**84**) appear to be simple oxidation products of peripentadenine (**81**). Figure 12 shows a proposed pathway for the biogenesis of these compounds from **81**. Anhydroperipentamine (**84**) can be formed from nucleophilic addition of the phenolic oxygen to the alpha position to the nitrogen. The same occurs in the formation of peripentamine (**83**), however in this example the nucleophile may be a hydroxide anion.

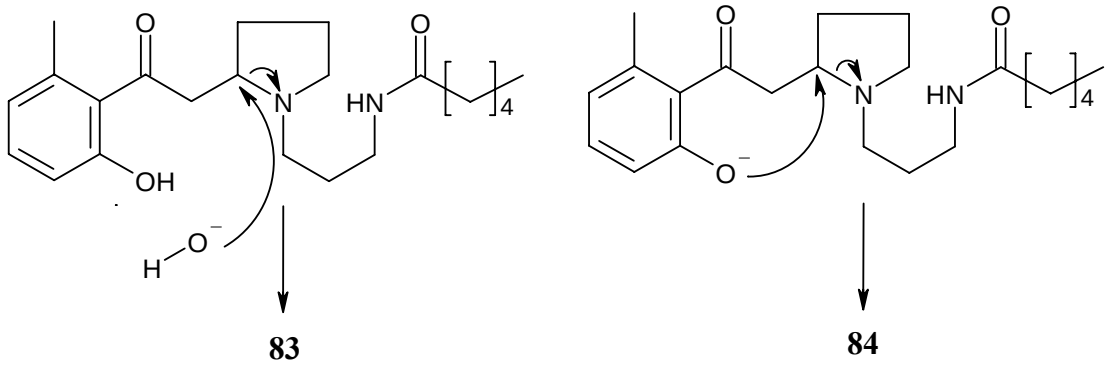

**83** **84**

**Figure 12.** The proposed formations of peripentamine (**83**) and anhydroperipentamine (**84**) by oxidation of peripentadenine (**81**).

The unique alkaloid mearsine (**85**) possesses the same isoquinuclidinone functionality as found in grandisine B (**74**). This suggests that the formation of these two compounds is related. Structure **86** has been proposed as the precursor of mearsine (**85**).[84] Amination of **86**, in the manner described for the formation of grandisine B in Figure 7, could afford mearsine (**85**).

### *1.4.6 The Value of Chemical Investigations of the Family Elaeocarpaceae*

The diverse chemical structures and the number of indole, indolizidine and pyrrolidine alkaloids isolated from the Elaeocarpaceae have led Collins *et al*. to claim that the family is one of the major alkaloid producing plant families.[67] Since only two of 40 species of Elaeocarpaceae in Queensland have been chemically investigated, potential exists for the discovery of structurally diverse novel indolizidine alkaloids from the remaining 38 species. Queensland species of *Aceratium*, *Sloanea,* and most of the *Elaeocarpus* species from PNG have not been investigated chemically.

### *1.4.7 The Extraction Process used in the Isolation of* **Elaeocarpus** *and* **Peripentadenia** *Alkaloids*

An acid-base extraction was employed in the isolation of the *Elaeocarpus* and *Peripentadenia* alkaloids. This has been viewed as a classic method for the purification of alkaloids. This method was particularly useful for the rapid separation of alkaloids from non-alkaloidal constituents. Acid-base extraction exploits the chemistry of the ionizable nitrogen found in alkaloids. Under acidic conditions the alkaloid is charged and water soluble, allowing non-charged organic soluble compounds to be easily removed by

partitioning with an organic solvent, typically $CHCl_3$. The acidic aqueous layer can then be basified, during which the alkaloid returns to its neutral state. Alkaloids can then be partitioned into an organic phase such as $CHCl_3$, which can be easily evaporated. The resulting residue usually affords a mixture of alkaloids.

An ethanol extract of the *Elaeocarpus* and *Peripentadenia* species was allowed to evaporate and an acid-base extraction was performed. The acid and base used in this procedure were $H_2SO_4$ and $NH_4OH$ respectively. The effects of $NH_4OH$ used during the extraction process have been documented.[86] The biogenesis of some *Elaeocarpus* and *Peripentadenia* alkaloids, such as elaeokanidine A (**80**) and mearsine (**85**), have not been explained. These compounds possess an extra nitrogen atom. Grandisine B (**74**)[69] is proposed to be formed from an amination reaction. Such reactions may therefore be responsible for the creation of elaeokanidine A (**80**) and mearsine (**85**). Ammonia is the probable source of the nitrogen in these amination reactions, suggesting grandisine B, mearsine and elaeokanidine A are ammonia artifacts, produced during the extraction procedure.

In a recent report, ammonia was shown to have an artifact inducing effect.[86] Ammonia was the base used in an acid-base extraction to isolate a series of epimeric alkaloids from the plant *Pandanus amaryllifolius* (Pandanaceae). 6-*Z*-Pandamarilactonine (**87**) is an example of an alkaloid isolated from this plant. In a second extraction of *P. amaryllifolius*, an acid-base purification was deliberately avoided. This yielded a different series of alkaloids, of which 6-*Z*-pandanamine (**88**) was an example. This compound was later found to readily produce 6-*Z*-pandamarilactonine (**87**) when reacted with $NH_4OH$. The conclusion from this study was that ammonia does generate artifacts when used during the extraction of *P. amaryllifolius*.[86]

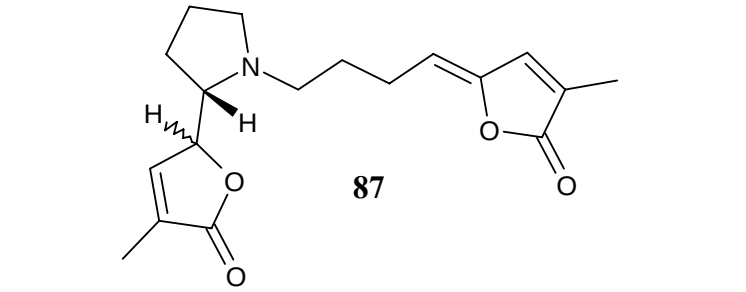

**87**

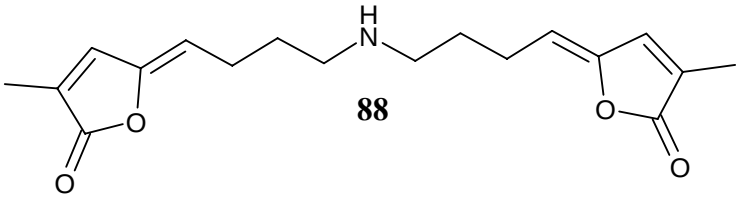

**88**

From this evidence, the mechanisms of the formation of elaeokanidine A (**80**) and mearsine (**85**) can be proposed. The formation of elaeokanidine A (**80**) (Scheme 1) occurs by nucleophilic attack of $NH_3$ to the β-position of the α–β unsaturated ketone in (**i**), affording the Michael adduct (**ii**). An intramolecular Michael addition shown in (**iii**) results in the formation of elaeokanidine A (**80**). The precursor (**i**) was surmised to be a dehydration product of (**i**) in Figure 5.

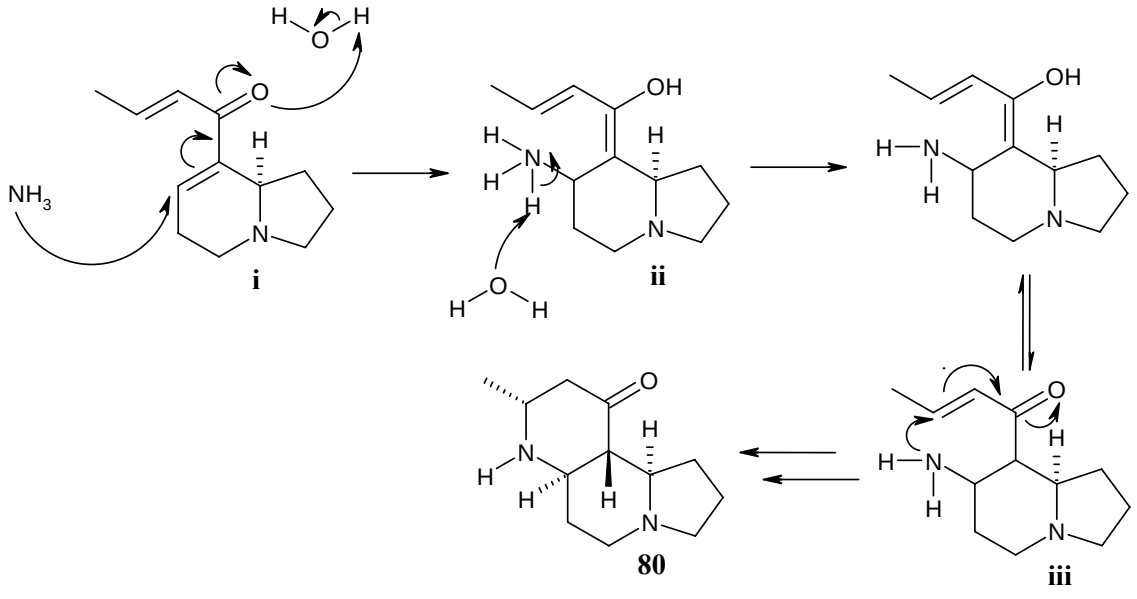

**Scheme 1.** The proposed mechanism of formation of elaeokanidine A (**80**).

The formation of mearsine (**85**) is proposed to occur from a similar Michael addition of ammonia (Scheme 2). Nucleopilic attack of **86** by $NH_3$ results in the adduct (**i**). An intramolecular cyclization resulting from a second nucleophilic attack by the amino group to the carbonyl yields (**ii**). The unstable aminoalcohol in B may spontaneously react to form mearsine (**85**). The conclusion from these proposals is that ammonia should be deliberately avoided in the extraction of plants of the family Elaeocarpaceae.

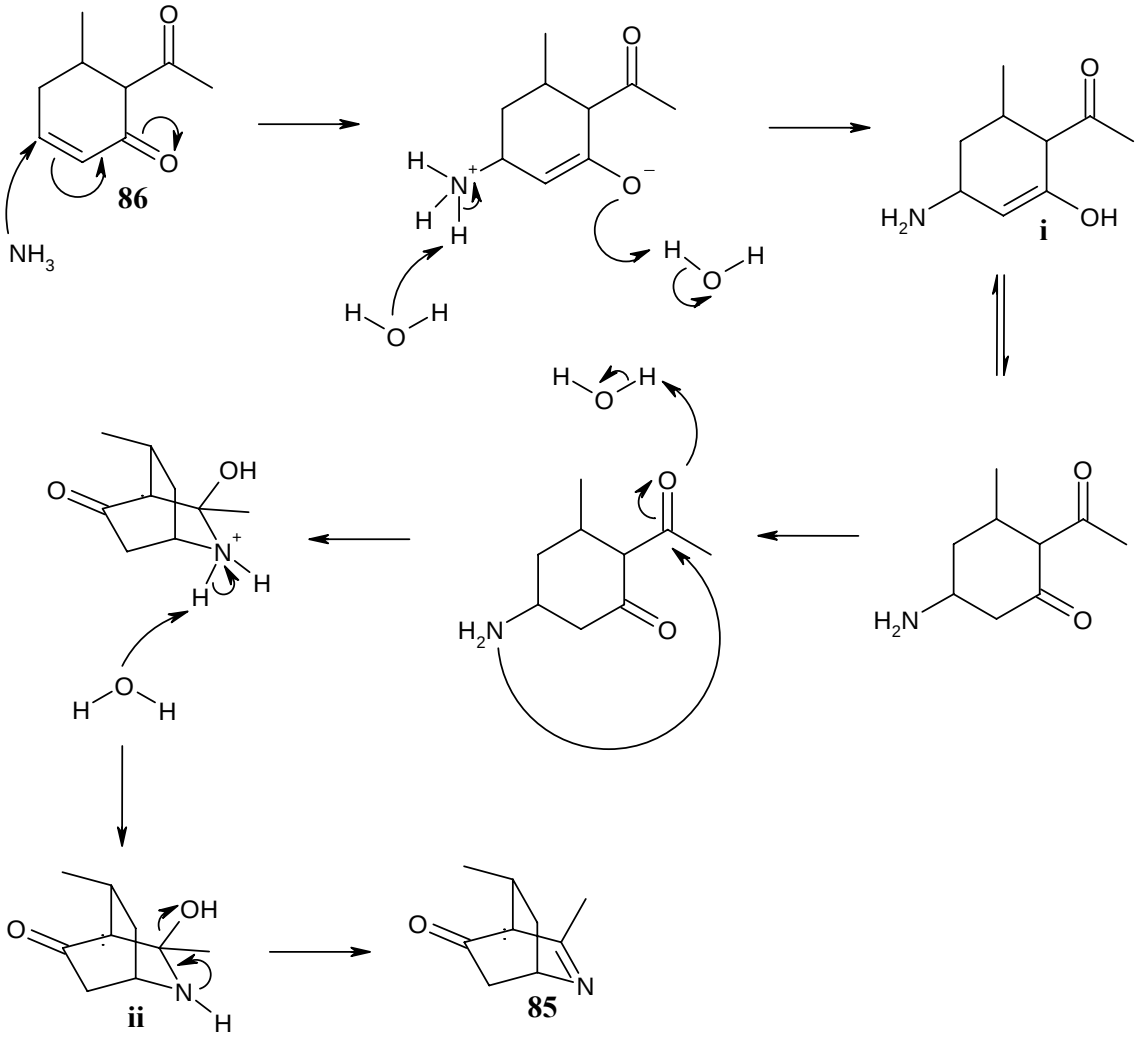


**Scheme 2.** The proposed mechanism of formation of mearsine (**85**) from **86**.

## 1.5 Pharmacological Activity of Indolizidine and *Elaeocarpus* Alkaloids

Plants of the genus *Elaeocarpus* have been reported to be of use as traditional medicines, particularly in India. *E. sphaericus* (*E. ganitrus*) is a tree found in the Himalayan region of India. The fruits of this plant are commonly known as Rudraksha and have been used in Ayurvedic traditional medicine for the treatment of mental diseases, epilepsy, asthma, hypertension, arthritis and liver diseases.[78, 79] Extracts of the fruits of *E. sphaericus* have been studied for pharmacological activity. These extracts were reported to exhibit sedative, antiepileptic, antihypertensive, antimicrobial and analgesic properties.[78, 79] An acetone extract of these fruits demonstrated antimicrobial activity against ten organisms, including *Staphylococcus aureus, Salmonella paratyphi*, and *Shigella dysenteriae*. This extract was found to contain mostly alkaloids and flavonoids. The antibacterial effects of several flavonoids have been demonstrated.[78]

Alkaloid containing extracts of *P. mearsii* and four *Elaeocarpus* species from PNG, including *E. densiflorus, E. dolichostylis, E. polydactylus* and *E. sphaericus*, have been tested for pharmacological activity and antitumour properites.[67] The extracts of *E. dolichostylis, E. polydactylus, E. sphaericus* and *P. mearsii* all exhibited cardiovascular effects. *E. densiflorus, E. polydactylus* and *E. sphaericus* extracts showed analgesic properties. Elaeocarpine (**60**) and isoelaeocarpine (**61**) were demonstrated to produce 50% analgesia in rats at 50mg/kg.[67] The alkaloids of *E. dolichostylis* also exhibited anticonvulsant and weak diuretic activity. Aqueous methanol extracts of *E. dolichostylis* and *E. polydactylus* were shown to inhibit the Walker 256 intramuscular tumour. The presence of alkaloids was confirmed in these extracts, although the constituents responsible for the antitumour activity were not identified.[67]

Further evidence for the potential analgesic properties of the *Elaeocarpus* alkaloids has been demonstrated with the biological evaluation of the *E. grandis* indolizidine alkaloids,

grandisine A (**73**), B (**74**) and isoelaeocarpiline (**63**). These compounds were shown to bind to the $\delta$ opioid receptor,[69] and may produce an analgesic effect. The binding affinities ($IC_{50}$) observed were 2.7 $\mu$M, 52.2 $\mu$M and 11 $\mu$M for grandisine A (**73**), B (**74**) and isoelaeocarpiline (**63**), respectively.

Pharmacological screening of extracts of New Zealand plants for inhibitory activity against HIV-1 protease identified the inhibitory effect of an extract of *E. hookerianus*.[87] However, flavonoids and not indolizidine alkaloids were found to be responsible for the inhibition. Two species of Elaeocarpaceae, *Aristotelia chilensis* and *Crinodendron hookerianum*, have been reported as plants of medicinal value in Chile.[88] Indole alkaloids have been isolated from *A. chilensis*. Plants from the family Elaeocarpaceae are also reported to be of medicinal value to primates. The capuchin monkeys (*Cebus capucinus)* of Costa Rica rub the leaves of species from the genus *Sloanea* into their fur for medicinal purposes.[89] However, these species of *Sloanea* have not been investigated chemically to identify the medicinally active principles.

Other indolizidine alkaloids isolated from a diverse range of organisms have also exhibited biological effects. Lycorine (**89**) has been isolated from several species of plants from the family Amaryllidaceae.[90, 91] This indolizidine alkaloid has been shown to exhibit a range of biological effects including acetylcholinesterase inhibition,[92] antimalarial activity[93] and cytotoxic effects against the human cancer cell-line HepG2.[94] One the most notable indolizidine alkaloids produced in the plant kingdom is castanospermine (**90**), a tetrahydroxy-indolizidine alkaloid from the seeds of the plant *Castanospermum australe* (Fabaceae). Castanospermine is a potent inhibitor of β-glucosidase, and shows potential as an inhibitor of the replication of HIV.[5] Castanospermine has been implicated in livestock poisoning.[5] The trihydroxy-indolizidine alkaloid swainsonine is an inhibitor of α–mannosidase and is a structural analogue of castanospermine.[95, 96]

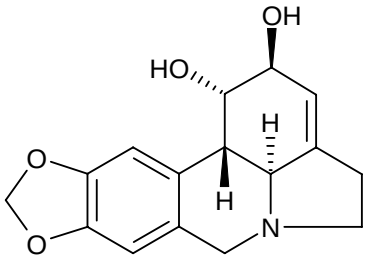


**89**

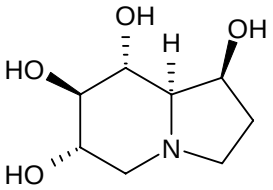


**90**

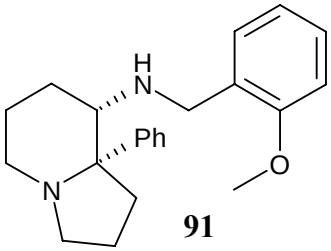


**91**

Indolizidine alkaloids are also reported to be potential substance P/neurokinin-1 receptor antagonists.[97] The indolizidine analogue (**91**) was prepared synthetically, based on the pharmacophore of a potent neurokinin-1 receptor antagonist. This receptor has been associated with several CNS diseases.[95]

Piclavine B (**92**) is an example of an indolizidine alkaloid from a marine organism. This compound, isolated from the tunicate *Clavelina picta,* has been shown to exhibit antimicrobial properties.[98] Chemical studies of microbes have yielded several indolizidines of which antibiotic A 58365A (**93**), louludinium (**94**) and indolizomycin (**95**) are examples. Antibiotic A 58365A (**93**) is an angiotensin converting enzyme inhibitor isolated from *Streptomyces chromofuscus*.[99, 100] Louludinium (**94**) was isolated from the cyanobacterium *Lyngbya gracilis*,[101] however any pharmacological significance of this compound was not identified. The triene antibiotic indolizomycin (**95**), isolated from the bacterium *Streptomyces griseus,* was shown to be weakly active against gram-positive and gram-negative bacteria.[102]

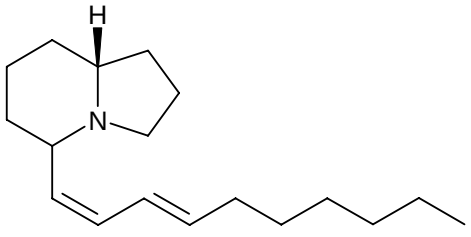


**92**

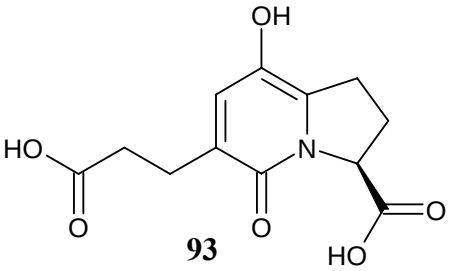


**93**

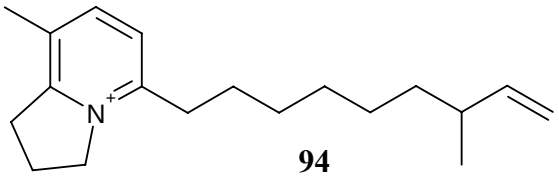

**94**

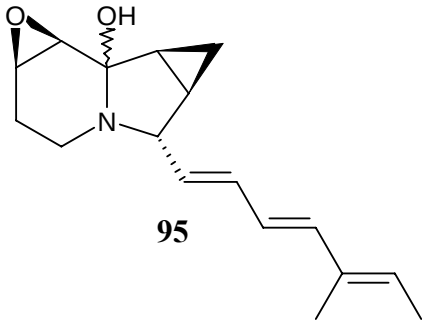

**95**

Arthropod indolizidine alkaloids also exhibit interesting pharmacology. This is exemplified by the pumiliotoxin series of alkaloids, of which pumiliotoxin A (**96**) is an example. These alkakoids are found in the skin of the South American frog *Dendrobates pumilio*.[60] These alkaloids are proposed to be of arthropod origin and are accumulated in *D. pumilio* through their diet of insects. The pumiliotoxins have been shown to have myotonic and cardiotonic activity through effects on sodium channels.[60] Another example of an arthropod indolizidine alkaloid is 3-hexyl-5-methylindolizidine (**97**). This compound was purified from the venom of thief ants, *Solenopsis* sp.[103]

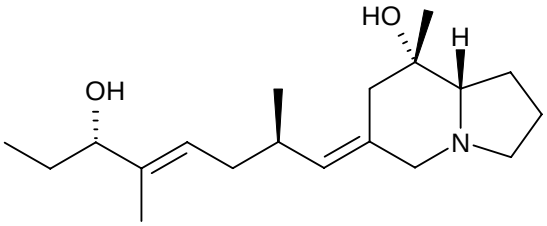

**96**

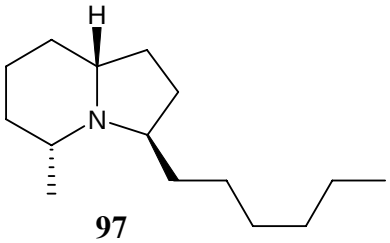

**97**

One of the only examples of an indolizidine alkaloid from mammals is 5-(3-furyl)-8-methyloctahydroindolizidine (**98**). This alkaloid was isolated from the scent glands of the Canadian beaver *Castor fiber*[36] which uses **98** as a territorial marker. This is the same animal from which the quinolizidine alkaloid (-)-castoramine (**20**) has been isolated.

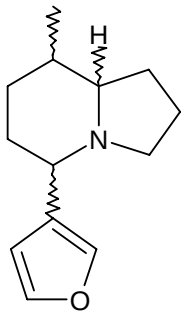


**98**

Indolizidine alkaloids are therefore an important structure class produced in nature. These alkaloids are produced by a wide variety of organisms and possess a broad range of pharmacological activities against a range of biological targets. Indolizidine alkaloids isolated from the family Elaeocarpaceae may offer biological activity against a variety of targets.

## 1.6 The Aims of the Chemical Investigation

The Elaeocarpaceae has been regarded as a major alkaloid containing family and to date no comprehensive chemical survey of plants of this family in Queensland or PNG has been undertaken. The aims of the research are to:

1) Identify new alkaloid producing species within the family Elaeocarpaceae.

2) Develop an efficient method for the extraction of alkaloids, which avoids the formation of artifacts.

3) Purify and elucidate the structures of novel alkaloids from plants of the family Elaeocarpaceae.

4) Determine if any of the isolated alkaloids have biological activity, with a focus on binding studies against the human $\delta$ opioid receptor.

5) Use selected alkaloid natural products isolated from the family Elaeocarpaceae as a template for synthetic modification.

A phytochemical survey was undertaken to identify new alkaloid producing species within the family *Elaeocarpaceae*. This will be discussed in chapter 2. The purification and structure elucidation of alkaloids from the species *E. habbeniensis*, *E. fuscoides*, *Peripentadenia* sp. and *E. grandis* is discussed in chapters 3 – 6, respectively. These species were identified as alkaloid containing from the phytochemical survey. The biological activity of the alkaloids isolated from these species against the human $\delta$ opioid receptor is discussed in detail in chapter 7. Chapter 8 details the synthetic manipulation of selected alkaloids from plants of the family Elaeocarpaceae.

## 1.7 References


1. Samuelsson, G., *Drugs of Natural Origin: A Textbook of Pharmacognosy*. 4th ed.; Swedish Pharmaceutical Press: Stockholm, **1999**.
2. Strohl, W. R., *Drug Discovery Today* **2000,** 5, 39 - 41.
3. Walsh, G., *Biopharmaceuticals: Biochemistry and Biotechnology*. 3rd ed.; J Wiley & Sons, Ltd: Chichester, **2003**.
4. Escohotado, A., *A Brief History of Drugs: from the stone age to the stoned age*. ed.; Park Street Press: Rochester, **1996**.
5. Hostettmann, K., Hamburger, M., *Search for New Lead Compounds of Natural Origin*. In *Perspectives in Medicinal Chemistry*, ed.; Testa, B., Kyburz, E., Fuhrer, W., Giger, R., Eds. Verlag Helvetica Chimica Acta: Basel, **1993**; pp. 475 - 488.

**6.** Newman, D. J., Cragg, G. M., Snader, K. M., *Nat Prod Rep* **2000,** 17, 215 - 234.

**7.** Roberts, M. F., Wink, M., *Introduction*. In *Alkaloids: Biochemistry, Ecology and Medicinal Applications*; Roberts, M. F., Wink, M., Eds. Plenum Press: New York, **1998**; pp. 1 - 7.

**8.** Balandrin, M. F., Kinghorn, A. D., Farnsworth, N. R., *Plant-Derived Natural Products in Drug Discovery and Development*. In *Human Medicinal Agents from Plants*; Balandrin, M. F., Kinghorn, A. D., Eds. American Chemical Society: Washington D. C., **1993**; pp. 2 - 12.

**9.** Triggle, D. J., *The Future of Medicinal Chemistry*. In *Perspectives in Medicinal Chemistry*; Testa, B., Kyburz, E., Fuhrer, W., Giger, R., Eds. Verlag Helvetica Chimica Acta: Basel, **1993**; pp. 3 - 12.

**10.** Harvey, A. L., *An introduction to drugs from natural products*. In *Drugs from Natural Products*; Harvey, A. L., Eds. Ellis Horwood Limited: Chichester, **1993**; pp. 1 - 6.

**11.** Foye, W. O., *Origins of Medicinal Chemistry*. In *Foye's Principles of Medicinal Chemistry*, 5th ed.; Williams, D. A., Lemke, T. L., Eds. Lippincott Williams and Wilkins: Philadelphia, **2002**; pp. 1 - 10.

**12.** Cordell, G. A., *Phytochemistry* **2000,** 55, 463 - 480.

**13.** Phillipson, J. D., *Phytochemistry* **2001,** 56, 237 - 243.

**14.** Gentry, A. H., *Tropical Forest Biodiversity and the Potential for New Medicinal Plants*. In *Human Medicinal Agents from Plants*; Balandrin, M. F., Kinghorn, A. D., Eds. American Chemical Society: Washington D. C., **1993**; pp. 13 - 24.

**15.** Mann, J., *Alkaloids*. In *Natural Products: Their Chemistry and Biological Significance*; Mann, J., Davidson, R. S., Hobbs, J. B., Banthorpe, D. V., Harborne, J. B., Eds. Longman: **1994**; pp. 389 - 446.

**16.** Drews, J., *Science* **2000,** 287, 1960 - 1964.

**17.** Schmeller, T., Wink, M., *Utilization of Alkaloids in Modern Medicine*. In *Alkaloids: Biochemistry, Ecology and Medicinal Applications*; Roberts, M. F., Wink, M., Eds. Plenum Press: New York, **1998**; pp. 435 - 459.

**18.** Tromans, A., *Nature* **2001,** 409, 28.

**19.** Conner, W. E., Boada, R., Schroeder, F. C., Gonzalez, A., Meinwald, J., Eisner, T., *PNAS* **2000,** 97, 14406 - 14411.

**20.** Dobler, S., Haberer, W., Witte, L., Hartmann, T., *J Chem Ecol* **2000,** 26, 1281 - 1298.

**21.** Dussourd, D. E., Ubik, K., Harvis, C. A., Resch, J., Meinwald, J., Eisner, T., *PNAS* **1988,** 85, 5992 - 5996.

**22.** Schneider, D., *Naturwissenschaften* **1992,** 79, 241 - 250.

**23.** Boppre, M., *Naturwissenschaften* **1986,** 73, 17 - 26.

**24.** Brown, K. S., *Nature* **1984,** 309, 707 - 709.

**25.** Dussourd, D. E., Harvis, C. A., Meinwald, J., Eisner, T., *PNAS* **1991,** 88, 9224 - 9227.

**26.** Schulz, S., Francke, W., Boppre, M., Eisner, T., Meinwald, J., *PNAS* **1993,** 90, 6834 - 6838.

**27.** Josephson, J., *Modern Drug Discovery* **2000,** May, 45 - 50.

**28.** Farnsworth, N. R., Bingel, A. S., *Problems and Prospects of Discovering New Drugs from Higher Plants by Pharmacological Screening*. In *New Natural Products and Plants Drugs with Pharmacological, Biological or Therapeutical Activity*; Wagner, H., Wolff, P., Eds. Springer-Verlag: New York, **1977**; pp. 1 - 22.

**29.** Phillipson, J. D., *Phytother Res* **1999,** 13, 2 - 8.

**30.** Waterman, P. G., *Chemical Taxonomy of Alkaloids*. In *Alkaloids: Biochemistry, Ecology and Medicinal Applications*, 1st ed.; Roberts, M. F., Wink, M., Eds. Plenum Press: New York, **1998**; p. 87

**31.** Mann, J., *Chemical Aspects of Biosynthesis*. 1st ed.; Oxford University Press: New York, **1994**.

**32.** Pengelly, A., *The Constituents of Medicinal Plants*. 1st ed.; CABI Publishing: Singapore, **2004**.

**33.** Cordell, G. A., Quinn-Beattie, M. L., Farnsworth, N. R., *Phytotherapy Research* **2001,** 15, 183 - 205.

**34.** Dewick, P. M., *Medicinal Natural Products: A Biosynthetic Approach*. 2nd ed.; Wiley: Chichester, **2001**.

**35.** Brielmann, H. L., *Phytochemicals: The Chemical Components of Plants*. In *Natural Products from Plants*; Kaufman, P. B., Cseke, L. J., Warber, S., Duke, J. A., Brielmann, H. L., Eds. CRC Press: Boca Raton, **1998**; pp. 1 - 36.

**36.** Maurer, B., Ohloff, B., *Helv Chim Acta* **1976,** 59, 1169 - 1176.

**37.** Wink, M., *A Short History of Alkaloids*. In *Alkaloids: Biochemistry, Ecology and Medicinal Applications*, 1st ed.; Roberts, M. F., Wink, M., Eds. Plenum Press: New York, **1998**; pp. 11 - 44.

**38.** Tursch, B., Daloze, D., Braekman, J. C., Hootele, C., Cravador, A., Losman, D., Karlsson, R., *Tetrahedron Lett* **1974,** 5, 409 - 472.

**39.** Schroder, F. C., Tolasch, T., *Tetrahedron* **1998,** 54, 12243 - 12248.

**40.** Laurent, P., Braekman, J. C., Daloze, D., Pasteels, J. M., *Tetrahedron Lett* **2002,** 43, 7465 - 7467.

**41.** Harvey, A., *Drug Discovery Today* **2000,** 5, 294 - 300.

**42.** Bindseil, K. U., Jakupovic, J., Wolf, D., Lavayre, J., Leboul, J., van der Pyl, D., *Drug Discovery Today* **2001,** 6, 840 - 847.

**43.** McChesney, J. D., *Biological and Chemical Diversity and the Search for New Pharmaceuticals and other Bioactive Natural Products*. In *Human Medicinal Agents from Plants*; Balandrin, M. F., Kinghorn, A. D., Eds. American Chemical Society: Washington D. C., **1993**; pp. 38 - 47.

**44.** O'Neill, M. J., Lewis, J. A., *The Renaissance of Plant Research in the Pharmaceutical Industry*. In *Human Medicinal Agents from Plants*; Balandrin, M. F., Kinghorn, A. D., Eds. American Chemical Society: Washington D. C., **1993**; pp. 48 - 55.

**45.** Lawrence, R. N., *Drug Discovery Today* **1999,** 4, 449 - 451.

**46.** Pietra, F., *Biodiversity and Natural Product Diversity*. 1st ed.; Elsevier Science: Amsterdam, **2002**.

**47.** Butler, M. S., *J Nat Prod* **2004,** 67, 2141 - 2153.

**48.** Williams, M., *Drug Design and Development: A Perspective*. In *Foye's Principles of Medicinal Chemistry*, 5th ed.; Williams, D. A., Lemke, T. L., Eds. Lippincott Williams and Wilkins: Philadelphia, **2002**; pp. 12 - 23.

**49.** Moore, P., *Superbugs: Rogue Diseases of the Twenty-First Century*. 1st ed.; Carlton Books Limited: London, **2001**.

**50.** Jarrott, B., *Chemistry in Australia* **2004,** April, 14 - 17.

**51.** Shu, Y.-Z., *J Nat Prod* **1998,** 61, 1053 - 1071.

**52.** Cragg, G. M., Newman, D. J., Snader, K. M., *J Nat Prod* **1997,** 60, 52 - 60.

**53.** Cordell, G. A., *Phytochem Rev* **2002,** 1, 261 - 273.

**54.** Newman, D. J., Cragg, G. M., Snader, K. M., *J Nat Prod* **2003,** 66, 1022 - 1037.

**55.** Lee, M.-L., Schneider, G., *J Comb Chem* **2001,** 3, 284 - 289.

**56.** Henkel, T., Brunne, R. M., Mueller, H., Reichel, F., *Angew Chem Int Ed* **1999,** 38, 643 - 647.

**57.** Tyler, V. E., *J Nat Prod* **1999,** 62, 1589 - 1592.

**58.** Proudfoot, J. R., *Bioorg Med Chem Lett* **2002,** 12, 1647 - 1650.

**59.** Heinrich, M., Teoh, H. L., *J Ethnopharm* **2004,** 92, 147 - 162.

**60.** Daly, J. W., *J Nat Prod* **1998,** 61, 162 - 172.

**61.** Angell, M., *The Truth About the Drug Companies*. 1st ed.; Random House: New York, **2004**.

**62.** Lee, K.-H., *J Nat Prod* **2004,** 67, 273 - 283.

**63.** Verpoorte, R., *Drug Discovery Today* **1998,** 3, 232 - 238.

**64.** Clark, A., *Natural Products*. In *Foye's Principles of Medicinal Chemistry*, 5th ed.; Williams, D. A., Lemke, T. L., Eds. Lippincott Williams and Wilkins: Philadelphia, **2002**; pp. 24 - 36.

**65.** Henderson, P. L., *Queensland Vascular Plants: Names and Distribution*; Queensland Herbarium: Brisbane, **1994**.

**66.** Personal communication G. Guymer (Queensland Herbarium).

**67.** Collins, D. J., Culvenor, C. C. J., Lamberton, J. A., Loder, J. W., Price, J. R., *Plants for Medicines: A Chemical and Pharmacological Survey of Plants in the Australian Region*. 1st ed.; CSIRO: Melbourne, **1990**.

**68.** Ray, A. B., Chand, L., Pandey, V. B., *Phytochemistry* **1979,** 18, 700 - 701.

**69.** Carroll, A. R., Arumugan, G., Quinn, R. J., Redburn, J., Guymer, G., Grimshaw, P., *J Org Chem* **2005,** 70, 1889 - 1892.

**70.** Johns, S. R., Lamberton, J. A., Sioumis, A. A., *Aust J Chem* **1969,** 22, 801 - 806.

**71.** Johns, S. R., Lamberton, J. A., Sioumis, A. A., *Chem Comm* **1968**, 410.

**72.** Johns, S. R., Lamberton, J. A., Sioumis, A. A., *Chem Comm* **1968**, 1324 - 1325.

**73.** Johns, S. R., Lamberton, J. A., Sioumis, A. A., Willing, R. I., *Aust J Chem* **1969,** 22, 775 - 792.

**74.** Johns, S. R., Lamberton, J. A., Sioumis, A. A., Wunderlich, J. A., *Chem Comm* **1968**, 290 - 291.

**75.** Johns, S. R., Lamberton, J. A., Sioumis, A. A., Suares, H., *Aust J Chem* **1971,** 24, 1679 - 1694.

**76.** Johns, S. R., Lamberton, J. A., Sioumis, A. A., Suares, H., Willing, R. I., *Chem Comm* **1970**, 804 - 805.

**77.** Johns, S. R., Lamberton, J. A., Sioumis, A. A., *Aust J Chem* **1969,** 22, 793 - 800.

**78.** Singh, R. K., Nath, G., *Phytother Res* **1999,** 13, 448 - 450.

**79.** Singh, R. K., Acharya, S. B., Bhattacharya, S. K., *Phytother Res* **2000,** 14, 36 - 39.

**80.** Hart, N. K., Johns, S. R., Lamberton, J. A., *Aust J Chem* **1972,** 25, 817 - 835.

**81.** Cseke, L. J., Kaufman, P. B., *How and Why These Compounds are Synthesized in Plants*. In *Natural Products from Plants*; Kaufman, P. B., Cseke, L. J., Warber, S., Duke, J. A., Brielmann, H. L., Eds. CRC Press: Boca Raton, **1998**; pp. 37 - 90.

**82.** Lamberton, J. A., Gunawardana, Y. A. G. P., Bick, I. R. C., *J Nat Prod* **1983,** 46, 235 - 247.

**83.** Bick, I. R. C., Gunawardana, Y. A. G. P., Lamberton, J. A., *Tetrahedron* **1985,** 41, 5627 - 5631.

**84.** Robertson, G. B., Tooptakong, U., Lamberton, J. A., Gunawardana, Y. A. G. P., Bick, I. R. C., *Tetrahedron Lett* **1984,** 25, 2695 - 2696.

**85.** Michael, J. P., Parsons, A. S., *Tetrahedron* **1996,** 52, 2199 - 2216.

**86.** Salim, A. A., Garson, M. J., Craik, D. J., *J Nat Prod* **2004,** 67, 54 - 57.

**87.** Wan, M., Bloor, S., Foo, L-Y., Loh, B-N., *Phytother Res* **1996,** 10, 589 - 595.

**88.** Niemeyer, H. M., *Biologically Active Compounds from Chilean Medicinal Plants*. In *Phytochemistry of Medicinal Plants*; Arnason, J. T., Mata, R., Romeo, J. T., Eds. Plenum Press: New York, **1995**; pp. 137 - 158.

**89.** Baker, M., *Amer J Primatology* **1996,** 38, 263 - 270.

**90.** Zhong, J., Zaiguo, L., Runqiu, H., *Nat Prod Rep* **2002,** 19, 454 - 476.

**91.** Zhong, J., *Nat Prod Rep* **2003,** 20, 606 - 614.

**92.** Elgorashi, E. E., Stafford, G. I., Van Staden, J., *Planta Med* **2004,** 70, 260 - 262.

**93.** Sener, B., Orhan, I., Satayavivad, J., *Phytother Res* **2003,** 17, 1220 - 1223.

**94.** Weniger, B., Italiano, L., Beck, J-P., Bastida, J., Bergonon, S., Codina, C., Lobstein, A., Anton, R., *Planta Med* **1995,** 61, 77 - 79.

**95.** Michael, J. P., *Nat Prod Rep* **2004**, 21, 625 - 649.

**96.** Molyneux, R. J., Gardner, D. R., James, L. F., Colegate, S. M., *J Chromatogr A* **2002**, 967, 57 - 74.

**97.** Chan, C., Cocker, J. D., Davies, H. G., Gore, A., Green, R. H., *Bioorg Med Chem Lett* **1996,** 6, 161 - 164.

**98.** Raub, M. F., Cardellina II, J. H., Spande, T. F., *Tetrahedron Lett* **1992,** 33, 2257 - 2260.

**99.** Fang, F. G., Danishefsky, S. J., *Tetrahedron Lett* **1989,** 30, 3621 - 3624.

**100.** Clive, D. L. J., Coltart, D. M., *Tetrahedron Lett* **1998,** 39, 2519 - 2522.

**101.** Yoshida, W. Y., Scheuer, P. J., *Heterocycles* **1998,** 47, 1023 - 1027.

**102.** Kim, G., Chu-Moyer, M. Y., Danishefsky, S. J., Schulte, G. K., *J Am Chem Soc* **1993,** 115, 30 - 39.

**103.** Gorman, J. S. T., Jones, T. H., Spande, T. F., Snelling, R. R., Torres, J. A., Garraffo, H. M., *J Chem Ecol* **1998,** 24, 933 - 943.

# CHAPTER 2 – Phytochemical Evaluation of Plants from the Family Elaeocarpaceae for Alkaloids

## 2.1 Introduction

The chemical screening of Australian plants for alkaloids was started by the CSIRO in the early 1940's.[1] The aim of this study was to identify new medicinal drugs and to investigate plants which are toxic to livestock.[2] The discovery of plants which produced alkaloids was the primary focus of the phytochemical survey, as alkaloids were considered to be medicinally important.[1] Over a 25 year period, this phytochemical survey evaluated more than 4000 species of higher plants. As a result, approximately 500 alkaloids were identified, including 200 new alkaloids.[3] Initial efforts of the survey were focused on plants from the rainforests of Queensland and northern New South Wales. Early testing indicated these regions produced a greater percentage of alkaloid containing species.[1] In 1963, the survey began the screening of plants from PNG, with a total of 2250 species screened for alkaloids. Among the plants identified by this survey as alkaloid containing were the five previously investigated New Guinean species of *Elaeocarpus*, and *Peripentadenia mearsii* from north Queensland. Extracts of *E. grandis* and *E. johnsonii* from Queensland were also reported to give positive alkaloid tests,[4] however these species were not chemically investigated during the survey.

The Australian phytochemical survey evolved from the success of a WWII project to discover new species which produced the alkaloid hyoscyamine (**99**). In 1878 two Australian species, *Duboisia myoporides* and *D. leichardtii,* were found to contain this alkaloid.[5] This discovery proved to be vital to the Australian Defence Forces Medical Equipment Control Committee (MECC), which made a list of essential drugs in 1940. Research efforts then focused on the production of these drugs locally, as established European sources of hyoscyamine (**99**) (*Atropa* and *Hyoscyamus* spp) were expected to

be compromised. The chemical company Drug Houses of Australia produced the required amount of hyoscyamine (**99**) to treat all of the D-Day landing troops for motion sickness.[5] In the late 1940's, the MECC approached the CSIRO to investigate other Australian plants for potential medicinal agents including alkaloids, saponins and cyanogenetic glycosides.[2] The importance of the CSIRO plant industry is still evident today in Tasmania where *Papaver somniferum* is cultivated and provides approximately 40% of the total legal worldwide production of medicinal opiates.[6]

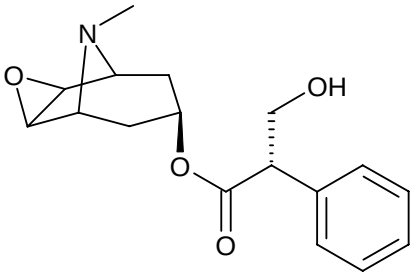


**99**

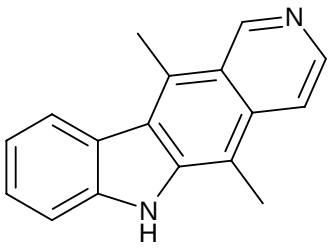


**100**

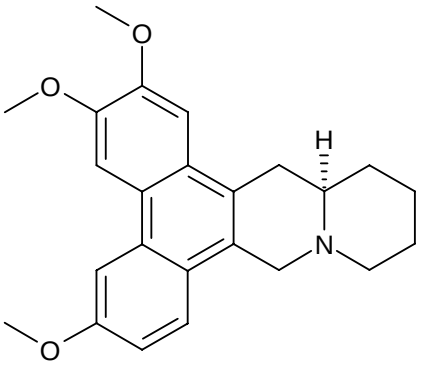


**101**

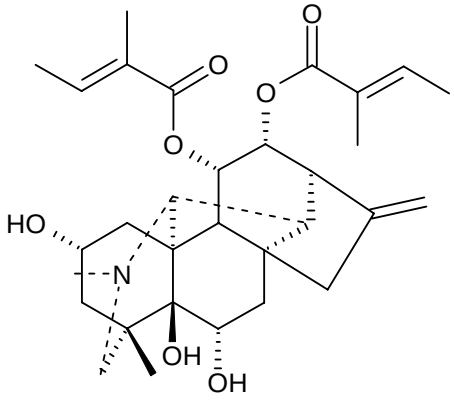


**102**

Examples of alkaloids isolated from plants identified in the alkaloid survey include several alkaloids with antitumour activities, such as ellipticine (**100**) from *Bleekeria coccinea* and *Ochrosia moorei* (Apocynaceae), cryptopleurine (**101**) from *Cryptocarya pleurosperma* (Lauraceae) and anopterine (**102**) from *Anopterus macleayanus* (Escaloniaceae).[1] Other alkaloids of medicinal value obtained from the survey included himbacine (**103**) from *Galbulimima belgraveana*, which shows hypotensive and anticonvulsant activity. Several alkaloids of unique structure were also encountered. These included the morphine-like alkaloid (+)-kreysiginine (**104**), which was isolated

from two Queensland species of the family Liliaceae, and the sulphur-containing indole and tropane alkaloids 4-methylthiocanthinone (**105**) and brugine (**106**), from *Pentaceras australis* (Rutacaeae) and *Bruguiera sexangula* (Sapotaceae), respectively. Several structurally complex alkaloids were discovered including himbosine (**107**), which was isolated from *Galbulimima belgraveana*, and hoveine (**108**) from *Hovea longipes*. Novel ring systems were also encountered in the structure of glochidicine (**109**), from the New Guinean plant *Glochidion philippicum* (Euphorbiaceae).[1] The plant *Ficus pantoniana* (Moraceae) was found to produce the first known flavonoidal alkaloids, of which ficine (**110**) is an example. The survey also identified several species that were toxic to livestock, many of which contained hepatotoxic pyrrolizidine alkaloids, of which jacobine (**111**) is an example.

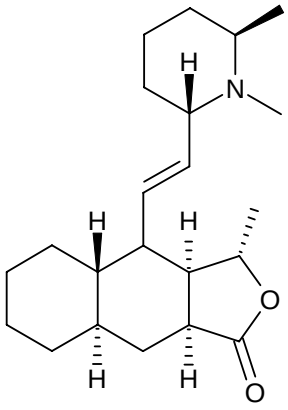


**103**

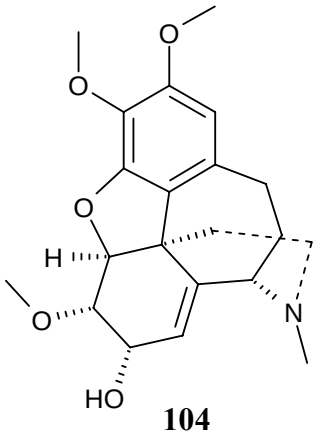


**104**

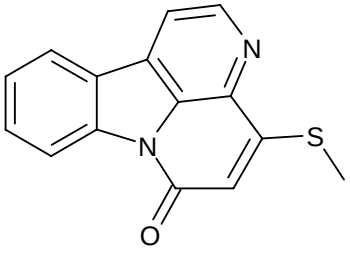


**105**

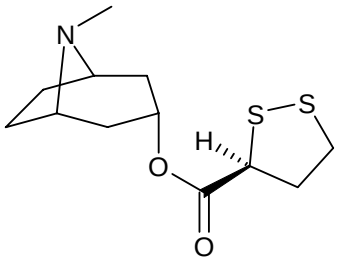


**106**

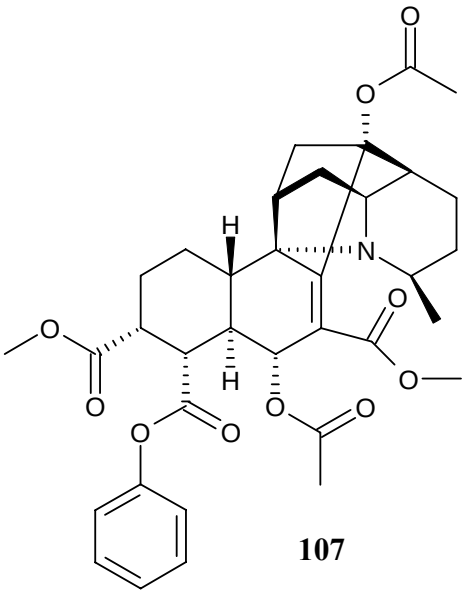

**107**

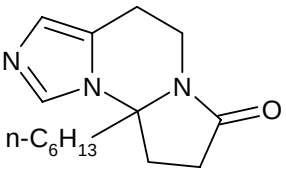

**109**

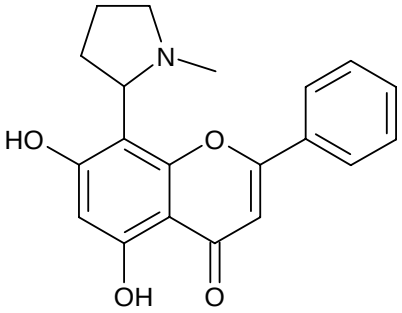

**110**

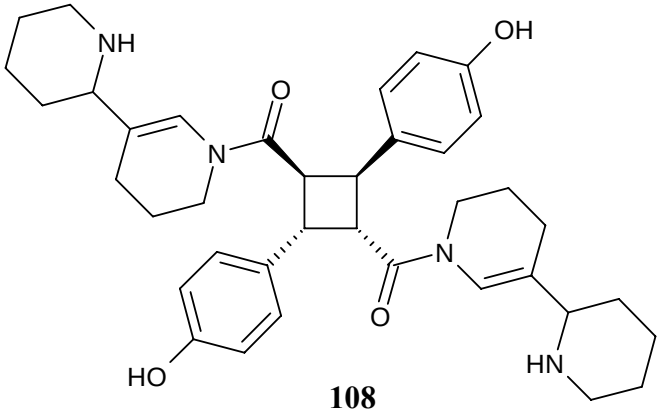

**108**

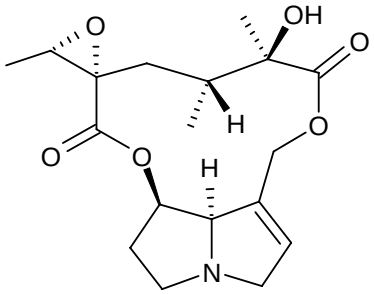

**111**

A phytochemical survey for alkaloids is therefore a rapid method of identifying alkaloid containing species from a large number of unknown or previously uninvestigated species. The results can direct chemical investigations toward alkaloid positive species.

## 2.2 Procedure of the CSIRO Phytochemical Survey

The survey for alkaloids operated on the principle of an alkaloid field test. The Culvenor and Fitzgerald alkaloid field test was employed in the survey.[1, 7] Up to four grams of leaves or soft stems were ground in a mortar and pestle and extracted with ammoniacal chloroform, which was partitioned with dilute sulphuric acid. An aliquot of the aqueous layer was then mixed with Mayer's reagent and silicotungstic acid, which are alkaloid testing reagents. In the case of a positive test, a precipitate is formed upon mixing the extract and the reagent. The density of the precipitate gives an estimate of the alkaloid content of the plant.[7]

Alkaloid detecting reagents are solutions of the salts of heavy metals. The most common reagents are Mayer's (potassium mercuric iodide), Ecolle's (silicotungstic acid), and Dragendorff's (potassium iodide-bismuth nitrate).[1, 8] The mechanism of action is proposed to occur via coupling of the reagent's heavy metal atom in the reagent with the nitrogen in the alkaloid to form ion pairs. The ion pairs from the insoluble precipitate. Using Dragendorff's reagent as an example, a reaction occurs between $BiI_4^-$ and the alkaloid as depicted in Figure 13.[9]

$$\text{alkaloid} + BiI_4^- \rightarrow (\text{alkaloid}^+)_n\,(BiI_4^-)_n$$

**Figure 13.** The interaction of bismuth tetraiodide with the nitrogen atom of an alkaloid.

The precipitating complex of Dragendorff's reagent, $BiI_4^-$, was determined by indirect flame atomic absorption spectrometry.[9] Dragendorff's reagent usually forms an orange-red coloured complex following reactions with alkaloids, although a range of colours have been observed from yellow/orange, red/black and pink to purple depending on the species or genus.[10] Studies on false-positive alkaloid tests using Dragendorff's reagent were found to result from reactions with nitrogenous (e.g. peptides) or non-nitrogenous

plant constituents. All non-nitrogenous compounds that were found to give strong positive reaction with the reagent were compounds containing oxygen.[11] The preferred method to rapidly remove non-nitrogenous metabolites from the extract is to perform an acid-base extraction followed by retesting of the extract.[10] The Culvenor-Fitzgerald method employs an acid-base extraction to ensure non-nitrogenous contaminants are limited. However, some limitations still apply. Glycosidal alkaloids and other very water soluble bases such as castanospermine (**90**) may not be extracted into chloroform. Alkaloids such as castanospermine are typically extracted with 25-50% aq. methanol/ethanol solutions and are separated from the extract via ion exchange chromatography.[12] Weak bases such as *N*-oxides, quaternary alkaloids and alkaloidal amides may not be detected. Also, if ammonia is used in the test, either in an acid-base or ammoniacal chloroform extraction, the ammonia can react with a non-basic constituent, giving rise to a basic product which is responsible for a positive test result.[1]

Phytochemical surveys can focus on species involved in ethnopharmacology, chemotaxonomy or chemical ecology.[13] The distribution of secondary metabolites is not random, therefore chemotaxonomic investigations directed at searching species within the same genera, or examining closely related species can yield a variety of secondary metabolites. Chemical ecology investigates the biochemical response of an organism to an environmental stimulant. This approach can increase the chances of identifying novel and bioactive secondary metabolites from a phytochemical survey. The ethnopharmacology approach was used by Coe and Anderson in a survey of the medicinal plants used by the Garifuna tribe of eastern Nicaragua for compounds of biological importance.[10] In a study of 229 species, 72% of the species tested positive for alkaloids with Dragenorff's reagent, emphasizing their biological importance.

## 2.3 Procedure and Results of the Phytochemical Survey of the Plants of the Family Elaeocarpaceae

Plants assessed for alkaloid content in this survey were selected on a chemotaxonomic basis, with a focus on species from the genus *Elaeocarpus*. The survey consisted of all available plant parts of the Elaeocarpaceae from Queensland, PNG and China in the Natural Product Discovery ground plant sample collection located at Griffith University. Dragendorff's reagent was used as the alkaloid detecting reagent in the survey with positive ESIMS as a selection tool. Individual plants parts were extracted with methanol. The extracts were evaporated to dryness, dissolved in 1M $H_2SO_4$ and partitioned twice with DCM. The pH of the aqueous layer was adjusted to pH 10 with $NH_3$. The basic aqueous layer was partitioned with DCM. The organic layer was evaporated and then dissolved in methanol and an aliquot was tested with Dragendorff's reagent. Appendix I lists all of the species tested. Table 1 represents all of the Dragendorff positive species in Queensland. For many of the species there were multiple collections and each collection is represented by the five-digit species-location code provided by the Queensland Herbarium. Table 2 lists the Dragendorff positive plant parts from PNG and China. Positive ESIMS was used as a secondary method to confirm the presence of alkaloids.

A total of 339 discrete plant parts were chemically screened. Eighteen leaf samples produced positive tests with Dragendorff's reagent, and only ten of these samples confirmed the presence of alkaloids by positive ESIMS. *E. grandis* and *P. mearsii* were the only two species from Queensland to produce a positive Dragendorff test and mass ion peaks in the positive ESIMS. This highlighted these species for further chemical investigations. Several species from PNG also showed the same result including all of the previously investigated species of *Elaeocarpus* from PNG in addition to two new species, *E. fuscoides* and *E. habbeniensis*. Chemical investigations of the alkaloid positive species of New Guinean *Elaeocarpus* have focused on these new species. The previously investigated species, *E. polydactylus, E. sphaericus, E. densiflorus* and *E. dolichostylus* were extracted and chromatographed, however significant amounts of pure compounds from these extract could not be obtained. Inspection of fractions revealed the same compounds that were later purified from *E. fuscoides*. *E. kaniensis* was also extracted, however alkaloids were lost during HPLC purification. No species of Elaeocarpaceae from China produced positive Dragendorff and positive ESIMS results.

**Table 1.** The Dragendorff positive extracts of species of Elaeocarpaceae from Queensland.[a] The five-digit species-location code was provided by the Queensland Herbarium.

| **Genus** | **Species** | **Plant parts** | **Alkaloid +** | ***m/z*** |
|---|---|---|---|---|
| *Aceratium* | *megalospermum* | 15560: St, M | M | |
| | | 23963: B, R, St, HW | - | |
| *Elaeocarpus* | *grahamii* | 21847: L, B, St, HW, M | M | |
| | *grandis* | 02031: Se, L, St | L | 260 |
| | | 21918: Se, L, B, St, HW, M | St , M | |
| | | 25523: L, B, St, HW | L, St | 260 |
| | *ruminatus* | 18113: Se, L, B, St | Se | |
| | | 22932: L, St | - | |
| | *sericopetalus* | 21909: Se, L, B, St, HW | Se | |
| | | 21871: B, St, M | - | |
| | sp. (Mt. Lewis | 17264: L, St | - | |
| | B.P.Hyland 2907) | 22897: Se, L, B, St, HW, M | L | |
| *Peripentadenia* | *mearsii* | 23959: L, Se, B, St | L, B, Se | 377 |
| *Sloanea* | *australis* | 00076: F, L, St | L, St | |
| | | 25905: L, B | - | |
| | | 25732: B, St | - | |
| | *macbrydei* | 18116: L, B, St | - | |
| | | 24058: L, Se, R, St, HW | Se, St | |
| | *woollsii* | 00224: Se | Se | |
| | | 00048: F, L, St | - | |

[a] See footnote on Table 2.

**Table 2.** The Dragendorff positive extracts of species of Elaeocarpaceae from PNG and China.[a]

| **Genus** | **Species** | **Location** | **Plant part** | **Alkaloid +** | ***m/z*** |
|---|---|---|---|---|---|
| *Dubouzetia* | *galorii* | PNG | L, B | L | |
| *Elaeocarpus* | *chiangiana* | China | B | B | |
| | *culminicola warb.* | PNG | L, B, St | L | |
| | *densiflorus* | PNG | L, B, R, Se | L, Se | 258 |
| | *dolichostylus* | PNG | L, R, St | L | 258 |
| | *dubia* | China | L, Fr | Fr | |
| | *fuscoides* | PNG | L, B, R | L | 258 |
| | *habbeniensis* | PNG | L, R | L | 280 |
| | *kaniensis* | PNG | L, B | L, B | 196 |
| | *lingualis* | PNG | L, B, Se | Se | |
| | *poculiferus* | PNG | L, B, R, Se | Se | |
| | *polydactylus* | PNG | L, B, R, St | L | 258 |
| | *ptilanthus* | PNG | L | L | |
| | *sphaericus* | PNG | L, B, R, HW | L | 258 |
| | *sylvestris* | China | B, R | R | |
| *Sloanea* | *arberrans* | PNG | L, R, B, St | L | |
| | *tieghemii* | PNG | L, R | L | |

[a] L = leaves; B = bark; R = roots; Se = seeds; St = stem; HW = heartwood; M = mix of plant parts (leaves, stem and bark); Fr = fruit; F = flower

## 2.4 Investigation of *Sloanea tieghemii*

### *2.4.1 The Isolation of 112 and 113*

The leaves of *S. tieghemii* were found to give a positive Dragendorff test, however no mass ion peaks were observed in the positive ESIMS. This suggested that a non-nitrogenous compound produced a reaction with the reagent. Leaves of *S. tieghemii* were extracted with methanol. The extract was filtered through PAG and evaporated. The residue was partitioned between DCM and $H_2O$. The aqueous layer was found to give a positive Dragendorff's test and was filtered through SCX resin. A load fraction was obtained and the SCX was washed with $H_2O$ before elution with NaCl. Testing of the NaCl eluted fraction yielded a negative result, however the load fraction produced a positive test. The SCX load fraction was evaporated and separated by C18 RP-MPLC, using a gradient of $H_2O$ to MeOH over 120 minutes and collecting 70 fractions. Fractions 37 to 47 were found to produce positive Dragendorff's tests and were combined. The negative ESIMS produced mass ion peaks of 689 and 691. The $^1H$ NMR spectra of these fractions revealed polyphenolic compounds. The combined fraction was separated into 50 fractions by isocratic C18 RP-HPLC with conditions of 1:4 $H_2O$:MeOH. Fractions 33, 34, 39 and 40 were found to give positive Dragendorff tests. Negative ESIMS revealed mass ion peaks of *m/z* 689 and 691 in fractions 33 – 34 and 39 – 40, respectively. The structures of two new compounds **112** and **113** were elucidated by 2D NMR from fractions 33 - 34 (30.6 mg, 0.038%) and 39 - 40 (28.6 mg, 0.036%), respectively.

Both **112** and **113** are small tannins, and were found to produce precipitates with Dragendorff's reagent at 0.1875 mg/mL. Their mechanism of action with Dragendorff's reagent is unknown. The conclusion drawn from these results was that Dragendorff positive extracts which did not yield a mass ion peak in the positive ESIMS should not be investigated, as non-nitrogenous metabolites may be present.

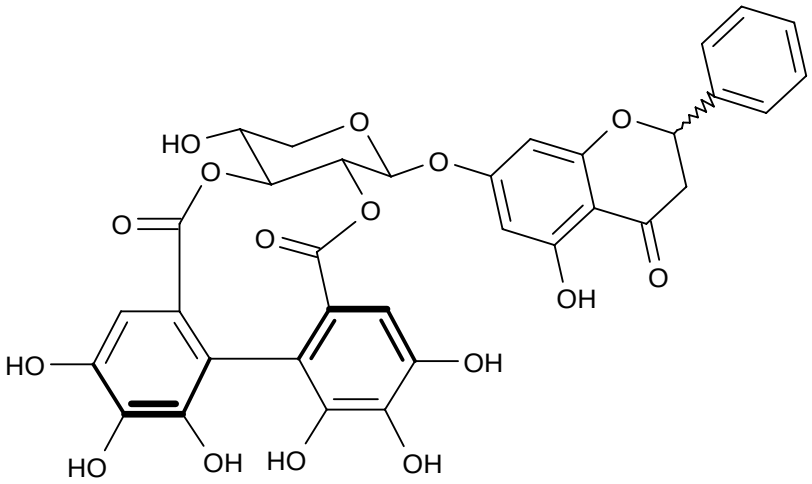

**112**

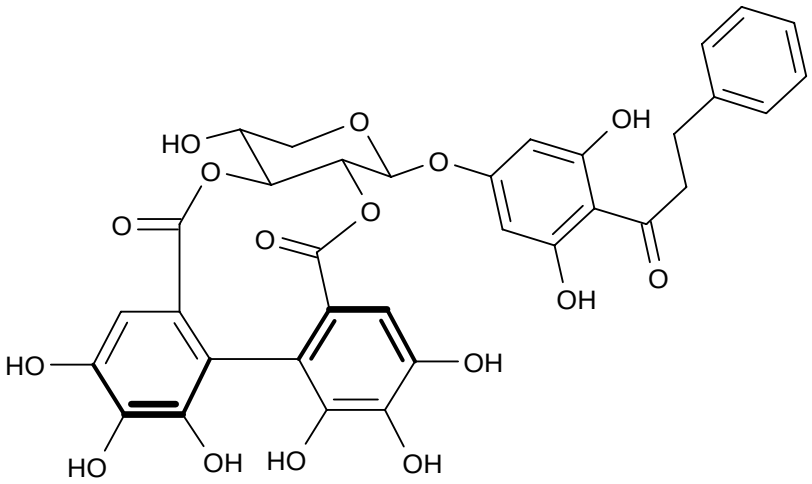

**113**

### *2.4.2 Structure Elucidation of 112*

The proton NMR spectra of **112** is represented in Figure 14. Resonances at δ 7.38 (1H, dd), 7.43 (2H, dd) and 7.51 (2H, d) in the $^{1}$H NMR spectrum of **112** indicated that a pendant or mono-substituted aromatic group was present. Four other downfield protons, all singlets, were observed in the $^{1}$H NMR spectrum of **112**, at 6.23, 6.27, 6.29 and 6.44 ppm. Interpretation of the HSQC spectrum revealed that these protons were bound to carbons at δ 96.6, 105.2, 95.5, and 104.7 ppm (Figure 15), respectively. The chemical shifts of these carbons at ~105 ppm suggested that they were *ortho* to an oxygenated

quaternary aromatic carbon. However, the carbons observed at ~95 ppm are consistent with carbons *ortho* to two oxygenated aromatic carbons.

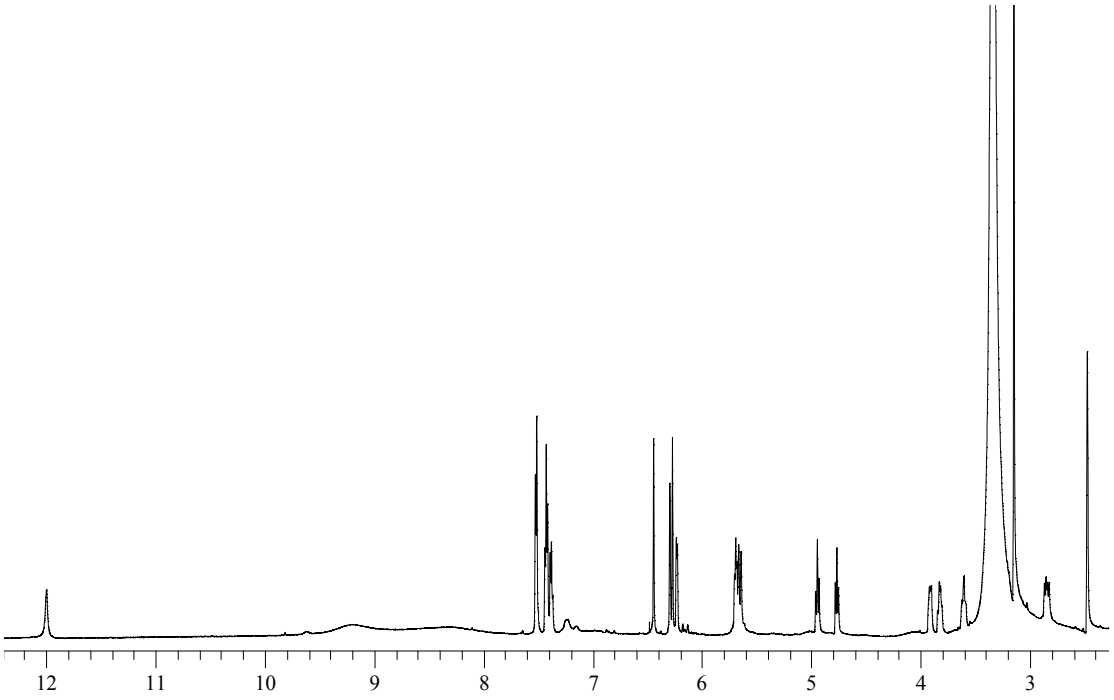


**Figure 14.** The $^{1}$H NMR spectrum of **112** at 500 MHz in $d_6$-DMSO.

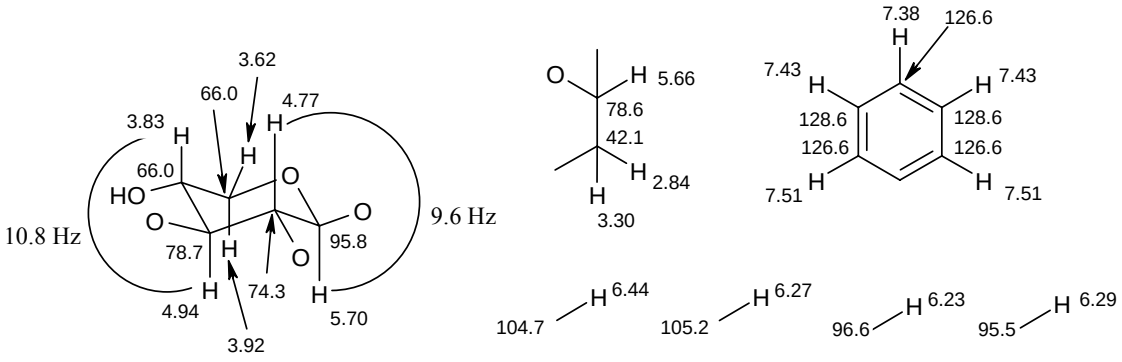


**Figure 15.** The partial structures of **112** established from COSY and HSQC spectra.

COSY experiments were used to establish the partial structures of **112** (Figure 15). The COSY spectrum of **112** displayed correlations from the oxygenated methine at 3.83 (H-4) to the oxygenated methylene (H-3) and the methine (H-5), which resonated at 3.62/3.92 and 4.94 ppm, respectively. COSY correlations were observed from H-22 (4.77 ppm) to H-5 and H-1 (5.70 ppm), which indicated that H-22 was adjacent to the oxygenated

methines H-1 and H-5. This completed the five carbon partial structure of **112**. Correlations in the HSQC spectrum of **112** demonstrated the attachment of all of these protons to oxygenated carbons. H-1 was shown to be bound to a carbon at 95.8 ppm (C-1), which is typical for an anomeric carbon. This also suggested that the five carbons of this partial structure formed the carbon skeleton of sugar moiety. Other correlations in the COSY spectrum of **112** enabled the connection of $CH_2$-31 to CH-32 as correlations were observed from the proton at 5.66 (H-32) to the protons at 2.84 (H-31a) and 3.30 (H-31b) ppm. Interpretation of the HSQC spectrum confirmed that the proton at 5.66 ppm was attached to an oxygenated carbon at 78.6 ppm, and the protons at 2.84 and 3.30 were attached the a methylene carbon at 45.2 ppm.

COSY correlations also confirmed the structure of the mono-substituted aromatic group in **112**. COSY correlations from the proton at 7.43 (H-35/37) to the protons at 7.51 (H-34/38) and 7.38 (H-36) enabled the construction of the phenyl moiety.

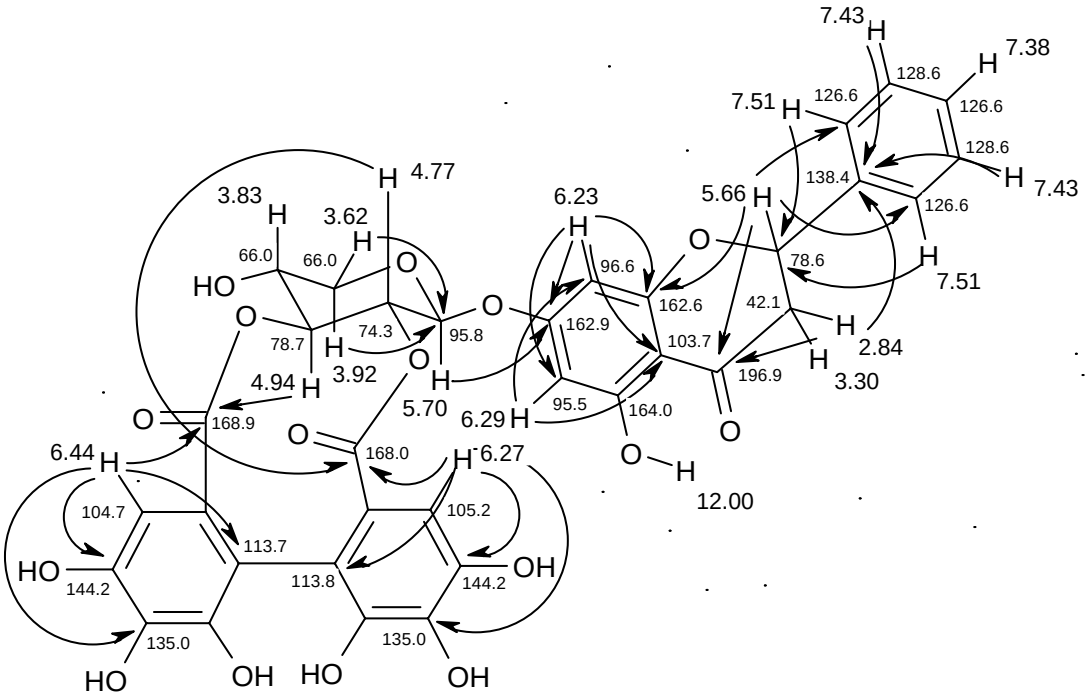


**Figure 16.** The connections of the partial structures of **112** established from HMBC spectra.

The partial structures in Figure 15 accounted for 16 carbons and 18 hydrogens in **112**. A total of 34 carbons were observed in the $^{13}C$ spectrum of **112**. This indicated that there were 18 quaternary carbons in **112**. Key HMBC correlations (Figure 16) were used to establish the connections of the partial structures of **112**.

The structure of the mono-substituted aromatic ring in **112** was secured by $^{3}J_{CH}$ correlations from H-35/37 (7.43) to a quaternary carbon at 138.4 ppm (C-33). Further three bond correlations from H-34/38 (7.51) to C-32 (78.6), from H-32 (5.66) to C-34/38 (126.6) and from H-31 (2.84/3.30) to C-33, indicated that the C-31-32 partial structure substituted the aromatic ring at position 33. HMBC correlations from H-31 and H-32 to a carbonyl carbon at 196.6 ppm (C-30) demonstrated that a ketone was adjacent to the H-31 methylene. Intense HMBC correlations were observed from the aromatic protons at 6.23 (H-25) and 6.29 (H-29) to C-29 (95.5) and C-25 (96.6), respectively. Both protons also displayed correlations to the quaternary carbon C-27 at 103.7 ppm. This indicated that C-27 was three bonds away from both H-25 and H-29, and that these protons were *meta* to each other. These interpretations secured the structure of a 1,3,4,5-tetra-substituted aromatic system. The establishment of an ether linkage between C-32 and C-26 was confirmed by HMBC correlations from H-32 to C-26 (162.6) and from H-25 to C-26. The connection of C-27 to C-30 was established from a correlation from H-31 to C-27. The structure of the flavanoid section of **112** was thus deduced. The chemical shift of C-27 was typical for a carbon which is alpha to three oxygenated carbons. The structure of the sugar moiety was deduced from HMBC correlations from H-3 (3.62/3.92) to the anomeric carbon C-1. HMBC correlations were observed from H-25 and the anomeric proton H-1 (5.70) to the quaternary aromatic carbon at 162.9 (C-24). This established the connection of the pentopyranose and flavanoid moieties via an ether link between C-1 and C-24. The protons H-5 (4.94) and H-22 (4.77) each displayed HMBC correlations to two different carbonyl carbons. These carbons were C-7 (168.9) and C-20 (168.0), respectively. This indicated that ester groups were attached via their oxygens to C-5 (78.7) and C-22 (74.3). HMBC correlations were observed from the two remaining aromatic protons, H-9 (6.44) and H-18 (6.27), to C-7 and C-20, respectively. This indicated that H-9 was three bonds away from C-7, and H-18 three bonds away from C-

20. Each of these protons displayed three other HMBC correlations to two oxygenated aromatic carbons and a quaternary aromatic carbon. Using H-18 as an example, these carbons were C-16 (135.0), C-17 (144.2) and C-14 (113.8).

Four carbons in the $^{13}C$ spectrum of **112**, at 124.1, 124.8 and two at 144.8 ppm, remained unassigned. C-8, C-19, C-12 and C-15 could not be assigned from HMBC correlations, however C-8 and C-19 are most likely the carbons at 124.1 and 124.8 ppm. This hypothesis is consistent with the published $^{13}C$ data of combreglutinin in acetone (**iii** in Figure 22). This data lists the carbons of the hexahydroxyphenoyl moiety alpha to the ester group at 126.1 and 123.9 ppm.[14] The remaining two carbons at 144.8 ppm can therefore be assigned as C-12 and C-15. This is also consistent with the published data.[14] The chemical shifts of these carbons suggested they were oxygenated. The resulting structure accounted for all but 8 Da. of the molecular weight of **112**. This indicated all eight oxygens attached to C-4, C-10-12, C-15-17, and C-28 were hydroxyls, and indicated there was a bond between C-13 and C-14. This secured the structure of the hexahydroxybiphenoyl system and thus the structure of **112** was established. The $^{1}H$, $^{13}C$ and HMBC NMR spectral data of **112** is detailed in Table 3.

Large coupling constants were observed for H-1, H-4, H-5 and H-22 in **112** (Figure 15). This demonstrated that these protons were all axial. The coupling constants of H-$31_{ax}$ (2.84) in **112** were 9.0 and 16.0 Hz. These large couplings can be attributed to axial and geminal couplings, respectively, therefore indicating that H-32 in **112** was also axial. The coupling constants of H-32 (3.0 and 13.2 Hz) are consistent for axial-equatorial (H-32/H-$31_{eq}$) and axial-axial (H-32/H-$31_{ax}$) couplings, respectively.

Inspection of the $^{13}C$ NMR spectrum of **112** revealed doubling of certain signals. In particular, two resonances were observed in a 1:1 ratio at δ 42.1, 138.4, 144.2, and 144.8 ppm with a less then 0.01 ppm difference in chemical shift. All other carbons were coincident. The doubling of certain signals was also evident in the $^{1}H$ NMR spectrum.

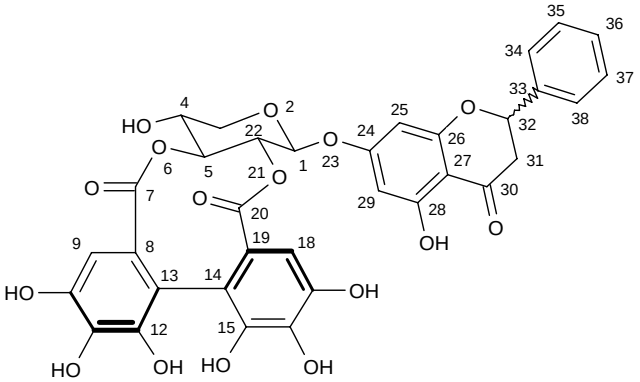

**Table 3.** $^{1}$H,[a] $^{13}$C[b] and HMBC NMR spectral data of **112**.[c]

| position | $\delta_C$ | $\delta_H$ (mult; *J* in Hz) | HMBC $^{2,3}J_{CH}$ |
|---|---|---|---|
| 1 | 95.8 | 5.70 (1H, d, 9.6) | 24 |
| 3 | 66.0 | 3.62 (1H, ddd, 4.2, 4.2, 12.6)<br>3.92 (1H, dd, 6.0, 13.8) | 1, 4, 5 |
| 4 | 66.0 | 3.83 (1H, ddd, 6.6, 10.8, 10.8) | 3, 5 |
| 5 | 78.7 | 4.94 (1H, dd, 9.6, 9.6) | 1, 3, 4, 7, 22 |
| 7 | 168.9 | - | - |
| 8 | 124.1 | - | - |
| 9 | 104.7 | 6.44 (1H, s) | 7, 10, 11, 13 |
| 10/17 | 144.2 | - | - |
| 11/16 | 135.0 | - | - |
| 12/15 | 144.8 | - | - |
| 13 | 113.7 | - | - |
| 14 | 113.8 | - | - |
| 18 | 105.2 | 6.27 (1H, s) | 14, 16, 17, 20 |
| 19 | 124.8 | - | - |
| 20 | 168.0 | - | - |
| 22 | 74.3 | 4.77 (1H, dd, 9.0, 9.0) | 1, 5, 20 |
| 24 | 162.9 | - | - |
| 25 | 96.6 | 6.23 (1H, s) | 24, 26, 27, 29 |
| 26 | 162.6 | - | - |
| 27 | 103.7 | - | - |
| 28 | 164.0 | - | - |
| 29 | 95.5 | 6.29 (1H, s) | 24, 25, 27 |
| 30 | 196.9 | - | - |
| 31 | 42.1 | 2.84 (1H, dd, 9.0, 16.0); 3.30 (1H, m) | 29, 30, 33; 30, 32, 33 |
| 32 | 78.6 | 5.66 (1H, dd, 3.0, 13.2) | 26, 30, 31, 33, 34, 38 |
| 33 | 138.4 | - | - |
| 34/38 | 126.6 | 7.51 (2H, d, 7.2) | 32, 34/38, 35/37, 36 |
| 35/37 | 128.6 | 7.43 (2H, dd, 6.6, 7.2) | 33, 35/37 |
| 36 | 126.6 | 7.38 (1H, dd, 6.6, 6.6) | 34/38 |
| C-28-OH | - | 12.00 (1H, brs) | - |

[a] At 600 MHz. [b] At 125 MHz. [c] In $d_6$-DMSO.

The proton, H-$31_{ax}$, was observed as two distinct doublet of doublets with identical coupling at δ 2.84 and 2.88 ppm, respectively. Doubling of the aromatic protons, H-25 and H-29, was also noted. These protons resonated at δ 6.23 and 6.25 ppm, and δ 6.29 and 6.30 ppm, respectively. All of these protons resonated as doublets with a coupling of 2.4 Hz. This coupling is a *meta* coupling between H-25 and H-29. The anomeric proton, H-1, was also observed as two doublets. These doublets, both 9.6 Hz, were observed at δ 5.70 and 5.72 ppm. All other protons were coincident. The same coupling constant determined for each of the anomeric protons suggested that **112** was not a mixture of anomers. Therefore, it can be concluded that **112** was present as a 1:1 mixture of diastereomers. This conclusion may provide evidence for the formation of **112** from a chalcone precursor (Figure 17). The Michael addition of a phenoxide ion to an α,β-unsaturated ketone in the chalcone precursor would yield the flavone moiety encountered in **112**. The resulting flavone would also be isomeric at the position beta to the ketone as the addition of the phenoxide ion can occur from either side of the double bond.

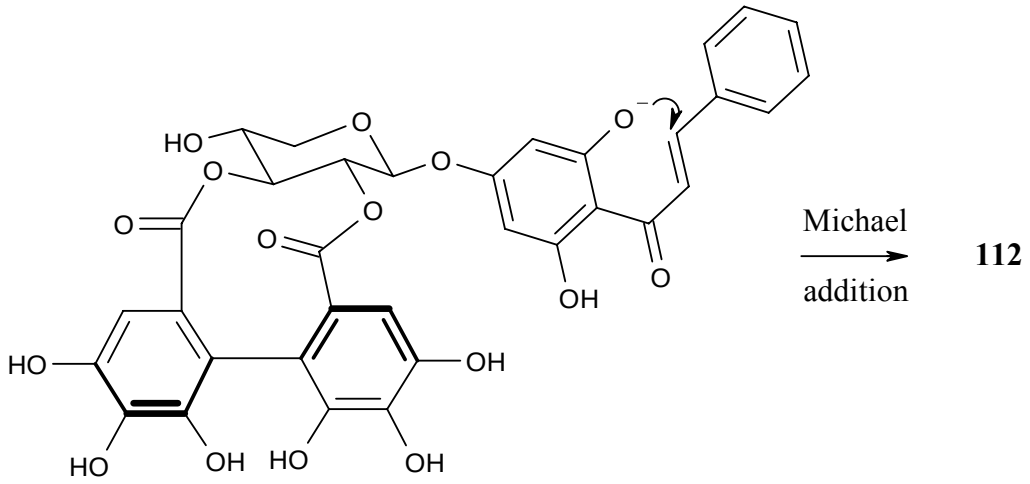


**Figure 17.** The proposed formation of **112** from a chalcone precursor via a Michael addition.

### *2.4.3 Structure Elucidation of 113*

The proton NMR spectra of **113** (Figure 18) displayed similar characteristics to the proton NMR spectrum of **112.** The $^{1}$H NMR spectrum of **113** demonstrated the same resonances consistent with a pendant aromatic group. These protons were observed at 7.16 (1H, dd), 7.24 (2H, dd), 7.26 (2H, d).

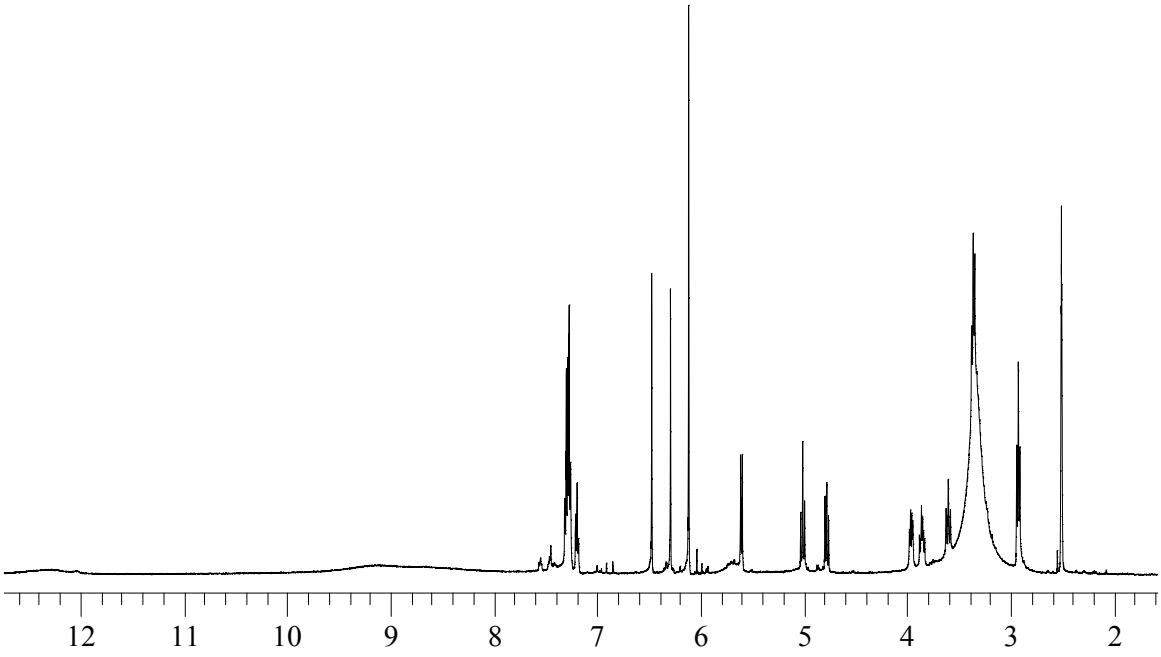


**Figure 18.** The $^{1}$H NMR spectrum of **113** at 500 MHz in $d_6$-DMSO.

The proton NMR spectrum of **113** also revealed four downfield protons, however only three singlets were observed, compared to four in the $^{1}$H NMR spectrum of **112**. One singlet, at 6.08, was equivalent to two protons and the remaining two singlets resonated at 6.26 and 6.44 ppm. Correlations observed in the HSQC spectrum of **113** indicated that both protons at 6.08 were attached to carbons at 95.1 and the other protons were bound to carbons at 105.8 and 105.2 ppm (Figure 19), respectively.

The protons between 3 and 6 ppm in both spectra were identical in multiplicity to the corresponding protons in the $^{1}$H NMR spectrum of **112**. However, slight differences in chemical shift were noted. The only differences between the spectra in this region were a doublet of doublets observed at 5.66 ppm in the $^{1}$H NMR spectrum of **112**, whereas this

proton was not observed in the $^{1}$H NMR spectrum of **113**. An extra proton was observed at 2.89 ppm (2H, t) in the proton spectrum of **113**, compared with a single proton at 2.84 ppm (1H, dd) in the $^{1}$H NMR spectrum of **112**.

Correlations observed in the COSY spectrum of **113** (Figure 19) enabled the construction of an identical five carbon fragment as for **112**. The carbon and proton chemical shifts between these two fragments in **112** and **113** were almost identical. The same connection in **113** between C-31 and C-32 was deduced from COSY correlations from a methylene at 2.89 (H-32) to another methylene at 3.33 (H-31). Correlations observed in the HSQC spectrum confirmed these protons were attached to carbons at 29.9 and 45.2 ppm, respectively. COSY correlations from the proton at 7.24 (H-35/37) to the protons at 7.26 (H-34/38) and 7.16 (H-36) confirmed the structure of the mono-substituted aromatic group **113**.

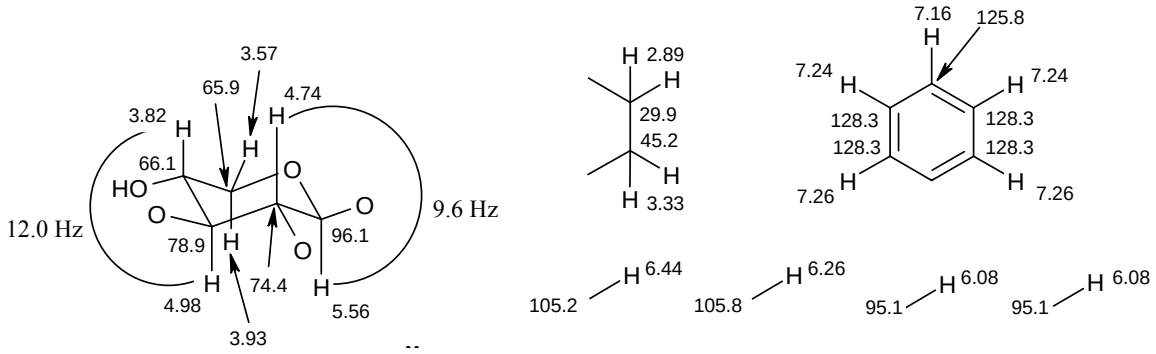


**Figure 19.** The partial structures of **113** established from COSY and HSQC spectra.

The partial structures in Figure 18 accounted for 16 carbons and 19 hydrogens in **113**. A total of 34 carbons were observed in the $^{13}$C spectrum. This indicated that there were 18 quaternary carbons in each molecule. Key HMBC correlations (Figure 20) were used to establish the connections of the partial structures of **113**.

The structure of the hexahydroxybiphenyl ester-linked pentopyranose system and the connection of the mono-substituted aromatic to the C-31-32 partial structure in **113** was deduced in an identical manner as for **112**. The only other HMBC correlations observed

from the methylenes H-32 (2.89) and H-31 (3.33) in **113** were to the carbonyl carbon at 204.9 ppm (C-30). This ketone adjacent to H-31 has shifted downfield from C-30 in **112**. This observation coupled with the absence of an HMBC correlation from H-32 to C-26 in **113**, suggested that the pyran ring of **112** was open in **113** to result in a dihydrochalcone. The final two aromatic protons at 6.08 ppm (H-25/29) formed part of the 1,3,4,5-tetra-substituted aromatic ring of the dihydrochalcone moiety in **113**. HMBC correlations were observed from H-25 to C-29, and H-29 to C-25, confirming they were *meta* to each other. Both of these protons displayed HMBC correlations to C-27 (104.6), the quaternary aromatic carbon alpha to the ketone. The ether linkage between the sugar moiety and the 1,3,4,5-tetra-substituted aromatic group was determined from HMBC correlations between H-1 (5.56) and H-25/29 to C-24 (162.2). Thus the structure of **113** was established. The $^{1}H$, $^{13}C$ and HMBC NMR spectral data of **113** is detailed in Table 4. Large coupling constants were observed for H-1, H-4, H-5 and H-22 in **113** (Figure 19). As with **112**, this demonstrated that these protons were all axial.

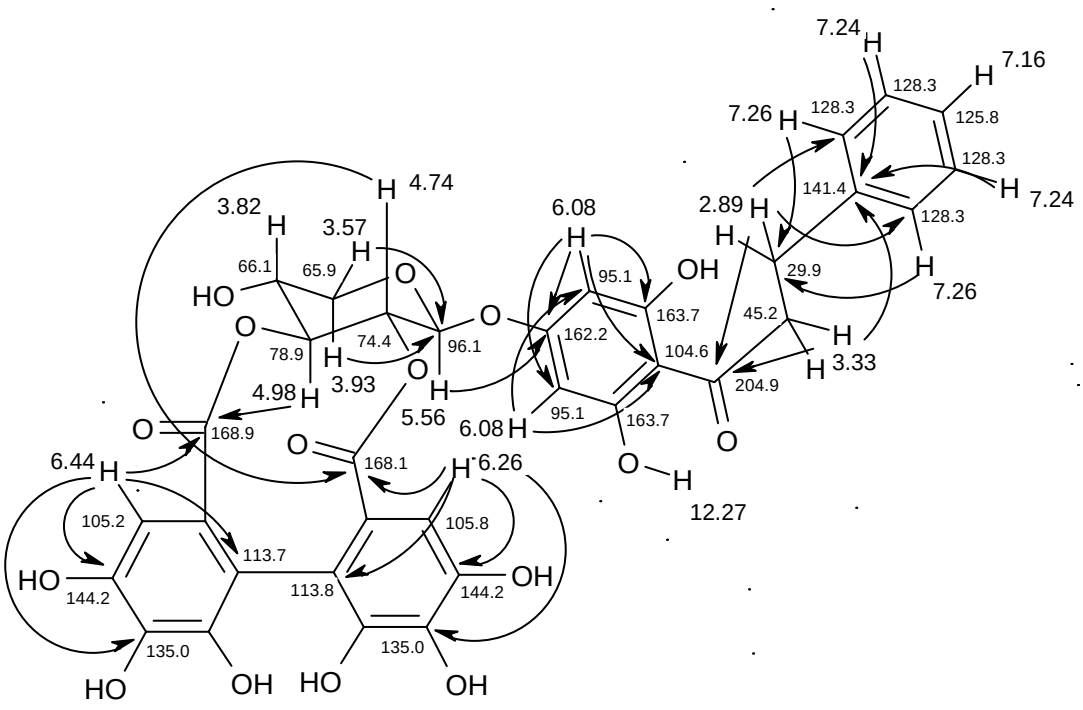


**Figure 20.** The connections of the partial structures of **113** established from HMBC spectra.

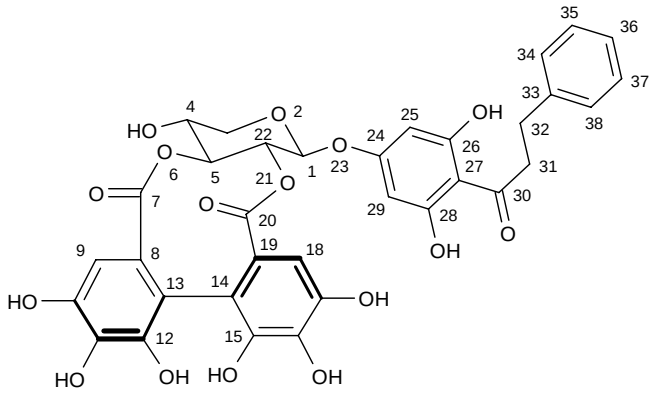

**Table 4.** $^{1}H$,[a] $^{13}C$[b] and HMBC NMR spectral data of **113**.[c]

| position | $\delta_C$ | $\delta_H$ (mult; *J* in Hz) | HMBC $^{2,3}J_{CH}$ |
|---|---|---|---|
| 1 | 96.1 | 5.56 (1H, d, 9.6) | 5, 22, 24 |
| 3 | 65.9 | 3.57 (1H, dd, 4.2, 10.8)<br>3.93 (1H, dd, 6.6, 13.8) | 1, 4, 5 |
| 4 | 66.1 | 3.82 (1H, ddd, 6.6, 12.0, 12.0) | 3, 5 |
| 5 | 78.9 | 4.98 (1H, dd, 9.0, 9.0) | 1, 3, 4, 7, 22 |
| 7 | 168.9 | - | - |
| 8 | 124.2 | - | - |
| 9 | 105.2 | 6.44 (1H, s) | 7, 10, 11, 13 |
| 10/17 | 144.2 | - | - |
| 11/16 | 135.0 | - | - |
| 12/15 | 144.7 | - | - |
| 13 | 113.7 | - | - |
| 14 | 113.8 | - | - |
| 18 | 105.8 | 6.26 (1H, s) | 14, 16, 17, 20 |
| 19 | 124.9 | - | - |
| 20 | 168.1 | - | - |
| 22 | 74.4 | 4.74 (1H, dd, 9.0, 9.0) | 1, 5, 20 |
| 24 | 162.2 | - | - |
| 25/29 | 95.1 | 6.08 (2H, s) | 24, 26, 27, 28, 25/29, 30 |
| 26/28 | 163.7 | - | - |
| 27 | 104.6 | - | - |
| 30 | 204.9 | - | - |
| 31 | 45.2 | 3.33 (2H, t, 10.8) | 30, 32, 33 |
| 32 | 29.9 | 2.89 (2H, t, 7.2) | 30, 31, 33, 34/38 |
| 33 | 141.4 | - | - |
| 34/38 | 128.3 | 7.26 (2H, d, 7.2) | 32, 34/38, 35/37, 36 |
| 35/37 | 128.3 | 7.24 (2H, dd, 6.6, 7.2) | 33, 35/37 |
| 36 | 125.8 | 7.16 (1H, dd, 6.6, 6.6) | 34/38 |
| C-28-OH | - | 12.27 (1H, br) | - |

[a] At 600 MHz. [b] At 125 MHz. [c] In $d_6$-DMSO.

Similarly with **112**, **113** may also be derived from a chalcone precursor (Figure 21). The chalcone precursor could be hydrogenated to yield the dihydrochalcone moiety encountered in **113**.

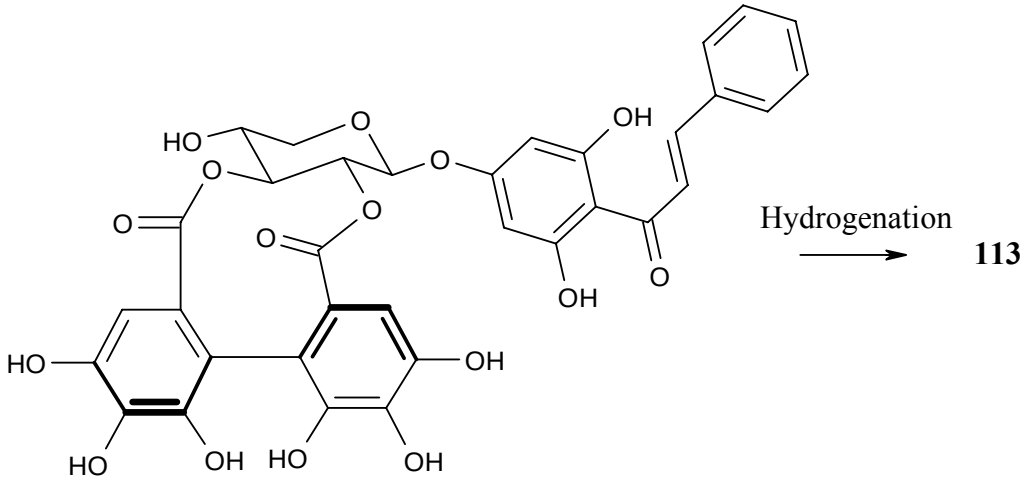


**Figure 21.** The proposed formation of **113** from a chalcone precursor via a hydrogenation reaction.

### *2.4.4 Determination of the Absolute Stereochemistry of the Diphenyl Group in 112 and 113*

The hexahydroxydiphenoyl moiety is widely known as a structural component of a broad class of natural products called ellagitannins.[15, 16] Over 500 ellagitannins are known,[15] however three examples are highlighted in Figure 20. These examples, 2,3-(*S*)-hexahydroxydiphenoyl-D-glucose, pedunculagin and combreglutinin all incorporate a D-glucose connected via ester linkages to a hexahydroxybiphenyl system. Compounds **112** and **113** are the first natural products which incorporate pentopyranose and hexahydroxydiphenoyl moieties.

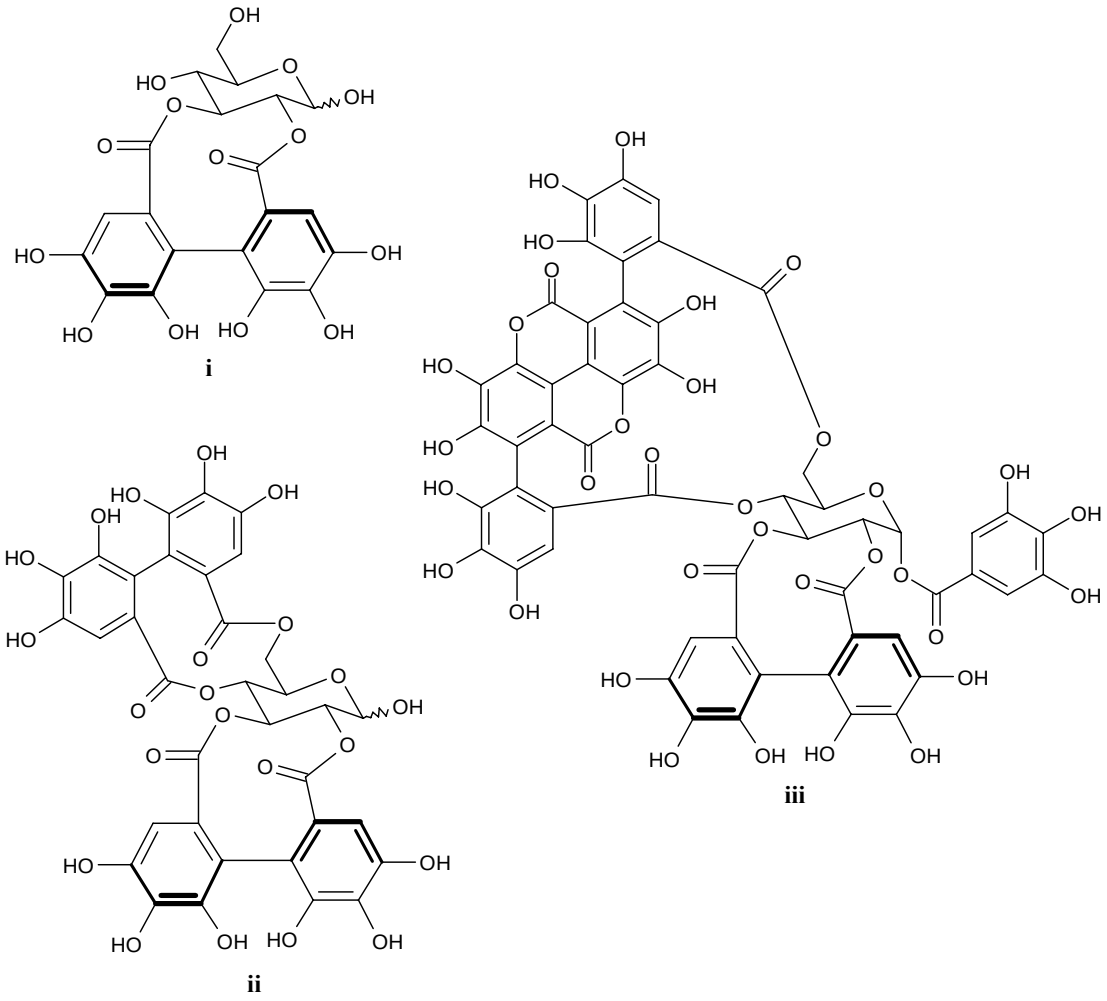


**Figure 22.** The structures of selected ellagitannins: 2,3-(*S*)-hexahydroxyphenoyl-D-glucose (**i**),[15] pedunculagin (**ii**),[16] and combreglutinin (**iii**).[15]

The diphenyl group has been recognized as a chiral system and the chirality of the hexahydroxydiphenyl is deduced from circular dichroism spectra.[17] The chirality of this group in 2,3-(*S*)-hexahydroxydiphenoyl-D-glucose, pedunculagin and combreglutinin has been assigned as *S*. Comparison of the CD spectra of **112** and **113** with that of pedunculagin[15, 16] and 2,3-(*S*)-hexahydroxydiphenoyl-D-glucose,[16, 17] indicated that the chirality of the biphenyl systems in **112** and **113** were also *S*. The CD spectrum in MeOH of pedunculagin has been reported as a deflection of +41.9 at 238 nm, -14.7 at 263 nm and +6.5 at 284 nm.[15] The CD spectrum in MeOH of 2,3-(*S*)-hexahydroxydiphenoyl-D-glucose has been reported as a deflection of +10.2 at 235 nm, -2.7 at 262 nm and -0.1 at 287 nm.[17] These deflections are dependent on the concentration of the sample. The

experimental CD spectra of **112** and **113** provided deflections of +42 at 232 nm, -18 at 265 nm, and +5 at 285 nm, and +52 at 232 nm, -18 at 265 nm and +5 at 285 nm, respectively. The sign of the deflection at ~235 nm is reported to be the diagnostic tool for the determination of the absolute configuration of the hexahydroxyphenoyl.[16] A positive deflection indicates an *S* configuration, whereas a negative deflection indicates an *R* configuration.[16] Therefore, the hexahydroxybiphenoyl moieties in both **112** and **113** are in an *S* configuration. The *S* configuration of the hexahydroxybiphenoyl moieties confirms the pentopyranose groups of **112** and **113** as D sugars (Appendix II). Molecular modeling of the *R* and *S* enantiomers of **113** indicated that the pentopyanoside present can only be a D sugar with an *S* configuration of the biphenyl.

## 2.5 The Application of Strong Cation Exchange to Alkaloid Isolation

Strong cation exchange resins consist of a sulfonic acid group covalently bound to an insoluble matrix. As an alkaloid containing extract is filtered through SCX resin, the protonated nitrogen atom of the cationic salt of the alkaloid forms an ionic bond with the negatively charged sulphonate group. Consequently, the alkaloid remains bound to the resin while other non-alkaloidal constituents of the extract are removed. The alkaloid can be displaced from the resin by a pH dependent elution, or by competition with the cation of a salt solution. This enables the separation of alkaloids from other compounds in the extract, and provides an alternative to an acid-base extraction.

The pH dependent elution of alkaloids is performed with base. The positive charge on the nitrogen atom is neutralized in the presence of base, eliminating the ionic interaction with the sulfonic acid group. The elution off SCX resin by competition with a cation provides a base-free alternative for the isolation of alkaloids. The atomic number, charge and concentration of a cation in solution influences the affinity of the cation to the sulphonate group and the cations ability to efficiently displace alkaloids.[18] At low aqueous concentrations, the exchange potential increases with valence.[18] At low concentrations

and constant valence, exchange potential increases with increasing atomic number. At high aqueous concentrations, exchange potential of monovalent cations increases, in contrast to the decreased exchange potential of divalent cations.[18] With these considerations, $Na^+$ was selected as the cation, at a concentration of 1M, for displacement of alkaloids from SCX resin. This enabled the base-free purification of alkaloids from the plants of the family Elaeocarpaceae.

## 2.6 Structure Elucidation Strategy

Structural elucidation of alkaloids purified from *E. habbeniensis, E. fuscoides, P. mearsii* and *E. grandis* was achieved by one and two dimensional NMR experiments. This has been the method of choice for elucidating structures of natural products since the 1970's.[19] 1D NMR techniques used include $^1H$ and $^{13}C$. Two dimensional NMR techniques used include COSY, HSQC, HMBC and ROESY experiments. These techniques are useful to determine the way chemical environments are interconnected within a molecule.[20] A COSY experiment provides correlations between geminal and vicinal $^1H$ nuclei.[20] HSQC and HMBC experiments are also 2D NMR techniques which are commonly used for the structure elucidation of natural products. An HSQC experiment shows $^1J_{CH}$ correlations of a $^1H$ nuclei to a $^{13}C$ nuclei. This allows the direct attachment of protons to carbons. Quaternary carbons or heteroatoms are not visible in an HSQC spectrum. An HMBC experiment, which can be considered an extension of the HSQC experiment, shows long range correlations from a $^1H$ nuclei to a $^{13}C$ nuclei, which are associated with two and three bond proton to carbon correlations. On rare occasions, four bond correlations are also witnessed but are generally regarded as lesser intensity signals compared to two and three bond correlations. A ROESY experiment can be used to determine the relative stereochemistry of a molecule. It depends on the nuclear Overhauser effect which couples $^1H$ nuclei close together in space.[21]

Advances in computational chemistry have allowed the visualization of molecular structures in three dimensions.[22] This technique has been termed molecular modeling. A

commonly applied method of molecular modeling is energy minimization. This process involves the adjustment of the 3-D arrangement of a structure to reduce its energy.[22] Molecules are known to intrinsically assume a low energy confirmation.[22] An important energy minimization technique is the Monte Carlo method.[22] This involves the generation of thousands of random configurations of a molecule and applying them to a Boltzmann probability theorem to determine the energy of each configuration.[22, 23] As a result, many high and low energy conformations are produced. The Monte Carlo conformational search has two distinct advantages in that it allows a configuration to be assessed independently based on its energy and the software was designed to search lower energy confirmations in greater depth.[22] The outcome of the conformational search can be regarded as a global energy minimum. The Monte Carlo method was applied to the alkaloids isolated from plants of the family Elaeocarpaceae.

## 2.7 References


1. Collins, D. J., Culvenor, C. C. J., Lamberton, J. A., Loder, J. W., Price, J. R., *Plants for Medicines: A Chemical and Pharmacological Survey of Plants in the Australian Region*. 1st ed.; CSIRO: Melbourne, **1990**.
2. Price, J. R., Lamberton, J. A., Culvenor, C. C. J., *Historical Records of Australian Science* **1993,** 9, 335 - 356.
3. Webb, L. J., Whitelock, D., Brereton, J. L. G.,, In *The Last of the Lands*, ed.; Eds. Jacaranda Press: **1989**; pp. 82 - 90.
4. Webb, L. J. *Australian Phytochemical Survey - Part 1*; Bulletin No. 241; CSIRO: Melbourne, **1949**.
5. Smith, R. J., *Chemistry in Australia* **1989**, 350 - 352.
6. Chitty, J. A., Allen, R. S., Fist, A. J., Larkin, P. J., *Functional Plant Biology* **2003**, 30, 1045 - 1058.
7. Culvenor, C. C. J., Fitzgerald, J. S., *J Pharm Sci* **1963,** 52, 303 - 304.
8. Farnsworth, N. R., *J Pharm Sci* **1966,** 55, 225 - 276.
9. Eisman, M., Gallego, M., Valcarel, M., *J Anal At Spectrom* **1993,** 8, 1117 - 1121.

**10.** Coe, F. G., Anderson, G. J., *J Ethnopharm* **1996,** 53, 29 - 50.

**11.** Habib, A. A., *J Pharm Sci* **1980,** 69, 37 - 40.

**12.** Molyneux, R. J., Gardner, D. R., James, L. F., Colegate, S. M., *J Chromatogr A* **2002**, 967, 57 - 74.

**13.** Waterman, P. G., *Natural products from plants: bioassay-guided separation and structural characterisation*. In *Drugs from Natural Products*, ed.; Harvey, A. L., Eds. Ellis Horwood Limited: Chichester, **1993**; pp. 7 - 17.

**14.** Jossang, A., Pousset, J-L., Bodo, B., *J Nat Prod* **1994,** 57, 732 - 737.

**15.** Feldman, K. S., Smith, R. S., *J Org Chem* **1996,** 61, 2606 - 2612.

**16.** Okuda, T., Yoshida, T., Hatano, T., *J Nat Prod* **1989,** 52, 1 - 31.

**17.** Okuda, T., Yoshida, T., Hatano, T., Koga, T., Toh, N., Kuriyama, K., *Tetrahedron Lett* **1982,** 23, 3937 - 3940.

**18.** *Dowex Exchange Resin Data Sheet*; Sigma-Aldrich: **1997**.

**19.** Mann, J., *Alkaloids*. In *Natural Products: Their Chemistry and Biological Significance*, 2nd ed.; Mann, J., Davidson, R. S., Hobbs, J. B., Banthorpe, D. V., Harborne, J. B., Eds. Longman: **1994**; pp. 389 - 446.

**20.** Byrne, L. T., *Nuclear Magnetic Resonance Spectroscopy: Strategies for Structural Determination*. In *Bioactive Natural Products: Detection, Isolation and Structural Determination*, 1st ed.; Colegate, S. M., Molyneux, R. J., Eds. CRC Press: Boca Raton, **1993**; pp. 75 - 104.

**21.** Field, L. D., Sternhell, S., Kalman, J. R., *Organic Structures from Spectra*. ed.; Wiley: Chichester, **1995**.

**22.** Billings, E., *Molecular Modeling and Drug Design*. In *Foye's Principles of Medicinal Chemistry*, ed.; Williams, D. A., Lemke, T. L., Eds. Lippincott Williams and Wilkins: Philadelphia, **2002**; pp. 68 - 85.

**23.** Morley, S. D., *The global minimum problem in molecular mechanics: Simulated annealing and related techniques*. In *Molecular Modelling and Drug Design*, 1st ed.; Vinter, J. G., Gardner, M., Eds. CRC Press: London, **1994**; pp. 89 - 136.

# CHAPTER 3 – Isolation and Structure Elucidation of Habbenine, a Novel Pyrrolidine Alkaloid from *Elaeocarpus habbeniensis*

## 3.1 Introduction

*Elaeocarpus habbeniensis* is a rainforest tree which grows in the mountainous regions of PNG. The local name for this tree is Kelo-Yombi-Kulgili.[1] An extract of the leaves of *E. habbeniensis* was identified as alkaloid containing by a positive Dragendorff's test. This extract displayed a mass ion peak in positive ESIMS analysis at *m/z* 280. This indicated that the extract was a likely source of alkaloids and warranted a full chemical investigation. This is the first chemical investigation of *E. habbeniensis*.

Leaves of *E. habbeniensis* were collected in January 1999 from the Manegilli village swamp forest, near Ialibu, in the southern highlands province of PNG. This chapter describes the isolation and structure elucidation of habbenine (**114**) from the leaves of this species.

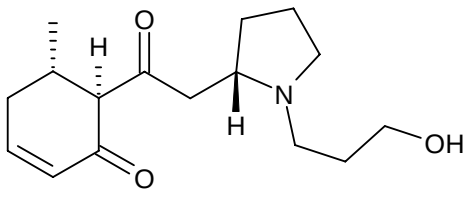


**114a**

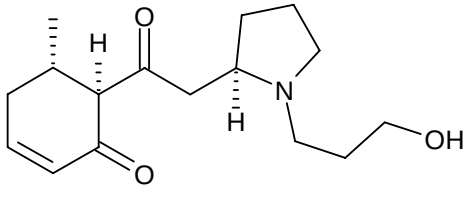


**114b**

## 3.2 The Isolation of Habbenine (114) from the Leaves of *E. habbeniensis*

The extraction of the leaves of *E. habbeniensis* and the isolation of habbenine (**114**) is shown in Scheme 3.

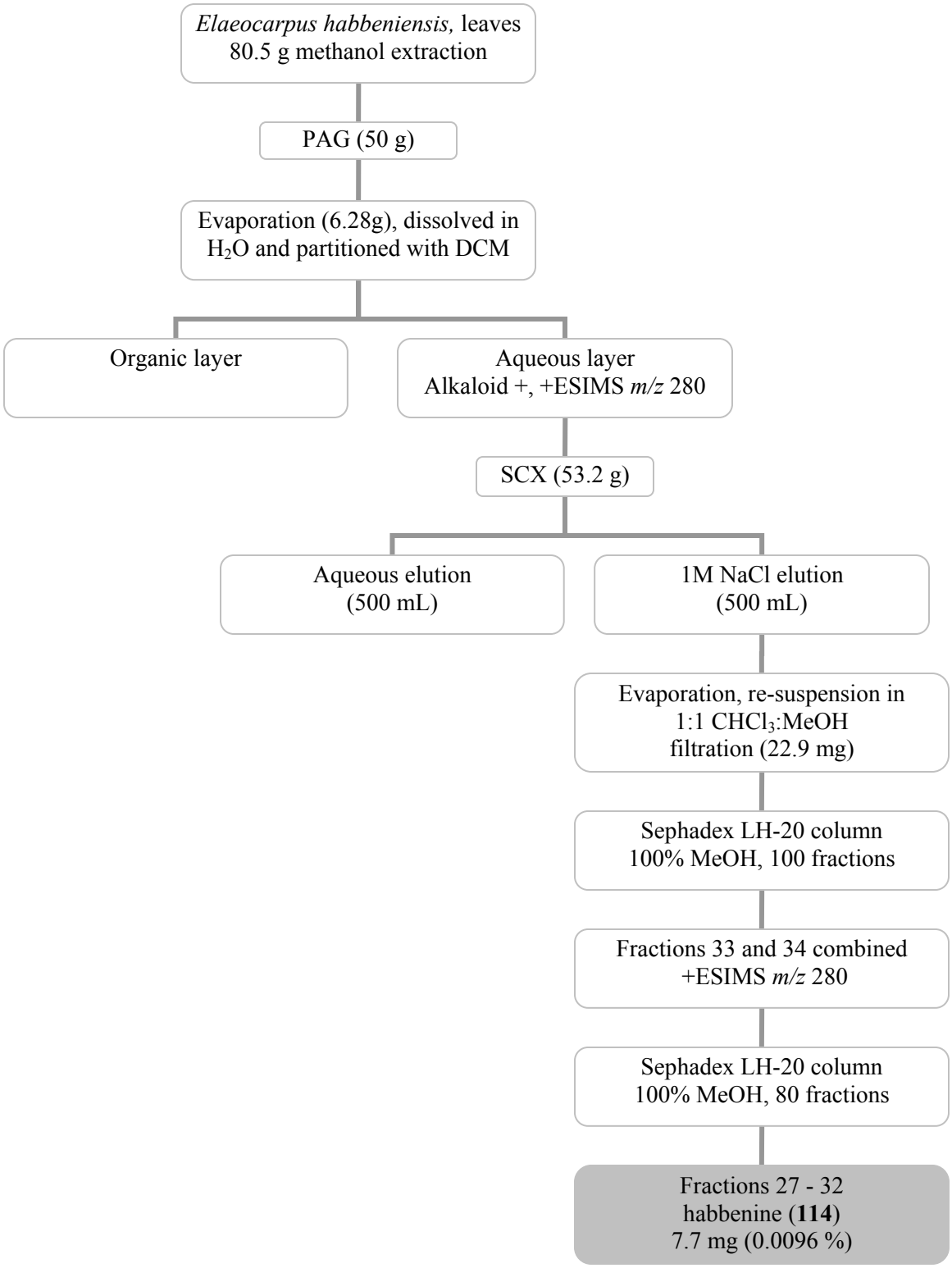


**Scheme 3.** The isolation of habbenine (**114**) from the leaves of *Elaeocarpus habbeniensis*.

The dried ground leaves of *E. habbeniensis* were extracted exhaustively with methanol. The MeOH extract was filtered through PAG (polyamide gel) to remove tannins and then evaporated. The residue was dissolved in $H_2O$ and partitioned with DCM. The aqueous layer gave a positive Dragendorff's test and a mass ion peak at *m/z* 280 in positive ESIMS. The aqueous layer was filtered through SCX resin. The SCX resin was washed with $H_2O$ before an alkaloid fraction was eluted with a 1M solution of NaCl. The alkaloid fraction was evaporated under vacuum and the residue suspended in a 1:1 mixture of $CHCl_3$:MeOH and filtered to remove NaCl. The filtrate was fractionated on a Sephadex LH-20 column eluting with 100% MeOH. Fractions were analysed by positive ESIMS and $^1$H NMR, and the alkaloid containing fractions were re-chromatographed on LH-20 to afford habbenine (7.7 mg, 0.0096%). The $^{13}$C NMR spectrum of **114** revealed a 1:1 mixture of diastereomers was present. Attempts to separate the diastereomers by C18 RP-HPLC, using isocratic conditions of 84:15:1 $H_2O$:MeOH:TFA, 89:10:1 $H_2O$:ACN:TFA and 85:7:7:1 $H_2O$:MeOH:ACN:TFA, were unsuccessful. An attempted separation using reverse phase HPLC on phenyl bonded silica, and isocratic elution with 94:5:1 $H_2O$:MeOH:TFA also proved unsuccessful.

## 3.3 Structure Elucidation of Habbenine (114)

Habbenine (**114**) was assigned a molecular formula $C_{16}H_{26}NO_3$ by high resolution positive electrospray mass measurement of the $[M + H]^+$ ion (280.18939). The $^1$H NMR spectrum of habbenine (**114**) is illustrated in Figure 23. Habbenine was observed as a mixture of tautomers in solution. The most noticeable difference between the two tautomers was in the chemical shifts of the olefinic protons. In the major tautomer, the olefinic protons resonated at δ 5.96 and 7.14 ppm, while in the minor tautomer they were observed at δ 6.06 and 6.67 ppm. Acquistion of the $^1$H NMR spectrum at 50$^o$ C saw no difference in the ratio of the tautomers. However, the ratios of the tautomers varied in different solvents. Solvents used in this study were $CD_3OD$, $CD_3CN$, $d_6$-DMSO and $CDCl_3$. A drop of concentrated TFA was added to habbenine which was dissolved in $d_6$-DMSO. This produced the best observed ratio of tautomers (Figure 23).

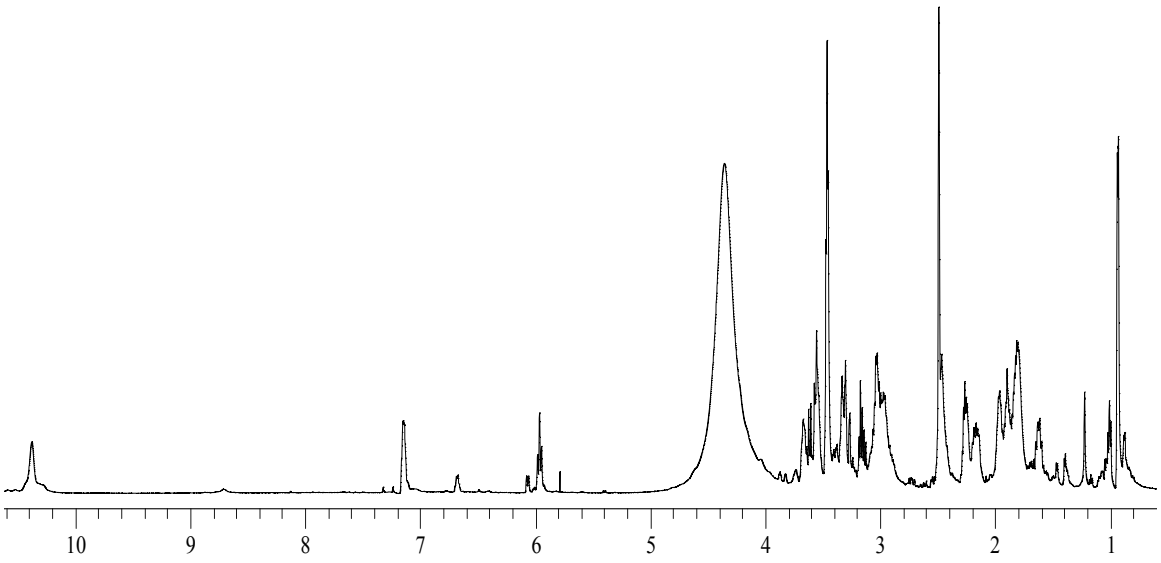


**Figure 23.** The $^{1}$H NMR spectrum of habbenine (**114**) at 600 MHz in $d_6$-DMSO with one drop of conc. TFA.

The existence of tautomers suggested the presence of a 1,3-diketo system within the molecule. This was supported by IR absorption bands at 1712 and 1674 $cm^{-1}$ and UV absorbances as 270 and 339 nm. The proton between the carbonyls of a 1,3-diketo system is acidic, allowing enol tautomerization with either ketone and resulting in a β-hydroxy-α,β-unsaturated ketone. The different ratios of the tautomers in each solvent was due to the dipole moments of the solvents. The $^{1}$H NMR spectra of **114** in $CD_3OD$ and $CD_3CN$ both produced similar ratios, due to the similar dipole moments of these solvents. The $^{1}$H NMR spectrum in $CDCl_3$ produced a greater proportion of the minor tautomer. The greater dipole moment of $CDCl_3$ enables increased stability of the more polar minor tautomer, thus altering the equilibrium. The di-keto tautomeric form was observed as the major isomer in a ratio of 4:1 in Figure 23, and allowed the structure of habbenine (**114**) to be determined.

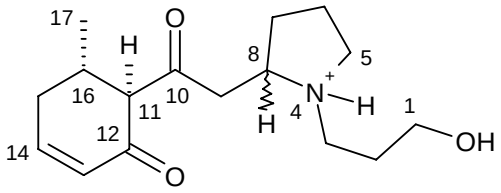


**Table 5.** $^{1}H$,[a] $^{13}C$[b] and HMBC NMR Spectral data of habbenine (**114a** and **b**)[c]

| position | $^{13}C$ | $^{1}H$, mult, *J* (Hz) | $^{13}C$ | $^{1}H$, mult, *J* (Hz) |
|---|---|---|---|---|
| 1 | 58.7 | 3.46 (2H, t, 6.0) | 58.7 | 3.46 (2H, t, 6.0) |
| 2 | 28.9 | 1.82 (2H, m) | 28.9 | 1.82 (2H, m) |
| 3 | 51.1 | 3.33 (1H, ddd, 4.2, 10.8) | 51.3 | 3.33 (1H, ddd, 4.2, 10.8) |
| | | 2.97 (1H, ddd, 2.4, 9.6) | | 2.97 (1H, ddd, 2.4, 9.6) |
| 4 | - | 10.38 (1H, br) | - | 10.38 (1H, br) |
| 5 | 53.1 | 3.55 (1H, m) | 53.0 | 3.55 (1H, m) |
| | | 3.04 (1H, ddd, 2.4, 7.8, 14.4) | | 3.04 (1H, ddd, 2.4, 7.8, 14.4) |
| 6 | 21.8 | 1.97 (1H, ddd, 2.4, 7.2, 15.0) | 22.0 | 1.97 (1H, ddd, 2.4, 7.2, 15.0) |
| | | 1.91 (1H, ddd, 3.6, 6.6, 13.2) | | 1.91 (1H, ddd, 3.6, 6.6, 13.2) |
| 7 | 30.2 | 2.26 (1H, ddd, 2.4, 6.6, 13.2) | 30.2 | 2.26 (1H, ddd, 2.4, 6.6, 13.2) |
| | | 1.62 (1H, ddd, 2.4, 9.0, 19.2) | | 1.62 (1H, ddd, 2.4, 9.0, 19.2) |
| 8 | 63.3 | 3.67 (1H, ddd, 4.2, 8.4, 9.0) | 63.4 | 3.67 (1H, ddd, 4.2, 8.4, 9.0) |
| 9 | 45.6 | 3.02 dd (8.4, 18.0) | 45.0 | 3.15 dd (8.4, 18.6) |
| | | 3.32 dd (4.2, 18.0) | | 3.28 dd (4.2, 18.6) |
| 10 | 206.6 | - | 206.6 | - |
| 11 | 66.3 | 3.55 (1H, d, 11.4) | 66.8 | 3.56 (1H, 11.4) |
| 12 | 197.8 | - | 197.8 | |
| 13 | 128.8 | 5.96 (1H, d, 9.6) | 128.8 | 5.97 (1H, d, 9.6 Hz) |
| 14 | 153.0 | 7.14 (1H, dd, 6.6, 9.6) | 153.0 | 7.19 (1H, dd, 6.6, 9.6) |
| 15 | 33.2 | 2.49 (1H, m) | 33.2 | 2.49 (1H, m) |
| | | 2.17 (1H, dd, 8.4, 11.4) | | 2.14 (1H, dd, 8.4, 11.4) |
| 16 | 32.4 | 2.47 (1H, m) | 32.0 | 2.49 (1H, m) |
| 17 | 19.9 | 0.93 (3H, d, 6.0) | 19.8 | 0.94 (3H, d 6.0) |

[a] At 600 MHz. [b] At 125 MHz. [c] In $d_6$-DMSO.

The $^{13}C$ and $^{1}H$ NMR spectral data for **114** is presented in Table 5. The $^{1}H$ NMR spectrum displayed signals for an exchangeable proton at δ 10.38 and two olefinic protons at 7.14 and 5.96 ppm. A methyl doublet was also observed, indicating the presence of a $CH_3$-CH moiety. Multiple signals were observed between δ 3 and 4 ppm, which indicated methines or methylenes bound to heteroatoms.

Inspection of the $^{13}C$ NMR spectrum revealed **114** was a 1:1 mixture of diastereomers. The chemical shifts of eight of the carbon atoms were identical for both diastereomers. However, some difference in chemical shift was observed for the remaining carbons. The largest differences in chemical shift were observed for C-3 (51.1/51.3), C-9 (45.6/45.0), C-11 (66.3/66.8) and C-16 (32.4/32.0). The proton chemical shifts were almost identical in both diastereomers except for the protons H-11 and $H_2$-9. Only the structure elucidation of one diastereomer is described.

Two ketone carbons were observed at δ 206.6 and 197.8 ppm in the $^{13}C$ NMR spectrum, with the latter indicative of an α,β-unsaturated ketone. Two $sp^2$ hybridized carbons were noted at δ 153.0 and 128.8 ppm. A group of six carbons were observed between δ 40 and 70 ppm, indicating carbons which were bound to heteroatoms. Five carbons were observed between δ 20 and 35 ppm. The methyl signal was observed at 19.9 ppm.

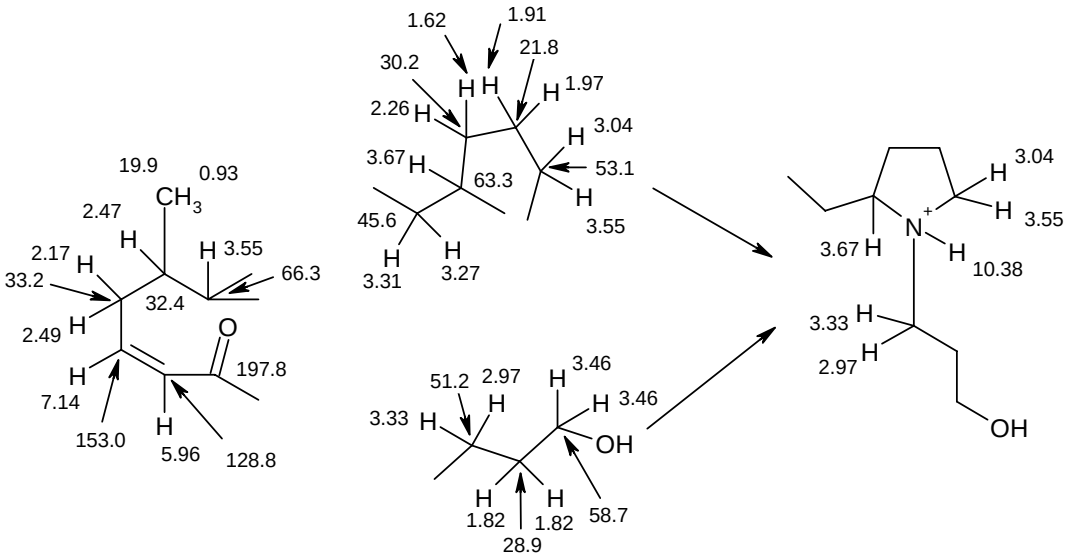


**Figure 24.** The partial structures of habbenine (**114**) established from COSY and HSQC experiments.

HSQC spectral data established the presence of 24 carbon bound protons (one methyl, eight methylenes, three methines and two olefinic protons). COSY and HSQC experiments established the partial structures illustrated in Figure 24. COSY correlations from the methylenes at δ 3.04/3.55 (H-5) and 2.26/1.62 ppm (H-7) to the methylene at δ 1.91/1.97 ppm (H-6) allowed the construction of the C-5 to C-7 carbon chain. Extension of this chain was permitted by correlations from H-7 to the methine at δ 3.67 ppm (H-8). The methylene at δ 3.31/3.27 ppm (H-9) was determined to be adjacent to H-8, due to COSY correlations between these protons. The C-1 to C-3 propanol group was assembled by COSY correlations from the methylenes at δ 3.33/2.97 (H-3) and 3.46 (H-1) to the methylene at 1.82 ppm (H-2). The HSQC spectrum indicated the protons of H-1 were attached to a carbon at δ 58.7 ppm. The proton and carbon chemical shifts of this methylene indicated it was oxygenated. MS evidence confirmed the presence of an alcohol. The connection of these partial structures into an *N*-propanolpyrrolidine group was deduced from COSY correlations between the exchangeable proton at δ 10.38 (H-4) and H-3, H-5 and H-8. The most intense COSY correlations from H-4 were observed to the protons at δ 2.97, 3.04 and 3.67 ppm, suggesting axial-axial configurations for these protons relative to the NH.

A second partial structure was assembled from the correlations of the olefinic protons at δ 7.14 and 5.96 ppm. HSQC correlations revealed that these protons were attached to carbons at δ 153.0 and 128.8 ppm, respectively. These are typical chemical shifts for the alpha and beta carbons of an α,β-unsaturated ketone. COSY correlations demonstrated that the methylene at δ 2.49/2.17 ppm (H-15) was adjacent to the olefinic proton at δ 7.14 ppm. Further correlations from H-15 to a proton at δ 2.47 ppm (H-16) allowed the connection of C-15 and C-16. The attachment of the methyl group (C-17) at δ 0.93 ppm to C-16 was demonstrated by a COSY correlation between H-16 and H-$17_{Me}$. The methine at δ 3.55 ppm was also determined to be adjacent to H-16 from a COSY correlation. The ketone at δ 206.6 ppm remained the only carbon unaccounted for from the $^{13}$C NMR spectrum, following the establishment of the partial structures of habbenine (**114**).

HMBC correlations (Figure 25) from H-$5_{ax}$ (3.04) to C-3 (51.1) and C-8, and H-3 (3.33/2.97) to C-8 supported the structure of the *N*-propanolpyrrolidine. The presence of the α,β-unsaturated ketone was confirmed by a correlation from the proton of the beta carbon H-14 (7.14) to C-12 (197.8). A methylcyclohexenone ring was secured by HMBC correlations from H-15 (2.49) and H-11 (3.55) to the C-17 methyl group (19.9), and from H-11 to the carbonyl C-12. H-11 exhibited a correlation to a second ketone at δ 206.6 ppm (C-10). As a result, a di-keto system was established. Strong correlations from the H-9 methylene (3.31/3.27) to C-10 allowed the connection of the methylcyclohexenone to the *N*-propanolpyrrolidine. Thus the structure of habbenine (**114**) was established. The proton H-8 showed no HMBC correlations.

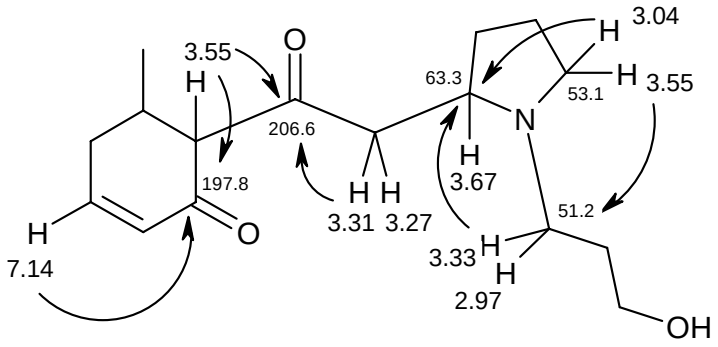


**Figure 25.** The key HMBC correlations used to establish the structure of habbenine (**114**).

The relative stereochemistry of H-11 and H-16 was established from ROESY correlations. Strong correlations were observed between the H-$17_{Me}$ and H-11 indicating a *cis* configuration between these protons, and therefore suggesting a *trans*-diaxial relationship between H-11 and H-16. A coupling constant of 11.4 Hz for H-11 confirmed the *trans* diaxial arrangement with H-16. The stereochemistry of H-8 relative to H-11 could not be determined as the distance between the two protons was too great for a ROESY correlation (Figure 26). However, both diastereomers had large couplings between H-11 and H-16. This indicated that both compounds had a *trans* diaxial arrangement between these protons. Therefore the two diastereomers differed only in the configuration at C-8.

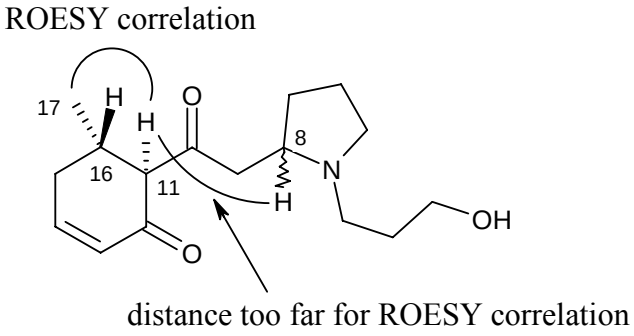


**Figure 26.** Depiction of the ROESY correlation observed between H-11 and H-$17_{Me}$.

The structure of the minor tautomer was proposed as **115**. However, the formation of other tautomers, such as **116** and **117**, are possible. Comparatively, structure **115** is considered to be the most thermodynamically stable, as a conjugated system is produced. Structure **117** is considered most unlikely as the proton (H-11) between the two carbonyls of **114** is more acidic than the protons of the α-methylene (H-9).

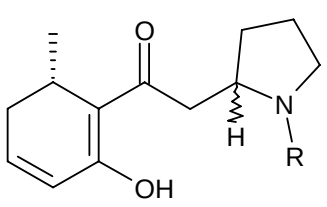


**115**

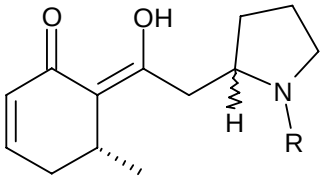


**116**

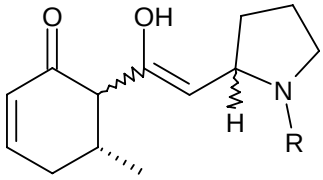


**117**

Habbenine (**114**) is proposed to be epimeric at C-8. In the previous report of the isolation of the pyrrolidine alkaloid peripentadenine (**81**) from *P. mearsii*, it was suggested that the proton alpha to the nitrogen was readily isomerized.[2] The same phenomenon may have occurred during the purification of **114**. Molecular modeling studies were performed on the proposed diastereomers of habbenine. The energy minimized structures of two isomers of habbenine are shown in Figure 27. The cyclohexenone ring is shown in a boat configuration. In both energy minimized structures, the *trans*-diaxial relationship was conserved between H-11 and H-16. The diastereomers only differ in the orientation of the pyrrolidine ring. An almost negligible difference in energy of the isomers in Figure 27 was noted. The first isomer, 16-*S*, 11-*S*, 8-*S*, produced a minimum energy value of 9.8254 kJ/mol, while the second isomer, 16-*S*, 11-*S*, 8-*R*, produced a value of 9.9784 kJ/mol.

This suggested that the three dimensional structures of both isomers were similar, thus making separation by HPLC difficult. The optical rotation of **114** was measured as $+13.73^{o}$.

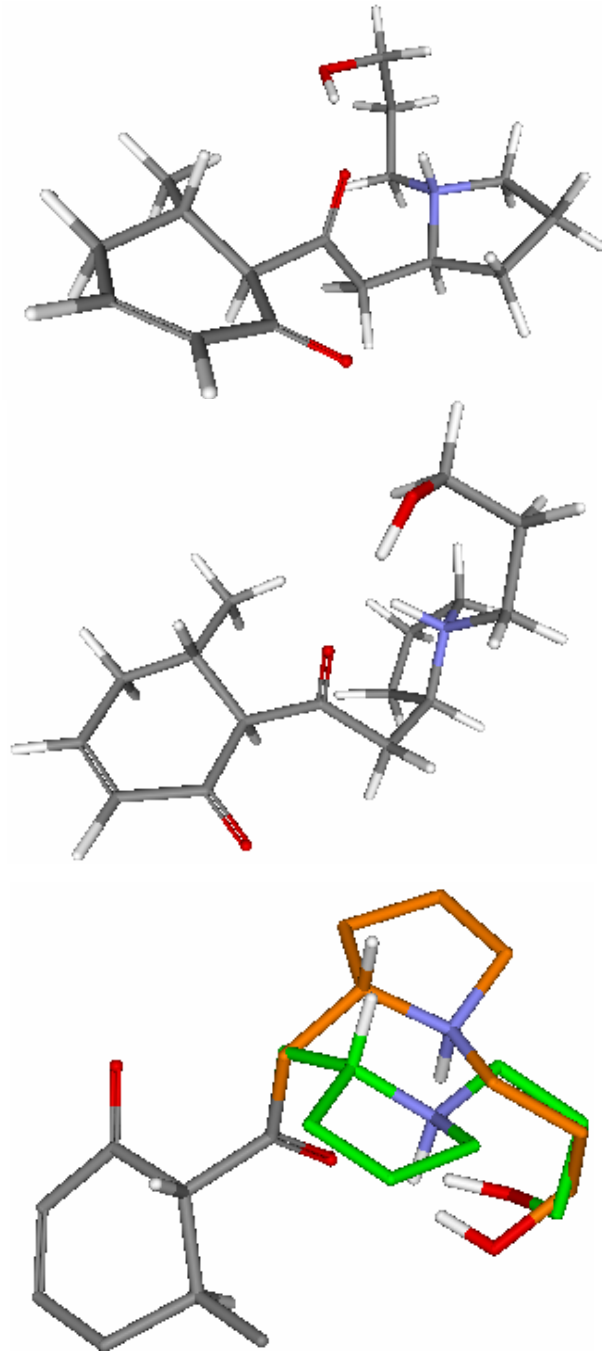

**Figure 27.** Comparison of the energy minimized structures of two diastereomers of habbenine (**114**).

## 3.4 The Proposed Biogenesis of Habbenine (114) and Chemotaxonomic Considerations

Habbenine (**114**) is a novel pyrrolidine alkaloid and the first pyrrolidine alkaloid isolated from a species of *Elaeocarpus*. Habbenine belongs to the same structure class as the pyrrolidine alkaloids isolated from *P. mearsii*. This may suggest a chemotaxonomic relationship between these two species. Habbenine could also have significance as a biogenetic precursor to the *P. mearsii* series of alkaloids. This will be discussed in chapter 5.

Chemotaxonomy is a term used for the clustering of species that possess similar chemistry or produce structurally related secondary metabolites. This suggests that the enzymatic processes of biosynthesis are preserved by chemotaxonomically related species. For example, genes encoding enzymes associated with the biosynthesis of monoterpene indole alkaloids for plants of the genus *Rauwolfia* (Apocynaceae) show high conservation amongst different species.[3] This suggests a close chemotaxonomic relationship between these species. This may indicate an evolutionary influence in the biosynthesis of alkaloids for the health of plants.[3]

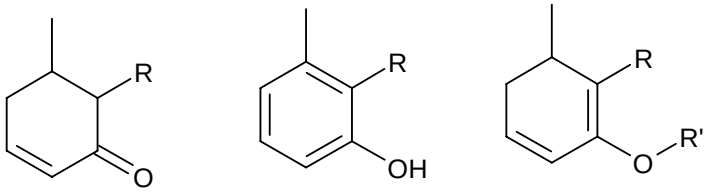


**118** **119** **120**

Habbenine (**114**) possesses similar structural features to the *Elaeocarpus* indolizidine alkaloids. The methylcyclohexenone moiety (**118**) of habbenine can be considered the hydrogenated precursor of the methylphenol (**119**) encountered in the structures of **61** – **63, 80** and **81**. The enol tautomer (**120**) of the methylcyclohexenone moiety has also been found in the indolizidine alkaloids **64** – **69** and **72**. The consensus between the polyketide condensation pathway of the *Elaeocarpus* alkaloids proposed by Johns and

Carroll suggests this pathway applies to the biogenesis of habbenine (**114**). I have proposed that the biogenesis of **114** could occur by one of two potential mechanisms.

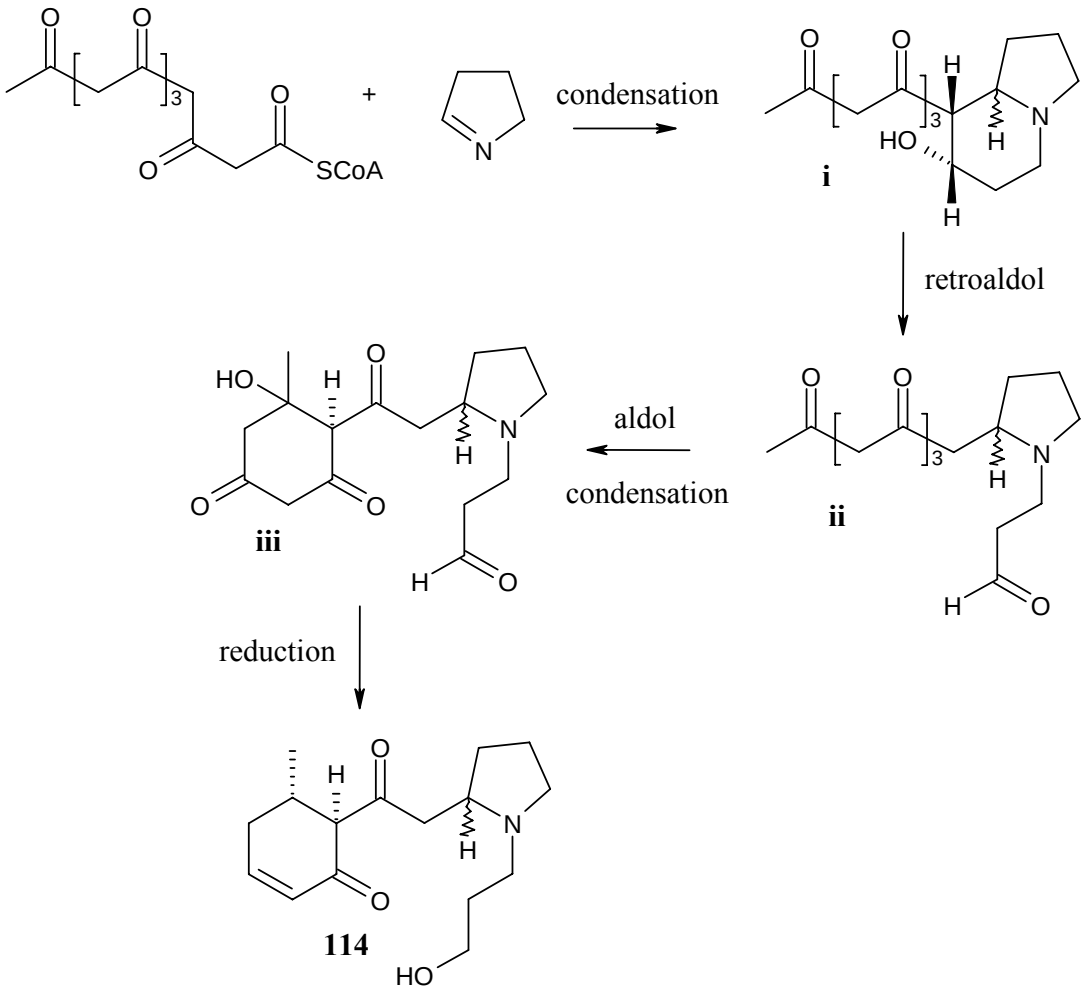


**Figure 28**. The proposed retroaldol biosynthetic pathway for the formation of habbenine (**114**).

The first mechanism is presented in Figure 28, which is proposed to occur in a similar manner to the $C_{16}$ *Elaeocarpus* indolizidine alkaloids. Condensation of a $C_{12}$ polyketide with dihydropyrrole yields the precursor (**i**). Enzymatic modification of (**i**) by a retroaldol reaction may produce the aldehyde precursor (**ii**). A subsequent aldol condensation would form the six-membered carbon ring in (**iii**). Reduction of the aldehyde in (**iii**) may yield the *N*-propanolpyrrolidine functionality. This functionality is a unqiue structural feature of habbenine (**114**) and distinguishes it from other *Elaeocarpus* and *Peripentadenia*

alkaloids. Further reduction of (**iii**) could lead to the formation of the methylcyclohexenone moiety.

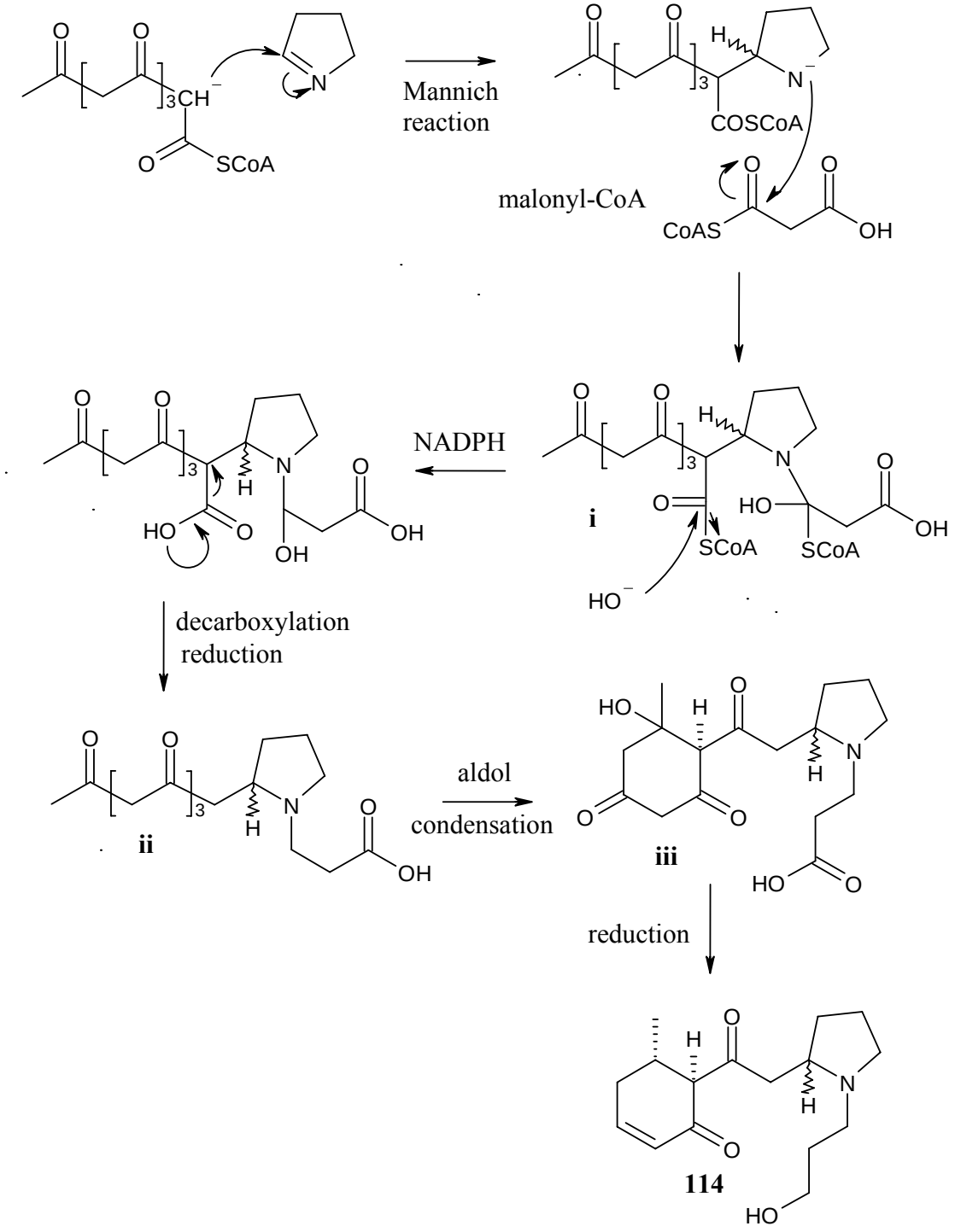


**Figure 29.** The proposed malonyl-CoA biosynthetic pathway for the formation of habbenine (**114**).

The second proposed biosynthesis of **114** (Figure 29) involves the addition of a $C_{10}$ polyketide, followed by nucleophilic attack of malonyl-CoA. The addition of a $C_{10}$ poplyketide to the dihydropyrrole could occur by a Mannich reaction. This type of reaction has been suggested in the formation of tropane alkaloids such as cocaine (**6**).[4]

Following the addition of the $C_{10}$ polyketide in Figure 29, the electron rich nitrogen could then act as a nucleophile in an attack of malonyl-CoA. The resulting adduct (**i**) could then undergo a hydrolysis and decarboxylation to yield (**ii**). Aldol condensation to give precursor (**iii**), and subsequent reduction would afford habbenine (**114**).

## 3.5 Habbenine as a Potential Inhibitor of Ion Channels

The carbon skeleton of habbenine (**114**) shows reasonable overlap with the structure of levobupivacaine (**121**). In 2000[5] levobupivacaine was approved as a local anaesthetic with a long mode of action.[6, 7] This compound has been shown to act as an inhibitor of voltage-gated sodium channels in peripheral nerves.[8] A potential side effect of this compound is cardiac depression.[6, 8] Habbenine (**114**) may therefore have potential as an inhibitor of sodium ion channels. However, no biological testing in this area was performed. There is the potential to evaluate habbenine against voltage-gated ion channels in the future.

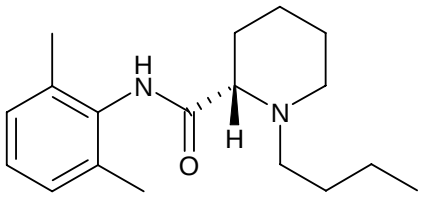


**121**

## 3.6 References


1. Communication with Topul Rali, collector.
2. Lamberton, J. A., Gunawardana, Y. A. G. P., Bick, I. R. C., *J Nat Prod* **1983,** 46, 235 - 247.
3. Saito, K., Murakoshi, I., *Genes in Alkaloid Metabolism*. In *Alkaloids: Biochemistry, Ecology and Medicinal Applications*, 1st ed.; Roberts, M. F., Wink, M., Eds. Plenum Press: New York, **1998**; pp. 147 - 157.
4. Dewick, P. M., *Medicinal Natural Products: A Biosynthetic Approach*. 2nd ed.; Wiley: Chichester, **2001**.
5. Proudfoot, J. R., *Bioorg Med Chem Lett* **2002,** 12, 1647 - 1650.
6. Kumar, S., Ramachandran, U., *Tetrahedron Lett* **2005,** 46, 19 - 21.
7. Bardsley, H., Gristwood, R., Baker, H., Watson, N., Nimmo, W., *Br J Clin Pharmacol* **1998**, 46, 245 - 249.
8. McLeod, G. A., Burke, D., *Anaesthesia* **2001,** 56, 331 - 341.

# CHAPTER 4 – Isolation and Structure Elucidation of Indolizidine Alkaloids from *Elaeocarpus fuscoides.*

## 4.1 Introduction

*Elaeocarpus fuscoides* Knuth. is a rainforest tree which grows in the mountainous regions of PNG. The phytochemical survey of the plants of the Elaeocarpaceae identified *E. fuscoides* as a potential source of alkaloids. This chapter is the first chemical investigation of this species. Leaves of *E. fuscoides* were collected in August 1999 from the Kirene forest, near Ialibu in the Southern Highlands Province of PNG. This chapter details the isolation and structural elucidation of four indolizidine alkaloids from this species, including the new compound elaeocarpenine (**122**). The known alkaloids isoelaeocarpicine (**62**), isoelaeocarpine (**61**) and elaeocarpine (**60**) were also purified from this plant. A base free extraction procedure was employed in the purification of alkaloids from the leaves of *E. fuscoides*. This investigation also reports the first complete discussion of the NMR data of **60** – **62**.[1]

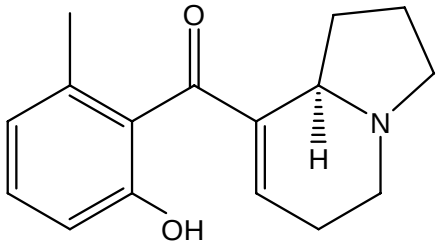


**122**

Elaeocarpenine (**122**) was purified from the extract as the major component. The diastereomers isoelaeocarpine (**61**) and elaeocarpine (**60**) were also isolated, with **61** purified as the major diastereomer. Treatment of elaeocarpenine **122** with $NH_3$ yielded a 1:1 mixture of the diastereomers **60** and **61**. It could therefore be hypothesized that elaeocarpenine (**122**) is the biogenetic precursor of **60** and **61**.

## 4.2 The Isolation of Indolizidine Alkaloids from the Leaves of *E. fuscoides*

The purification of elaeocarpenine (**122**), isoelaeocarpine (**61**), elaeocarpine (**60**) and isoelaeocarpicine (**62**) is depicted in Scheme 4. The alkaloids were isolated as their TFA salts, as a consequence of the use of TFA during the extraction procedure. A methanol extract of the leaves of *E. fuscoides* was filtered through SCX resin. The resin was washed sequentially with methanol and water prior to elution with 1M NaCl. The alkaloids were eluted in the NaCl fraction. Separation was achieved by C18 RP silica gel chromatography. NaCl was removed by washing with copious amounts of $H_2O$ prior to elution of the alkaloids with 1%TFA/MeOH.

The resulting alkaloid fraction was separated by preparative C18 RP-HPLC, using a linear gradient from $H_2O$ to 1%TFA/MeOH over 100 minutes. Fifty fractions were collected and analysed by positive ESIMS. Mass ion peaks were observed at *m/z* 276 in fractions 13 – 20, and *m/z* 258 in fractions 21 - 24 and 26 – 31. The $^1$H NMR spectra of individual fractions showed semi-pure isoelaeocarpicine (**62**) in fractions 13 - 20, pure elaeocarpenine (**122**) in fractions 21 - 24, and a mixture of two compounds in fractions 26 - 31. Fractions 21 - 24 were combined to yield elaeocarpenine (**122**) (94.7 mg, 0.079%).

Fractions 13 - 20 were combined and separated by semi-preparative C18 RP-HPLC employing a gradient of 3:1 $H_2O$: 1%TFA/MeOH to 1%TFA/MeOH over 15 minutes. The presence of isoelaeocarpicine (**62**) was monitored by positive ESIMS, and the fractions were combined to yield isoelaeocarpicine (**62**) (4.0 mg, 0.0033%).

Purification of the two compounds detected in fractions 26 - 31 was performed by C18 RP-HPLC, with a gradient of 1:1 $H_2O$: 1%TFA/MeOH to 1%TFA/MeOH over 15 minutes. Analysis of the fractions afforded isoelaeocarpine (**61**), 38.7 mg (0.032%) and elaeocarpine (**60**), 17.6 mg (0.011%).

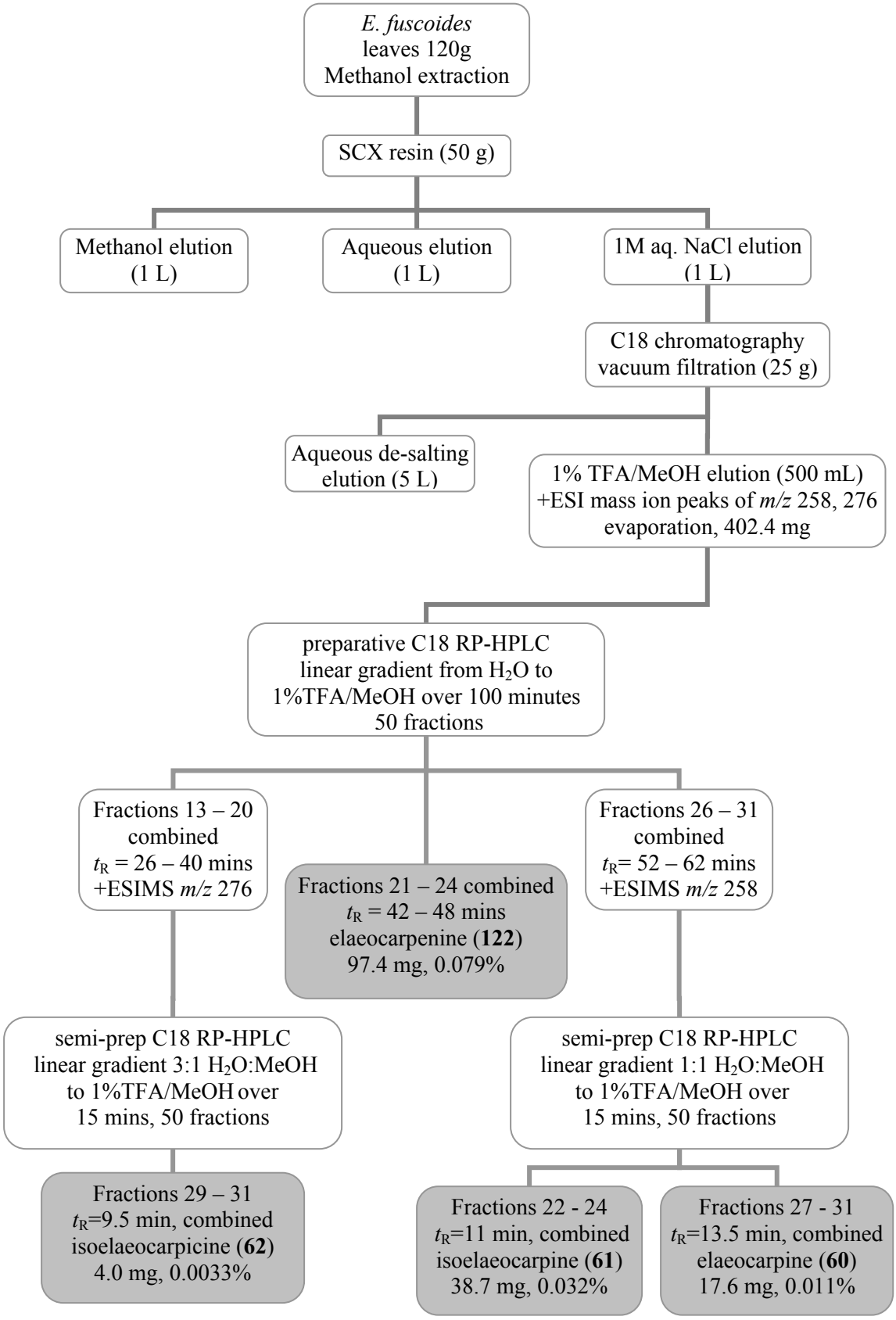


**Scheme 4.** The isolation of indolizidine alkaloids from *E. fuscoides*.

## 4.3 Structure Elucidation of Elaeocarpenine (122)

Elaeocarpenine (**122**) was assigned the molecular formula $C_{16}H_{20}NO_2$ by high resolution positive electrospray mass measurement of the $[M + H]^+$ ion (258.1490). Inspection of the $^1H$ NMR spectrum of **122** (Figure 30) revealed the presence of an olefinic methyl group (δ 2.02 ppm) and four olefinic protons. Two of these protons were doublets, δ 6.72 and 6.68, and one was a triplet at 7.12 ppm. This suggested a 1,2,3-tri-substituted aromatic system. The fourth olefinic proton, δ 6.60 ppm, resonated as a broad triplet. The upfield region of the spectrum contained signals at δ 1.18, 3.16, 3.57 and 4.51 which integrated to one proton each, δ 2.07 and 3.31 which integrated to two protons each, and δ 2.53 ppm which integrated to three protons.

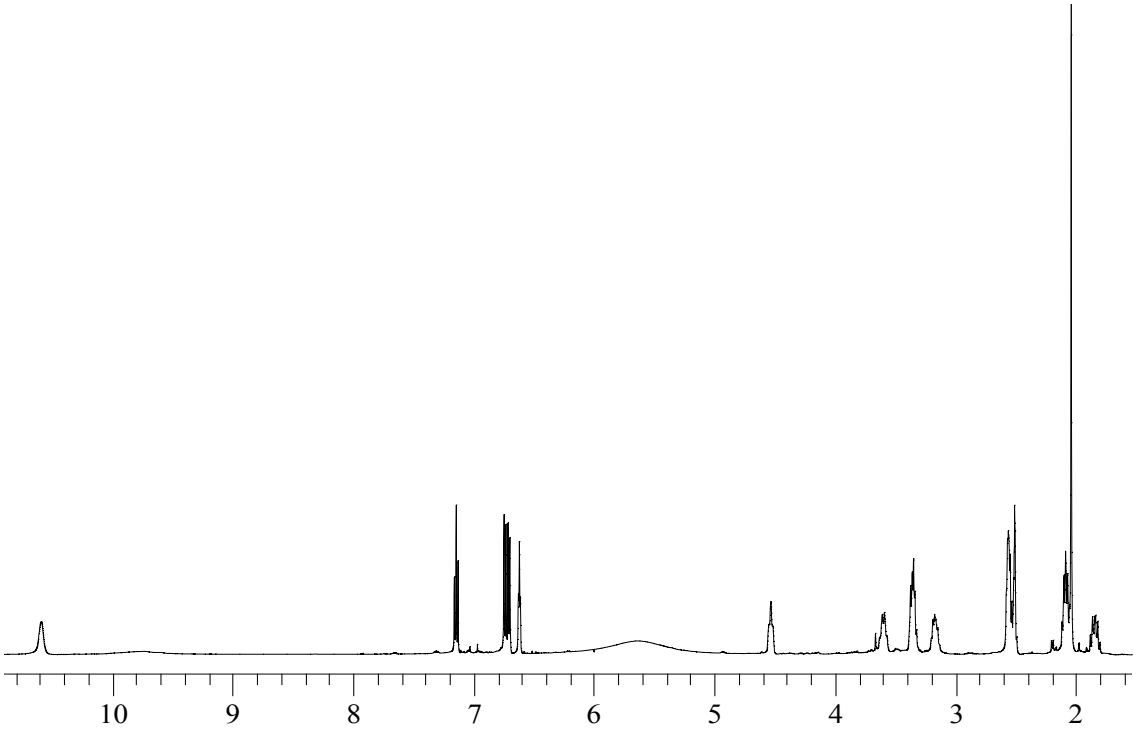


**Figure 30.** The $^1H$ NMR spectrum of elaeocarpenine (**122**) at 600 MHz in $d_6$-DMSO.

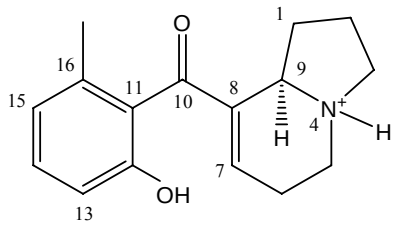


**Table 6.** $^{1}H$,[a] $^{13}C$[b] and HMBC NMR spectral data of elaeocarpenine (**122**)[c]

| position | $\delta_C$ | $\delta_H$ (mult; *J* in Hz) | HMBC $^{2,3}J_{CH}$ |
|---|---|---|---|
| 1 | 28.2 | 2.53 (1H, m) | 2, 3, 8, 9 |
| | | 1.81 (1H, ddd, 6.0, 10.8, 15.6) | |
| 2 | 20.6 | 2.07 (2H, t, 8.4) | 1, 3, 9 |
| 3 | 52.7 | 3.57 (1H, dd, 2.4, 13.2) | 1, 2, 5, 9 |
| | | 3.31 (1H, m) | |
| 4 | - | 10.82 (1H, s) | - |
| 5 | 43.4 | 3.31 (1H, m) | 3, 6, 7, 9 |
| | | 3.16 (1H, br) | |
| 6 | 22.5 | 2.53 (2H, m) | 5, 7, 8 |
| 7 | 140.4 | 6.60 (1H, dd, 4.8, 4.8) | 5, 6, 9, 10 |
| 8 | 135.5 | - | - |
| 9 | 58.1 | 4.51 (1H, brdd, 9.6, 9.6) | 1, 5, 7, 8 |
| 10 | 196.7 | - | - |
| 11 | 126.0 | - | - |
| 12 | 154.2 | - | - |
| 13 | 113.0 | 6.72 (1H, d, 9.6) | 10, 11, 12, 15, 16 |
| 14 | 129.9 | 7.12 (1H, dd, 9.6, 9.0) | 11, 12, 13, 15, 16 |
| 15 | 120.5 | 6.68 (1H, d, 9.0) | 10, 11, 12, 13, 14, 16, 17 |
| 16 | 136.5 | - | - |
| 17 | 18.4 | 2.02 (3H, s) | 11, 15, 16 |

[a] At 600 MHz. [b] At 125 MHz. [c] In $d_6$-DMSO.

The $^{13}C$ NMR spectrum of **122** showed 16 carbons. The chemical shifts of two carbons at δ 154.2 and 196.7 ppm indicated that an oxygenated aromatic carbon and α,β-unsaturated ketone were present. This was confirmed by an IR absorption band at 1683 $cm^{-1}$. A further seven carbons resonated in the downfield region of the $^{13}C$ spectrum. Carbons at δ 43.4, 52.7 and 58.1 ppm were observed and suggested that these carbons were bound to heteroatoms. The remaining signals comprised a methyl at δ 18.4 and three aliphatic methylenes at δ 20.6, 22.5 and 28.2 ppm. The $^{1}H$ and $^{13}C$ NMR spectral data of **122** is shown in Table 6.

An HSQC experiment established the presence of 18 carbon bound protons (one methyl, five methylenes, one methine and four olefinic protons). The partial structures illustrated in Figure 31 were established from a COSY experiment. The first aliphatic fragment was assembled from correlations from the methylene protons H-3 and H-11 at δ 3.57/3.31 and 2.53/1.81, respectively, to the methylene H-2 at 2.07 ppm. The attachment of the methine proton at δ 4.51 ppm (H-9) was determined from a COSY correlation to the methylene protons at position 1 (δ 2.53/1.81 ppm). A second aliphatic fragment was constructed from correlations from the H-5 methylene protons at δ 3.31/3.16 and the olefinic proton at 6.60 (H-7) to the methylene protons at 2.53 ppm (H-6). This partial structure accounted for two olefinic carbons. The final fragment was formed from correlations from the aromatic doublets δ 6.68 and 6.72 to 7.12 ppm. An aromatic ring was constructed from these protons and the six remaining $sp^2$ hybridized carbons. The HSQC spectrum demonstrated that the proton at δ 6.72 (H-13) was attached to a carbon at δ 113.0 ppm. In an aromatic system, this chemical shift is typical for a carbon that is *ortho* to an oxygenated quaternary carbon. Strong COSY correlations from the exchangeable proton at δ 10.82 to 4.51, 3.16, and 3.57 suggested C-3, C-5 and C-9 formed the *N*-carbons of the pyrrolidine ring.

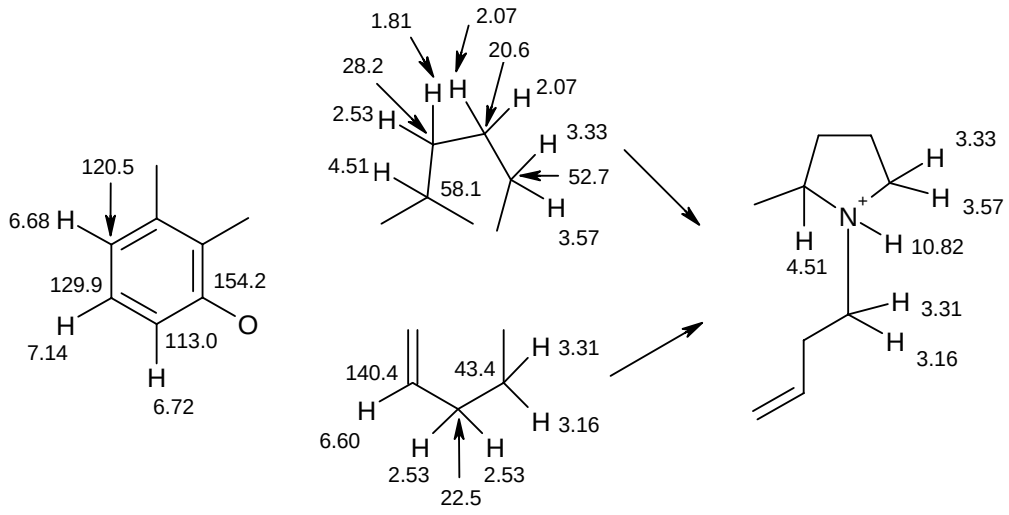


**Figure 31.** Partial structures of elaeocarpenine (**122**) established from COSY and HSQC experiments.

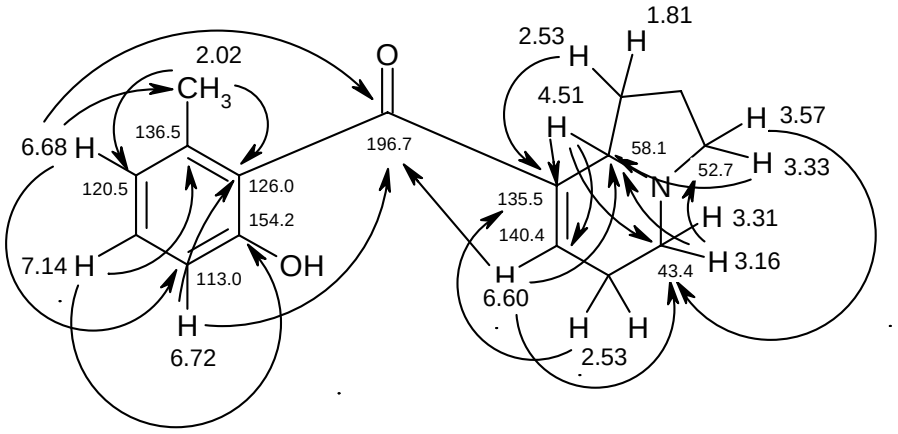


**Figure 32.** Key HMBC correlations used to establish the structure of elaeocarpenine (**122**).

Correlations observed in an HMBC experiment (Figure 32) established the connection of the partial structures. Correlations from the methylene H-3 (3.31/3.57) to C-5 (43.4), from H-3 and H-5 (3.31/3.16) to C-9 (58.1), from H-9 (4.51) to C-5 and C-7 (140.4), and from H-1 (2.53/1.81) and H-7 (6.60) to C-8 (135.5), secured the structure of the indolizidine moiety. The methylphenol moiety was constructed from correlations of H-

$17_{Me}$ (2.02) to C-15 (120.5), H-14 (7.12) to C-16 (136.5), H-15 (6.68), H-13 (6.72) and H-$17_{Me}$ to C-11 (126.0), and from H-14 to the phenolic carbon C-12 (154.2). The indolizidine and methylphenol moieties were connected by correlations from H-7 to the ketone C-10 (196.7), and four-bond correlations from H-13 and H-15 to C-10. Thus the structure of the salt of elaeocarpenine (**122**) was established.

The stereochemistry of H-9 relative to H-4 is proposed to be *trans*-diaxial. This was supported by the two large coupling constants observed for H-9 ($J$ = 9.6, 9.6) which is typical for an axial proton. An intense COSY correlation between δ 4.51 (H-9) and 10.82 (H-4), provided further evidence for the axial-axial relationship between these protons. An analogous measurement has been observed between the proton alpha to the nitrogen and the nitrogen lone pair in other indolizidine[1] structures. Therefore, the same *trans*-diaxial configuration may exist in elaeocarpenine trifluoroacetate (**122**). The energy minimized structure of elaeocarpenine (**122**) is shown in Figure 33. The six membered nitrogen heterocycle is depicted in a pseudo-boat conformation.

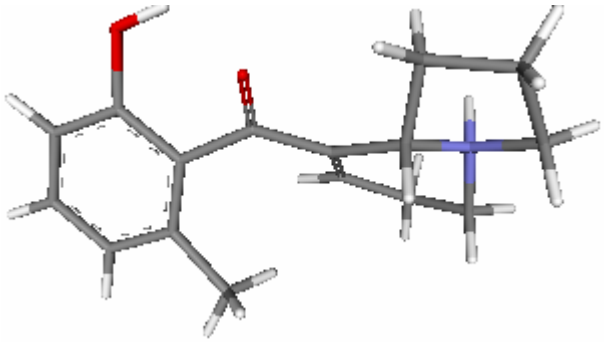

**Figure 33**. The energy minimized structure of elaeocarpenine (**122**).

The measurement of the optical rotation of the new compound elaeocarpenine (**122**) provided a value of $0^{o}$, indicating that elaeocarpenine was isolated as a racemate.

## 4.4 Structure Elucidation of Isoelaeocarpicine (62)

The $^{1}H$ NMR spectrum of isoelaeocarpicine (**62**) in $d_6$-DMSO (Figure 34), compared well with the previously published spectrum which was acquired at 100 MHz in $CDCl_3$.[2] The most noticeable difference between these spectra was the observation of the exchangeable protons in Figure 34. The positive ESI mass spectrum of isoelaeocarpicine (**62**) showed a dehydration product which could be elaeocarpenine (**122**). The reported mass spectrum also showed a dehydration product.[1] The $^{1}H$ and $^{13}C$ NMR spectral data of **62** is detailed in Table 7.

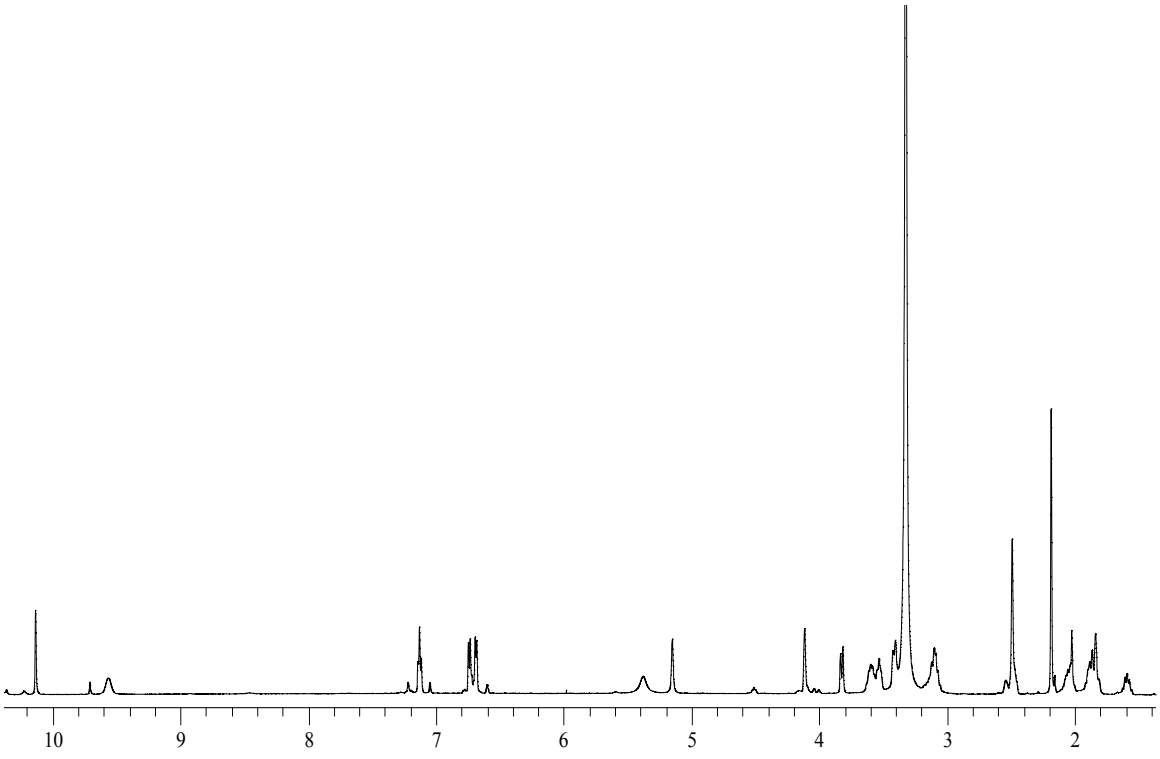


**Figure 34**. The $^{1}H$ NMR spectrum of isoelaeocarpicine (**62**) acquired at 600 MHz in $d_6$-DMSO.

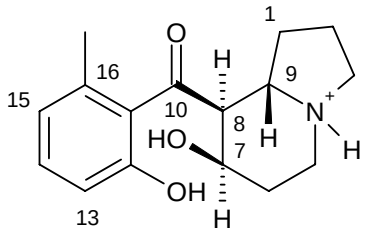


**Table 7.** $^{1}H$,[a] $^{13}C$[b] and HMBC NMR Spectral data of isoelaeocarpicine (**62**)[c]

| position | $\delta_C$ | $\delta_H$ (mult; *J* in Hz) | HMBC $^{2,3}J_{CH}$ |
|---|---|---|---|
| 1 | 26.6 | 2.49 (1H, m) | 2, 3, 8, 9 |
| | | 1.61 (1H, ddd, 2.4, 10.8, 18.0) | |
| 2 | 19.2 | 2.03 (1H, dddd, 1.8, 6.0, 6.0, 15.6) | 1, 3, 9 |
| | | 1.84 (1H, dddd, 2.4, 11.4, 11.4, 18.0) | |
| 3 | 51.3 | 3.59 (1H, ddd, 2.4, 2.4, 9.6) | 1, 5, 9 |
| | | 3.08 (1H, m) | |
| 4 | - | 9.56 (1H, br) | |
| 5 | 44.8 | 3.41 (1H, dd, 2.4, 12.6) | 6, 7 |
| | | 3.08 (1H, m) | |
| 6 | 30.9 | 1.87 (2H, t, 16.8) | 5, 7, 8, 10 |
| 7 | 63.1 | 4.12 (1H, br) | 5, 6, 9, 10 |
| 8 | 56.2 | 3.82 (1H, brd, 10.8) | |
| 9 | 60.4 | 3.53 (1H, ddd, 2.4, 11.4, 11.4) | |
| 10 | 203.0 | - | |
| 11 | 125.7 | - | |
| 12 | 154.8 | - | |
| 13 | 113.3 | 6.74 (1H, d, 7.8) | 10, 11, 12, 15, 16 |
| 14 | 130.6 | 7.13 (1H, dd, 7.8, 7.8) | 11, 12, 13, 15, 16 |
| 15 | 121.6 | 6.68 (1H, d, 7.8) | 11, 12, 13, 14, 16, 17 |
| 16 | 136.5 | - | |
| 17 | 19.2 | 2.19 (3H, s) | 10, 11, 15, 16 |
| C-7-OH | - | 5.15 (1H, s) | |
| C-12-OH | - | 10.13 (1H, s) | |

[a] At 600 MHz. [b] At 125 MHz. [c] In $d_6$-DMSO.

Figure 34 reveals the presence of an aromatic methyl group and three aromatic protons. A slight difference in the chemical shift of the methyl group in isoelaeocarpicine, δ 2.19, was noted when compared to elaeocarpenine (**122**) (δ 2.02 ppm). The aromatic protons resonated at δ 7.13, 6.74 and 6.68 ppm respectively, which is almost identical to the chemical shifts of the aromatic protons of elaeocarpenine (**122**). Other signals in the upfield region of the $^{1}H$ spectrum contained resonances at δ 1.61, a multiplet at 1.85 which intregrated to three protons, a proton at 2.03 (1H, m), and a group of four signals between 3.0 and 3.6 ppm. The signal at δ 3.08 ppm integrated to two protons. A resonance at δ 4.12 indicated an oxygenated methine, and another proton was observed at 3.82 ppm.

The $^{13}C$ spectrum of isoelaeocarpicine (**62**) showed a carbonyl carbon at δ 203.0 ppm. This was a significant shift downfield of 6.3 ppm from the carbonyl carbon observed in elaeocarpenine (**122**) and suggested a saturated ketone was present in isoelaeocarpicine (**62**). Six carbons were observed between δ 110 and 160 ppm, suggesting the presence of an aromatic ring. The carbon chemical shift at δ 154.8 ppm was indicative of an oxygenated aromatic carbon. Five carbons were observed between δ 40 and 70 ppm, which indicated the presence of either bridge-head carbons or carbons bound to heteroatoms. The remaining signals comprised two carbons at δ 19.2, and methylene carbons at 26.6 and 30.9 ppm.

The partial structures depicted in Figure 35 were established from correlations observed in the COSY and HSQC spectra of isoelaeocarpicine (**62**). The HSQC correlations indicated 16 carbon bound protons were present in (**62**) comprising one methyl, five methylenes, three methines, and three olefinic protons. An aromatic fragment was constructed from the three $sp^2$ hybridized protons. The doublet of doublets at δ 7.13 correlated to two doublets at 6.68 and 6.74 ppm in the COSY spectrum. The presence of an oxygenated carbon *ortho* to H-13 (δ 6.74 ppm) was determined in the same manner as for elaeocarpenine (**122**). A partial structure comprising an eight carbon fragment was assembled from COSY correlations between the methylene protons at H-3 and H-1 at 3.08/3.59 and 2.49/1.61, respectively, to the methylene protons H-2 (2.03/1.84).

Correlations from H-2 to H-9 (δ 3.53 ppm) allowed the connection of these protons. The proton at δ 3.82 (H-8) showed a correlation to H-9, indicating these two methines were adjacent to each other. An oxygenated methine at δ 4.12 (H-7) was found to correlate to H-8, to the exchangeable proton at 5.15 ppm and to the H-6 methylene at 1.87 ppm. This allowed the attachment of H-7 to H-8 and H-6, and confirmed the presence of a hydroxyl group at this position. Further correlations from H-6 to 3.08/3.41 allowed the attachment of the H-5 methylene. Correlations from the exchangeable proton at δ 9.56 ppm (H-4) to H-9 and the two methylenes H-3 and H-5, allowed the structure of the indolizidine moiety to be confirmed. Thus the two partial structures of isoelaeocarpicine (**62**) were established.

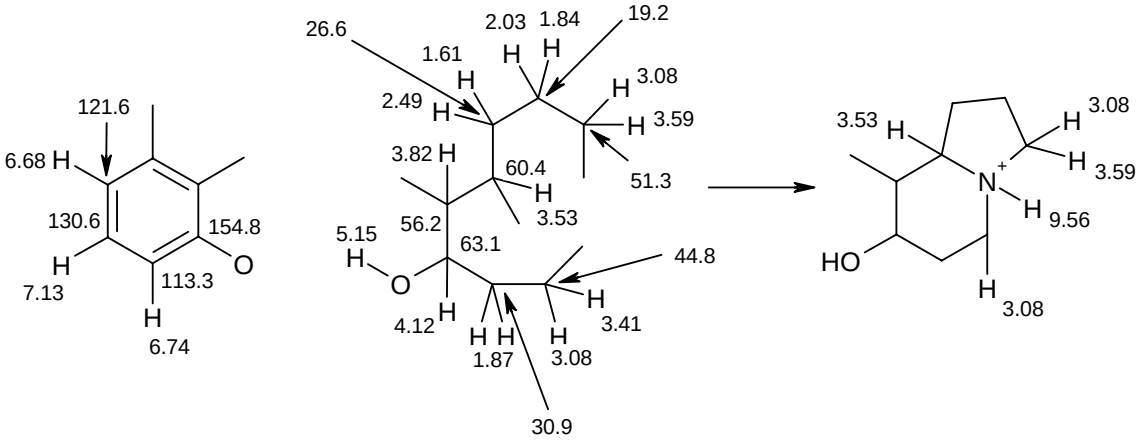


**Figure 35.** Partial structures of isoelaeocarpicine (**62**) established from COSY and HSQC experiments.

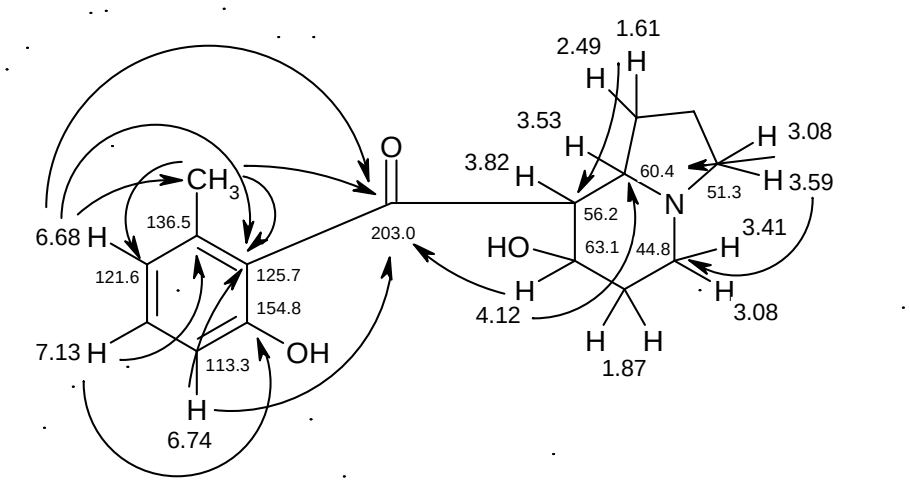


**Figure 36.** Key HMBC correlations used to establish the structure of isoelaeocarpicine (**62**).

HMBC correlations (Figure 36) from H-15 (6.68) to C-$17_{Me}$ (19.2), and from H-$17_{Me}$ (2.19) to C-15 (121.6) and C-11 (125.7) secured the structure of the methylphenol moiety. A correlation from H-14 (7.13) to C-12 (154.8) confirmed the position of the phenol and correlations from H-13 (6.74) and H-15 (6.68) to C-11 (125.7) provided further evidence for the structure. The 7-hydroxyindolizidine group was confirmed by HMBC correlations from H-3 (3.08/3.59) to C-5 (44.8) and C-9 (60.4), H-1 (2.49/1.61) to C-8 (56.2), and H-7 (4.12) to C-9 (60.4). No HMBC correlations were observed for H-8 (3.82) or H-9 (3.53). The connection of the 7-hydroxyindolizidine and the methylphenol moieties was confirmed by a correlation from H-7 (4.12) to C-10 and by four bond correlations from H-$17_{Me}$ (2.19), H-15 (6.68) and H-13 (6.74) to the carbonyl carbon at 203.0 (C-10). Thus the 2D structure of isoelaeocarpicine (**62**) was established and agrees with the structure published by Johns *et al*.[1] The energy minimized structure of isoelaeocarpicine is depicted in Figure 37.

The stereochemistry of H-8 relative to H-9 was established as axial-axial from the large coupling constant of 10.8 Hz between H-8 and H-9 (lit. 11.0 Hz).[1] H-7 resonated as a broad singlet. The relationship between H-4 (9.56) and H-9 is also proposed to be axial-axial, as a strong COSY correlation was observed. A ROESY correlation between H-7 and H-8 indicated a *cis* configuration, (Figure 38) suggesting that H-7 was equatorial. The relative stereochemistry determined for isoelaeocarpicine (**62**) is therefore consistent with the literature. The reported optical rotation for **62** was $+29^{o}$,[1] and the measured optical rotation of isoelaeocarpicine trifluoroacetate was $+9.25^{o}$. The rotation determined in this study was on the TFA salt in MeOH compared to the reported rotation of the free base in chloroform. In the work of Johns *et al.*,[1] only the relative stereochemistry of (+)-isoelaeocarpicine was reported, however the relationship between the optical rotation and absolute stereochemistry of elaeokanine C (**77**) was highlighted by synthetic studies.[2] Elaeokanine C (**77**) possesses the same 7-hydroxy-8-ketoindolizidine group as isoelaeocarpicine (**62**). The optical rotation of synthetic 7-*S*-8-*R*-9-*R* elaeokanine C was +36.9, and this indicated that (+)-isoelaecarpicine was purified as the 7-*S*-8-*R*-9-*R* isomer.

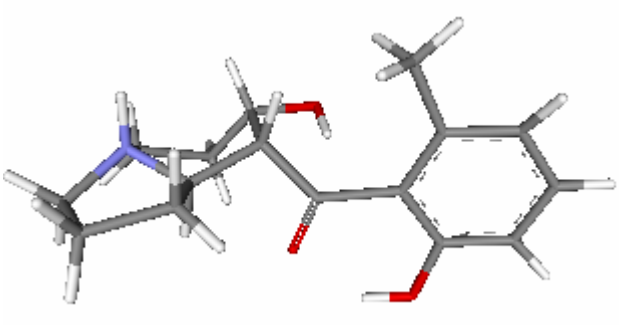

**Figure 37**. The energy minimized structure of isoelaeocarpicine (**62**).

The sharpness of the hydroxyl exchangeable protons at δ 10.13 and 5.15 ppm suggested hydrogen bonding interactions with the oxygen of the ketone. These interactions are shown in Figure 38 and may lead to the formation of pseudo-six-membered rings.

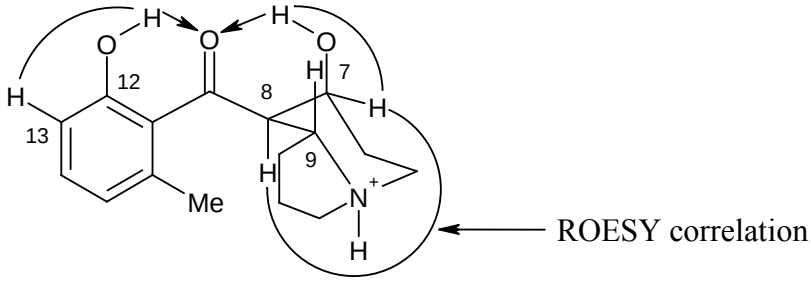


**Figure 38.** The H-bond interactions and ROESY correlations observed for isoelaeocarpicine (**62**).

## 4.5 Structure Elucidation of Isoelaeocarpine (61)

The $^{1}$H NMR spectrum of isoelaeocarpine (**61**) (Figure 39) shows three aromatic protons, a doublet of doublets at δ 7.47, and two doublets at 6.96 and 6.91 ppm. A proton was observed at 4.91 ppm (1H, brs) which suggests a proton bound to an oxygenated carbon. This proton shifted upfield to a narrow doublet at δ 4.65 ppm, $J$ = 2.5 Hz in the $^{1}$H NMR spectrum acquired in $CD_2Cl_2$. In the published spectrum of isoelaeocarpine (100 MHz in $CDCl_3$)[1] this proton resonated as a narrow doublet of doublets at 4.64 ppm. The published spectrum also contained two doublets and a doublet of doublets in the aromatic region.

The upfield region of the $^{1}$H NMR spectrum of **61** consisted of an olefinic methyl group at δ 2.55, a broad signal at 1.90 which integrated to three protons, and a group of signals which integrated to one proton each at δ 1.78, 2.08, 2.29, 2.82, 3.07, 3.28, 3.45, 3.60 and 3.65 ppm. A total of 18 protons were found. The $^{1}$H and $^{13}$C NMR spectral data of isoelaeocarpine (**61**) are detailed in Table 8. The methyl groups in elaeocarpenine (**122**) and isoelaeocarpicine (**62**) were observed at δ 2.02 and 2.19 ppm, respectively. The downfield shift of the aromatic methyl group of isoelaeocarpine (**61**) (δ 2.55) suggests that it was significantly deshielded by the adjacent carbonyl.

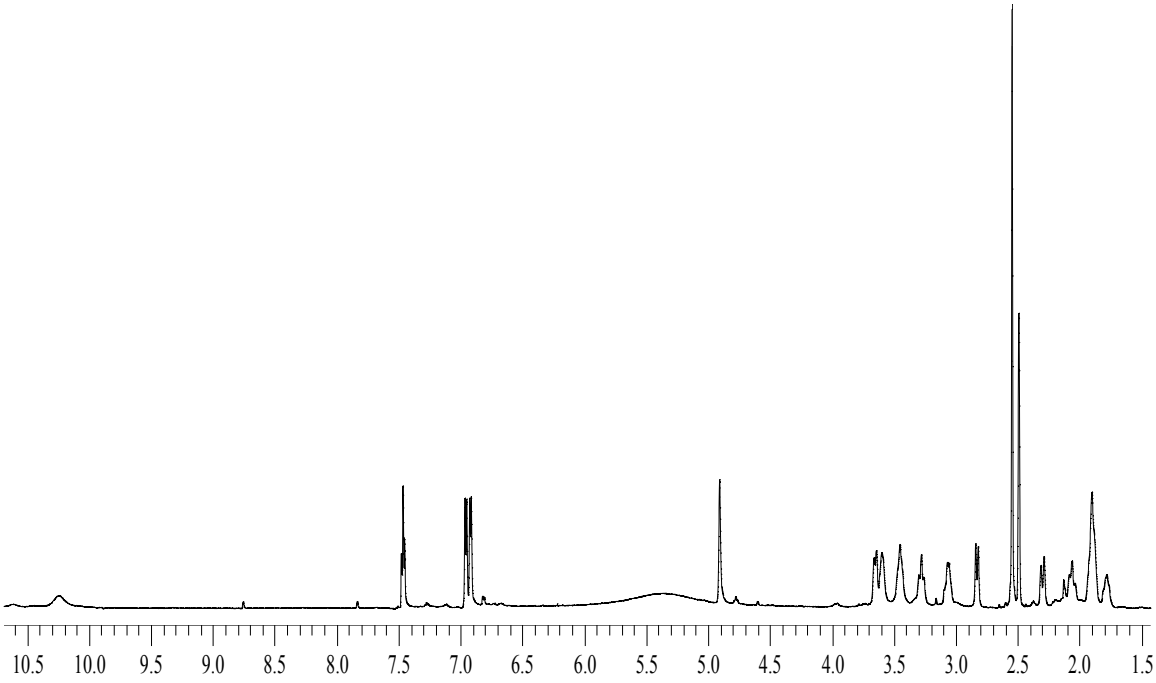


**Figure 39**. The $^{1}$H NMR spectrum of isoelaeocarpine (**61**) at 600 MHz in $d_6$-DMSO.

The $^{13}$C NMR spectrum of **61** showed a total of 16 carbons, the same number of carbons as elaeocarpenine (**122**) and isoelaeocarpicine (**62**). The positive ESIMS of isoelaeocarpine (**61**) showed a mass ion peak of *m/z* 258, which was identical to that of elaeocarpenine (**122**). However, the $^{13}$C NMR spectrum of **61** was distinctly different to that of **122**. Six $sp^2$ hybridized carbons were found, including an oxygenated quaternary carbon at δ 162.9 ppm. A ketone carbonyl carbon was observed at δ 194.6, and an oxygenated carbon at 74.5 ppm was also noted. The chemical shift of this carbon was typical for a carbon that was bound to an ether group. The remaining eight carbons were observed between δ 20 and 70 ppm.

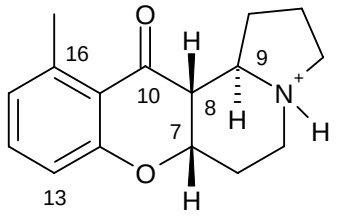


**Table 8.** $^{1}H$,[a] $^{13}C$[b] and HMBC NMR Spectral data of isoelaeocarpine (**61**).

| position | $\delta_C$ | $\delta_H$ (mult; *J* in Hz) | HMBC $^{2,3}J_{CH}$ |
|---|---|---|---|
| 1 | 28.7 | 1.78 (1H, ddd, 2.4, 10.8, 17.4) | 2, 3, 8, 9 |
| | | 1.90 (1H, m) | |
| 2 | 21.0 | 1.90 (2H, m) | 1, 3, 9 |
| 3 | 54.0 | 3.07 (1H, ddd, 2.4, 9.6, 18.0) | 1, 2, 9 |
| | | 3.60 (1H, ddd, 2.1, 2.1, 10.2) | |
| 4 | - | 10.23 (1H, brs) | |
| 5 | 47.4 | 3.28 (1H, ddd, 3.3, 12.0, 12.0) | 6, 7, 9 |
| | | 3.65 (1H, brdd, 2.4, 13.8) | |
| 6 | 30.2 | 2.29 (1H, brdd, 3.8, 15.6) | 5, 7, 8 |
| | | 2.08 (1H, brdd, 4.8, 15.6) | |
| 7 | 74.5 | 4.91 (1H, brs) | 5, 9 |
| 8 | 54.0 | 2.82 (1H, brd, 12.0) | 1, 9, 10 |
| 9 | 59.6 | 3.45 (1H, ddd, 6.0, 12.0, 12.0) | 2 |
| 10 | 194.6 | - | |
| 11 | 119.1 | - | |
| 12 | 162.9 | - | |
| 13 | 116.3 | 6.96 (1H, d, 7.8) | 10, 11, 12, 15 |
| 14 | 135.2 | 7.47 (1H, dd, 7.8, 7.8) | 12, 13, 15, 16 |
| 15 | 125.1 | 6.91 (1H, d, 7.8) | 10, 11, 12, 13, 16, 17 |
| 16 | 142.9 | - | |
| 17 | 23.1 | 2.55 (3H, s) | 10, 11, 15, 16 |

[a] At 600 MHz in $d_6$-DMSO. [b] At 125 MHz in $CD_2Cl_2$.

An HSQC experiment established the presence of 19 carbon bound protons, including one methyl, five methylenes, three methines and three aromatic protons. A COSY experiment was used to establish the partial structures illustrated in Figure 40. A 1,2,3-tri-substituted aromatic group was assembled from the six $sp^2$ hybridized carbons and COSY correlations from H-14 (δ 7.47) to H-13 (6.96) and H-15 (6.91 ppm). The HSQC spectrum demonstrated H-13 was attached to a carbon at δ 116.3 ppm, which indicated this proton was *ortho* to an oxygenated quaternary carbon. An eight-carbon partial structure was assembled from correlations from the H-2 methylene at δ 1.90 to the methylene protons H-1 (δ 1.90/1.78 ppm) and H-3 (δ 3.07/3.60 ppm). The connection between H-1 and H-9 was confirmed from COSY correlations from H-1 to δ 3.45 ppm (H-9). The methine H-8 (δ 2.82 ppm) correlated to H-9 and H-7 (δ 4.91 ppm) allowing, the attachment of C-7 (δ 74.5 ppm) and C-9 (δ 59.6 ppm) to C-8 (δ 54.0 ppm). The attachment of C-6 to C-7 and C-5 was deduced through COSY correlations from the H-6 methylene (δ 2.08/2.29 ppm) to H-5 (δ 3.28/3.65 ppm) and H-7. An exchangeable proton was observed at 10.23 ppm, however no COSY correlations were observed from this proton. An indolizidine functionality could not be created from the eight-carbon partial structure from COSY correlations.

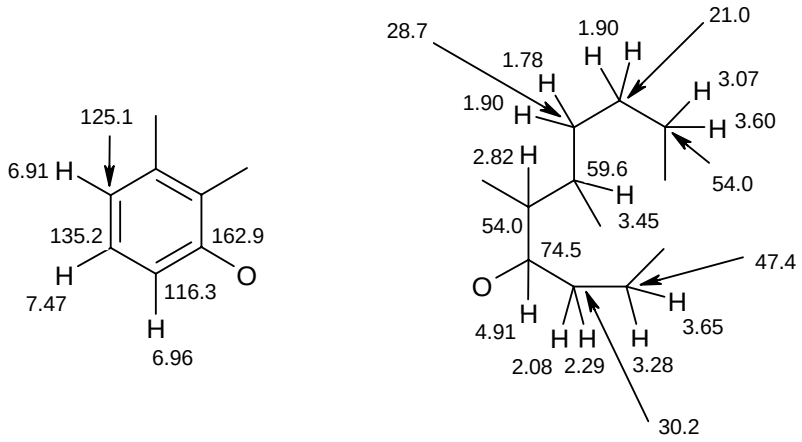


**Figure 40.** The partial structures of isoelaeocarpine (**61**) established from HSQC and COSY experiments.

HMBC correlations (Figure 41) from H-5 (δ 3.28/3.65 ppm), H-3 (δ 3.60/3.07 ppm) and H-7 (δ 4.91 ppm) to C-9 (δ 59.6 ppm) secured the structure of the indolizidine moiety. A

correlation was observed from H-8 (δ 2.82 ppm) to the ketone carbonyl carbon at δ 194.6 ppm (C-10). This established the structure of a 7-oxy-8-ketoindolizidine moiety. The structure of the tri-substituted aromatic group was confirmed by correlations from the methyl group (H-17, δ 2.55 ppm) to C-11 (δ 119.1 ppm), C-15 (δ 125.1 ppm) and C-16 (δ 142.9 ppm), from H-15 (6.91) to C-17 (23.1), from H-14 (δ 7.47 ppm) to C-12 (δ 162.9 ppm) and C-16 (δ 142.9 ppm), and H-13 (6.96) to C-11 (119.1). Four-bond correlations from H-$17_{Me}$, H-13 and H-15 to the ketone carbonyl carbon C-10 allowed the connection of the tri-substituted aromatic to the ketone of the indolizidine moiety. An ether linkage between C-7 and C-12 was suggested by MS evidence and by the carbon chemical shift of C-7. H-7 showed no HMBC correlation to C-12. The absence of an HMBC correlation from H-7 to C-12 was suggestive of a 90$^{o}$ torsion angle between H-7 and C-12. Thus the structure of the salt of isoelaeocarpine (**61**) was established.

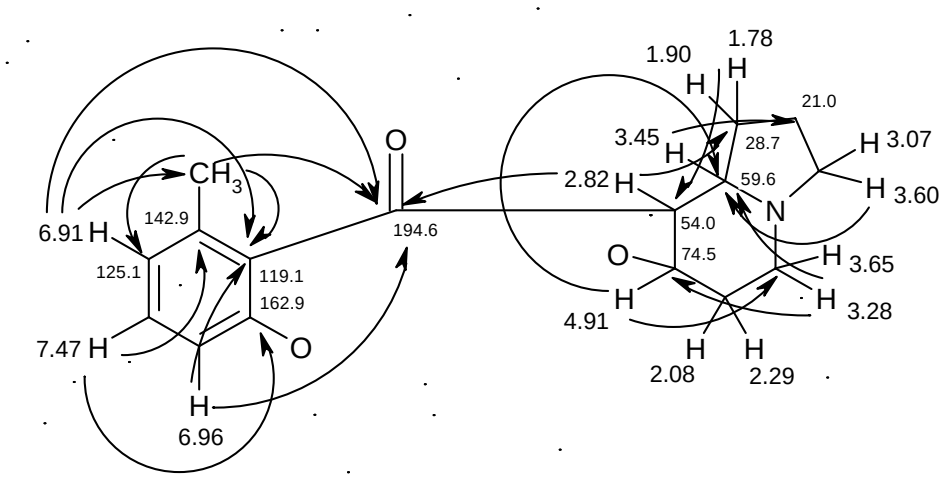


**Figure 41.** Key HMBC correlations used to establish the structure of isoelaeocarpine (**61**).

Coupling constants and ROESY correlations were used to establish the relative stereochemistry of isoelaeocarpine (**61**). No coupling information could be determined for H-7, however H-8 and H-9 both exhibited large couplings of 12.0 Hz. This suggested that H-8 and H-9 are both axial. A ROESY correlation between H-8 and H-7 (Figure 42) suggested these protons were *cis* to each other, therefore indicating H-7 was equatorial. The absence of a ROESY correlation from H-9 to either H-8 or H-7 suggested that this

proton is *trans* to both of these protons. H-7 exhibited a coupling constant of 2.5 Hz in the $^1$H NMR spectrum in $CD_2Cl_2$ which was typical for an equatorial proton. This coupling may be to either H-8, H-$6_{ax}$ or H-$6_{eq}$. Thus the relative stereochemistry of isoelaeocarpine (**61**) was established and was consistent with the published structure.

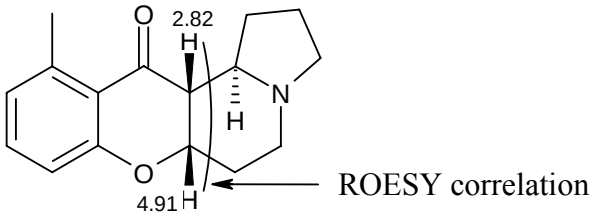


**Figure 42.** The key ROESY correlations of isoelaeocarpine (**61**).

The optical rotation of isoelaeocarpine (**61**) was measured as +14.49$^o$, indicating that **61** had been isolated as a partial racemate. Isoelaeocarpine (**61**) and elaeocarpine (**60**) were both reported to have high optical rotations.[1] The energy minimized structure of **61** is represented in Figure 43.

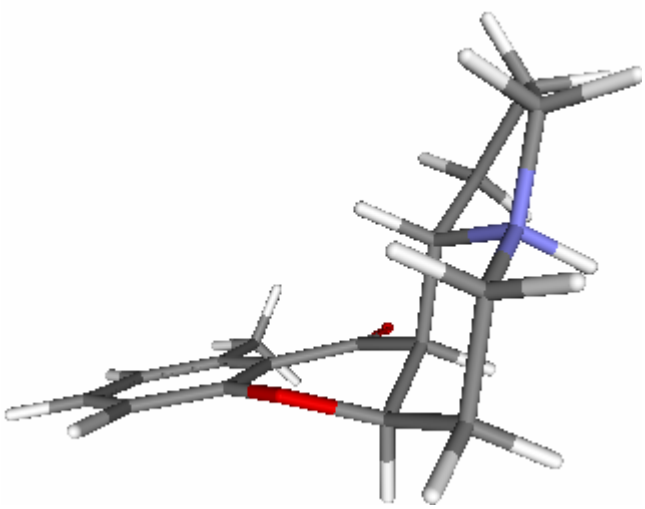

**Figure 43**. The energy minimized structure of isoelaeocarpine (**61**).

## 4.6 Structure Elucidation of Elaeocarpine (60)

Three aromatic protons, two doublets at δ 6.90 and 6.91 ppm, and a doublet of doublets at 7.43 ppm were observed in the $^{1}$H NMR spectra of elaeocarpine (**60**) in $d_6$-DMSO (Figure 44). Figure 44 was similar to Figure 39 in that it also possessed an oxygenated methine proton, resonating at 4.60 ppm. This was a significant upfield (0.31 ppm) shift from that observed in isoelaeocarpine (**61**). The positive LRESIMS of elaeocarpine (**60**) was identical to that of isoelaeocarpine (**61**), suggesting **60** was an isomer of **61**. Additional information gained from Figure 44 suggested the presence of an aromatic methyl group at δ 2.52 ppm. A group of five signals between 3.0 and 4.0 ppm and seven protons from 1.77 to 3.0 ppm, were consistent for the protons of the indolizidine functionality.

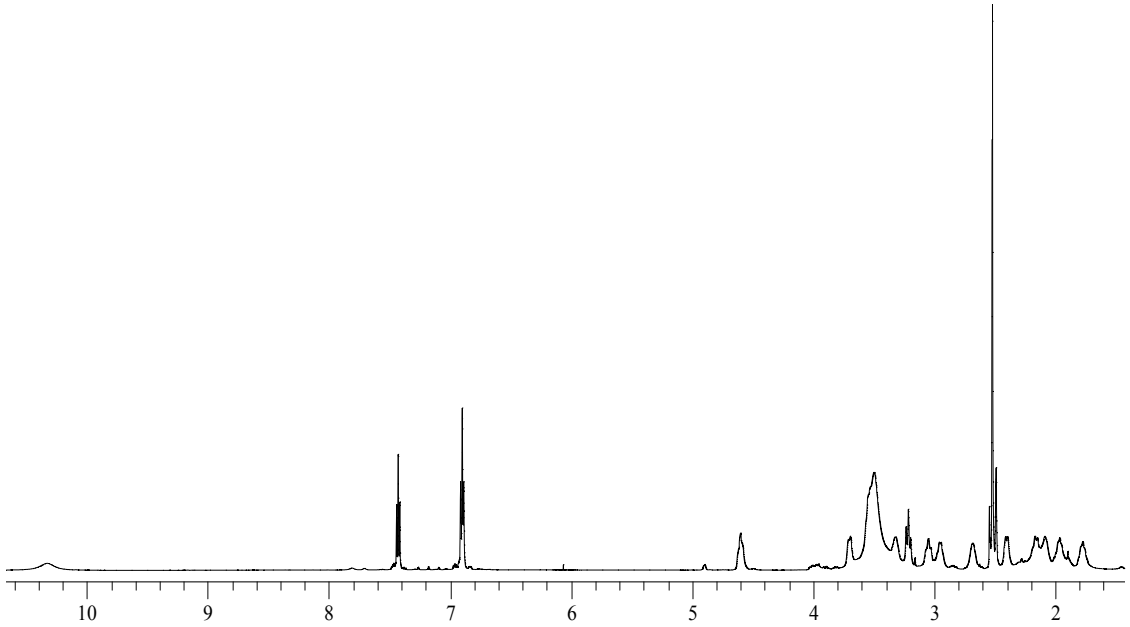


**Figure 44**. The $^{1}$H NMR spectrum of elaeocarpine (**60**) at 600 MHz in $d_6$-DMSO.

The $^{1}$H NMR spectrum of **60** was also acquired in $CD_2Cl_2$ and the oxygenated methine proton (H-7) at δ 4.60 shifted upfield to a ddd at δ 4.26 ppm, $J$ = 3.0, 7.5, 12.5 Hz. This was found to be analogous with the proton at 4.15 ppm in the published spectrum of elaeocarpine at 100 MHz in $CDCl_3$.[1] This proton exhibited couplings of 11.8 and 7.8 Hz in the published spectrum. The $^{1}$H and $^{13}$C NMR spectral data for elaeocarpine (**60**) is detailed in Table 9.

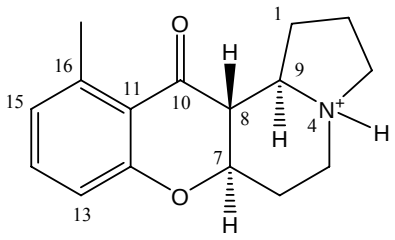


**Table 9.** $^{1}H$,[a] $^{13}C$[b] and HMBC NMR Spectral data of elaeocarpine (**60**).

| position | $\delta_C$ | $\delta_H$ (mult; *J* in Hz) | HMBC $^{2,3}J_{CH}$ |
|---|---|---|---|
| 1 | 29.7 | 2.68 (1H, br) | 2, 9 |
| | | 1.77 (1H, ddd, 1.8, 11.4, 18.0) | |
| 2 | 22.1 | 1.96 (1H, brdd, 10.8, 10.8) | 1, 3 |
| | | 2.09 (1H, br) | |
| 3 | 52.5 | 3.50 (1H, m) | 2, 5, 9 |
| | | 2.95 (1H, brdd, 9.6, 18.0) | |
| 4 | - | 10.36 (1H, br) | |
| 5 | 48.8 | 3.03 (1H, ddd, 3.0, 12.6, 18.0) | 3, 6, 7, 9 |
| | | 3.69 (1H, brdd, 4.8, 13.2) | |
| 6 | 30.3 | 2.15 (1H, ddd, 4.8, 12.0, 12.0) | 5, 7, 8 |
| | | 2.40 (1H, brdd, 3.6, 13.8) | |
| 7 | 77.8 | 4.60 (1H, ddd, 4.4, 12.0, 12.0) | |
| 8 | 52.8 | 3.21 (1H, dd, 11.4, 11.4) | 1, 7, 9, 10 |
| 9 | 63.7 | 3.32 (1H, brdd, 10.8, 10.8) | |
| 10 | 193.4 | - | |
| 11 | 120.0 | - | |
| 12 | 162.3 | - | |
| 13 | 116.0 | 6.90 (1H, d, 7.8) | 10, 11, 12, 14, 15 |
| 14 | 135.2 | 7.43 (1H, dd, 7.8, 7.8) | 11, 12, 16 |
| 15 | 125.2 | 6.90 (1H, d, 7.8) | 10, 11, 13, 14, 16, 17 |
| 16 | 142.3 | - | |
| 17 | 22.7 | 2.52 (3H, s) | 10, 11, 15, 16 |

[a] At 600 MHz in $d_6$-DMSO. [b] At 125 MHz in $CD_2Cl_2$.

The $^{13}C$ NMR spectrum of elaeocarpine (**60**) was almost identical to the spectrum of isoelaeocarpine (**61**), showing six aromatic protons and a ketone carbonyl carbon. The major differences were the shift of C-7 (74.5) and C-9 (59.6) in **61** to 77.8 and 63.7 in **60** respectively.

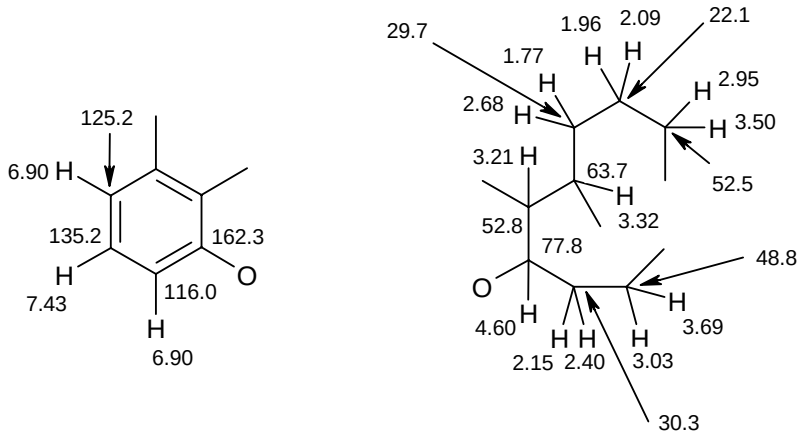


**Figure 45**. The partial structures of elaeocarpine (**60**) established from HSQC and COSY experiments.

The HSQC spectrum of **60** demonstrated the same number of methyls, methylenes, methines and olefinic protons as for isoelaeocarpine (**61**). The same partial structures as **61** were also determined for elaeocarpine (**60**) from a COSY experiment (Figure 45). An aromatic group was constructed from the six aromatic carbons and from COSY correlations from δ 7.43 (H-14) to 6.90 ppm (H-13 and H-15). HSQC correlations showed two carbons at δ 125.2 and 116.0 ppm for the protons at δ 6.90 ppm. The chemical shift of C-13 was consistent with a carbon *ortho* to an oxygenated quaternary carbon. The eight carbon skeleton of the indolizidine moiety was constructed from COSY correlations between δ 1.96/2.09 (H-2), 2.95/3.50 (H-3) and 1.77/2.68 ppm (H-1). COSY correlations from H-1 to H-9 (δ 3.32 ppm) determined the connection of these protons. Correlations observed from H-8 to H-9 and H-7 (δ 4.60 ppm) enabled the attachment of C-8 to C-9, and the oxygenated carbon C-7 to C-8. The H-6 methylene protons (δ 2.15/2.40 ppm) correlated to H-7 and H-5 (δ 3.03/3.69 ppm), which completed the carbon backbone of the indolizidine moiety. No COSY correlations were observed from the H-4 exchangeable proton (δ 10.36), and as a result an indolizidine functionality could not be constructed from COSY correlations.

HMBC correlations (Figure 46) from H-3 (δ 3.50/2.95 ppm) and H-5 (δ 3.03/3.69 ppm) to C-9 (δ 63.7 ppm) secured the structure of the 7-oxyindolizidine moiety. H-8 (δ 3.21 ppm) showed a correlation to the ketone carbonyl carbon C-10 (δ 193.4 ppm). The aromatic group was confirmed by HMBC correlations in an identical manner to that for isoelaeocarpine (**61**). The connection of the aromatic group to the 7-oxy-8-ketoindolizidine was established by four-bond correlations from H-$17_{Me}$ (δ 2.52), H-15 and H-13 to C-10. As with isoelaeocarpine (**61**), no HMBC correlation was observed in elaeocarpine (**60**) from H-7 (4.60) to C-12. However, the same conclusion can be drawn from MS evidence that an ether link exists between C-7 (77.8) and C-12 (162.3) in elaeocarpine (**60**). Therefore the structure of **60** was established.

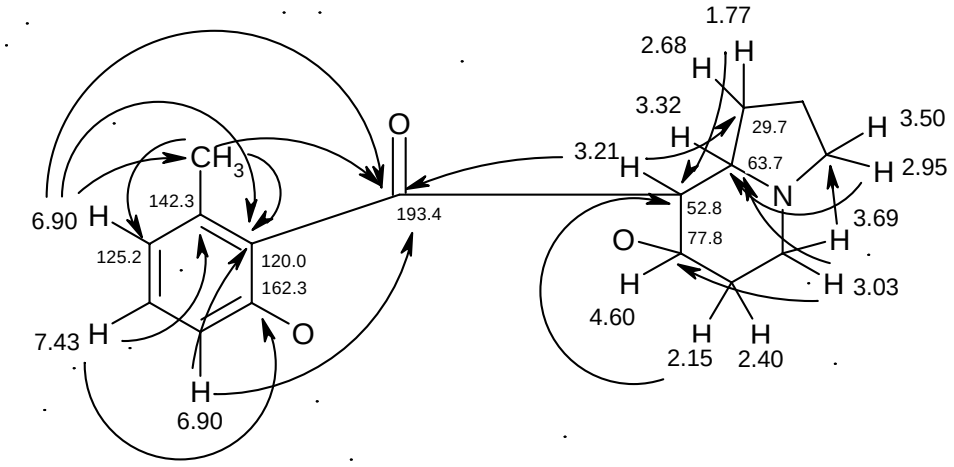


**Figure 46.** Key HMBC correlations used to establish the structure of elaeocarpine (**60**).

The relative stereochemistry of elaeocarpine (**60**) was established from coupling constants. The proton at δ 3.21 ppm (H-8) exhibited two large couplings, both being 11.4 Hz. These values are typical for axial-axial couplings. This infers that a *trans*-diaxial coupling exists between H-7 and H-8, and H-8 and H-9 (δ 3.32 ppm). Large couplings of 10.8 and 12.0 Hz were observed for H-9 and H-7, respectively, which provides further evidence for their axial configurations. Thus the relative stereochemistry of elaeocarpine (**60**) was established. This proves that **60** is an isomer of **61**, by variation of the stereochemistry at H-7. This is consistent with the literature.[1] ROESY correlations

(Figure 47) supported this, with correlations from H-7 to H-9 and H-$5_{ax}$ (3.03), suggesting 1-3-diaxial relationships for these protons.

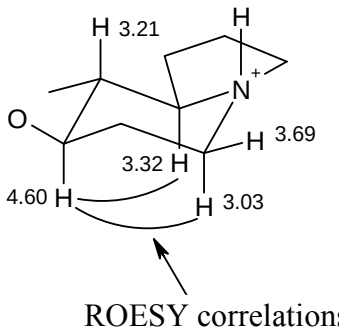


**Figure 47.** The key ROESY correlations of elaeocarpine (**60**).

The energy minimized structure of elaeocarpine (**60**) is shown in Figure 48. Measurement of the optical rotation of **60** produced a value of +12.36°. The literature values are +206 and -210° for enantiomerically pure forms of elaeocarpine.[1] This suggests that elaeocarpine (**60**) was isolated as a partial racemate with a slight excess of the (+)-enantiomer.

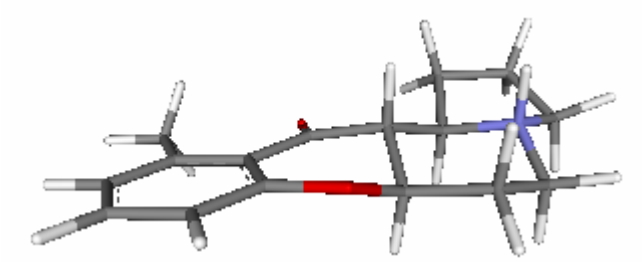

**Figure 48**. The energy minimized structure of elaeocarpine (**60**).

## 4.7 The Conversion of Elaeocarpenine (122) to Isoelaeocarpine (61) and Elaeocarpine (60)

The conversion of elaeocarpenine (**122**) to isoelaeocarpine (**61**) and elaeocarpine (**60**) was observed upon reacting **122** (5.2 mg) with ammonia in methanol. The reaction

mixture was separated by reversed phase semi-preparative HPLC, employing a gradient from 3:1 to 1:3 $H_2O$:MeOH over 10 minutes. This afforded isoelaeocarpine (**61**) (1.2 mg) and elaeocarpine (**60**) (1.2 mg). The optical rotations of **61** and **60** purified from this reaction were +11.43 and +9.66$^o$ (c 0.067, MeOH), respectively. This suggests that **122** was isolated as a partial racemate.

This observation suggests ammonia promotes ring closure by removal of the acidic phenolic proton to form the phenoxide ion via and subsequent intra-molecular Michael addition to form an ether linkage (Figure 49). The attack of the phenoxide ion occurs from either side of the ring which results in epimerization at position C-7. This provides justification for employing an ammonia free extraction process.

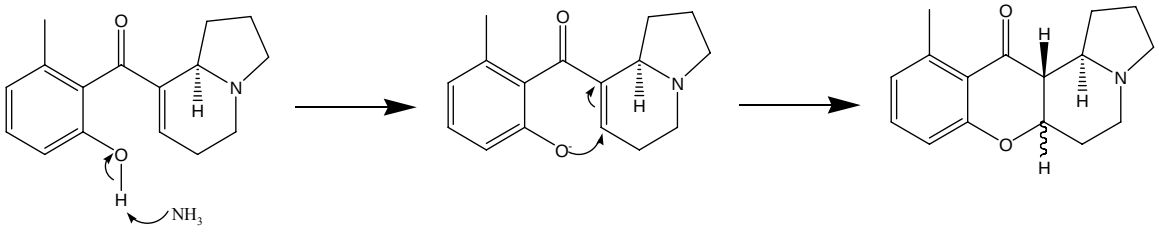


**Figure 49.** The ammonia promoted ring closure of elaeocarpenine (**122**).

## 4.8 Proposed Biogenesis of the *E. fuscoides* Alkaloids

I propose the biogenesis of the *E. fuscoides* alkaloids as shown in Figure 50, which can be considered an extension of the polyketide condensation pathway previously proposed for the Elaeocarpaceae alkaloids. The condensation product (**i**) can undergo an aldol condensation to create a six membered ring in (**ii**). Subsequent reduction may lead to isoelaeocarpicine (**62**). Further reduction of **62** could yield elaeocarpenine (**122**). Cyclization of **122** would result in the formation of elaeocarpine (**60**) and isoelaeocarpine (**61**).

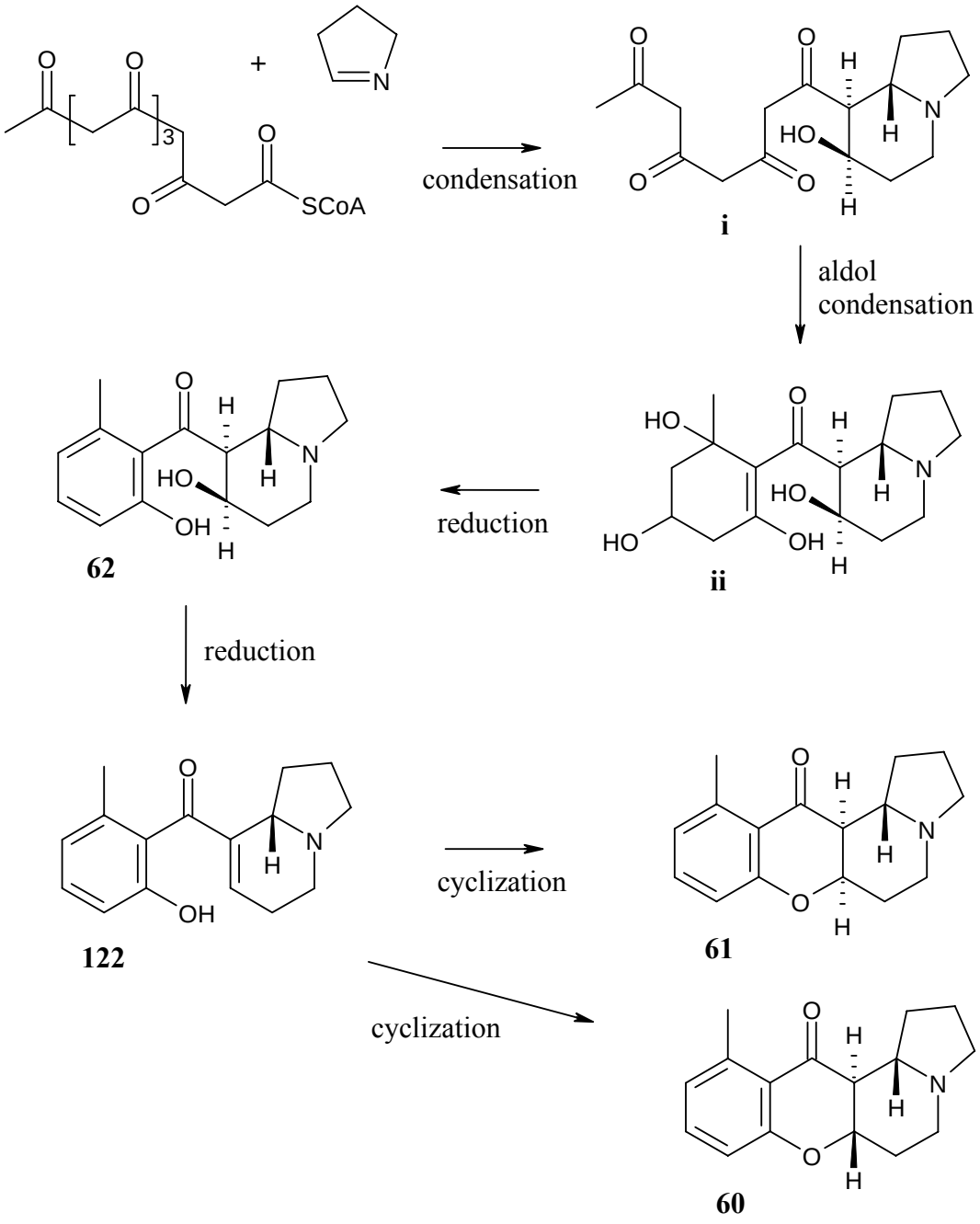


**Figure 50.** The proposed biogenesis of the *E. fuscoides* alkaloids.

## 4.9 References


1. Johns, S. R., Lamberton, J. A., Sioumis, A. A., Willing, R. I., *Aust J Chem* **1969,** 22, 775 - 792.
2. Arai, Y., Kontani, T., Koizumi, T., *Tetrahedron: Asymmetry* **1992,** 3, 535 - 538.

# CHAPTER 5 – Isolation and Structure Elucidation of Novel Alkaloids from *Peripentadenia mearsii*.

## 5.1 Introduction

The genus *Peripentadenia* comprises two species, *P. mearsii* and *P. phelpsii*.[1] These species are rainforest trees which grow in north Queensland. The bark and leaves of *P. mearsii* collected from Boonjie have been the focus of previous chemical investigations.[2, 3] Peripentadenine (**81**) was identified as the major alkaloid constituent of bark extracts and the only constituent of leaf extracts.[2] Dinorperipentadenine (**82**), peripentamine (**83**), anhydroperipentamine (**84**) and mearsine (**85**) were also isolated from the bark.

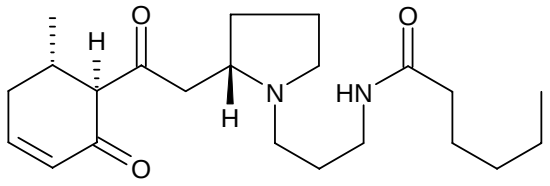

**123a**

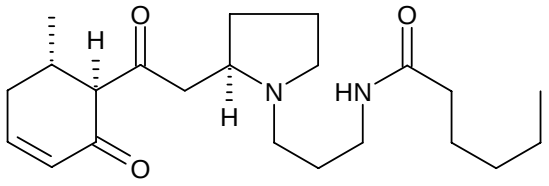

**123b**

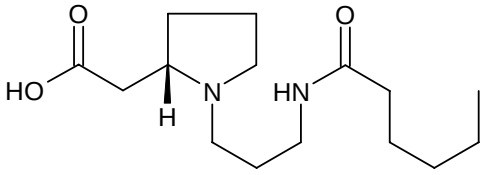

**124**

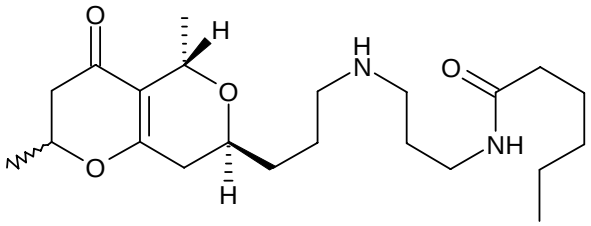

**125**

*P. mearsii* was identified as an alkaloid producing species following a positive result in the phytochemical survey. The positive ESIMS of the extract of *P. mearsii* revealed a mass ion peak at *m/z* 377. *P. phepsii* was not evaluated for alkaloids in the Elaeocarpaceae phytochemical survey. This investigation focuses on a comparative investigation of *P. mearsii* by an ammonia-free extraction protocol.

This chapter details the isolation and structure elucidation of the new pyrrolidine alkaloid peripentonine (**123**) from the leaves and seeds of *P. mearsii*. Peripentadenine (**81**) was only isolated from the bark of this species. Two novel alkaloids, mearsamine 1 (**124**) and 2 (**125**) were also isolated from the leaves of *P. mearsii*. All of these compounds were isolated as their TFA salts.

## 5.2 Isolation of Peripentonine (123), Peripentadenine (81), and Mearsamine 1 (124) and 2 (125)

The isolation procedures for two separate collections for the leaves of *P. mearsii* are illustrated in Schemes 5 and 6. The first collection was extracted with methanol and the extract was evaporated. The resulting residue was dissolved in $H_2O$ and partitioned three times with DCM. The aqueous layer provided a positive result in a Dragendorff's test. The aqueous layer was then filtered through SCX resin and peripentonine (**123**) was eluted with 1M NaCl. Evaporation of this salt solution, followed by re-suspension in 1:1 $CHCl_3$:MeOH and filtration yielded pure peripentonine (**123**) (45.5 mg, 0.108 %).

The second collection of the leaves of *P. mearsii* was also extracted with methanol. The extract was filtered through SCX resin under vacuum and washed sequentially with MeOH and $H_2O$. Alkaloids were eluted from the SCX resin with 1M NaCl. The separation of salt from the alkaloids was facilitated by filtration through C18. The NaCl was removed by extensive washing of the C18 with $H_2O$. An alkaloid fraction was produced by elution with 1% TFA/MeOH. Mass ion peaks of *m/z* 285, 377, and 395

were detected in this fraction in the positive ESI mass spectrum. This fraction was separated into 50 fractions by preparative C18 RP-HPLC, utilizing a gradient from $H_2O$ to 1% TFA/MeOH over 100 minutes. Fractions 22 and 23 afforded pure mearsamine 1 (**124**) (11.2 mg, 0.0221%), fraction 25 yielded pure mearsamine 2 (**125**) (13.2 mg, 0.0260%) and fractions 28 – 32 yielded pure peripentonine (**123**) (33.2 mg, 0.636%).

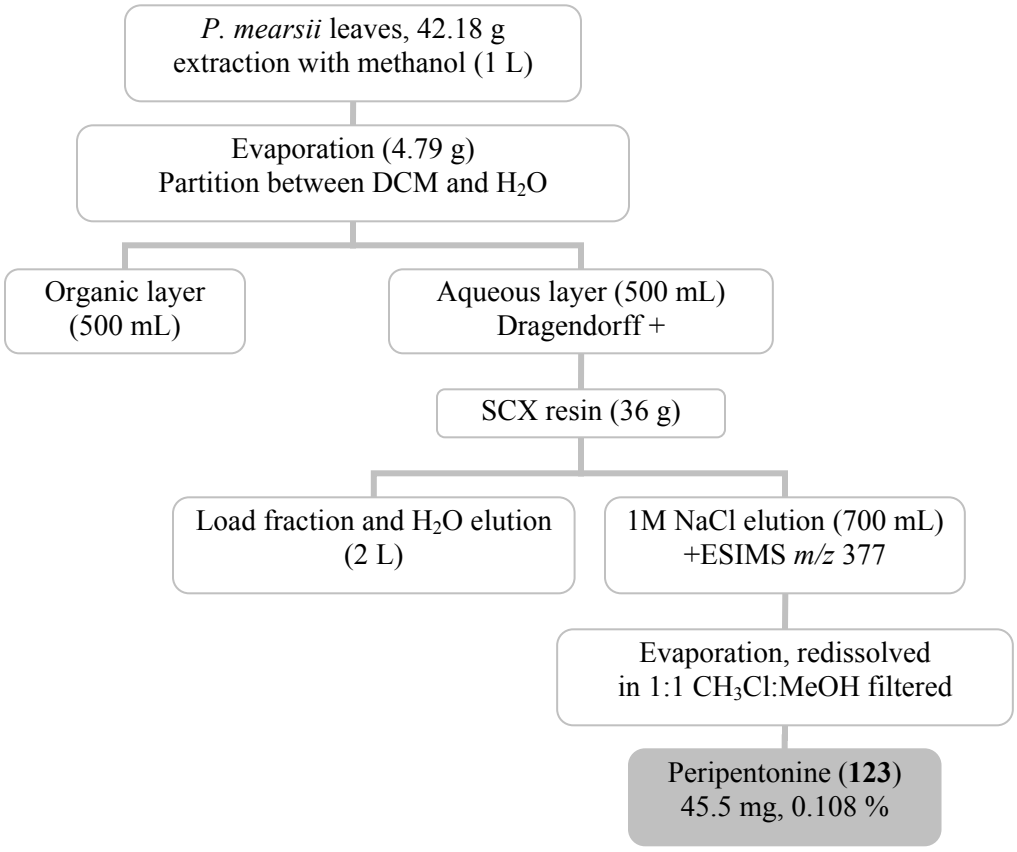


**Scheme 5.** Isolation scheme for the purification of peripentonine (**123**) from the leaves of *P. mearsii*.

The extraction of the bark and seeds of *P. mearsii* is illustrated in Schemes 7 and 8 respectively. Purification was achieved by methanol extraction, SCX/C18 filtration and preparative C18 gradient HPLC, as discussed for the leaves of *P. mearsii*. The bark yielded peripentadenine (**81**) (19.0 mg, 0.0127 %) from fractions 34 - 36 of the preparative C18 HPLC separation. Peripentonine (**123**) (18.7 mg, 0.0468 %) was purified from the seeds, eluting in fractions 34 - 36 of the preparative C18 HPLC separation. A

second extraction of the bark of *P. mearsii* was performed in an identical manner to that described for the bark, which also yielded peripentadenine (**81**) (3.2 mg, 0.0064 %).

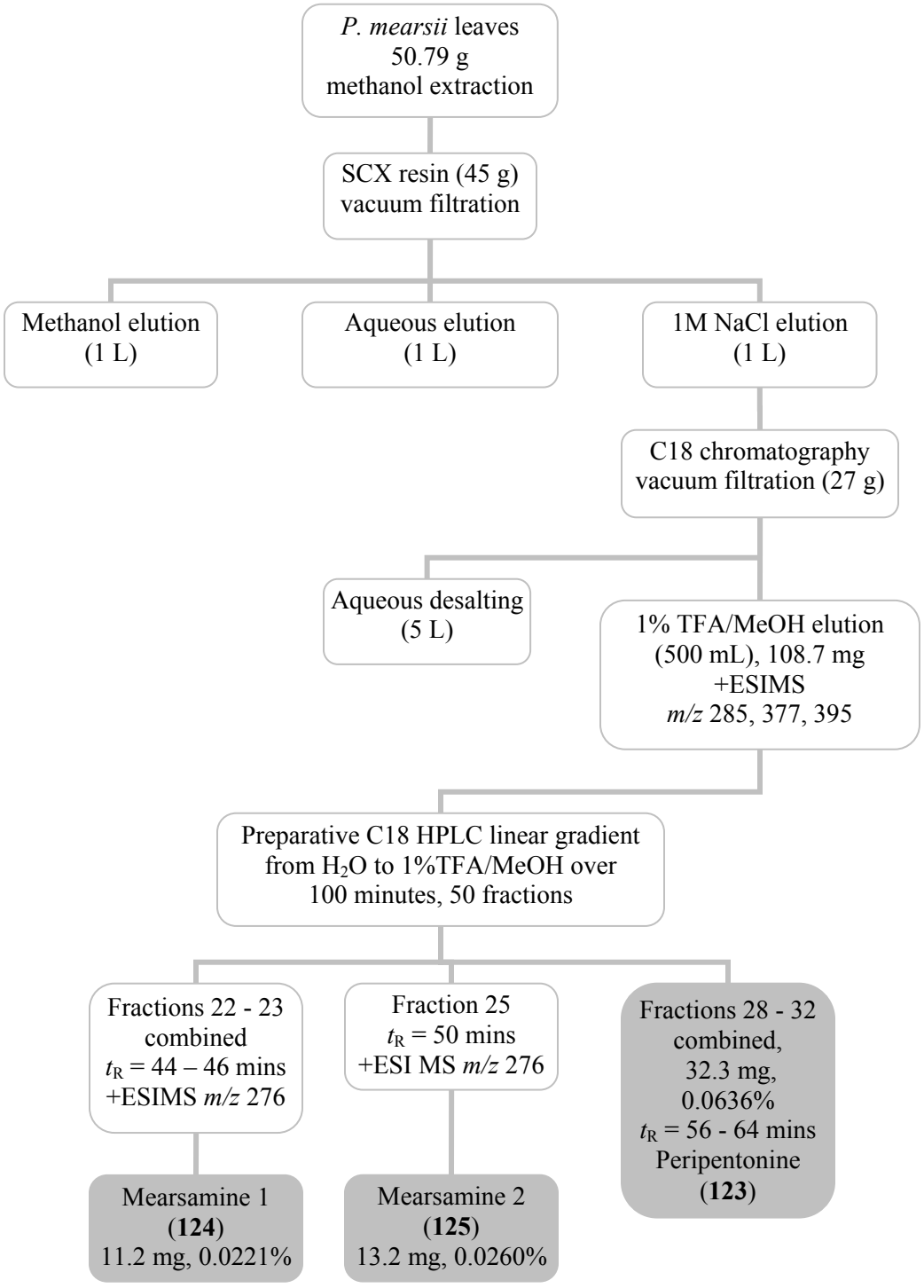


**Scheme 6.** The isolation scheme for the purification of mearsamine 1 (**124**), 2 (**125**) and peripentonine (**123**) from the leaves of *P. mearsii*.

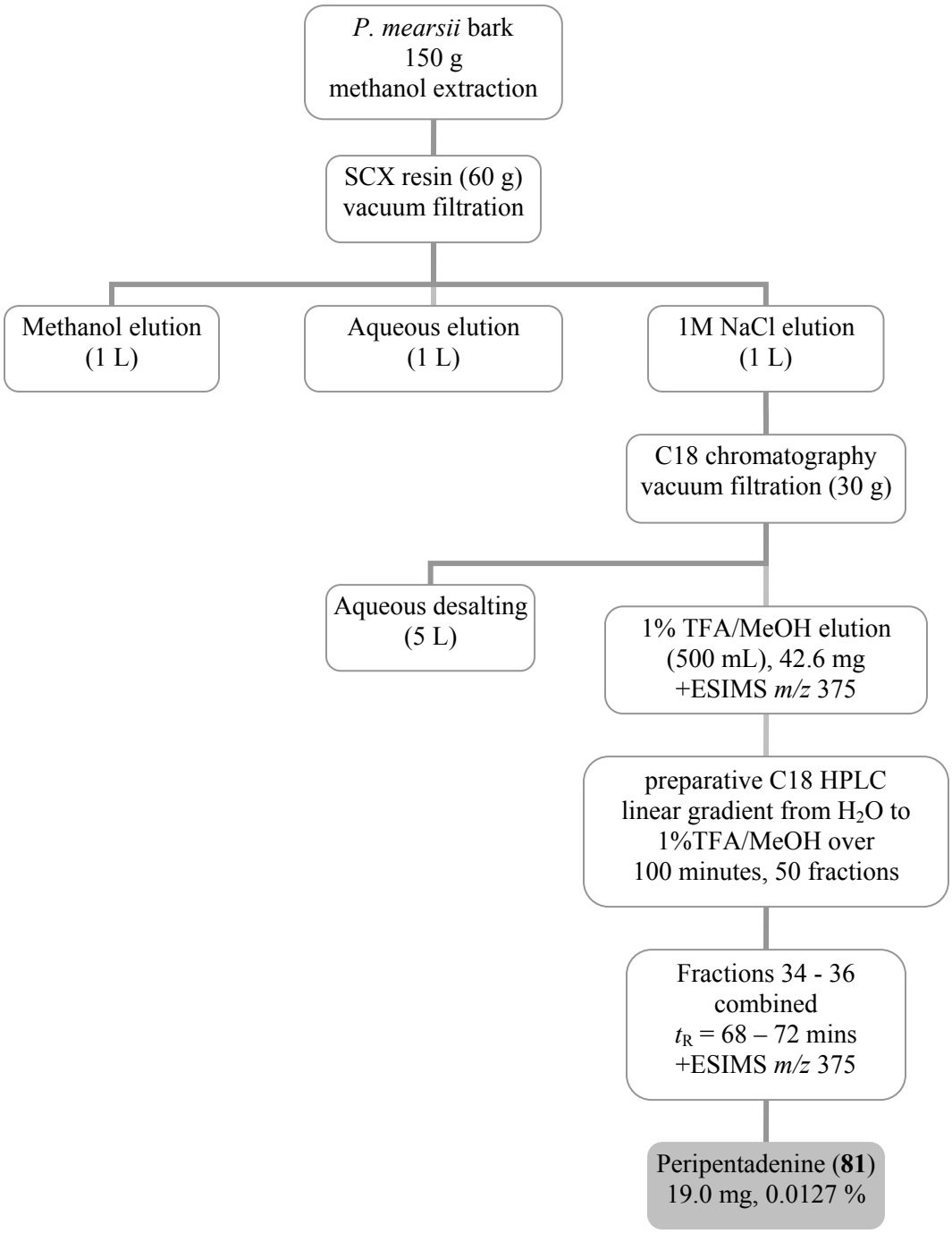


**Scheme 7.** The isolation scheme for the purification of peripentadenine (**81**) from the bark of *P. mearsii*.

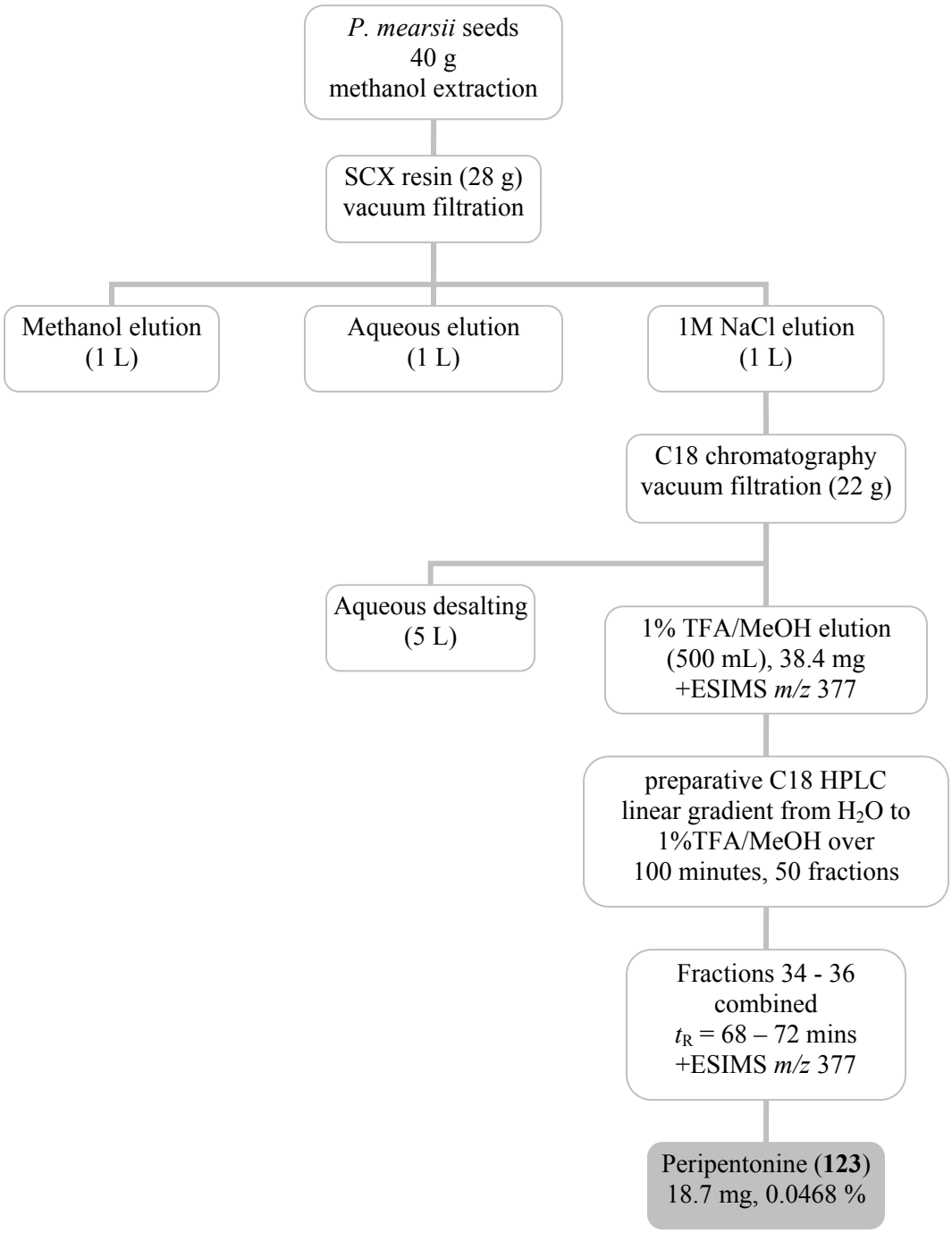


**Scheme 8.** The isolation scheme for the purification of peripentonine (**123**) from the seeds of *P. mearsii*.

## 5.3 Structure Elucidation of Peripentonine (123)

Peripentonine (**123**) was assigned a molecular formula $C_{22}H_{37}N_2O_3$ by high resolution positive electrospray mass measurement of the $[M + H]^+$ ion 377.279196 (calculated for 377.279869). Peripentonine was found to exist as a mixture of tautomers in solution. As with habbenine (**114**), the difference between the two tautomers was evident in the olefinic region. Inspection of the $^1H$ NMR spectrum (Figure 51) revealed that the major tautomer possessed proton signals at δ 5.97 and 7.11, whereas signals at 6.06 and 6.63 ppm were attributed to the minor tautomer. The chemical shifts of the olefinic protons from the major and minor tautomer of peripentonine were almost identical to those observed for habbenine (**114**). This suggested that peripentonine contained the same 1,3-diketo system as found in habbenine.

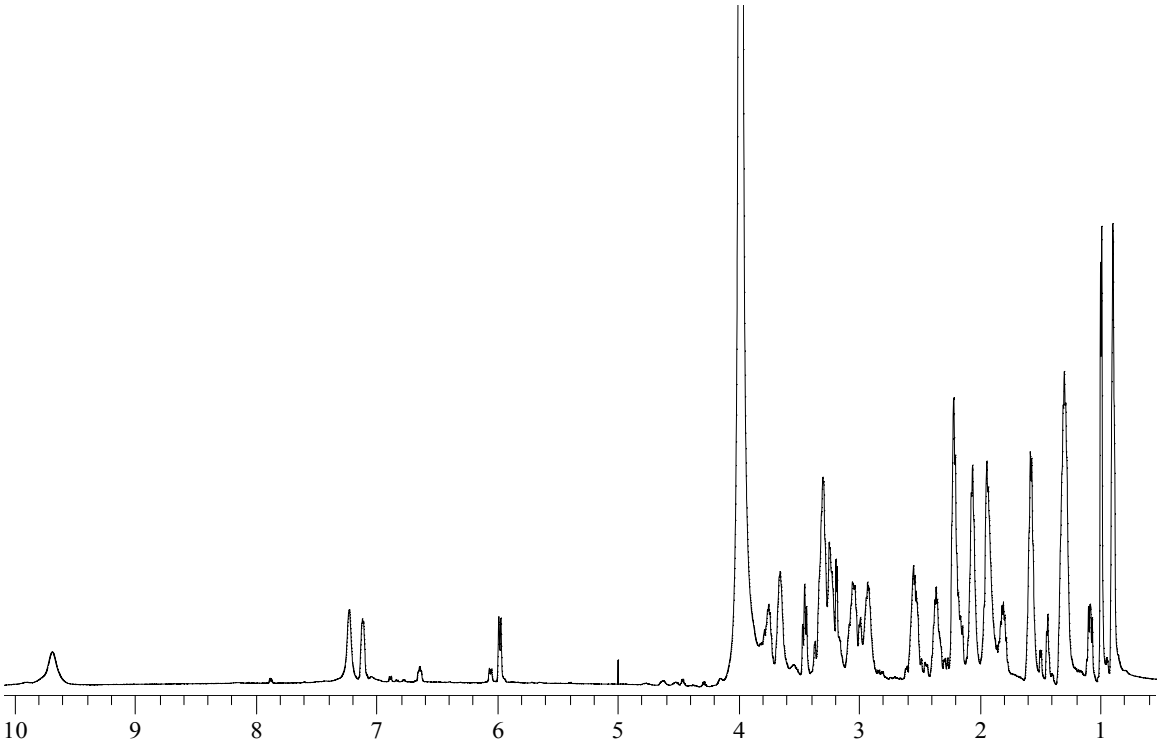


**Figure 51.** The $^1H$ NMR spectrum of peripentonine (**123**) at 600 MHz in $CD_3CN$ with one drop of conc. TFA.

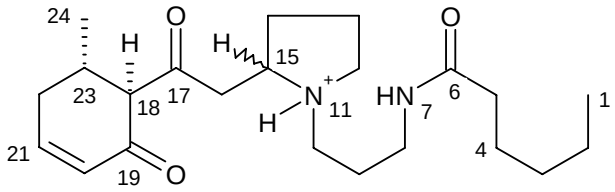


**Table 10.** $^{13}C^{a}$ and $^{1}H^{b}$ NMR spectral data for peripentonine[c] (**123a** and **b**).

| atom | $^{13}C$, δ | $^{1}H$, δ, mult, *J* (Hz) | $^{13}C$, δ | $^{1}H$, δ, mult, *J* (Hz) |
|---|---|---|---|---|
| 1 | 13.4 | 0.89 (3H, br) | 13.4 | 0.89 (3H, br) |
| 2 | 21.7 | 1.30 (2H, m) | 21.5 | 1.30 (2H, m) |
| 3 | 31.7 | 1.30 (2H, m) | 31.7 | 1.30 (2H, m) |
| 4 | 25.3 | 1.58 (2H, m) | 25.4 | 1.57 (2H, m) |
| 5 | 35.7 | 2.21 (2H, m) | 35.7 | 2.21 (2H, m) |
| 6 | 176.3 | - | 176.2 | - |
| 7 | - | 7.23 (1H, br) | - | 7.23 (1H, br) |
| 8 | 36.0 | 3.30 (2H, m) | 35.9 | 3.30 (2H, m) |
| 9 | 25.7 | 1.93 (2H, m) | 25.8 | 1.93 (2H, m) |
| 10 | 51.5 | 2.93 (1H, ddd, 6.0, 6.0, 13.2) | 51.2 | 2.93 (1H, ddd, 6.0, 6.0, 13.2) |
| | | 3.23 (1H, ddd, 5.4, 5.4, 13.8) | | 3.23 (1H, ddd, 5.4, 5.4, 13.8) |
| 11 | - | 9.69 (1H, br) | - | 9.69 (1H, br) |
| 12 | 53.1 | 3.05 (1H, m) | 53.0 | 3.05 (1H, m) |
| | | 3.65 (1H, brdd, 6.6, 13.8) | | 3.65 (1H, brdd, 6.6, 13.8) |
| 13 | 22.3 | 2.06 (2H, m) | 22.3 | 2.06 (2H, m) |
| 14 | 29.8 | 1.81 (1H, ddd, 2.4, 7.7, 15.6) | 29.8 | 1.81 (1H, ddd, 2.4, 7.7, 15.6) |
| | | 2.36 (1H, brdd, 6.6, 13.8) | | 2.36 (1H, brdd, 6.6, 13.8) |
| 15 | 64.0 | 3.78 (1H, brdd, 7.2, 13.8) | 64.2 | 3.78 (1H, brdd, 7.2, 13.8) |
| 16 | 44.8 | 3.18 (1H, dd, 6.0, 14.4) | 44.9 | 3.00 (1H, dd, 6.0, 14.4) |
| | | 3.30 (1H, dd, 7.8, 14.4) | | 3.18 (1H, dd, 7.8, 14.4) |
| 17 | 206.1 | - | 206.0 | - |
| 18 | 66.5 | 3.45 (1H, d, 9.6) | 66.5 | 3.46 (1H, d, 9.6) |
| 19 | 197.2 | - | 197.2 | - |
| 20 | 128.3 | 5.97 (1H, d, 10.2) | 128.3 | 5.97 (1H, d, 10.2) |
| 21 | 152.2 | 7.11 (1H, ddd, 4.6, 7.2, 9.6) | 152.4 | 7.11 (1H, ddd, 4.6, 7.2, 9.6) |
| 22 | 33.0 | 2.16 (1H, m) | 32.9 | 2.16 (1H, m) |
| | | 2.52 (1H, m) | | 2.55 (1H, m) |
| 23 | 31.9 | 2.55 (1H, m) | 31.7 | 2.55 (1H, m) |
| 24 | 19.1 | 0.99 (3H, d, 6.6) | 19.0 | 0.99 (3H, d, 6.6) |

[a]At 125 MHz. [b]At 600 MHz. [c]In $CD_3CN$.

The ratios of the tautomers of peripentonine were also found to vary in different solvents. Acquistion of the $^{1}H$ NMR spectrum (Figure 51) in $CD_3CN$ with one drop of conc. TFA provided the best ratio of tautomers (6:1) and allowed the structure of peripentonine (**123**) to be detemined. Proton NMR spectra were acquired in a number of different solvents: $d_6$-DMSO, $d_5$-pyridine, $CD_3OD$ and $CD_3CN$. Spectra acquired in $CD_3OD$ and $CD_3CN$ gave the greatest difference in the ratios of the tautomers, whereas the spectrum acquired in $d_5$-pyridine gave a 1:1 ratio of the tautomers.

In addition to the olefinic signals, Figure 51 revealed two methyl groups at δ 0.89 and 0.99 ppm. Other resonances were found at δ 1.30, which integrated to four protons, and signals at 1.57, 1.93, 2.06, 2.21, 2.53 ppm which all integrated to two protons. The signal at δ 3.30 ppm integrated to three protons.

The $^{13}C$ NMR spectrum of **123** indicated that peripentonine was purified as a mixture of diastereomers. Similarly with habbenine (**114**), several carbons were identical in chemical shift and others were in a ratio of approximately 1:1. Since **123** and **114** were structurally similar, it was speculated that the diastereomers of peripentonine (**123**) could not be separated.

The structure elucidation of only one isomer of **123** will be discussed. A total of 36 carbons were observed in the $^{13}C$ NMR spectrum of peripentonine (**123**), however 22 carbons could be assigned to each diastereomer with eight carbons coincident in both diastereomers. Two $sp^2$ hybridized carbons at δ 152.2 and 128.3, and three carbonyl carbons at 176.3, 206.1 and 197.2 ppm were observed for one isomer. The carbonyl carbon at δ 197.2 ppm was indicative of an α,β-unsaturated ketone. The chemical shifts of the olefinic carbons were typical for carbons alpha and beta to a ketone. The carbonyl at δ 206.1 ppm was indicative of a saturated ketone. The remaining carbonyl carbon, resonating at δ 176.3 ppm, could be either an amide, ester or a carboxylic acid. Five carbons resonated between δ 40 and 70 ppm, suggesting bridgeheads or carbons bound to oxygen or nitrogen. Two methyl carbons resonated at δ 19.1 and 13.4, and a group of ten

aliphatic carbons were observed between 20 and 40 ppm. The $^{1}H$ and $^{13}C$ NMR spectral data for peripentonine (**123**) is detailed in Table 10.

HSQC spectral data established the presence of 35 carbon bound protons including two methyls, 12 methylenes, three methines, and two olefinic protons. COSY and HSQC experiments were used to establish the partial structures of **123** (Figure 52). A pentyl group was deduced from COSY correlations from the methyl protons at δ 0.89 (H-1) to the H-2 methylene at 1.30 ppm. COSY correlations were observed from the protons at δ 1.57 (H-4 methylene) to the protons of H-5 (2.21) and H-3 (1.30 ppm). HSQC correlations from the protons at δ 1.30 ppm to two carbons at δ 21.7 and 31.7 ppm confirmed that there were two methylenes at 1.30 ppm (H-2 and H-3). The connection between C-2 and C-3 was suggested upon comparison with other *Peripentadenia* alkaloids. No HSQC correlations were observed for the proton at δ 7.23 ppm, however this proton correlated to the protons at δ 3.30 ppm (H-8) in the COSY spectrum. The HSQC spectrum demonstrated that the protons at δ 3.30 ppm were attached to a carbon at δ 36.0 ppm. This carbon chemical shift was consistent with a carbon attached to the nitrogen atom of an amide. This suggested that the resonance at δ 7.23 (H-7) in the $^{1}H$ spectrum was an amide proton. A COSY correlation from H-8 to the protons at δ 1.93 (H-9) established the connection of C-8 to C-9, and correlations from H-9 to protons at δ 2.93/3.23 ppm indicated that H-10 was adjacent to H-9. This established the propylamide partial structure. Another aliphatic partial structure was assembled from COSY correlations between the H-13 methylene (δ 2.06 ppm) and the protons at δ 3.05/3.65 (H-12) and 1.81/2.36 ppm (H-14). COSY correlations from the proton at δ 3.78 ppm (H-15) to the protons at δ 1.81/2.36 (H-14) and δ 3.18/3.30 (H-16) demonstrated that the H-15 methine was vicinal to both the methylenes H-14 and H-16. COSY correlations were observed from the exchangeable proton at δ 9.69 ppm to the protons at δ 2.93, 3.05 and 3.78 ppm, which allowed the attachment of a nitrogen to C-15, C-12 and C-10 to establish a pyrrolidine-*N*-propylamide partial structure. Another partial structure was created from COSY correlations from the olefinic protons at δ 5.97 (H-20) and 7.11 ppm (H-21) to each other. Other correlations from H-21 to the protons at δ 2.16/2.52 (H-22) indicated that a methylene was vicinal to this olefinic proton. The proton at δ 2.55 ppm

(H-23) correlated to the protons of H-22 and methyl protons at δ 0.99 ppm (H-24), indicating that a -CH-$CH_3$ group was attached to C-22. COSY correlations from H-23 to a proton at δ 3.45 ppm (H-18) demonstrated that another methine was adjacent to H-23. Thus the partial structures of peripentonine (**123**) were established.

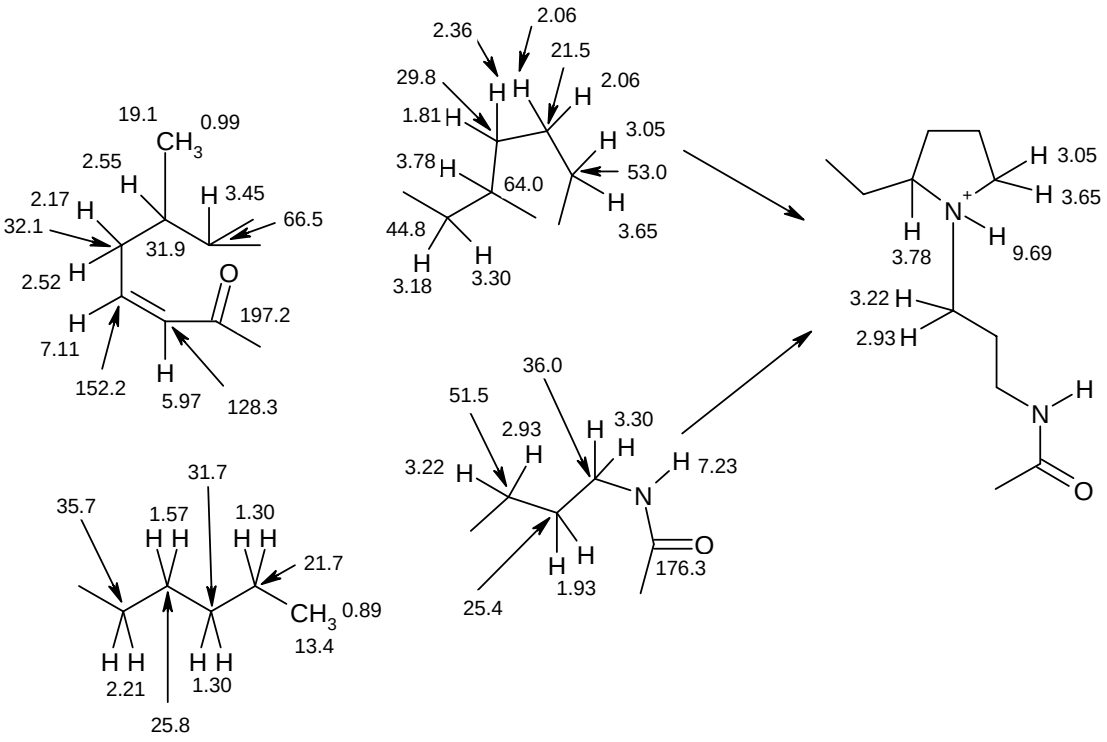


**Figure 52**. The partial structures of peripentonine (**123**) established from COSY and HSQC experiments.

The structure of the pyrrolidine-*N*-propylamide functionality was secured from HMBC correlations from H-12 (3.05/3.65) and H-10 (2.93/3.23) to C-15 (64.0), and from H-10 to C-12 (53.1) (Figure 53). HMBC correlations were observed from the protons at δ 1.57 (H-4) and 2.21 ppm (H-5) to the carbonyl carbon of C-6 (176.3), which allowed the connection of the pentyl partial structure to the amide carbonyl carbon. No HMBC correlations were observed from the amide proton (7.23). The structure of the 1,3-diketo-methylcyclohexenone moiety was confirmed by correlations from H-18 (3.45) to the ketone carbonyl carbons at 197.2 (C-19) and 206.1 (C-17) and to the methyl group C-24 (19.1). HMBC correlations from the olefinic proton at δ 7.11 (H-21) to the carbonyl

carbon at 197.2 ppm (C-19) confirmed the position of the ketone carbonyl carbon. The connection of the pyrrolidine-*N*-propylhexanamide structure to the 1,3-diketo-methylcyclohexenone was deduced from interpretation of an HMBC correlation from the protons at δ 3.18/3.30 ppm (H-16) to the ketone carbonyl carbon C-17. Thus the structure of peripentonine (**123**) was established.

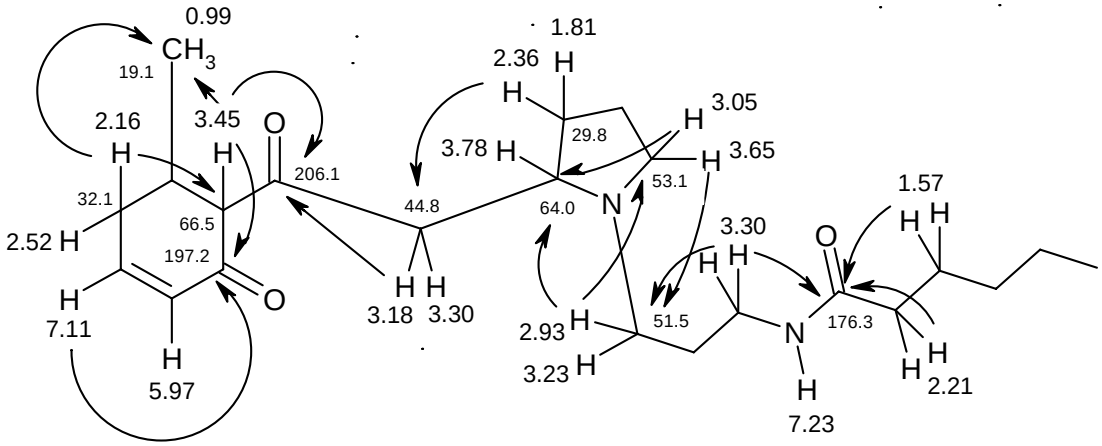


**Figure 53.** Connection of the partial structures of peripentonine (**123**) established from key HMBC correlations.

The only significant difference in the chemical shift of the protons in the two diastereomers of peripentonine (**123**) was observed for the protons attached to C-16. The protons of the C-16 methylene were observed at δ 3.18/3.30 ppm in one isomer, and at δ 3.00/3.18 ppm in the other isomer. The protons at δ 3.45 and 3.46 ppm (H-18) in the $^{1}$H spectrum each resonated as doublets with similar coupling constants, of 9.6 and 10.8 Hz, respectively. Both of these coupling constants were consistent with a *trans* diaxial configuration between H-18 and H-23. A correlation in the ROESY spectrum was also observed between the methyl group H-24 and H-18. This indicated a *cis* arrangement between the methyl group and H-18, and supported the axial configurations for both H-18 and H-23. This indicated that the relative stereochemistry of H-18 and H-23 was the same in both diastereomers, and therefore suggested that peripentonine (**123**) was isomeric at C-15. The significant difference in the chemical shifts of the protons attached to C-16 between the two isomers supports the isomerism at C-15. Inspection of the energy

minimized diastereomers at C-8 of habbenine (**114**) (Figure 27) demonstrates that the methylenes alpha to the ketone of each isomer are in different orientations relative to the ketone and pyrrolidine ring. This difference in three-dimensional arrangement accounts for the variation in chemical shift of the protons of C-9 in **114** and C-16 in **123**. The molecular modeled diastereomers of habbenine (**114**) also suggested that the chemical environments of the other protons and carbons were similar, thus resulting in little difference between the chemical shifts of the protons and carbons of each diastereomer. The energy minimized structure of one isomer of peripentonine (**123**) is illustrated in Figure 54.

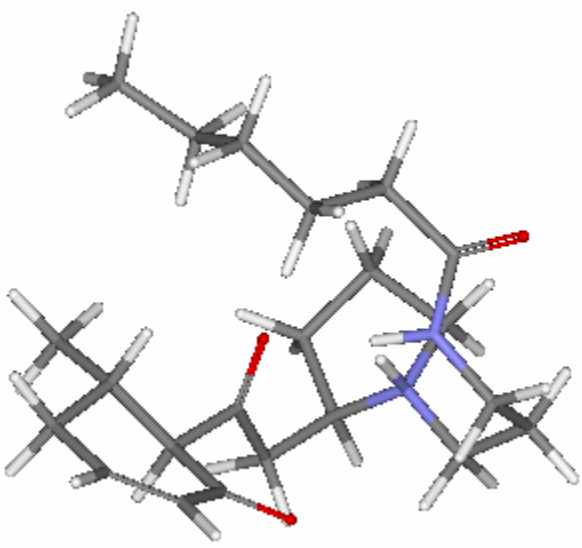

**Figure 54.** The energy minimized structure of peripentonine (**123**).

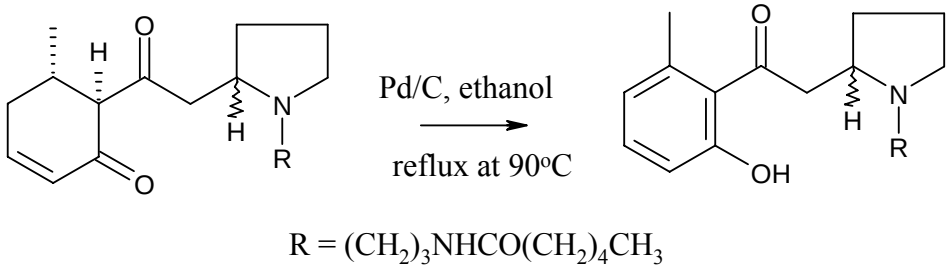


$R = (CH_2)_3NHCO(CH_2)_4CH_3$

**Figure 55.** The dehydrogenation of peripentonine (**123**) in the presence of Pd/C to yield peripentadenine (**81**).

The dehydrogenation of peripentonine (**123**) (Figure 55) with Pd/C in ethanol at 90ºC produced peripentadenine (**81**) in 63% yield. The $^1$H NMR spectrum ($d_6$-DMSO) of the product was identical to the natural product. The optical rotation of peripentadenine (**81**) produced from this reaction was $0^o$. This indicated that **81** was present as a racemate and confirmed that **123** was epimeric at C-15.

## 5.4 Structure Elucidation of Peripentadenine (81)

The $^1$H NMR spectrum of peripentadenine (**81**) (Figure 56) revealed the distinguishing signals of a propylhexanamide chain as observed in peripentonine (**123**). A downfield shift of the amide proton from δ 7.23 in **123** to 7.92 ppm in peripentadenine (**81**) was the only difference in the propylhexanamide signals between the two spectra. This was deemed to be a solvent dependent shift.

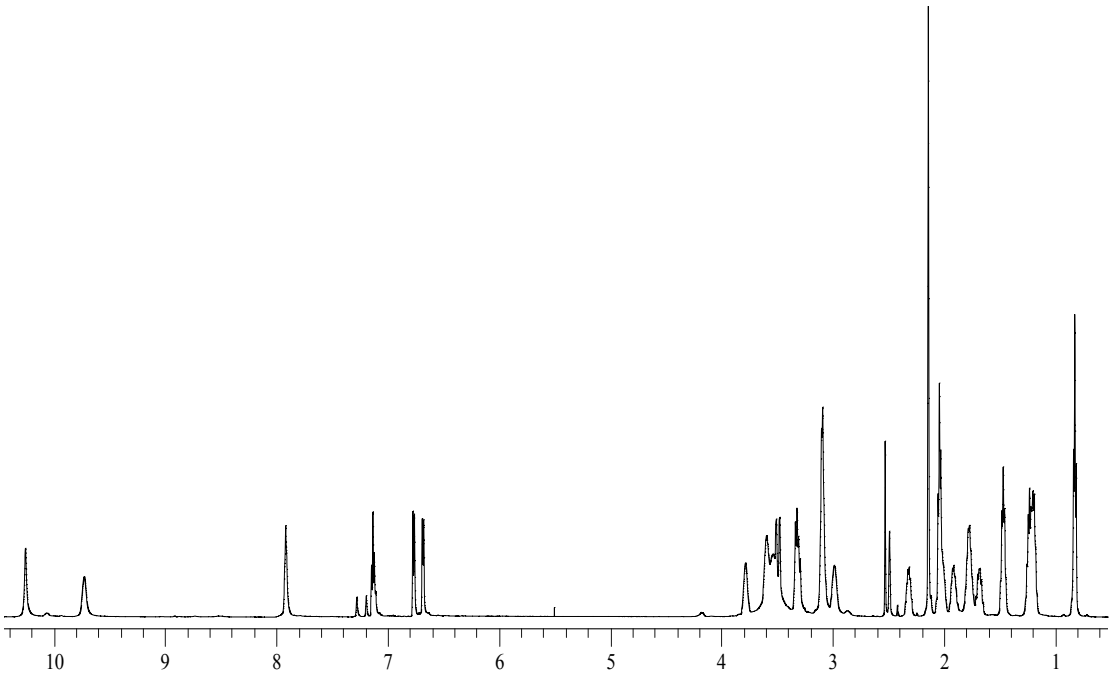


**Figure 56**. The $^1$H NMR spectrum of peripentadenine (**81**) at 600 MHz in $d_6$-DMSO.

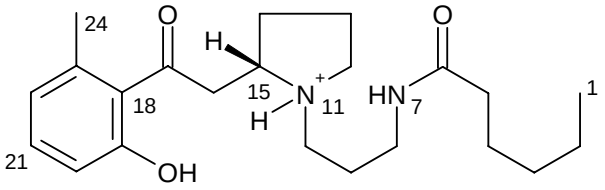


**Table 11.** $^{13}C^{a}$ and $^{1}H^{b}$ NMR spectral data for peripentadenine[c] (**81**).

| position | $^{13}C$, δ | $^{1}H$, δ, mult, *J* (Hz) | HMBC $^{2,3}J_{CH}$ |
|---|---|---|---|
| 1 | 13.7 | 0.82 (3H, t, 7.2) | 2, 3 |
| 2 | 21.8 | 1.24 (2H, t, 7.2) | 1, 3, 4 |
| 3 | 30.8 | 1.21 (2H, t, 7.2) | 1, 2 , 4, 5 |
| 4 | 24.8 | 1.47 (2H, t, 7.2) | 2, 3, 5, 6 |
| 5 | 35.3 | 2.04 (2H, t, 7.2) | 3, 4, 6 |
| 6 | 172.5 | - | - |
| 7 | - | 7.92 (1H, s) | 5, 6, 8 |
| 8 | 35.6 | 3.09 (2H, t, 7.2) | 6, 9, 10 |
| 9 | 25.5 | 1.77 (2H, t, 7.2) | 8, 10 |
| 10 | 50.8 | 2.99 (1H, ddd, 6.6, 12.6, 12.6) | 8, 9, 12, 15 |
| | | 3.33 (1H, m) | |
| 11 | - | 9.73 (1H, br) | - |
| 12 | 52.6 | 3.09 (1H, m) | 13, 14, 15 |
| | | 3.54 (1H, brdd, 5.4, 12.6) | |
| 13 | 21.3 | 1.91 (1H, dddd, 2.4, 7.2, 7.2, 13.2) | 12, 14, 15 |
| | | 2.00 (1H, m) | |
| 14 | 29.4 | 1.68 (1H, brdd, 8.4, 16.4) | 12, 13, 15, 16 |
| | | 2.32 (1H, brdd, 6.6, 13.8) | |
| 15 | 63.4 | 3.79 (1H, brdd, 9.0, 9.0) | 14, 16 |
| 16 | 44.7 | 3.30 (1H, dd, 9.6, 18.0) | 14, 15, 17 |
| | | 3.49 (1H, dd, 3.6, 18.0) | |
| 17 | 203.4 | - | - |
| 18 | 127.7 | - | - |
| 19 | 154.7 | - | - |
| 20 | 113.5 | 6.77 (1H, d, 7.8) | 17,18,19,20,22, 23 |
| 21 | 130.6 | 7.13 (1H, dd, 7.8, 7.8) | 18, 19, 20, 22, 23 |
| 22 | 121.1 | 6.68 (1H, d, 7.8) | 17,18,19,20,23,24 |
| 23 | 135.8 | - | - |
| 24 | 19.0 | 2.14 (3H, s) | 18, 22, 23 |
| 19-OH | - | 10.26 (1H, s) | - |

[a]At 125 MHz. [b]At 600 MHz. [c]In $d_6$-DMSO.

Three aromatic protons were observed at δ 6.68, 6.77 and 7.13 ppm in Figure 56, in contrast to the two olefinic protons observed for peripentonine. The published $^{1}H$ (270 MHz)[2] and $^{13}C$ (100 MHz)[3] NMR spectra ($CDCl_3$) of peripentadenine compared well with the $^{1}H$ and $^{13}C$ NMR spectral data (Table 11), although **81** was isolated as the TFA salt.

The $^{13}C$ NMR spectrum of peripentadenine (**81**) revealed a total of 22 carbons, including six $sp^2$ hybridized carbons which were assigned to an aromatic ring. One of these signals was a carbon at δ 154.7 ppm, which is suggestive of an oxygenated aromatic carbon. Two carbonyl carbons were observed, including the amide carbonyl of the hexanamide group at δ 172.5, and a ketone carbonyl at 203.4 ppm. Two methyl carbons resonated at δ 19.0 and 13.7 ppm, the latter belonging to the hexanamide group. Eight carbons were observed between 20 and 40 ppm. All of these carbons were very similar to the chemical shifts of the carbons of the pyrrolidine-*N*-propylhexanamide functionality of peripentonine (**123**). Three carbons at δ 63.4, 52.6 and 50.8 ppm were almost identical in chemical shift to nitrogen bound carbons of the pyrrolidine-*N*-propyl group.

HSQC spectral data established the presence of 32 carbon bound protons including two methyls, 11 methylenes, one methine, and three aromatic protons. The partial structures in Figure 57 were assembled from interpretation of data from COSY and HSQC experiments. The C-1 to C-5 pentyl chain was deduced from COSY correlations from the H-2 methylene (δ 1.24 ppm) to the H-1 methyl at 0.82 ppm and to the H-3 methylene at 1.21 ppm, and correlations from the H-4 methylene at δ 1.47 to 1.21 (H-3) and 2.04 ppm (H-5). COSY correlations from H-8 (δ 3.09 ppm) to protons at δ 7.92 (H-7) and 1.77 (H-9) demonstrated that the amide proton and H-9 methylene were adjacent to the H-8 methylene. Correlations from H-9 were also observed to the protons at δ 2.99 and 3.33 ppm, indicating the H-10 methylene was adjacent to H-9. This enabled the formation of the C-8 to C-10 propylamide partial structure. The C-12 to C-16 partial structure was assembled from COSY correlations from the H-13 methylene (δ 1.91/2.00 ppm) to the methylenes of H-14 and H-12 at δ 1.68/2.32 and 3.09/3.54 ppm, respectively. COSY correlations were observed from the methine at δ 3.79 ppm (H-15) to H-14 and the

protons at 3.30/3.49 ppm. This indicated that H-15 was adjacent to H-14 and the methylene H-16. COSY correlations were observed from the exchangeable proton δ 9.73 ppm (H-11) to the methylenes H-10 and H-12, and the methine H-15. This enabled the construction of a pyrrolidine-*N*-propylamide partial structure. A 1,2,3-tri-substituted aromatic ring was assembled from COSY correlations between the aromatic proton at δ 7.13 (H-21) and the protons at 6.68 (H-22) and 6.77 (H-20) ppm. HSQC data indicated that H-20 was attached to a carbon at δ 113.5 ppm, suggesting an oxygen atom substituted the *ortho* carbon.

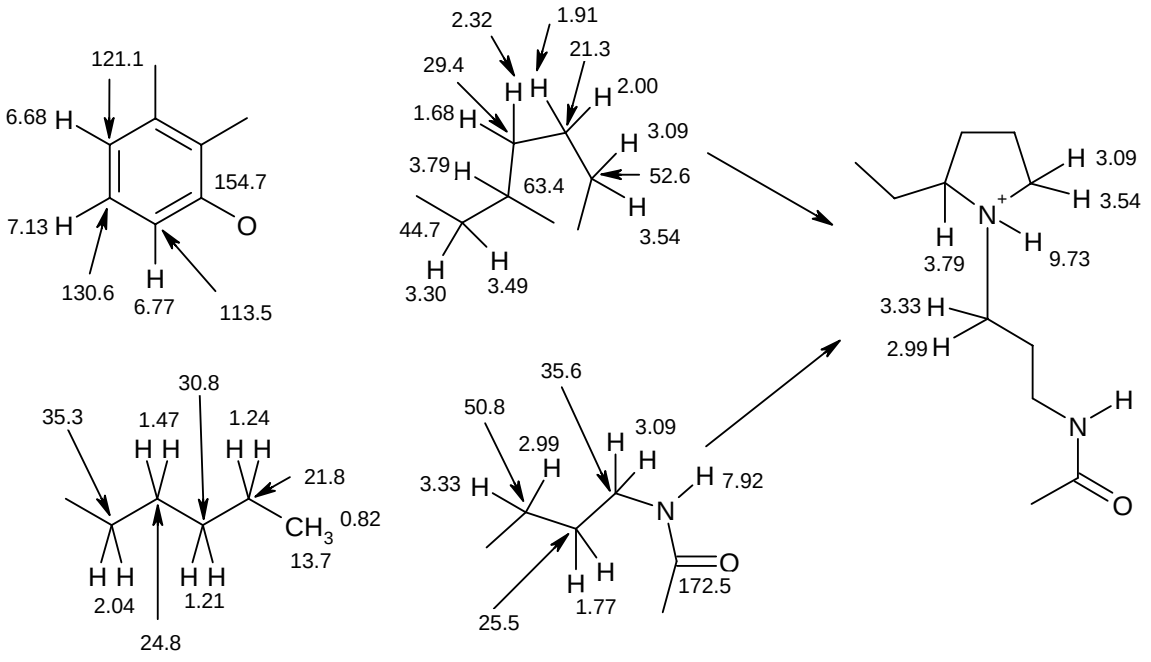


**Figure 57.** The partial structures of peripentadenine (**81**) established from COSY and HSQC experiments.

The structure of the pyrrolidine-*N*-propylamide moiety was confirmed by HMBC correlations (Figure 58) from H-10 to C-15 (δ 63.4 ppm) and to C-12 (δ 52.6 ppm), and from H-12 to C-15 and C-10 (δ 50.8 ppm). Correlations were observed from the amide proton (H-7) to the carbonyl carbon C-6 (δ 172.5 ppm) and to C-8 (δ 35.6 ppm) and C-5 (δ 35.3 ppm). This enabled the connection of the pentyl chain partial structure to the amide group of the pyrrolidine-*N*-propylamide partial structure. This connection was

supported by HMBC correlations from H-4 (δ 1.47), H-5 (δ 2.04) and H-8 (δ 3.09) to the carbonyl carbon at δ 172.5 ppm (C-6). The structure of a methylphenol group was secured by HMBC correlations from H-22 (δ 6.68 ppm) to the methyl carbon C-24 (δ 19.0 ppm) and to the quaternary aromatic carbon at δ 127.7 ppm (C-18). Correlations were also observed from the methyl protons at δ 2.14 ppm (H-24) and from H-20 (δ 6.77 ppm) to C-18. The position of the phenolic group was confirmed by a $^{3}J_{CH}$ correlation from H-21 (δ 7.13 ppm) to the oxygenated aromatic carbon C-19 (δ 154.7 ppm). Correlations from the C-16 methylene protons (δ 3.30/3.49) to the carbonyl carbon C-17 (δ 203.4) indicated that a ketone was adjacent to this methylene. Four-bond correlations from the aromatic protons H-22 and H-20 to C-17, allowed the connection of the methylphenol partial structure to the pyrrolidine-*N*-propylhexanamide. Thus, the structure of the salt of peripentadenine (**81**) was established. The sharpness of the exchangeable proton at δ 10.26 ppm in Figure 46 suggested the phenolic proton was hydrogen bonded to the oxygen of the ketone.

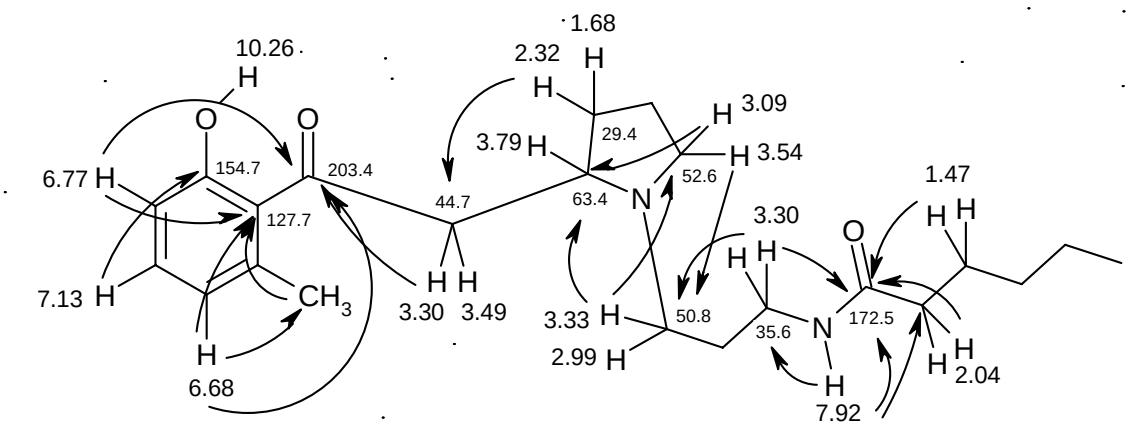


**Figure 58.** Connection of the partial structures of peripentadenine (**81**) established from key HMBC correlations.

In the previous report of the structure elucidation of peripentadenine (**81**) the compound was isolated as the free base and was a racemate, since an optical rotation close to zero was observed. Racemization was postulated to occur during extraction with ammonia.[2] The TFA salt of peripentadenine (**81**) had a *trans*-diaxial relationship between H-15 and

H-11, since a strong COSY correlation was observed between H-15 and H-11. The optical rotation of **81** was also observed to be $0^{o}$, indicating the compound was a racemate. The energy minimized structure of peripentadenine (**81**) is shown in Figure 59.

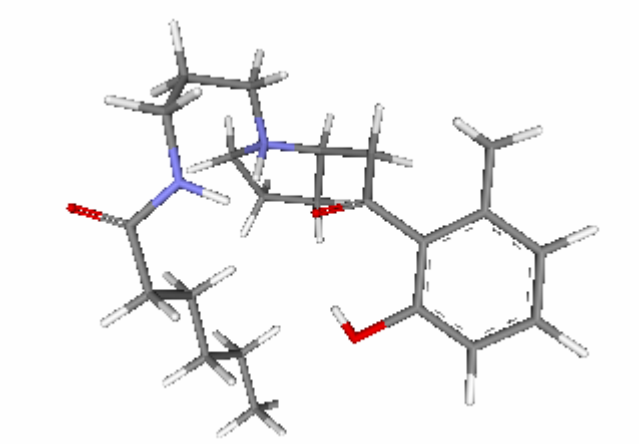

**Figure 59.** The energy minimized structure of peripentadenine (**81**).

## 5.5 Structure Elucidation of Mearsamine 1 (124)

Mearsamine 1 (**124**) was assigned the molecular formula $C_{15}H_{28}N_2O_3$ by high resolution positive electrospray mass measurement of the $[M + H]^+$ ion at *m/z* 285.215921 (calculated for 285.217269). The major peaks at 3404, 1683 and 1200 $cm^{-1}$ in the IR spectrum of **124** indicated the presence of a hydroxyl, a carbonyl, and carbon-nitrogen bonds, respectively. Inspection of the $^1H$ NMR spectrum of mearsamine 1 (Figure 60) reveals a much simpler spectrum when compared to those of peripentonine (**123**) and peripentadenine (**81**) (Figures 51 and 56, respectively). The $^1H$ NMR spectrum of mearsamine 1 (**124**) showed significant homology with the spectra of peripentonine (**123**) and peripentadenine (**81**). In particular, signals for the pyrrolidine and propylhexanamide moieties were consistent. However, Figure 60 shows the absence of signals corresponding to olefinic protons. An amide signal was observed at δ 7.90 and an exchangeable proton at δ 9.48 ppm. The absence of a C-24 methyl group was also noted in Figure 60. The molecular formula of the pyrrolidine-*N*-propylhexanamide moiety

found in peripentadenine **(81)** is $C_{13}H_{25}N_2O$. When this is subtracted from the molecular formula determined for mearsamine 1 (**124**), the remainder is $C_2H_3O_2$. This suggests the absence of a six-membered ring in **124**.

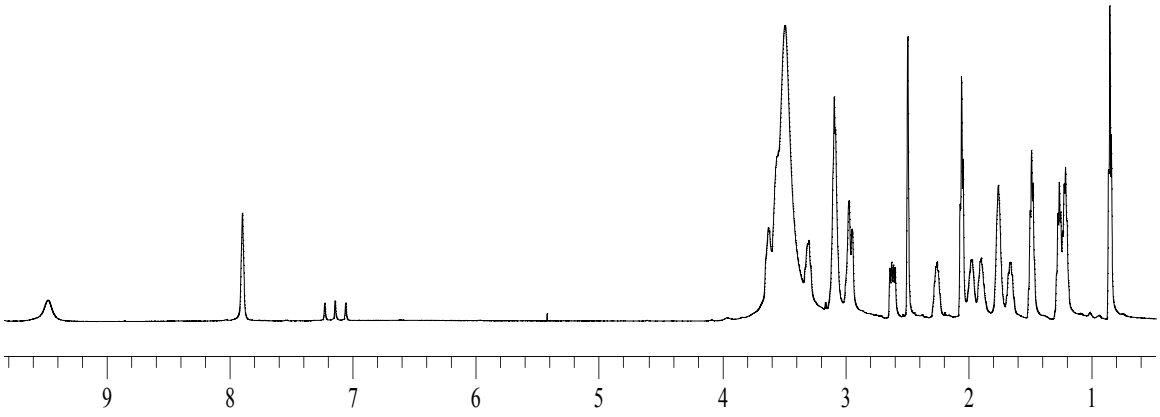


**Figure 60**. The $^1$H NMR spectrum of mearsamine 1 (**124**) at 600 MHz in $d_6$-DMSO.

The $^{13}$C NMR spectrum of mearsamine 1 (**124**) contained 15 carbons. Two carbonyl carbons were found at δ 172.5 and 171.2 ppm. One of these was the amide carbonyl of the hexanamide group, and the molecular formula suggested the other carbonyl carbon was part of a carboxylic acid. The chemical shifts of several carbons were identical to the pyrrolidine-*N*-propylhexanamide carbons of peripentadenine (**81**). The only difference in the $^{13}$C NMR spectrum of mearsamine 1, excluding the absence of aromatic carbons, was the upfield shift of C-16 from δ 44.7 in **81** to 35.4 ppm in **124**. The $^{13}$C and $^1$H NMR spectral data for mearsamine 1 (**124**) is represented in Table 12.

Analysis of HSQC spectral data established the presence of 26 carbon bound protons including one methyl, 11 methylenes, and one methine. The partial structures of mearsamine 1 (**124**) shown in Figure 61 were deduced from HSQC and COSY spectra. The propylamide and pentyl partial structures and the carbon backbone of the pyrrolidine, were elucidated in an identical manner as for **123** and **81**.

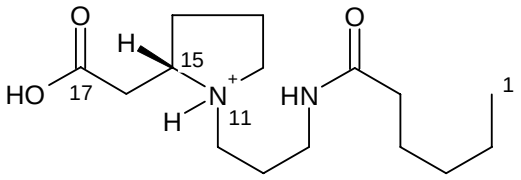


**Table 12.** $^{13}C^{a}$ and $^{1}H^{b}$ NMR spectral data for mearsamine 1[c] (**124**).

| position | $^{13}C$, δ | $^{1}H$, δ, mult, *J* (Hz) | HMBC $^{2,3}J_{CH}$ |
|---|---|---|---|
| 1 | 13.8 | 0.85 (3H, t, 7.2) | 2, 3 |
| 2 | 22.0 | 1.26 (2H, t, 7.2) | 1, 3, 4 |
| 3 | 30.9 | 1.22 (2H, t, 7.2) | 1, 2 , 4, 5 |
| 4 | 24.8 | 1.48 (2H, t, 7.2) | 2, 3, 5, 6 |
| 5 | 35.3 | 2.05 (2H, t, 7.2) | 3, 4, 6 |
| 6 | 172.5 | - | - |
| 7 | - | 7.90 (1H, s) | 5, 6, 8 |
| 8 | 35.6 | 3.08 (2H, t, 7.2) | 6, 9, 10 |
| 9 | 25.5 | 1.76 (2H, brt, 7.2) | 8, 10 |
| 10 | 51.2 | 2.97 (1H, m) | 9, 12 |
| | | 3.29 (1H, ddd, 2.4, 9.6, 19.8) | |
| 11 | - | 9.48 (1H, br) | - |
| 12 | 52.9 | 3.08 (1H, m) | 13, 14, 15 |
| | | 3.55 (1H, brdd, 4.8, 9.6) | |
| 13 | 21.4 | 1.89 (1H, dddd, 7.2, 7.2, 7.2, 15.6) | 12, 14, 15 |
| | | 1.97 (1H, dddd, 5.4, 5.4, 5.4, 13.2) | |
| 14 | 29.3 | 1.66 (1H, ddd, 7.8, 7.8, 15.4) | 12, 13, 15, 16 |
| | | 2.25 (1H, ddd, 6.6, 6.6, 14.4) | |
| 15 | 64.0 | 3.62 (1H, br) | 17 |
| 16 | 35.4 | 2.62 (1H, dd, 9.0, 16.8) | 14, 17 |
| | | 2.94 (1H, dd, 4.8, 16.8) | |
| 17 | 171.2 | - | - |

[a]At 125 MHz. [b]At 600 MHz. [c]In $d_6$-DMSO.

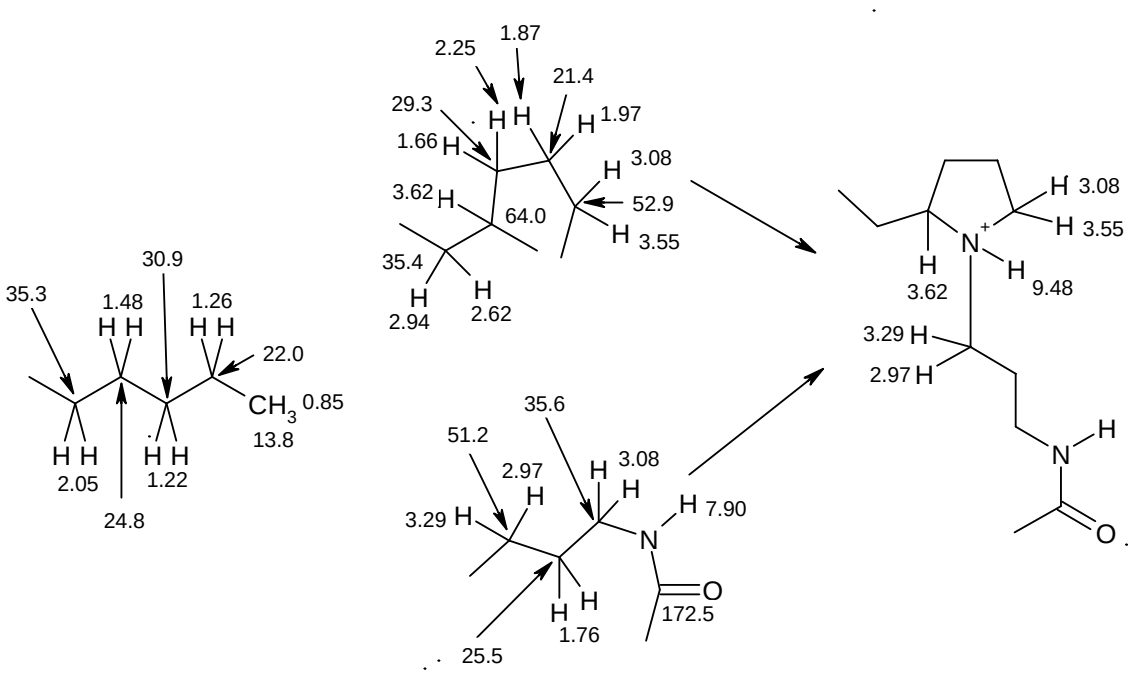


**Figure 61.** The partial structures of mearsamine 1 (**124**) established from COSY and HSQC experiments.

The pyrrolidine and propylamide fragments were linked by COSY correlations to the N-H exchangeable proton at δ 9.48 ppm (H-11). The chemical shifts of all of these protons were within ±0.05 ppm range of the chemical shifts of the pyrrolidine-*N*-propylhexanamide protons of peripentadenine (**81**). The only exceptions were the chemical shift of H-15, where a difference of 0.17 ppm was observed, and a significant shift of the H-16 methylene to δ 2.62/2.94 in mearsamine 1 (**124**) from 3.30/3.49 ppm in peripentadenine (**81**).

HMBC correlations (Figure 62) secured the structure of the propylhexanamide in an identical manner as for peripentadenine (**81**). HMBC correlations from the methylene protons at δ 3.29/2.97 (H-10) to C-12 (52.9) and C-15 (64.0), and from 3.08/3.55 (H-12) to C-10 (51.2 ppm) and C-15 confirmed the connection of a propyl group to the nitrogen of the pyrrolidine. Correlations from the H-14 methylene (δ 1.66/2.25) and from H-15 (3.62) to C-16 (35.4) confirmed the position of the H-16 methylene (2.62/2.94). HMBC correlations from H-16 and H-15 to a carbonyl carbon at δ 171.2 ppm (C-17) indicated

that a carbonyl carbon was vicinal to the methylene of C-16. This carbonyl was assigned to a carboxylic acid, as an oxygen and hydrogen were the only two atoms unaccounted for from the molecular formula. Thus the structure of the TFA salt of mearsamine 1 (**124**) was established.

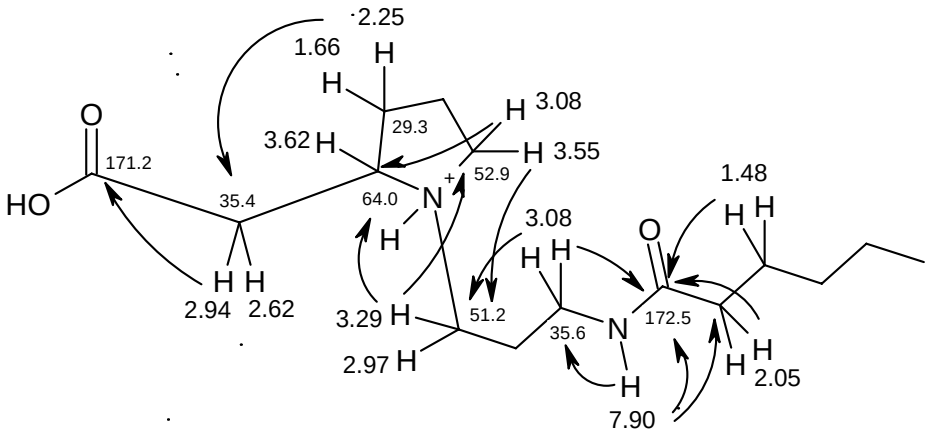


**Figure 62.** Connection of the partial structures of mearsamine 1 (**124**) established from key HMBC correlations.

The orientation of H-15 (δ 3.62) relative to H-11 (δ 9.48) can be regarded as axial-axial due to an intense COSY correlation between these protons. The optical rotation of mearsamine 1 (**124**) was -5.81°. The energy minimized structure of **124** is illustrated in Figure 63.

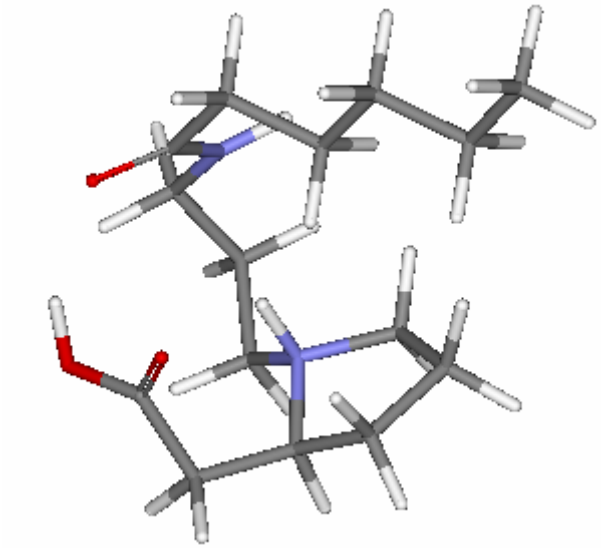

**Figure 63.** The energy minimized structure of mearsamine 1 (**124**).

## 5.6 Structure Elucidation of Mearsamine 2 (125)

Mearsamine 2 (**125**) was assigned a molecular formula $C_{22}H_{39}N_2O_4$ by high resolution positive electrospray mass measurement of the $[M + H]^+$ ion 395.290601 (calculated for 395.290434). This indicated that **125** contained the same number of carbons as peripentonine (**123**) and peripentadenine (**81**), however it also possessed an extra oxygen atom. The major peaks at 3457, 3288, 1677 and 1187 $cm^{-1}$ in the IR spectrum of **125** indicated the presence of an -OH and -NH, a carbonyl, and carbon-nitrogen bonds, respectively. The $^1H$ NMR spectrum of mearsamine 2 (**125**) (Figure 64) contained the characteristic signals for a propylhexanamide chain, however the downfield region of the spectrum was unique when compared to the other *Peripentadenina* alkaloids. The absence of olefinic and exchangeable protons in Figure 64 was one of the distinguishing features.

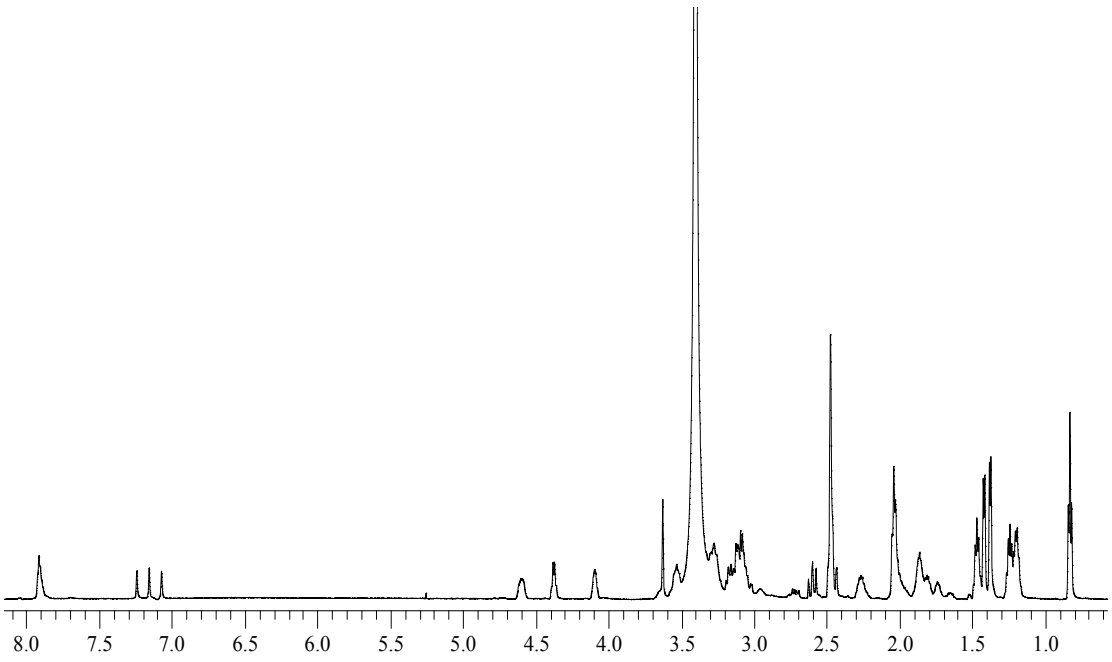


**Figure 64**. The $^1H$ NMR spectrum of mearsamine 2 (**125**) at 600 MHz in $d_6$-DMSO.

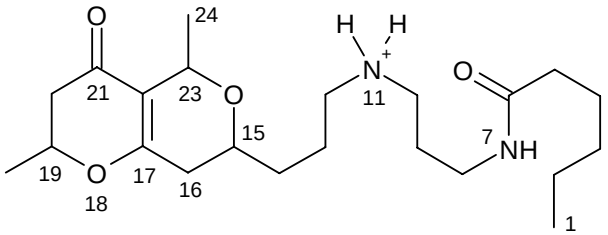


**Table 13.** $^{13}C^{a}$ and $^{1}H^{b}$ NMR spectral data for mearsamine 2[c] (**125**)

| position | $^{13}C$, δ | $^{1}H$, δ, mult, *J* (Hz) | HMBC $^{2,3}J_{CH}$ |
|---|---|---|---|
| 1 | 13.8 | 0.83 (3H, t, 7.2) | 2, 3 |
| 2 | 21.8 | 1.25 (2H, t, 7.2) | 1, 3, 4 |
| 3 | 30.9 | 1.20 (2H, t, 7.2) | 1, 2 , 4, 5 |
| 4 | 24.8 | 1.47 (2H, t, 7.2) | 2, 3, 5, 6 |
| 5 | 35.6 | 2.03 (2H, t, 7.2) | 3, 4, 6 |
| 6 | 172.5 | - | - |
| 7 | - | 7.91 (1H, s) | 5, 6, 8 |
| 8 | 35.4 | 3.10 (2H, m) | 6, 9, 10 |
| 9 | 21.8 | 1.87 (2H, t, 7.2) | 8, 10 |
| 10 | 55.8 | 3.28 (2H, m) | 8, 9, 12 |
| 12 | 58.6 | 3.53 (1H, ddd, 5.4, 7.2, 12.6) | 10, 13, 14, 15 |
| | | 3.17 (1H, ddd, 2.4, 9.6, 12.6) | |
| 13 | 20.1 | 2.03 (2H, t, 7.2) | 12, 14, 15 |
| 14 | 29.6 | 2.27 (1H, ddd, 7.2, 7.2, 15.0) | 12, 13, 15, 16 |
| | | 1.81 (1H, ddd, 6.6, 6.6, 13.8) | |
| 15 | 66.7 | 4.10 (1H, br) | 17 |
| 16 | 29.8 | 3.15 (1H, dd, 11.4, 10.8) | 14, 15, 17, 22 |
| | | 2.49 (1H, m) | |
| 17 | 168.0 | - | - |
| 19 | 75.9 | 4.60 (1H, ddd, 4.2, 7.2, 14.4) | - |
| 20 | 41.8 | 2.60 (1H, dd, 15.6, 15.6) | 19, 21, 19-Me |
| | | 2.47 (1H, m) | |
| 21 | 188.4 | - | - |
| 22 | 108.7 | - | - |
| 23 | 56.8 | 4.37 (1H, q, 6.6) | 15, 17, 21, 22, 24 |
| 24 | 16.4 | 1.42 (3H, d, 6.6) | 22, 23 |
| 19-Me | 19.9 | 1.38 (3H, d, 6.6) | 19, 20, 21 |

[a]At 125 MHz. [b]At 600 MHz. [c]In $d_6$-DMSO.

Figure 64 shows a methyl triplet at δ 0.83 ppm, two methyl doublets at 1.38 and 1.42, two methylenes at 1.20 and 1.25, and a signal at 2.03 ppm which integrated to three protons. A group of five signals were found between δ 3.00 and 3.60 ppm, indicating possible methylenes or methines bound to heteroatoms. Three protons resonated at δ

4.10, 4.37 and 4.60 ppm, which are typical chemical shifts for oxygenated methine protons. A signal at δ 7.91 ppm was observed, which is consistent with the chemical shift in DMSO for the amide proton H-7 of peripentadenine (**81**) and mearsamine 1 (**124**).

The $^{13}$C NMR spectrum of mearsamine 2 (**125**) contained signals for seven carbons which were almost identical to the chemical shifts of C-1 to C-6 and C-8 in peripentadenine (**81**) and mearsamine 1 (**124**). Four other methylene carbons were observed between δ 20 and 40 ppm. Two additional methyl groups were found at δ 16.4 and 19.9 ppm. Signals observed at δ 55.8, 56.8, 58.6, 66.7 and 75.9 ppm suggest carbons bound to heteroatoms. Three downfield signals were observed, other than the amide carbonyl carbon, which resonated at δ 108.7, 168.0 and 188.4 ppm. The carbon at δ 188.4 was indicative of an α,β-unsaturated ketone. The alpha and beta carbons are the carbons at δ 108.7 and 168.0 ppm, respectively. In this system the chemical shift of the α-carbon has shifted upfield, whereas the β-carbon has shifted downfield, relative to typical chemical shifts for such carbons. This suggested an electron withdrawing atom, possibly an oxygen, was attached to the β-carbon. The $^{1}$H and $^{13}$C NMR spectral data of mearsamine 2 (**125**) is shown in Table 13.

HSQC spectral data established the presence of 36 carbon bound protons including three methyls, 12 methylenes and three methines. A COSY experiment allowed the construction of the partial structures illustrated in Figure 65. A pentyl chain partial structure was assembled in an identical manner as for mearsamine 1 (**124**) and peripentadenine (**81**), with the chemical shifts of H-1 to H-5 almost identical for all three compounds. The chemical shifts and COSY correlations of the amide proton H-7 and the H-8 methylene also matched the same protons in **81** and **124**, however the methylene H-9 (δ 1.87) was shifted downfield. COSY correlations were observed from this proton to the methylenes H-8 (δ 3.10) and H-10 (δ 3.28). This enabled the construction of a propylamide partial structure. Another aliphatic fragment was assembled from correlations from the methylene at δ 2.03 (H-13) to the methylene protons H-12 and H-14, at δ 3.53/3.17 and 2.27/1.81 ppm respectively. COSY correlations from H-14 to the proton at δ 4.10 ppm (H-15) indicated that this oxygenated methine was adjacent to H-14.

COSY correlations from the H-16 methylene protons at δ 3.15/2.49 ppm to H-15, demonstrated that this methylene was vicinal to H-15. Two final partial structures were created by correlations from the methyl group at δ 1.42 (H-24) to the oxygenated methine at 4.37 (H-23). COSY correlations were observed from the proton of another oxygenated methine at δ 4.60 (H-19) to the protons of a methyl group at δ 1.38 (H-$19_{Me}$), and methylene protons at δ 2.60/2.47 ppm (H-20). The proton at δ 4.60 was bound to a carbon at 75.9 ppm, which was characteristic of an ether.

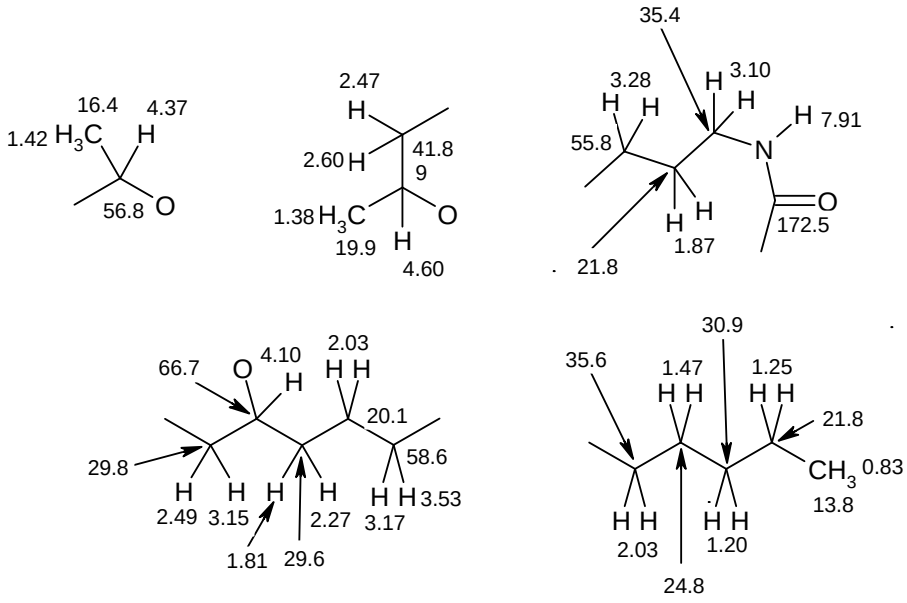


**Figure 65.** The partial structures of mearsamine 2 (**125**) established from COSY and HSQC experiments.

Only two HMBC correlations (Figure 66) were observed from the H-24 methyl group (δ 1.42 ppm) to the oxygenated methine C-23 (δ 56.8) and quaternary olefinic carbon C-22 (δ 108.7). The proton H-23 (δ 4.37) exhibited $^{3}J_{CH}$ correlations to the ketone carbonyl at δ 188.4 (C-21), C-17 (δ 168.0) and C-15 (δ 66.7). This confirmed that H-23 was attached to C-22, the α-carbon of the α,β-unstaturated ketone. The correlation from H-23 to C-15 suggested an ether linkage between C-15 and C-23. The structure of a pyran ring was deduced from a $^{3}J_{CH}$ correlation from H-15 (δ 4.60) to C-17. The structure of the pyran was supported by HMBC correlations from the methylene H-16 (3.15/2.49) to C-17 and

C-22. Correlations from H-16 to C-14 (δ 29.6), and H-14 (δ 1.81/2.27) to C-16 (δ 29.8) provided further evidence for the positioning of H-14 vicinal to H-15. The H-20 methylene (δ 2.60/2.47) displayed $^{2}J_{CH}$ correlations to the ketone carbonyl C-21 (δ 188.4), which allowed the connection of the -$CH_2$-CH($CH_3$)-O- partial structure to the ketone. The methyl group at δ 1.38 (H-$19_{Me}$) of this partial structure displayed only two HMBC correlations to C-19 (δ 75.9) and C-20 (δ 41.8), supporting the position of H-20 as vicinal to C-21. No HMBC correlations were observed from H-19 (δ 4.60), however an ether linkage between C-19 and C-17 was determined on the basis of the chemical shifts of these carbons and MS evidence. This secured the structure of the bi-pyrano ring system. An unusual four-bond correlation was observed from the proton at δ 3.53 ppm (H-$12_{\alpha}$) to C-15. A linkage between the pentyl chain and the propylamide, to create a propylhexanamide group, was confirmed by correlations from H-7 (δ 7.91), H-8 (δ 3.10), C-5 (δ 2.03) and H-4 (δ 1.47) to the amide carbonyl carbon at δ 172.5 ppm (C-6). HMBC correlations from H-12 (δ 3.53/3.17) to C-10 (55.8) and from H-10 (δ 3.28) to C-12 (58.6) allowed the connection of the propylhexanamide to the end of the propyl group of the bi-pyrano structure, via an amine linkage. Thus the structure of mearsamine 2 (**125**) was established. Grandisine A (**73**) contains the same bi-pyrano ring system.

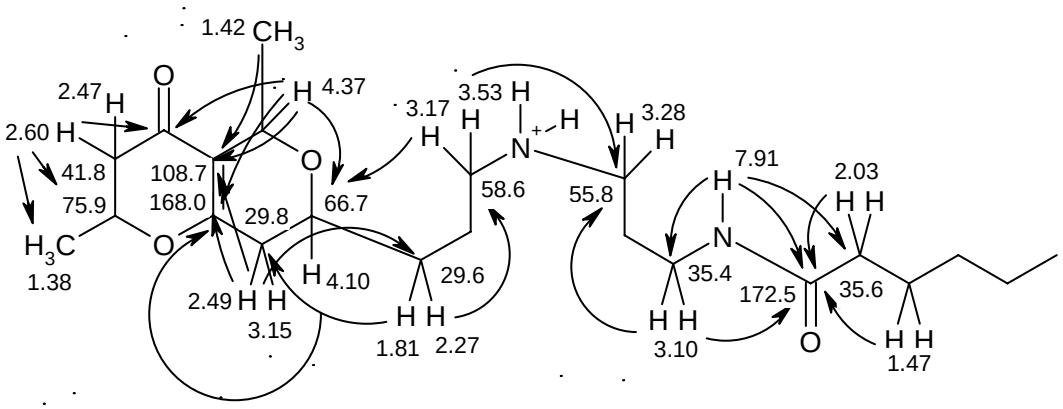


**Figure 66.** Connection of the partial structures of mearsamine 2 (**125**) established from key HMBC correlations.

Coupling constants were used to assign axial configurations for two of the three chiral centres in **125**. The proton at δ 4.60 (H-19, ddd) exhibited three couplings of 4.2, 7.2 and 14.4 Hz. The coupling of 14.4 Hz indicated that a *trans*-diaxial relationship exists between H-$20_{ax}$ (2.60, dd, $J$ = 15.6, 15.6) and H-19. Both couplings are characteristic of geminal and axial-axial couplings. The same diaxial configuration was observed between these two protons in grandisine A (**73**). Couplings of 16.8 and 13.2 Hz were observed for the H-$20_{ax}$ equivalent proton in **73**. A correlation in the ROESY spectrum from 4.60 to 2.47 suggested these protons were in a *cis* arrangement and supported the *trans*-diaxial configuration between 4.60 and 2.60 (Figure 67). An axial configuration was also determined for H-15 (4.10, br) from coupling constants. The two large couplings determined for H-$16_{ax}$ (3.15, dd, 11.4, 10.8 Hz) indicate geminal and axial-axial couplings This is supported by a ROESY correlation (Figure 67) between H-$16_{eq}$ (δ 2.49) and H-15, indicating a *cis* relationship. The stereochemistry of H-23 (4.37) relative to H-15 could be determined as equatorial by ROESY correlations. A correlation was observed between H-24 (δ 1.42) and H-15 (Figure 67), suggesting the methyl group and this proton were on the same face of the ring. A subsequent correlation from H-23 to H-$16_{ax}$ also suggested these two protons were on the same face, therefore securing the equatorial assignment for H-23. However, the stereochemistry of H-19 relative to H-24 or H-15 could not be established. Therefore two structures (Figure 68) of mearsamine 2 are possible. The energy minimized structure of mearsamine 2 (**125**) is shown in Figure 69.

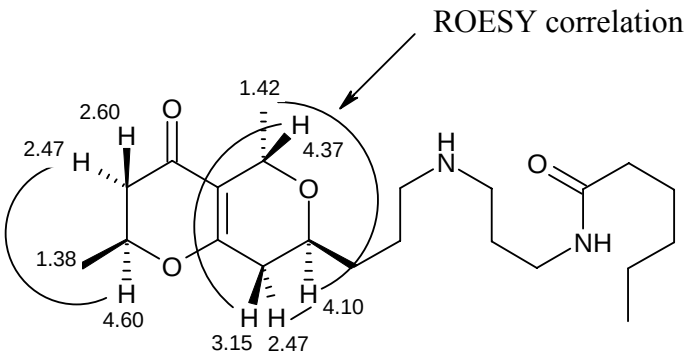


**Figure 67.** Key ROESY correlations for mearsamine 2 (**125**).

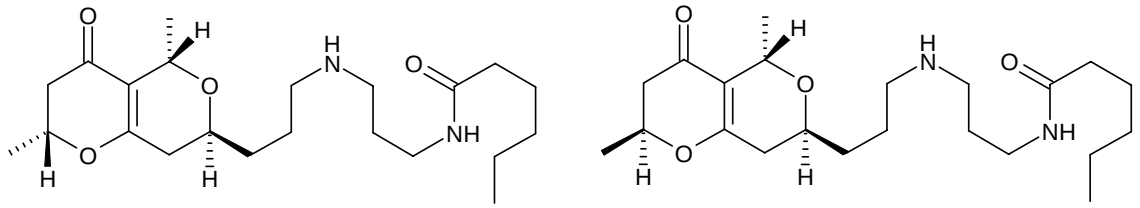

**Figure 68.** The two possible structures of mearsamine 2 (**125**).

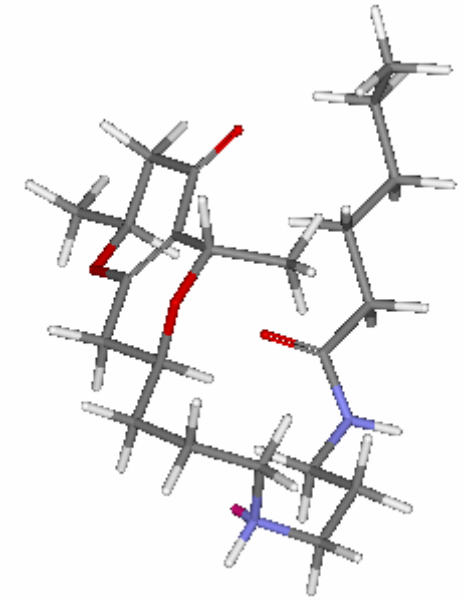

**Figure 69.** The energy minimized structure of one of the possible structures of mearsamine 2 (**125**).

## 5.7 Proposed Biogenesis of *Peripentadenia* Alkaloids and Chemotaxonomic Considerations

Plants from the genus *Peripentadenia* have provided some diverse chemical structures which show similarities to compounds isolated from other plants from the *Elaeocarpaceae*. Peripentonine (**123**) contains the same methylcyclohexenone moiety as

habbenine (**114**). Peripentadenine (**81**) possesses a methyl phenolic group which has also been encountered in isoelaeocarpicine (**62**) and elaeocarpenine (**122**). *P. mearsii* also produced compounds which are unique to the genus, such as mearsamine 1 (**124**) and 2 (**125**). An interesting observation from both species is that peripentadenine (**81**) was exclusive to the bark of this species and peripentonine (**123**) was only found in the leaves and the seeds of *P. mearsii*. Peripentadenine (**81**) has also previously been isolated from the leaves and bark of *P. mearsii*.

I propose that the biogenesis of the *Peripentadenia* alkaloids is an extension of either of the habbenine (**114**) pathways (Figure 70). The precursor (**i**) can theoretically be produced by either the retro-aldol or malonyl-CoA pathways proposed for habbenine. Transamination of (**i**) could yield (**ii**), which can undergo an amide coupling with hexanoic acid. An amino acid may provide the nitrogen for the transamination reaction. This may yield the propylhexanamide derivative (**iii**), which can be regarded as a common precursor of mearsamine 2 (**125**), peripentonine (**123**) and peripentadenine (**81**).

Reduction of (**iii**) may yield peripentonine (**123**), and further reduction of **123** could lead to peripentadenine (**81**). A ring opening of the six-membered ring in (**iii**) via a retro-aldol reaction could lead to (**iv**), a precursor of mearsamine 2 (**125**). The subsequent formation of the bi-pyrano ring system was modeled on the proposed biogenesis of grandisine A (**73**).[5] The formation of the alcohols in (**v**) could occur by the reduction of the two methyl ketones. Nucleophilic attack of the alcohol shown in (**v**) to the α-methine of the pyrrolidine may lead to the ring opening of the pyrrolidine and formation of a six membered pyran ring in (**vi**). Attack of the second alcohol onto the carbonyl carbon of the ketone in the pyran ring could yield the bicyclic structure (**vii**). Dehydration of (**vii**) would produce the α,β-unsaturated ketone and yield mearsamine 2 (**125**).

Mearsamine 1 (**124**) is proposed to be the product of a retro-Claisen condensation reaction on peripentonine (**123**) (Figure 71). Peripentonine was proposed as the source of mearsamine 1, as both compounds were only found in the leaves of *P. mearsii*.

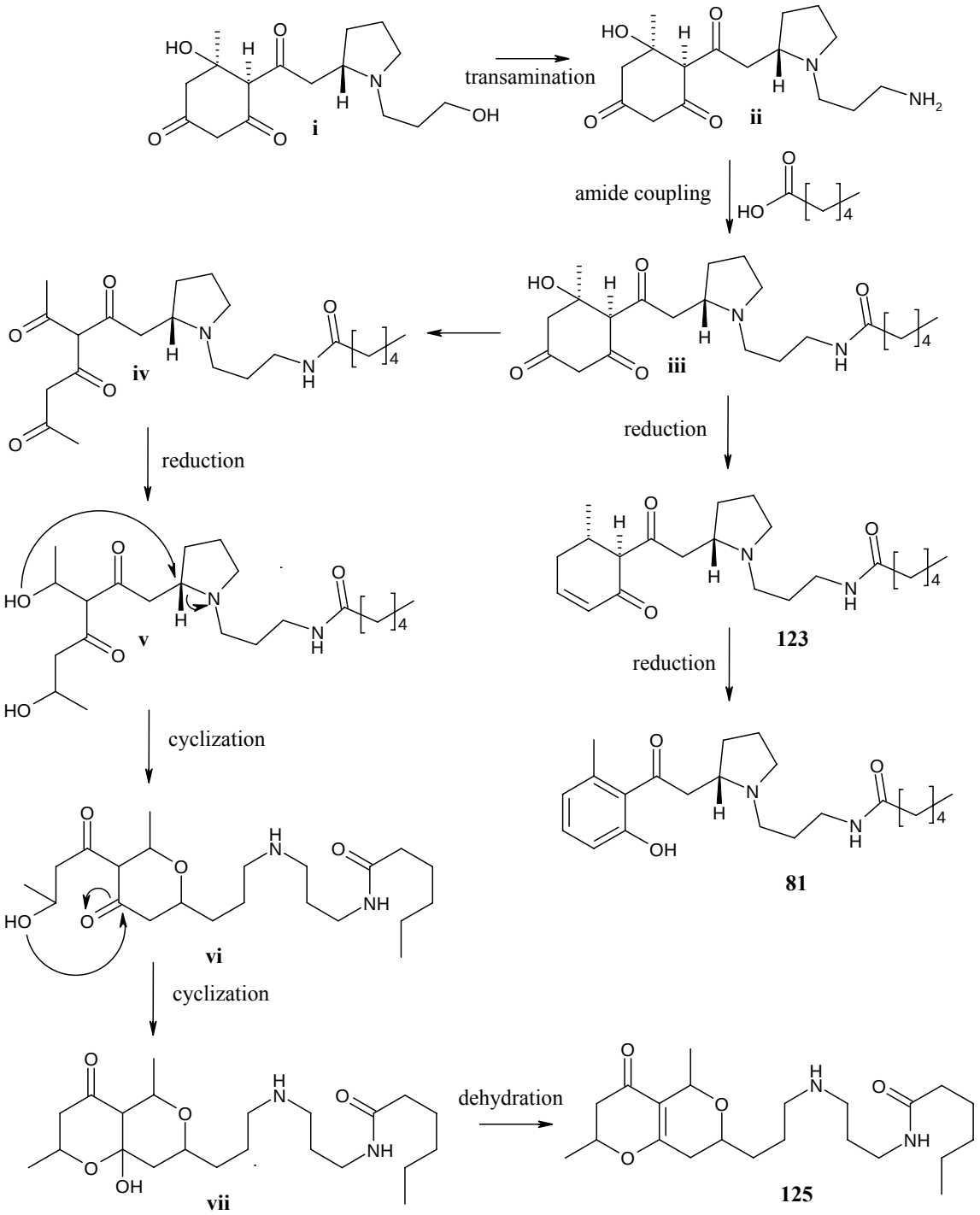


**Figure 70.** Proposed biogenesis of the *Peripentadenia* alkaloids peripentonine (**123**), peripentadenine (**81**) and mearsamine 2 (**125**).

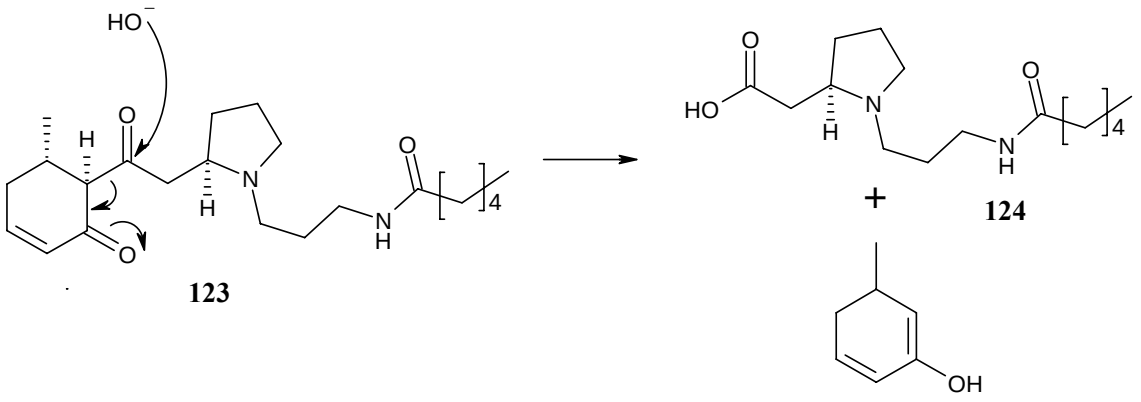


**Figure 71.** Proposed biogenesis of mearsamine 1 (**124**) by a retro-Claisen condensation of peripentonine (**123**).

## 5.8 References


1. Henderson, P. L., *Queensland Vascular Plants: Names and Distribution*. ed.; Queensland Herbarium: Brisbane, **1994**.
2. Lamberton, J. A., Gunawardana, Y. A. G. P., Bick, I. R. C., *J Nat Prod* **1983,** 46, 235 - 247.
3. Bick, I. R. C., Gunawardana, Y. A. G. P., Lamberton, J. A., *Tetrahedron* **1985,** 41, 5627 - 5631.
4. Mazzini, C., Sambri, L., Regeling, H., Zwanenburg, B., Chittenden, G. J. F., *JCS Perkin 1* **1997**, 3351 - 3356.
5. Carroll, A. R., Arumugan, G., Quinn, R. J., Redburn, J., Guymer, G., Grimshaw, P., *J Org Chem* **2005,** 70, 1889 - 1892.

# CHAPTER 6 – The Isolation and Structure Elucidation of Novel Indolizidine Alkaloids from *Elaeocarpus grandis*.

## 6.1 Introduction

*Elaeocarpus grandis* is a rainforest tree which grows along the east coast of Queensland, Australia, in sub-tropical rainforests and along creeks and rivers.[1] *E. grandis* is commonly known as the blue quandong, due to the characteristic blue colour of its fruits (Appendix III). *E. grandis* has recently been shown to be a source of indolizidine alkaloids.[2] This chapter describes the chemical investigation of this species. Two different extraction procedures were used in this investigation.

Leaves of *E. grandis* were collected in December 2001 from Mt Tambourine in South East Queensland. This sample was subjected to chemical investigation employing a base free SCX (strong cation exchange) extraction protocol. The new indolizidine alkaloids grandisine C (**127**), D (**126**), and E (**128**), as well as the known alkaloid isoelaeocarpiline (**63**) were purified from this extract.

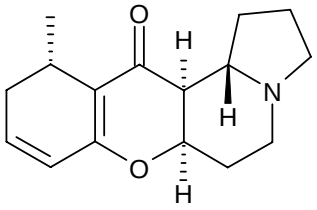


**63**

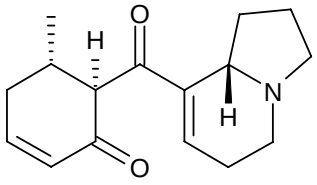


**126**

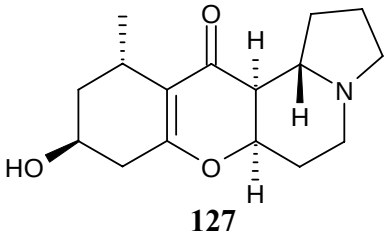


**127**

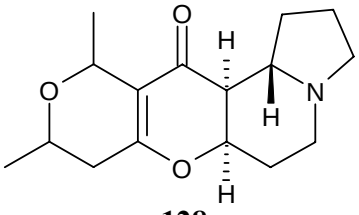


**128**

A second collection of the leaves of *E. grandis* was made in January 2004 from North Queensland. The sample was extracted and alkaloids were isolated by an acid-base protocol. This yielded **63**, **126**, **127** in addition to the novel indolizidine alkaloids grandisine F (**129**), G (**130**) and **131**. Compound **131** was isolated as a mixture of diastereomers. Another fraction contained a mixture of diastereomers of grandisine F (**129**). Grandisine F and G were proposed to be formed from the addition of ammonia to grandisine D (**126**). This study also reports the first complete discussion of the NMR data of isoelaeocarpiline (**63**).

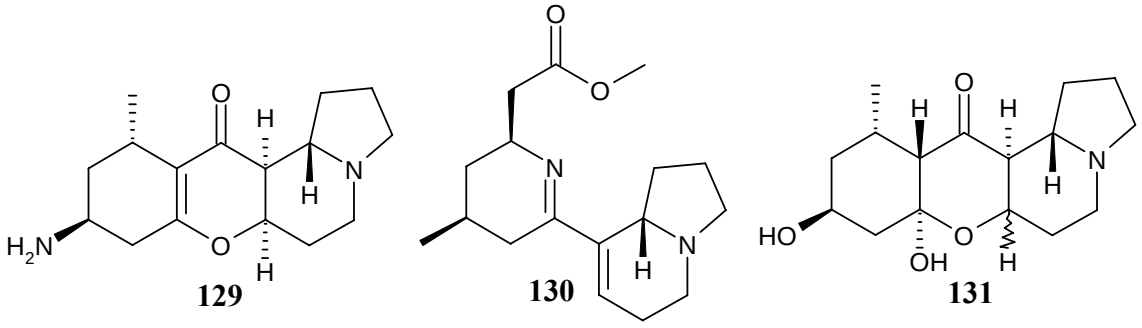


## 6.2 The Isolation of Grandisine C (127), D (126) and E (128) from *E. grandis* by an SCX Extraction Procedure

The purification of isoelaeocarpiline (**63**), grandisine C (**127**), D (**126**), and E (**128**) is depicted in Scheme 9. A methanol extract of the leaves of *E. grandis* was filtered through strongly acidic ion exchange resin. After washing the resin with methanol and water, the alkaloids were eluted with 1M NaCl. The eluant was filtered through C18 and the C18 was washed with copious amounts of water, before the alkaloids eluted with 1%TFA/MeOH.

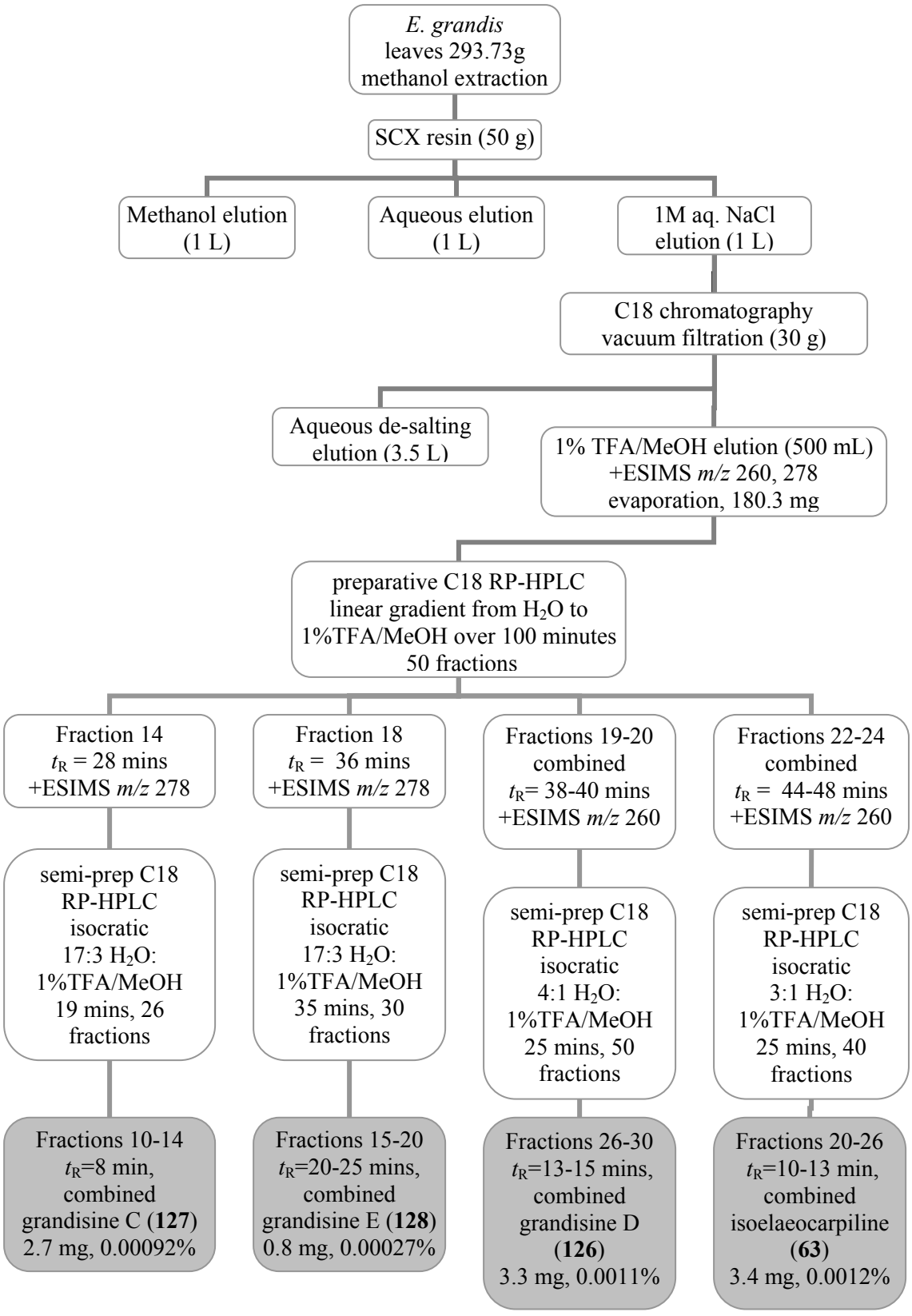


**Scheme 9.** The isolation of indolizidine alkaloids from *E. grandis*.

Mass ion peaks at *m/z* 260 and 278 were detected by positive ESIMS in the alkaloid fraction. This fraction was separated by preparative C18 RP-HPLC, using a linear gradient from $H_2O$ to 1%TFA/MeOH over 100 minutes. Fifty fractions were collected and analysed by positive ESIMS. Mass ion peaks at *m/z* 278 in fractions 14 and 18, and *m/z* 260 in fractions 19 - 24, were observed. The $^1$H NMR spectra of individual fractions showed semi-pure grandisine C (**127**) and E (**128**) in fractions 14 and 18, respectively. Fractions 19 and 20, and 22 - 24 were combined to yield semi-pure grandisine D (**126**) and isoelaeocarpiline (**63**), respectively.

Isoelaeocarpiline (**63**), grandisine C (**127**), D (**126**) and E (**128**) were further purified by isocratic C18 RP-HPLC. Conditions of 17:3 $H_2O$:1%TFA/MeOH were used to purify grandisine C (**127**) (2.7 mg, 0.00092%) and E (**128**) (0.8mg, 0.00027%). Grandisine D (**126**) (3.3 mg, 0.0011%) was purified from fractions 19 – 20 employing 4:1 $H_2O$:1%TFA/MeOH. Isoeleaocarpiline (**63**) (3.4 mg, 0.0012%) was purified from fractions 22 – 24 via C18 RP-HPLC using isocratic elution with 3:1 $H_2O$:1%TFA/MeOH. All compounds were isolated as their TFA salts.

## 6.3 Structure Elucidation of Isoelaeocarpiline (63)

The $^1$H NMR spectrum of isoelaeocarpiline (**63**) (Figure 72) was consistent in the olefinic region with that of the published spectrum.[3] The upfield region of Figure 72 was distinctly different to the published spectrum, since **63** was originally isolated as the free base. Figure 72 shows two olefinic protons at δ 6.32 and 5.94 ppm, in addition to a broad signal at δ 4.58 ppm. A methyl group was found at δ 0.88 ppm. Multiplets at δ 2.15, 1.69 and 1.80 ppm integrated to four, three and two protons respectively. Isoelaeocarpiline was converted to its free base by an acid/base partition and all NMR spectra were subsequently recorded in chloroform.

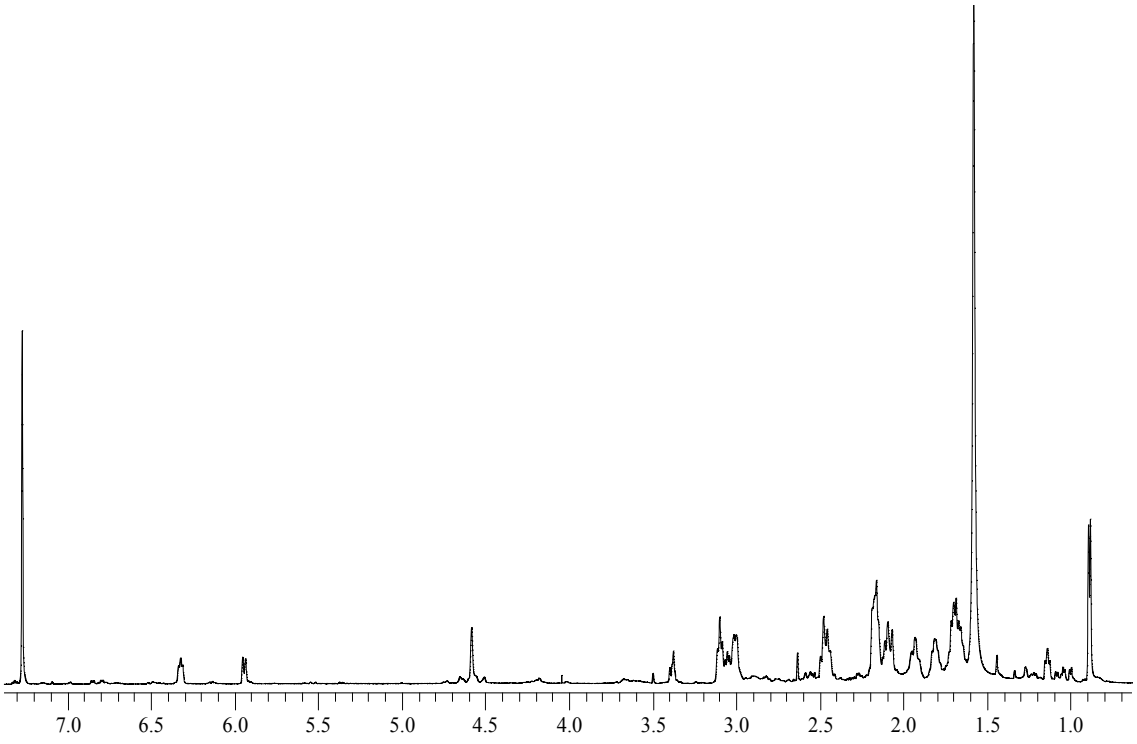


**Figure 72.** The $^{1}H$ NMR spectrum of isoelaeocarpiline (**63**) at 600 MHz in $CDCl_3$.

A total of 16 carbons were observed in the $^{13}C$ NMR spectrum of isoelaeocarpiline (**63**), including four olefinic carbons. An olefinic carbon was observed at δ 164.3 ppm, indicating an oxygenated quaternary carbon. An α,β-unsaturated ketone carbonyl carbon was found at δ 192.5 ppm. The signal at δ 76.4 ppm was consistent with a carbon attached to an ether oxygen. Carbons at δ 54.0, 47.7, 52.8 and 60.5 ppm were indicative of bridgehead or heteroatom bound carbons. In addition, six aliphatic carbons were also observed. The $^{13}C$ and $^{1}H$ NMR spectral data can be found in Table 14.

The partial structures of isoelaeocarpiline (**63**) (Figure 73) were established from HSQC and COSY spectra. One methyl, six methylenes, four methines and two olefinic protons were established from the HSQC spectrum. COSY correlations from H-14 (δ 6.32 ppm) to the olefinic proton H-13 (δ 5.94 ppm) and to the H-15 methylene (δ 2.17/2.45 ppm) enabled the attachment of the double bond to the H-15 methylene. This methylene in turn

correlated to a methine at δ 3.05 ppm (H-16). The attachment of a methyl group (H-17$_{Me}$) to this methine was deduced from a COSY correlation from δ 0.88 to 3.05 ppm.

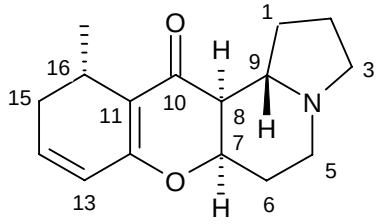


**Table 14.** $^{1}$H,[a] $^{13}$C[b] and HMBC NMR spectral data of isoelaeocarpiline (**63**)[c]

| position | $\delta_C$ | $\delta_H$ (mult; *J* in Hz) | HMBC ($^{2,3}J_{CH}$) |
|---|---|---|---|
| 1 | 29.2 | 1.68 (1H, m); 1.72 (1H, m) | 2, 9 |
| 2 | 21.3 | 1.66 (1H, m); 1.82 (1H, brdd, 8.4, 16.8) | 1, 3 |
| 3 | 54.0 | 2.16 (1H, m); 3.08 (1H, brdd, 9.0, 9.0) | 1, 2, 9 |
| 5 | 47.7 | 2.48 (1H, m); 3.00 (1H, ddd, 2.4, 4.8, 11.4) | 6, 7, 9 |
| 6 | 30.3 | 1.94 (1H, ddd, 5.4, 5.4, 13.8); 2.07 (1H, m) | 5 |
| 7 | 76.4 | 4.58 (1H, br) | 5, 9 |
| 8 | 52.8 | 2.19 (1H, m) | 9, 10 |
| 9 | 60.5 | 2.10 (1H, m) | 1, 2, 5 |
| 10 | 192.5 | - | - |
| 11 | 112.8 | - | - |
| 12 | 164.3 | - | - |
| 13 | 122.5 | 5.94 (1H, d, 9.6) | 11, 15 |
| 14 | 139.7 | 6.32 (1H, brdd, 9.6, 9.6) | 12 |
| 15 | 31.9 | 2.17 (1H, m); 2.45 (1H, m) | 13, 14, 16, 17 |
| 16 | 22.5 | 3.05 (1H, dq, 6.6, 6.6) | 10, 11, 12, 14, 15, 17 |
| 17 | 18.6 | 0.88 (3H, d, 6.6) | 11, 15, 16 |

[a] At 600 MHz. [b] At 125 MHz. [c] In $CDCl_3$.

An eight carbon partial structure was assembled by COSY correlations from the H-2 methylene (δ 1.66/1.82 ppm) to the methylenes H-3 (δ 2.16/3.08 ppm) and H-1 (δ 1.72/1.68 ppm). A COSY correlation from H-1 to the proton at δ 2.10 ppm (H-9) enabled the connection of C-1 to C-9. H-8 (δ 2.19 ppm) was determined to be adjacent to H-9 from a COSY correlation. A correlation from H-8 to H-7 (δ 4.58 ppm) allowed the connection of C-8 to the oxygenated methine at δ 76.4 ppm (C-7). COSY correlations were observed from the methylene at δ 2.07/1.94 ppm (H-6) to the methylene at δ 3.00/2.48 ppm (H-5) in addition to H-7. This completed the carbon backbone of an

indolizidine moiety. However, in contrast to elaeocarpenine (**122**) and isoelaeocarpicine (**62**), an indolizidine functionality could not be determined from the COSY spectrum of **63**, as no correlations were observed from an H-4 exchangeable proton.

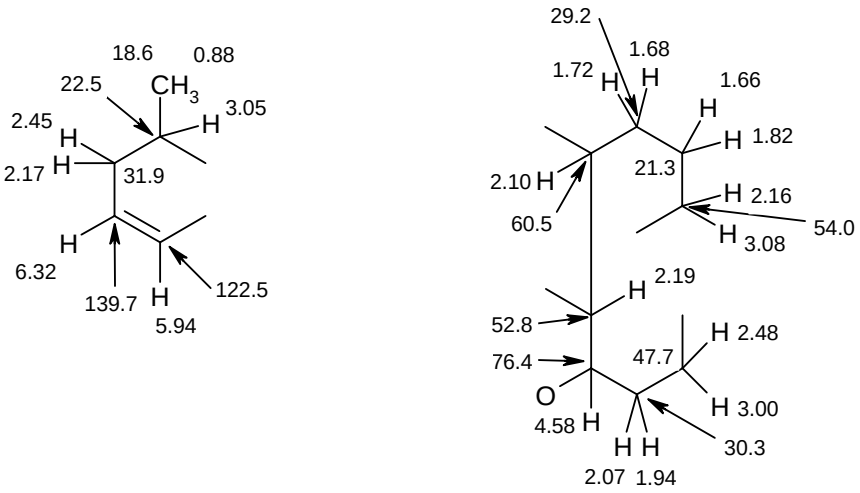


**Figure 73.** The partial structures of isoelaeocarpiline (**63**) established from HSQC and COSY experiments.

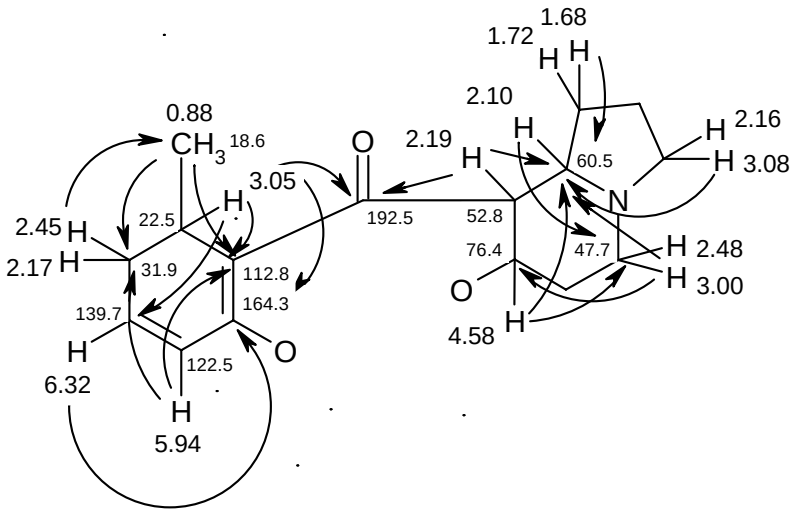


**Figure 74.** The key HMBC correlations for isoelaeocarpiline (**63**).

HMBC correlations (Figure 74) from H-1 (1.72/1.68), H-3 (2.16/3.08), H-5 (2.48/3.00), H-7 (4.58) and H-8 (2.19) to C-9 (60.5) secured the structure of the 7-oxyindolizidine

moiety. Correlations from H-9 (2.10) and H-7 to C-5 (47.7) provided further evidence for this structure. An HMBC correlation from H-8 to the ketone carbonyl carbon at 192.5 ppm (C-10) demonstrated the presence of a 7-oxy-8-ketoindolizidine group. A 1-methyl-3-oxycyclohexadiene ring was formed from the remaining partial structure by HMBC correlations from H-16 (3.05) and H-14 (6.32) to the oxygenated olefinic carbon at δ 164.3 ppm (C-12). The structure of this ring was supported by correlations from H-16 and H-13 (5.94) to C-11, a quaternary olefinic carbon at δ 112.8 ppm. The methyl group H-17 (0.88) showed correlations to C-15 (31.9) and C-11. An HMBC correlation from H-16 to C-10 determined that this tri-substituted cyclohexadiene system was connected to the ketone of the 7-oxy-8-ketoindolizidine. An ether linkage between C-7 and C-12 was suggested from MS evidence and the chemical shifts of these carbons, despite the absence of an HMBC correlation from H-7 to C-12. Thus the structure of isoelaeocarpiline (**63**) was established.

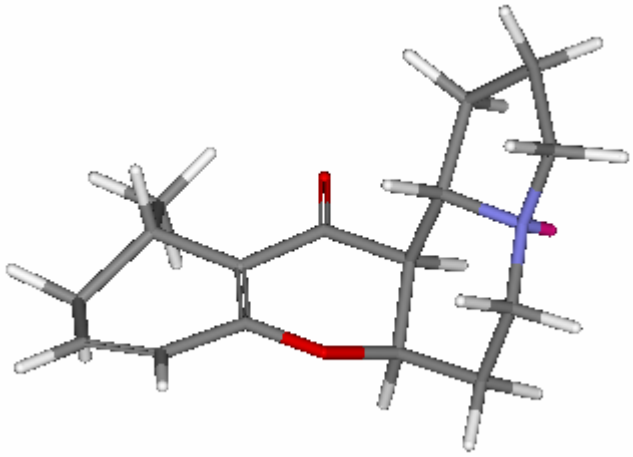

**Figure 75.** The energy minimized structure of isoelaeocarpiline (**63**).

The relative stereochemistry of **63** was established from coupling constants and ROESY correlations. The coupling information from H-16 is not consistent with an equatorial proton. Inspection of the energy minimized structure of **63** (Figure 75) shows the methyl group and H-16 in pseudo equatorial and axial positions due to the twisted boat conformation of the cyclohexadiene ring. Therefore, it can be suggested that the methyl group is therefore pseudo equatorial and H-16 pseudo axial. An axial-equatorial relationship was established between H-7 and H-8 from the ROESY correlation between

these two protons. This indicates a *cis* relationship. The absence of a ROESY correlation between H-8 and H-9 is consistent with an axial-axial relationship between these protons. Therefore H-7 is equatorial, and H-8 and H-9 are both axial. No coupling information could be determined in support of these assignments. ROESY correlations from H-8 and H-9 to other protons in the indolizidine ring were not easily distinguished due to the close chemical shifts of these protons. The relative stereochemistry of isoelaeocarpiline is consistent with the literature.[3] Measurement of the optical rotation of isoelaeocarpiline (**63**) produced a value of +112.10$^{o}$. The literature value was -400$^{o}$,[3] which indicated that **63** was purified as a partial racemate, with an excess of the (+)-enantiomer.

## 6.4 Structure Elucidation of Grandisine D (126)

Grandisine D (**126**) was assigned a molecular formula $C_{16}H_{22}NO_2$ by positive HRESI mass measurement of the $[M + H]^+$ ion 260.16502 (calculated for 260.16451). The positive LRESIMS of grandisine D (**126**) is identical to that of isoelaeocarpiline (**63**). Three olefinic protons were observed in the $^1$H NMR spectrum of grandisine D (Figure 76). Two of these protons were similar in multiplicity to the olefinic protons of isoelaecarpiline (**63**), however the significant shift of H-14 in **63** (δ 6.32 ppm) to δ 7.13 ppm in **126** was noted. The chemical shift of H-13 (δ 5.94 ppm) in **63** was identical in chemical shift to H-13 in grandisine D. A methyl group was noted at δ 0.84 ppm, in addition to signals at δ 2.00 and 2.60 ppm, which integrated to two protons each. Two signals were observed close together at δ 4.30 ppm.

The $^{13}$C NMR spectrum of grandisine D (**126**) showed 16 carbons, including four olefinic carbons at δ 151.6, 140.1, 137.7 and 128.4 ppm. Two carbonyl carbons were found at δ 196.6 and 198.3 ppm, which are typical chemical shifts for α,β-unsaturated ketones. Four carbons were observed between 40 and 60 ppm, indicating bridgehead carbons or carbons

bound to heteroatoms. Six aliphatic carbons were observed between 15 and 40 ppm. The $^{13}C$ and $^{1}H$ NMR spectral data are presented in Table 15.

The UV spectrum of grandisine D (**126**) revealed maxima at 267 and 325 nm, which are characteristic for saturated and α,β-unsaturated ketones, respectively. The major absorbances at 3419, 1652 and 1125 $cm^{-1}$ in the IR spectrum of **126** indicated the presence of a hydroxyl, a carbonyl, and carbon-nitrogen bonds, respectively.

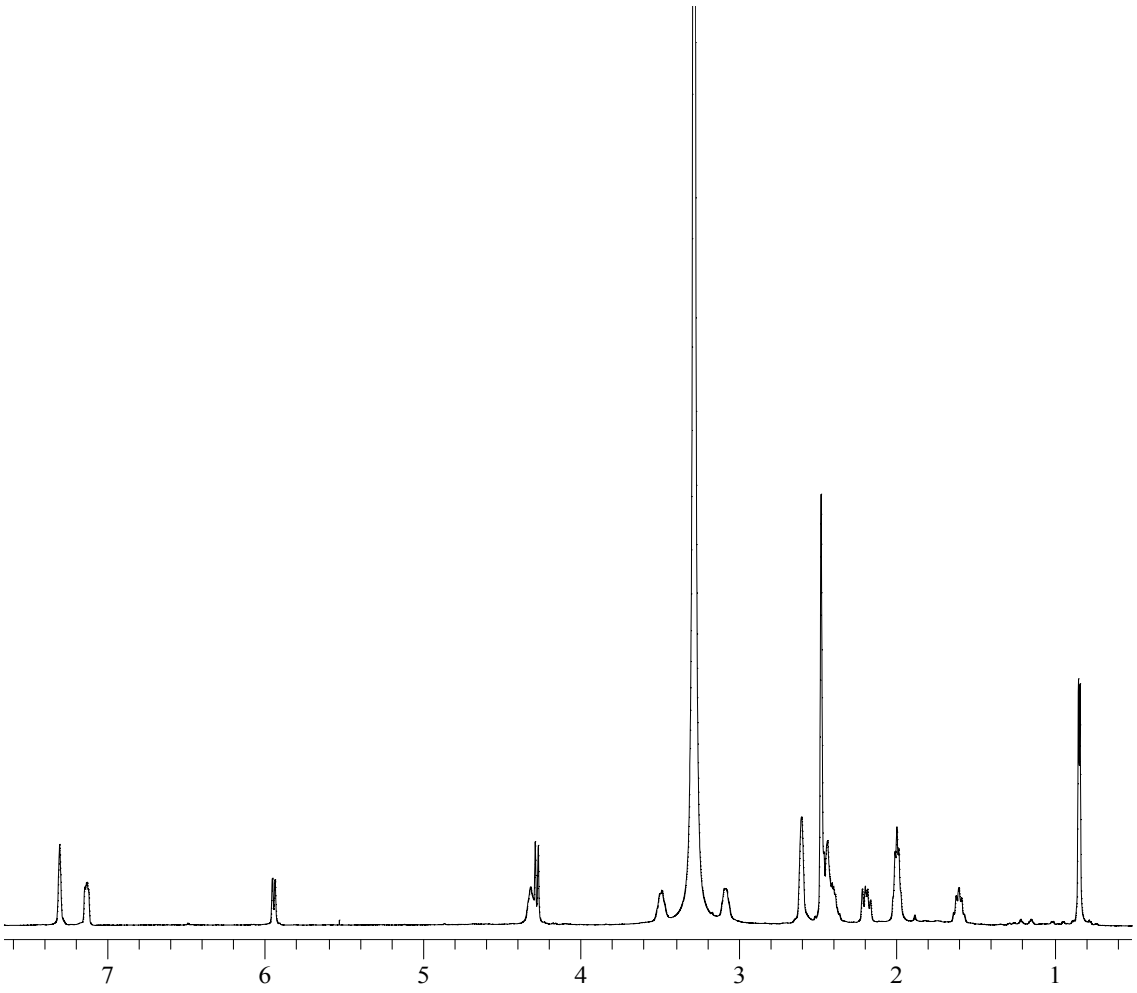


**Figure 76.** The $^{1}H$ NMR spectrum of grandisine D (**126**) at 600 MHz in $d_6$-DMSO.

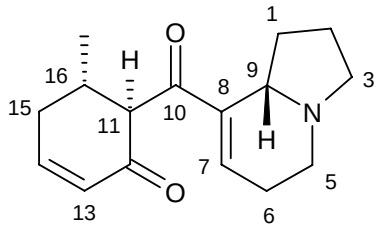


**Table 15.** $^{1}H$,[a] $^{13}C$[b] and HMBC NMR spectral data of grandisine D (**126**)[c]

| position | $\delta_C$ | $\delta_H$ (mult; *J* in Hz) | HMBC ($^{2,3}J_{CH}$) |
|---|---|---|---|
| 1 | 28.2 | 1.62 (1H, dddd, 8.4, 9.6, 9.6, 9.6); 2.40 (1H, dddd, 8.4 9.6, 9.6, 9.6) | 8, 9 |
| 2 | 20.3 | 2.00 (2H, dd, 7.8, 7.8) | 1, 3, 9 |
| 3 | 52.9 | 3.28 (1H, m); 3.48 (1H, ddd, 10.8, 10.8, 10.8) | 1, 5, 9 |
| 4 | - | 10.25 (1H, br) | |
| 5 | 43.2 | 3.28 (1H, m); 3.09 (1H, ddd, 8.4, 8.4 13.2) | 9 |
| 6 | 23.0 | 2.60 (2H, br) | 8 |
| 7 | 140.1 | 7.30 (1H, brdd, 4.0, 4.0) | 5, 6, 9, 10 |
| 8 | 137.7 | - | - |
| 9 | 58.0 | 4.32 (1H, brdd, 7.8, 7.8) | - |
| 10 | 198.3 | - | - |
| 11 | 59.3 | 4.29 (1H, d, 11.4) | 10, 12, 15, 16, 17 |
| 12 | 196.6 | - | - |
| 13 | 128.4 | 5.94 (1H, d, 10.2) | 15 |
| 14 | 151.6 | 7.13 (1H, ddd, 4.6, 7.2, 9.0) | 12, 15, 16 |
| 15 | 32.6 | 2.20 (1H, brdd, 12.0, 18.0); 2.44 (1H, br) | 11, 13, 14, 16 |
| 16 | 33.0 | 2.42 (1H, dq, 6.6, 6.6, 12.0) | 10, 11, 15, 17 |
| 17 | 19.1 | 0.84 (3H, d, 6.6) | 11, 15, 16 |

[a] At 600 MHz. [b] At 125 MHz. [c] In $d_6$-DMSO.

The partial structures of **126** (Figure 77) were established from HSQC and COSY correlations. HSQC spectral data established the presence of 21 carbon bound protons, one methyl, six methylenes, three methines and three olefinic protons. An α,β-unsaturated ketone functionality was assembled from COSY correlations observed between the olefinic protons at δ 5.94 (H-13) and 7.13 ppm (H-14). The chemical shifts of these protons and their attached carbons were typical for this type of system. Correlations from the methylene H-15 at δ 2.44/2.20 ppm allowed the connection of C-14 and C-15. COSY correlations between H-16 (δ 2.42 ppm) and H-15 demonstrated that these protons were adjacent. Further correlations from H-16 to H-$17_{Me}$ (δ 0.84 ppm) and H-11 (δ 4.29 ppm) enabled the connection of the methyl group and C-11 methine to C-16. Another partial

structure was determined by COSY correlations from the C-1 methylene at δ 2.40/1.62 ppm to the methine proton at δ 4.32 ppm (H-9) and a methylene at δ 2.00 ppm (H-2). Correlations were also observed from H-2 to the methylene at δ 3.28/3.48 ppm (H-3), which completed a four carbon aliphatic fragment. A third partial structure was constructed from COSY correlations from the methylene signal at δ 2.60 (H-6) to 3.09/3.28 ppm (H-5) and to an olefinic proton at δ 7.30 ppm (H-7). This accounted for the four olefinic carbons in the $^{13}$C NMR spectrum.

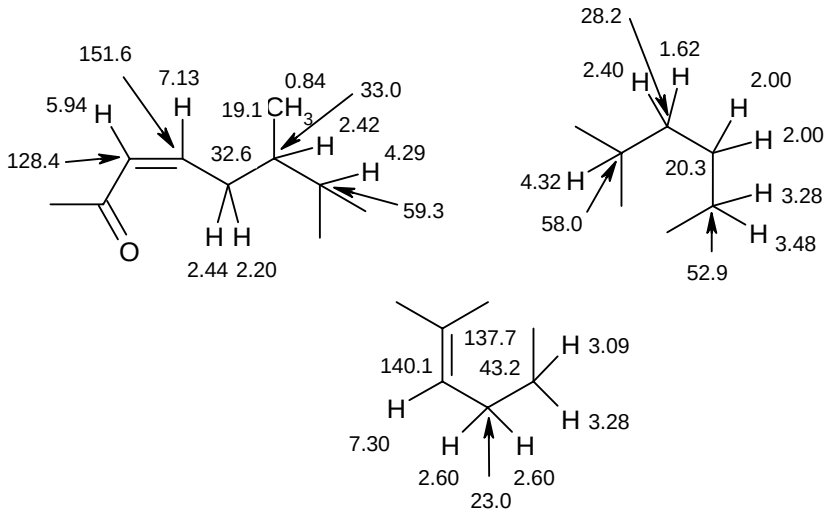


**Figure 77.** The partial structures of grandisine D (**126**) established from HSQC and COSY experiments.

HMBC correlations (Figure 78) from H-1 (2.40/1.62), H-3 (3.28/3.48), H-5 (3.09/3.28) and H-7 (7.30) to C-9 (58.0) allowed the connection of two partial structures to create a 7,8-dihydroindolizidine moiety. Correlations from H-1 and H-6 (2.60) to C-8 (137.7), and from H-7 to C-5 (43.2) provided further evidence for this functionality and confirmed the presence of the double bond. The structure of the methylcyclohexenone moiety was secured by correlations from H-11 (4.29) and H-14 (7.13) to the ketone carbonyl C-12 (196.8). This allowed the connection of C-11 (59.3) and C-12, to create the cyclohexenone ring. HMBC correlations from the methyl group (0.84) to C-15 (32.6) and C-11 (59.3) supported this structure. The connection of the methylcyclohexenone to the 7,8-dihydroindolizidine was facilitated by correlations from H-7, H-11 and H-16 (2.42) to

the ketone carbonyl C-10 (198.3). Thus the structure of grandisine D (**126**) was established.

Grandisine D was found to have the same indolizidine functionality as elaeocarpenine (**122**), and the same methylcyclohexenone moiety and 1,3-diketo system found in habbenine (**114**) and peripentonine (**123**). Unlike **114** and **123**, grandisine D (**126**) was not found to tautomerize in solution. Grandisine D possesses two α,β-unsaturated ketones, as opposed to **114** and **123** which only contain one each. The presence of the second α,β-unsaturated ketone in grandisine D stablizes the 1,3-diketo system, and tautomerisation is not observed.

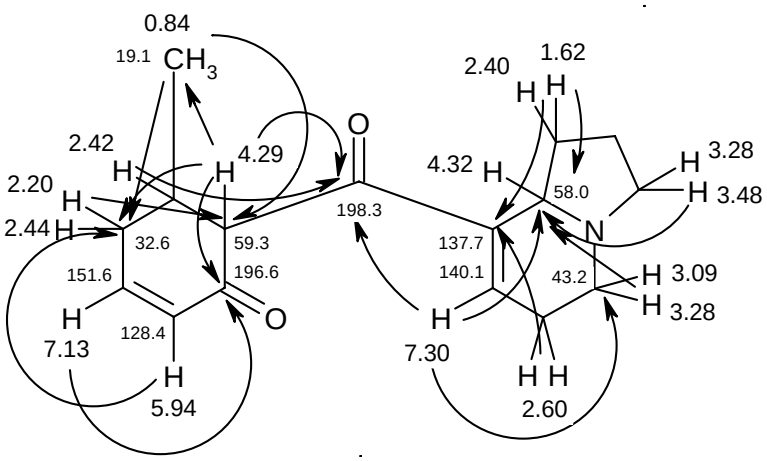


**Figure 78.** The key HMBC correlation used to establish the structure of grandisine D (**126**).

The relative stereochemistry of grandisine D (**126**) was established from coupling constants and ROESY correlations. A large axial coupling of 11.4 Hz was observed for H-11. As H-16 is the only adjacent proton, this indicates an axial-axial arrangement between these protons. This was supported by a correlation in the ROESY spectrum between H-$17_{Me}$ and H-11, demonstrating these protons were *cis* to each other. This also indicated that the methyl group was equatorial. The stereochemistry of H-9 relative to H-11 could be deduced from two key ROESY correlations. A strong ROESY correlation between H-7 and H-11 indicated that they were very close. A weak correlation between

H-$17_{Me}$ and H-$1_{\alpha}$ (δ 1.62) indicated that the methyl group was on the same face as this proton. This orientation is only possible with the stereochemistry depicted. In the other *Elaeocarpus* and *Peripentadenina* alkaloids, COSY correlations from the H-4 exchangeable proton enabled the assignment of H-9 as axial. However, no COSY correlations were observed for H-4 in grandisine D. The orientation of H-9 in grandisine D (**126**) can be assigned as axial following inspection of the coupling constants for H-9 (7.8, 7.8 Hz). Mearsurement of the optical rotation of grandisine D (**126**) provided a value of +18.34°. The energy minimized structure of **126** is shown in Figure 79.

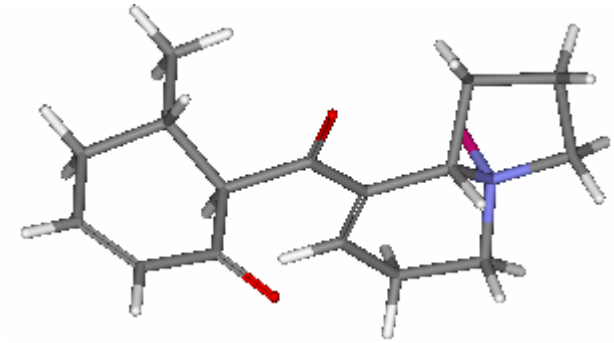

**Figure 79.** The energy minimized structure of grandisine D (**126**).

## 6.5 Structure Elucidation of Grandisine C (127)

A molecular formula of $C_{16}H_{24}NO_3$ was determined for grandisine C (**127**) following positive high resolution mass spectral analysis of the molecular ion $[M + H]^+$ 278.14709 (calculated for 278.17507). This demonstrated that **127** was heavier than isoelaeocarpiline (**63**) by the atomic mass of $H_2O$. The upfield region of the $^1H$ NMR spectrum of grandisine C (**127**) (Figure 80) was found to be almost identical to that of isoelaeocarpiline (**63**). The only difference was the downfield shift of the methyl group from 0.88 ppm in isoelaeocarpiline (**63**) to δ 1.04 in grandisine C. Other distinguishing features of the $^1H$ NMR spectrum of **127** were the absence of olefinic protons and the

appearance of resonances at δ 4.17, 2.66 and 2.24 ppm. The resonance at δ 4.17 ppm indicated a proton which was attached to an oxygenated carbon. This suggested that the double bond of isoelaeocarpiline (**63**) was hydrated in grandisine C (**127**).

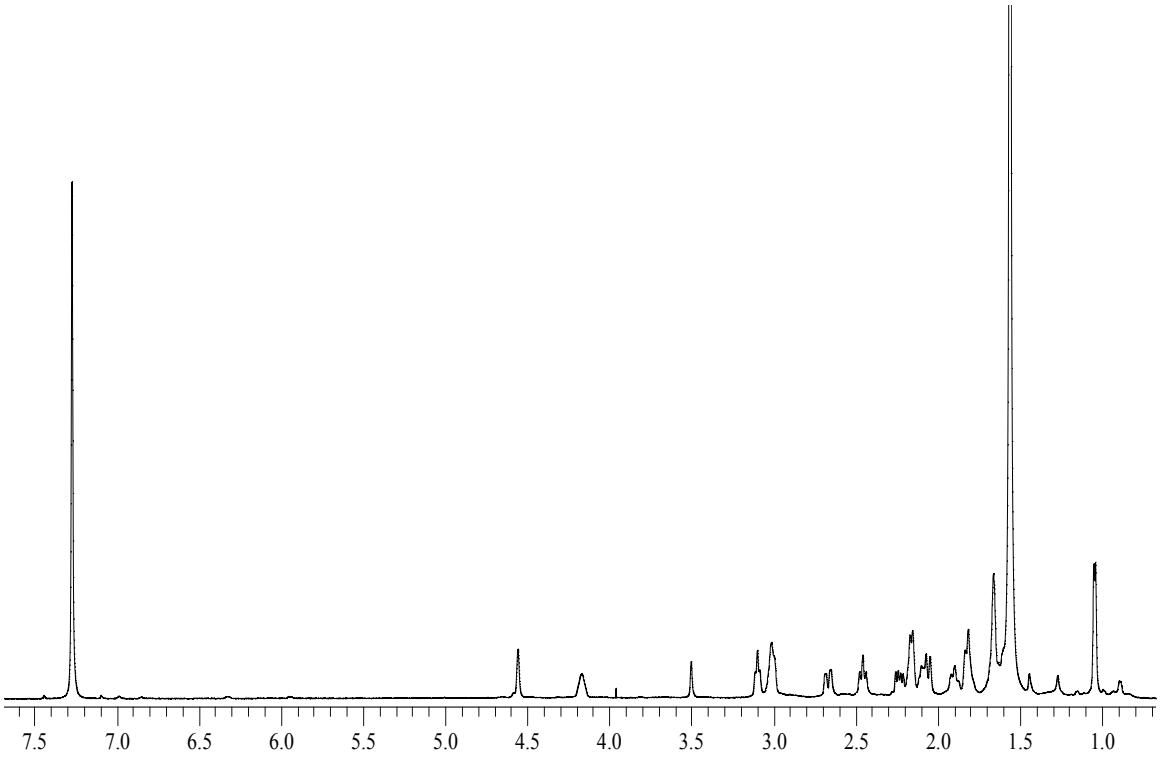


**Figure 80.** The $^{1}$H NMR spectrum of grandisine C (**127**) at 600 MHz in $CDCl_3$.

This hypothesis was supported by investigation of the $^{13}$C NMR spectrum of grandisine C (**127**). An absence of two olefinic carbons was noted upon comparison with the $^{13}$C NMR spectrum of isoelaeocarpiline (**63**). Three carbons at δ 63.8, 39.4 and 38.2 ppm, were unique to the $^{13}$C NMR spectrum of **127**. The carbon at δ 63.8 ppm was indicative of an oxygenated aliphatic carbon. The carbons associated with the 7-oxy-8-ketoindolizidine were almost identical to the chemical shifts of the same carbons in isoelaeocarpiline (**63**). Two $sp^2$ hybridized carbons at δ 116.3 and 168.1 ppm were also observed in the $^{13}$C NMR spectrum of grandisine C (**127**), which were shifted upfield from the quaternary olefinic carbons at δ 112.8 and 164.3 ppm in **63**. The $^{13}$C and $^{1}$H NMR spectral data of

grandisine C (**127**) can be found in Table 16. Grandisine C was converted to its free base via an acid/base partition and all NMR spectra were acquired in chloroform.

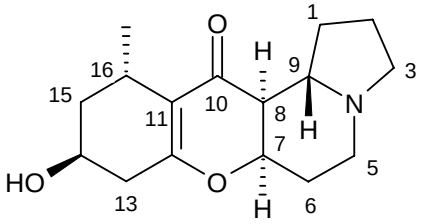


**Table 16.** $^{1}$H,[a] $^{13}$C[b] and HMBC NMR spectral data of grandisine C (**127**)[c]

| position | $\delta_C$ | $\delta_H$ (mult; *J* in Hz) | HMBC ($^{2,3}J_{CH}$) |
|---|---|---|---|
| 1 | 28.4 | 1.66 (2H, m) | 2, 3, 9 |
| 2 | 21.2 | 1.66 (1H, m); 1.82 (1H, brd, 9.0) | 3, 9 |
| 3 | 53.8 | 2.26 (1H, d, 9.6); 3.11 (1H, brdd, 9.0, 9.0) | 1, 2, 5, 9 |
| 5 | 47.6 | 2.47 (1H, brdd, 12.0, 12.0); 3.01 (1H, ddd, 2.4, 2.4, 12.0) | 6, 7, 9 |
| 6 | 30.0 | 1.91 (1H, ddd, 2.0, 4.8, 14.4); 2.07 (1H, ddd, 2.4, 2.4, 15.6) | - |
| 7 | 75.5 | 4.56 (1H, br) | - |
| 8 | 52.2 | 2.16 (1H, m) | 10 |
| 9 | 60.0 | 2.10 (1H, m) | - |
| 10 | 192.7 | - | - |
| 11 | 116.3 | - | - |
| 12 | 168.1 | - | - |
| 13 | 38.2 | 2.24 (1H, dd, 10.2, 18.0); 2.66 (1H, dd, 6.0, 18.0) | 11, 12, 14, 15 |
| 14 | 63.8 | 4.17 (1H, br) | - |
| 15 | 39.4 | 1.60 (1H, m); 1.82 (1H, m) | 13, 14, 16, 17 |
| 16 | 25.4 | 3.02 (1H, m) | 11, 12, 14, 15, 17 |
| 17 | 20.2 | 1.04 (3H, d, 6.6) | 11, 15, 16 |

[a] At 600 MHz. [b] At 125 MHz. [c] In $CDCl_3$.

The partial structures of grandisine C (**127**), illustrated in Figure 81, were established from correlations observed in the HSQC and COSY spectra. The presence of one methyl, seven methylenes and five methines was established from the HSQC spectrum. The indolizidine carbon skeleton was assembled in an identical fashion to that of isoelaeocarpiline (**63**). The chemical shifts of the protons and carbons of this partial structure were almost identical to those found in **63**. A second aliphatic partial structure

was constructed from COSY correlations observed from the methine at δ 3.02 ppm (H-16) to a methyl group at δ 1.04 ppm and to a methylene at δ 1.60/1.82 ppm (H-15). A COSY correlation determined the proton at δ 4.17 ppm (H-14) was adjacent to H-15. The connection of a methylene at δ 2.66/2.44 ppm (H-13) to H-14 was established from COSY correlations.

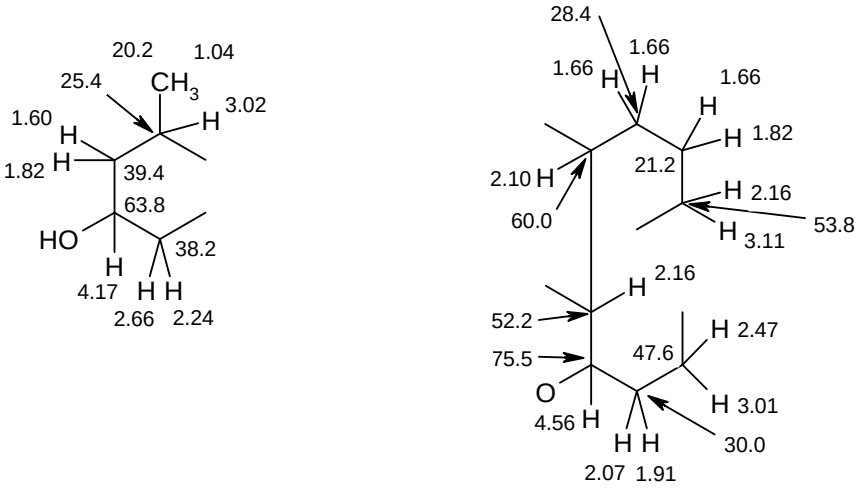


**Figure 81.** The partial structures of grandisine C (**127**) established from HSQC and COSY experiments.

HMBC correlations (Figure 82) from H-1 (1.66), H-3 (2.16/3.11) and H-5 (2.47/3.01) to C-9 (60.0) secured the structure of the indolizidine moiety. Other correlations from H-5 to C-7 (75.5) and from H-6 (2.07/1.91) to C-8 (52.2) supported the presence of the oxygenated carbon at C-7. An HMBC correlation from H-8 (2.16) to the ketone carbonyl C-10 (192.7) confirmed the structure of a 7-oxy-8-ketoindolizidine moiety. The presence of a 1-methyl-3-oxy-5-hydroxycyclohex-2-ene ring was deduced by HMBC correlations from H-16 (3.02) to the olefinic quaternary carbon C-11 (116.3), and to the oxygenated carbons C-12 (168.1) and C-14 (63.8). The presence of the double bond was confirmed by correlations from H-13 (2.66/2.24) to C-12 and C-11. No HMBC correlations were observed from H-14 (4.17). A connection between the 7-oxy-8-ketoindolizidine and cyclohexene ring could not be established, as no HMBC correlations were observed from H-16 to the ketone carbonyl C-10. H-7 also showed no HMBC correlation to C-12.

However, the structure of grandisine C (**127**) was determined from MS evidence. The similar spectral properties of grandisine C (**127**) and isoelaeocarpiline (**63**) also supported the structure of **127**.

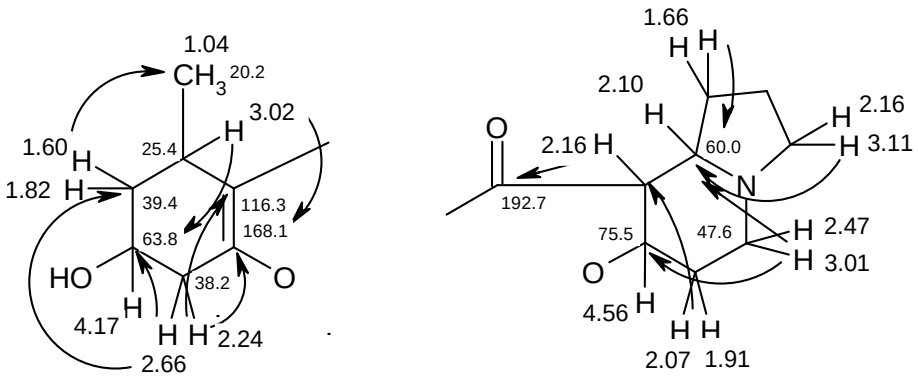


**Figrure 82.** The key HMBC correlations used to establish the structure of grandisine C (**127**).

The two dimensional structure was therefore determined to be the same as that of rudrakine (**72**). No information regarding the three dimensional structure of **72** has been reported in the literature.[4] Different spectral properties were observed between these compounds, namely the methyl group was observed at 1.20 ppm, and H-7 at 4.15 ppm in the $^{1}$H NMR spectrum of rudrakine (**72**). Therefore grandisine C (**127**) can be considered an isomer of rudrakine. The relative stereochemistry of **127** was determined from ROESY correlations and comparison with the spectra data of isoelaeocarpiline (**63**). A ROESY correlation was observed between H-14 and H-17$_{Me}$, which demonstrated that these protons were on the same face of the cyclohexene ring. This enabled both the methyl group and H-14 to be assigned axial configurations. These protons would be too far apart for a ROESY correlation in this system if they were both equatorial. Consequently, the H-14 and H-17$_{Me}$ protons were close enough to exhibit a ROESY correlation in a 1,3-diaxial relationship. Two large couplings of 10.2 and 18.0 Hz were observed for H-13$_{ax}$ (2.24), which supports an axial-axial relationship between this proton and H-14. The relative stereochemistry of H-7, H-8 and H-9 in **127** can be considered the same as in isoelaeocarpiline (**63**), as no major differences were observed in the chemical

shifts of the protons of the indolizidine moiety. The energy minimized structure of grandisine C (**127**) is represented in Figure 83.

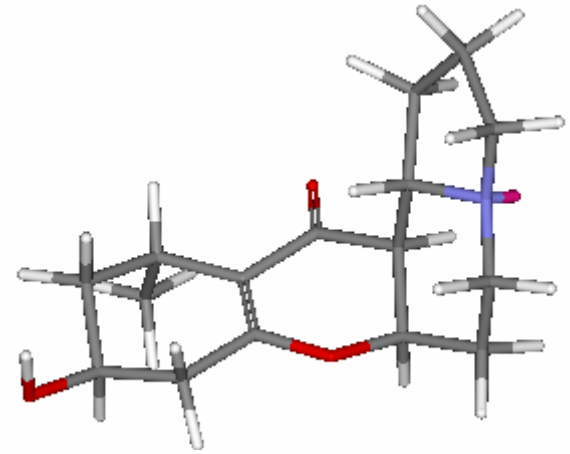

**Figure 83.** The energy minimized structure of grandisine C (**127**).

## 6.6 Structure Elucidation of Grandisine E (128)

Analysis of the molecular ion $[M + H]^+$ 278.17578 (calculated for 278.17507) by positive HRESIMS allowed a molecular formula of $C_{16}H_{24}NO_3$ to be assigned to grandisine E (**128**) . This provided the same molecular formula as grandisine C (**127**), however the $^1H$ NMR spectrum of grandisine E (**128**) was vastly different to the $^1H$ NMR spectrum of grandisine C (**127**). Two methyl doublets at δ 1.27 and 1.33 ppm were observed in the $^1H$ NMR spectrum of **128**, in addition to the absence of olefinic protons. Protons at δ 4.03, 4.59 and 4.83 ppm were observed, indicating these protons were attached to oxygenated aliphatic carbons. A large water peak at δ 3.30 ppm obscured some signals. A broad signal at δ 1.80 ppm integrated to five protons. Grandisine E was converted to its free base via an acid/base partition and all NMR spectra were acquired in chloroform

Carbons of similar chemical shift to the carbons of the 7-oxy-8-ketoindolizidine moiety in isoelaeocarpiline (**63**) and grandisine C (**127**) were observed in the $^{13}C$ NMR spectrum of grandisine E (**128**). Two olefinic carbons were found at δ 113.7 and 167.8 ppm, which

were similar to the chemical shifts of C-11 and C-12 in **63** and **127**. Two oxygenated carbons were observed at δ 66.8 and 62.4 ppm. This indicated that grandisine E (**128**) contained an aliphatic ether linkage, as the molecular formula demonstrated that two hydroxyl groups could not be present. The $^{13}C$ and $^{1}H$ NMR spectral data can be found in Table 17.

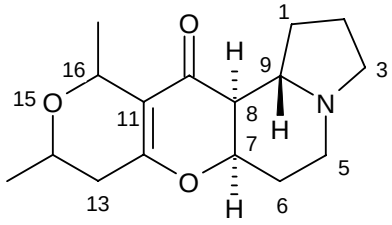


**Table 17.** $^{1}H$,[a] $^{13}C$[b] and HMBC NMR spectral data of grandisine E (**128**)[c]

| position | $\delta_C$ | $\delta_H$ (mult; *J* in Hz) | HMBC ($^{2,3}J_{CH}$) |
|---|---|---|---|
| 1 | 29.5 | 1.67 (2H, m) | 2 |
| 2 | 21.2 | 1.67 (1H, m); 1.81 (1H, brdd, 9.0, 16.8) | 3 |
| 3 | 54.1 | 2.13 (1H, ddd, 2.4, 7.2, 18.0)<br>3.09 (1H, brdd, 7.8, 7.8) | 1, 9 |
| 5 | 47.4 | 2.45 (1H, m); 3.00 (1H, dd, 5.4, 10.8) | 6, 7, 9 |
| 6 | 30.9 | 1.93 (1H, dddd, 3.6, 3.6, 12.0, 12.0)<br>2.06 (1H, brddd, 2.4, 2.4, 15.0) | 5 |
| 7 | 75.8 | 4.59 (1H, brdd, 2.4, 2.4) | - |
| 8 | 51.7 | 2.20 (1H, m) | 6, 9, 10 |
| 9 | 60.1 | 2.20 (1H, m) | 2, 5 |
| 10 | 191.2 | - | - |
| 11 | 113.7 | - | - |
| 12 | 167.8 | - | - |
| 13 | 35.6 | 2.20 (2H, m) | 11, 12, 14 |
| 14 | 62.4 | 4.03 (1H, dq, 6.0, 6.0, 6.0) | 16, 14-Me |
| 16 | 66.8 | 4.83 (1H, q, 6.6) | 11, 12, 14, 17 |
| 17 | 18.8 | 1.27 (3H, d, 6.6) | 11, 16 |
| 14-Me | 21.5 | 1.33 (3H, d, 6.6) | 13, 14 |

[a] At 600 MHz. [b] At 125 MHz. [c] In $CDCl_3$.

The presence of two methyls, six methylenes and five methines was determined from the HSQC spectrum. The partial structures (Figure 84) were established from HSQC and COSY spectral data. An eight carbon skeleton of the indolizidine moiety was assembled in an identical manner to isoelaeocarpiline (**63**) and grandisine C (**127**). A $CH_3$-CH-O- partial structure was supported by a COSY correlation from the methyl group H-17 (1.27)

to the proton at δ 4.83 ppm (H-16). This proton was bound to a carbon at δ 66.8 ppm. Another partial structure was constructed from correlations between the proton at δ 4.03 (H-14) to a methyl at 1.33 (H-$14_{Me}$) and to a methylene at 2.20 ppm (H-13). The proton at δ 4.03 was bound to an oxygenated carbon at 62.4 ppm. An intense correlation in the HSQC spectrum inferred that two protons at 2.20 ppm were bound to the carbon at 35.6 ppm. MS evidence allowed these partial structures to be connected via an ether linkage.

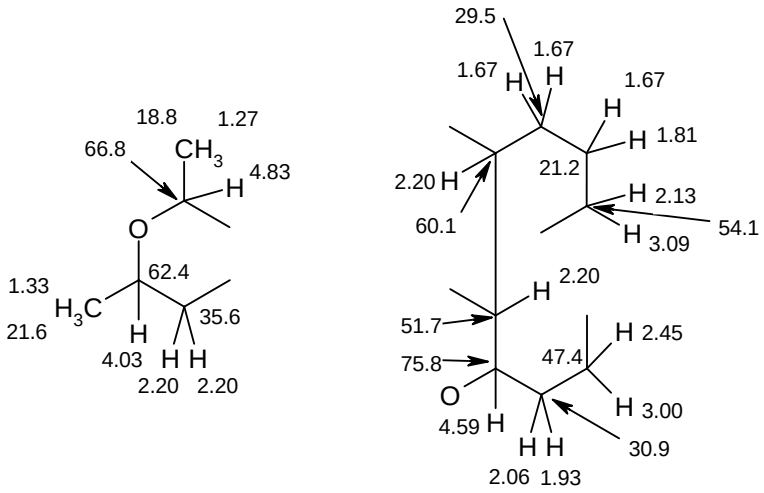


**Figure 84.** The partial structures of grandisine E (**128**) established from HSQC and COSY experiments.

HMBC correlations (Figure 85) secured the structure of the 7-oxy-8-ketoindolizidine moiety by correlations from H-1 (1.67), H-3 (2.13/3.09), H-5 (2.45/3.00) and H-8 (2.20) to C-9 (60.1). Correlations from H-9 (2.20) to C-5 (47.4), H-3 to C-7 (75.8) and from H-8 to C-6 (30.9) provided further evidence for this structure. A correlation was observed from H-8 to the ketone carbonyl C-10 at δ 191.2 ppm. The ether linkage between C-16 (66.8) and C-14 (62.4) was demonstrated by HMBC correlations from H-16 (4.83) to C-14 (62.4), and from H-14 (4.03) to C-16 (66.8). Two HMBC correlations were observed from H-$17_{Me}$ (1.27) to C-16 and to a quaternary olefinic carbon (C-11, 113.7). Correlations to C-14 and C-13 (35.6) were observed from the methyl group at 1.33 (H-$14_{Me}$). Correlations from H-16 were observed to C-11 and to a second quaternary olefinic carbon C-12 (167.8). This confirmed the presence of a fully substituted double bond

adjacent to C-16. HMBC correlations observed from H-13 (2.20) to both of these olefinic carbons allowed the formation of a dihydropyran ring. No HMBC correlations were observed from H-16 to C-10 in grandisine E (**128**) to enable the connection of the dihydropyran ring to the keto group of the indolizidine. As with grandisine C (**128**), MS evidence suggested that the dihydropyran ring was joined to the indolizidine via the ketone C-10, and the chemical shifts of C-7 and C-12 indicated an ether linkage existed between these carbons. Thus the structure of grandisine E (**128**) was established.

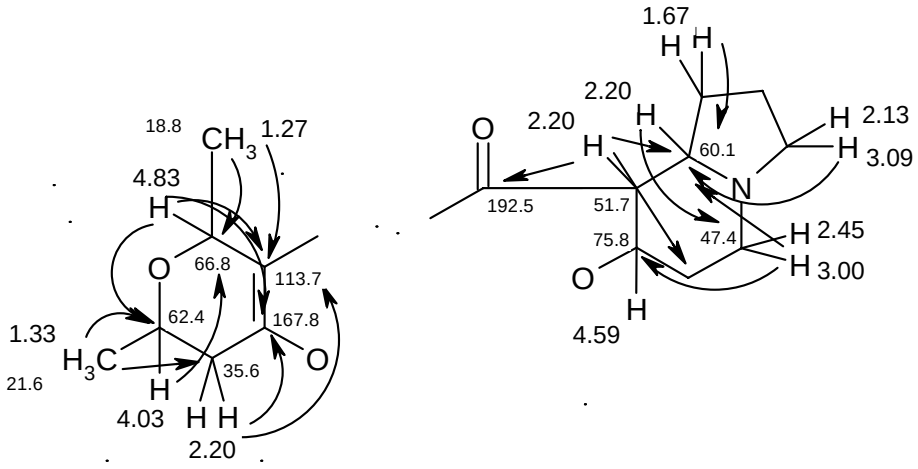


**Figure 85.** The key HMBC correlations for grandisine E (**128**).

The relative stereochemistry of the three chiral centres of the indolizidine moiety of **128** was found to be that same as that of grandisine C (**127**) and isoelaeocarpiline (**63**), on the basis of almost identical chemical shifts. This was supported by a ROESY correlation from H-7 to H-8, indicating an equatorial-axial relationship. ROESY correlations from H-8 and H-9 could not be observed since these protons have the same chemical shift. In the same manner as for grandisine C (**127**), a ROESY correlation demonstrated that a 1,3-diaxial configuration exists between H-14 and H-$17_{Me}$. The distance between the protons of the dihydropyran ring and the indolizidine moiety was too great to enable unambiguous assignment of the stereochemistry of chiral centres H-14 and H-16 relative to H-8 and H-7. Therefore two isomers are possible, as shown in the energy minimized structures of grandisine E (**128**) in Figure 86.

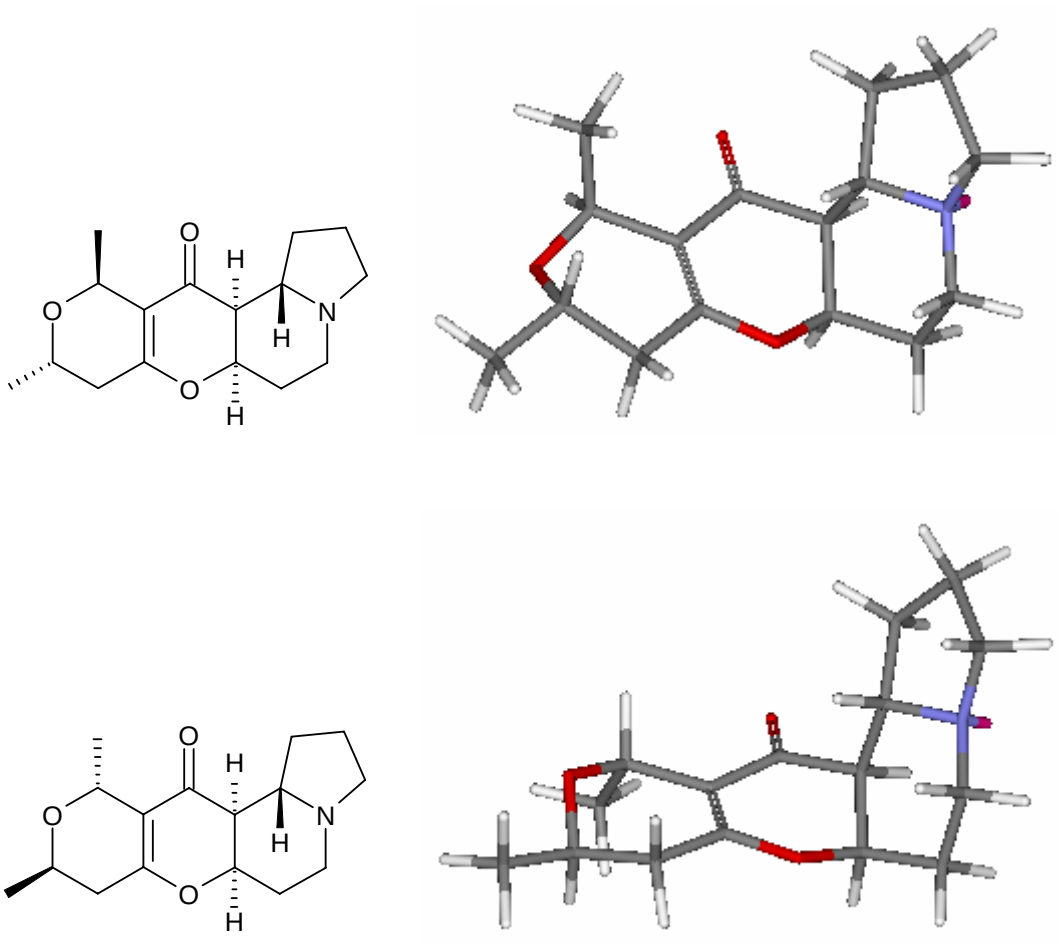


**Figure 86.** The energy minimized structures of two possible structures of grandisine E (**128**).

## 6.7 The Isolation of Grandisine F (129), G (130) and 131 from *E. grandis* by an Acid/Base Extraction Procedure

The ground, dried leaves of *E. grandis* were extracted with a small volume of 28% $NH_3$ solution followed by an exhaustive extraction with DCM (Scheme 10).

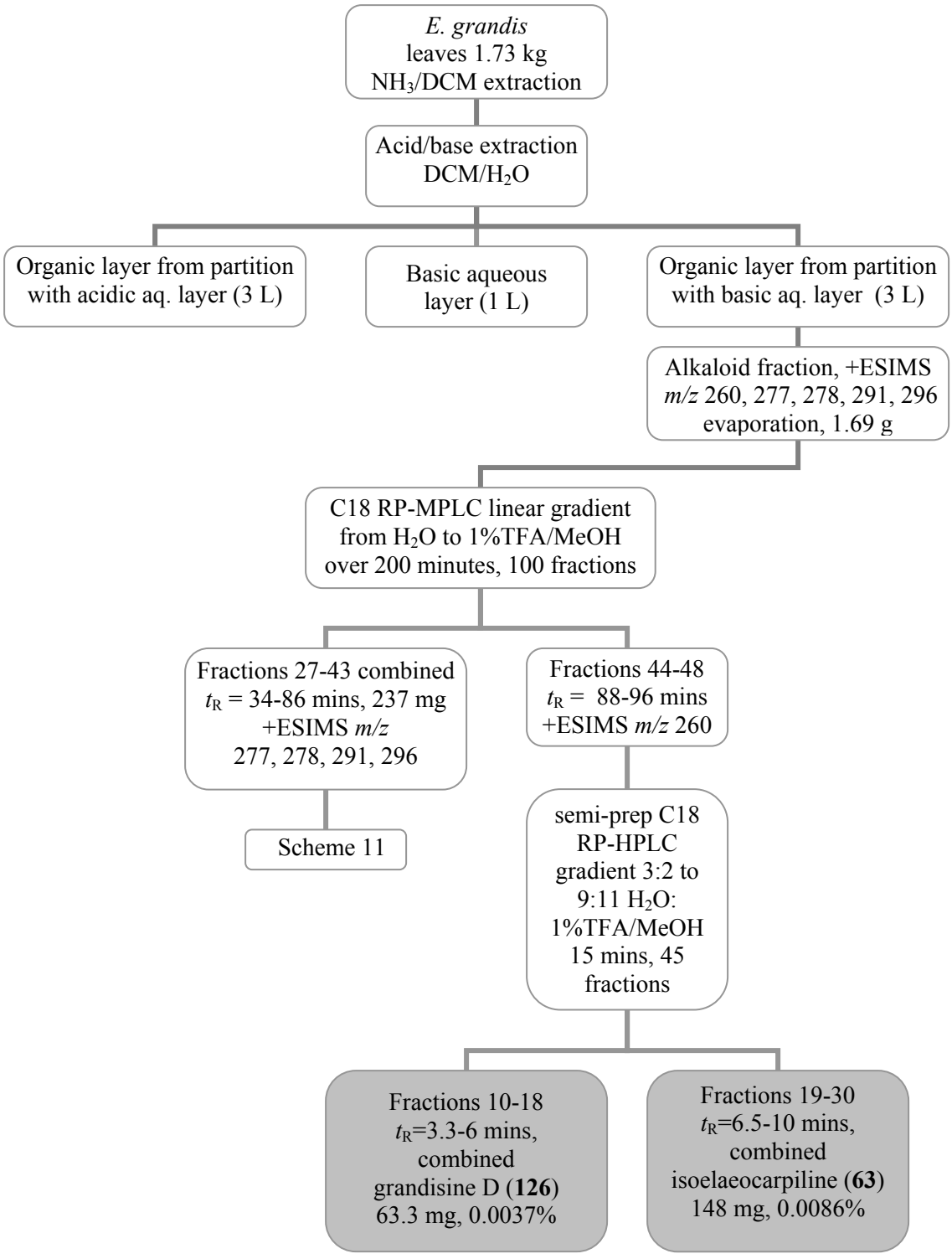


**Scheme 10.** The extraction of the leaves of *E. grandis* by an acid/base procedure and the purification of grandisine D (**126**) and isoelaeocarpiline (**63**).

The DCM extract was separated from the aqueous ammonia. The volume of the organic extract was reduced under vacuum and the residue was subsequently partitioned with dilute $H_2SO_4$ (pH 1). The aqueous layer was then basified with $NH_3$ to pH 10 and partitioned with DCM. The presence of alkaloids in this organic layer was determined by positive ESIMS. This alkaloid fraction was evaporated to dryness and separated into 100 fractions by C18 silica gel RP-MPLC, using a gradient of $H_2O$ to 1%TFA/MeOH over 200 minutes (Scheme 10).

Two sets of pooled fractions were obtained from the MPLC separation. Fractions 27 to 43, and 44 to 48 were combined on the basis of similar $^1$H NMR spectra and mass ion peaks in the positive ESIMS. The combined fractions (27 – 43) contained mass ion peaks at *m/z* 277, 278, 291 and 296. The purification of grandisine C (**127**), F (**129**), G (**130**) and **131** from this fraction is described in Scheme 11.

A mass ion peak at *m/z* 260 was detected in the combined fractions 44 – 48. Analysis of this fraction by $^1$H NMR demonstrated a mixture of grandisine D (**126**) and isoelaeocarpiline (**63**) was present. A C18 RP-HPLC gradient of 3:2 to 9:11 $H_2O$:1%TFA/MeOH over 15 minutes was used to separate this fraction (Scheme 10). A total of 45 fractions were collected. Fractions 10 to 18 yielded **126** (63.3 mg, 0.0037%), and **63** (148 mg, 0.0086%) was obtained from fractions 19-30.

Scheme 11 illustrates the purification of the pooled fraction 27 to 43. Initial separation into 50 fractions was achieved via preparative C18 RP-HPLC using a gradient of $H_2O$ to 1:4 $H_2O$/1%TFA over 100 minutes. Pure grandisine C (**127**) (6.8 mg, 0.00039%) was obtained in fractions 10 to 17. A mass ion peak at *m/z* 296 was observed in fractions 18 to 25 by positive ESIMS. These fractions were combined and analysis by $^1$H NMR revealed a mixture of two compounds. Purification of this mixture was achieved by a C18 RP-HPLC gradient of 4:1 to 3:2 $H_2O$:1%TFA/MeOH. A pure mixture of two diastereomeric compounds **131** (2.1 mg) was obtained from the eluting fractions. Separation of the diastereomers proved unsuccessful by C18 RP-HPLC isocratic conditions of 4:1 $H_2O$:1%TFA/MeOH. However, the structures of two isomers of **131** were proposed.

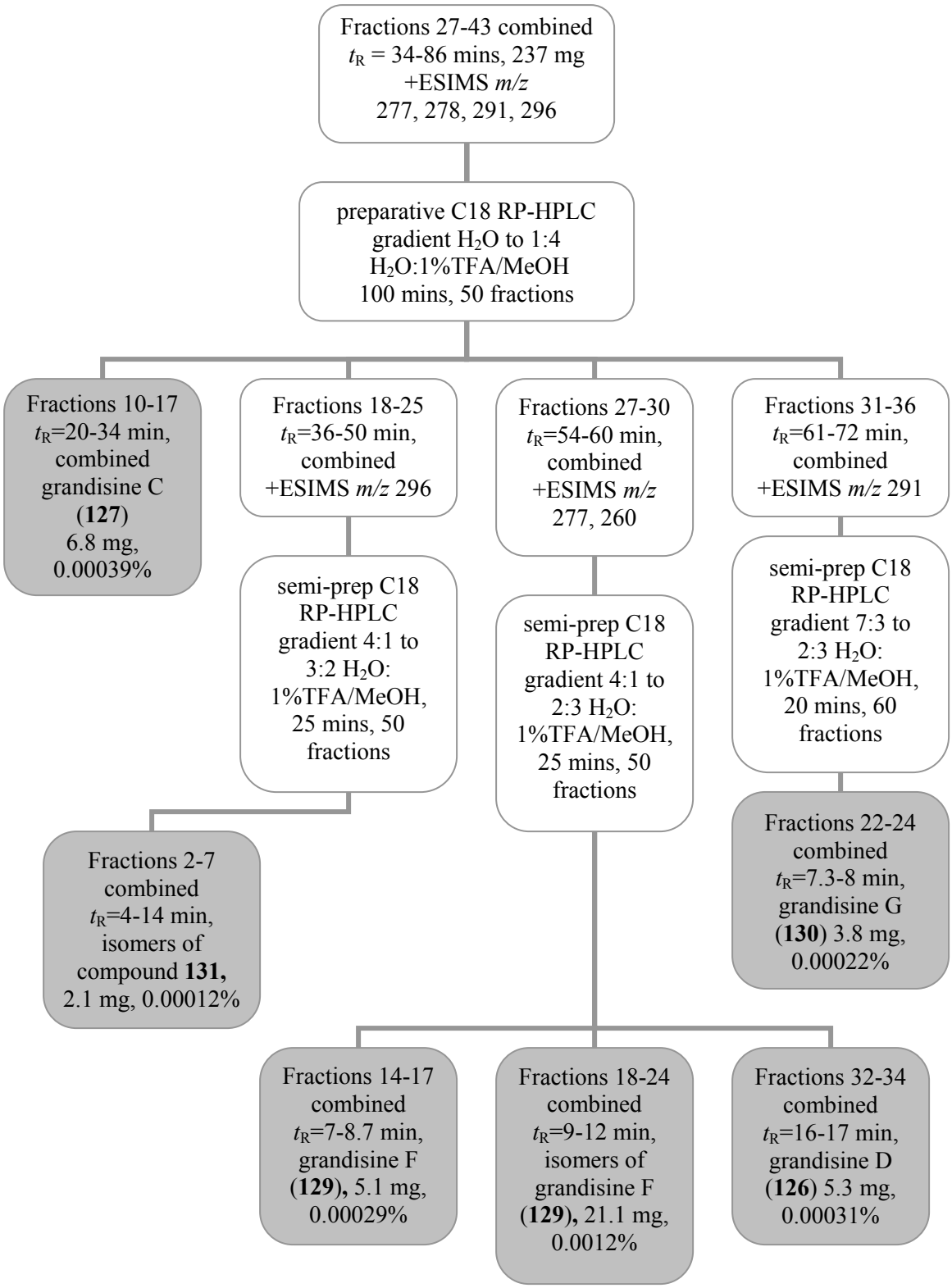


**Scheme 11.** The purification of grandisine C (**127**), D (**126**), F (**129**), G (**130**) and compounds **131a** and **b**.

Mass ion peaks at *m/z* 277 and 260 were detected in fractions 27 to 30 from the preparative C18 RP-HPLC fractionation (Scheme 11). These fractions were combined and separated by semi-preparative C18 RP-HPLC into 50 fractions by a gradient of 4:1 to 2:3 $H_2O$:1%TFA/MeOH over 25 minutes. Mass ion peaks at *m/z* 277 and 260 were observed in fractions 14 – 24 and 32 – 34, respectively. Analysis by $^1$H NMR revealed fractions 32 to 34 to be grandisine D (**126**). Fractions 14 – 17 were combined to yield grandisine F (**129**) (5.1 mg, 0.00029%). Analysis of fractions 18 – 24 by $^1$H NMR demonstrated that the fractions were a mixture of two major and two minor compounds. These fractions were combined to yield a mixture of isomers of grandisine F (**129**) (21.1 mg, 0.0012%).

The mass ion peak at m/z 291 was detected by positive ESIMS in fractions 31 to 36 from the preparative C18 RP-HPLC fractionation (Scheme 11). These fractions were combined and purification of grandisine G (**130**) was achieved by a C18 RP-HPLC gradient of 7:3 to 2:3 $H_2O$:1%TFA/MeOH. Sixty fractions were collected over 20 minutes. Analysis of the fractions by positive ESIMS and $^1$H NMR yielded grandisine G (**130**) in fractions 22 – 24 (3.8 mg, 0.00022%).

## 6.8 Structure Elucidation of Grandisine F (129)

A molecular formula of $C_{16}H_{25}N_2O_2$ was determined for grandisine F (**129**) following positive HRESIMS measurement of the molecular ion $[M + H]^+$ 277.190345 (calculated for 277.191054). This was found to be 17 Da. heavier than isoelaeocarpiline (**63**), which is equivalent to the presence of an additional $H_3N$. Inspection of the $^1$H NMR spectrum of **129** (Figure 87) revealed an absence of olefinic protons. Grandisine F was observed to be the major compound in Figure 78, however small amounts of minor isomers are observed.

The $^1$H NMR spectrum of **129** contained similar chemical shifts and multiplicity of protons to those observed in the $^1$H NMR spectrum of isoelaeocarpiline (**63**), particularly

in the upfield region from δ 1.5 to 3.0 ppm. This suggested that grandisine F (**129**) also possessed an indolizidine group. A methyl doublet was found at δ 0.98 and a triplet of doublets at 1.4 ppm. A narrow doublet at δ 4.51 ppm was almost identical to H-7 (δ 4.58 ppm) of isoelaeocarpiline (**63**). A unique feature of Figure 87 was the broad signal at δ 3.19 ppm. Grandisine F was converted to a free base by an acid/base partition and NMR spectra were acquired in $CD_2Cl_2$.

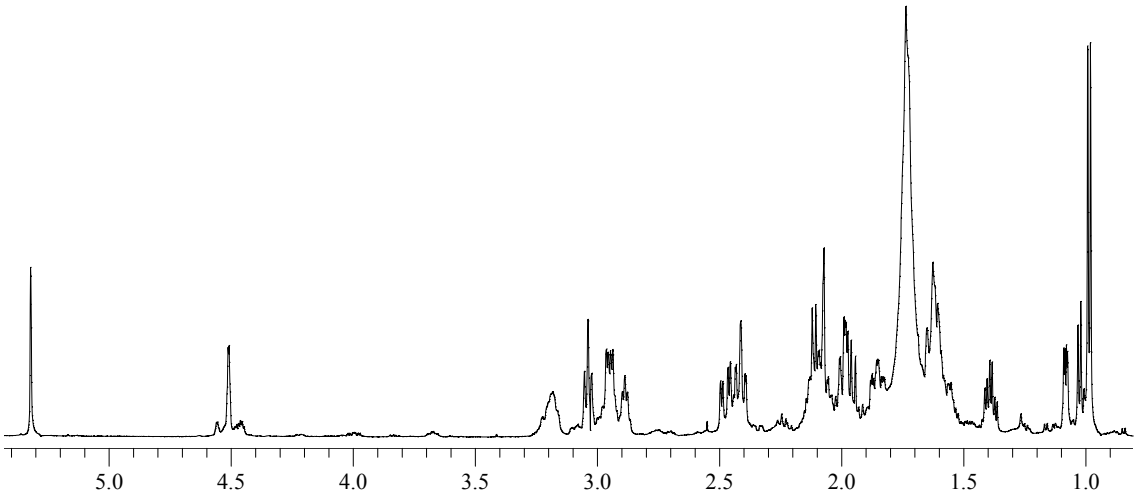


**Figure 87.** The $^1$H NMR spectrum of grandisine F (**129**) in $CD_2Cl_2$.

The $^{13}$C NMR spectrum of grandisine F (**129**) revealed two olefinic carbons at δ 115.6 and 169.0, and a carbonyl carbon at 193.1 ppm. The chemical shifts of these carbons were similar to those of C-10 to C-12 of the α,β-unsaturated ketone found in isoelaeocarpiline. Several carbons were also found to be identical to the indolizidine carbons (C-1 to C-9) of **63**. The remaining signals in the $^{13}$C NMR of **129** were a methyl carbon at δ 20.4 and carbons at 26.4, 39.5, 40.7 and 43.3 ppm. The $^{13}$C and $^1$H NMR spectral data for **129** can be found in Table 18.

The partial structures of **129** (Figure 88) were determined from correlations observed in HSQC and COSY spectra. An eight carbon partial structure was constructed in identical fashion as for isoelaeocarpiline (**63**), grandisine C (**127**) and E (**128**), with many of the carbon and proton chemical shifts almost identical. A second partial structure was

assembled from correlations from the proton at δ 3.19 ppm (H-14) to two methylenes at 2.49/1.99 and 1.39/1.63 ppm, H-13 and H-15 respectively. A COSY correlation from the proton at δ 2.89 ppm (H-16) to the methyl group at δ 1.00 ppm (H-17) and to H-15 established the connection of the methine of H-16 to the methylene of H-15 and to H-$17_{Me}$. The HSQC spectrum demonstrated that the proton at δ 3.19 (H-14) was attached to a carbon at 43.3 ppm. The chemical shift of both this proton and carbon indicated that an amino group was attached to C-14. In contrast, the same position in grandisine C (**127**) yielded an oxygenated methine with carbon and proton chemical shifts of δ 63.8 and 4.17 ppm, respectively. The molecular formula of **129** also provided support for the presence of an amino group.

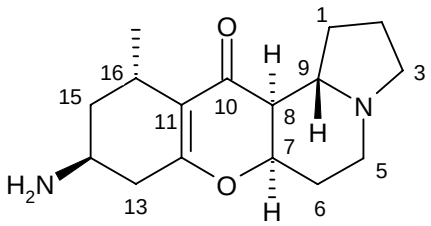


**Table 18.** $^{1}H$,[a] $^{13}C$[b] and HMBC NMR spectral data of grandisine F (**129**)[c]

| position | $\delta_C$ | $\delta_H$ (mult; *J* in Hz) | HMBC ($^{2,3}J_{CH}$) |
|---|---|---|---|
| 1 | 28.9 | 1.56 (1H, m); 1.63 (1H, m) | 2, 3, 9, 10 |
| 2 | 21.2 | 1.63 (1H, m); 1.74 (1H, m) | 3, 9 |
| 3 | 54.0 | 2.13 (1H, m); 3.05 (1H, brdd, 9.0, 9.0) | 1, 2, 9 |
| 5 | 47.8 | 2.40 (1H, ddd, 3.0, 11.4, 15.0) | 6, 7, 9 |
| | | 2.95 (1H, ddd, 1.2, 4.8, 11.4) | 6, 7, 9 |
| 6 | 31.1 | 1.85 (1H, dddd, 3.0, 5.4, 13.8, 15.0); | 7, 8 |
| | | 1.99 (1H, dddd, 1.2, 3.0, 3.0, 13.8) | |
| 7 | 76.2 | 4.51 (1H, ddd, 3.0, 3.0, 2.4) | 5, 9, 10 |
| 8 | 52.6 | 2.10 (1H, m) | 1, 9, 10 |
| 9 | 60.4 | 2.10 (1H, m) | 2 |
| 10 | 193.1 | - | - |
| 11 | 115.6 | - | - |
| 12 | 169.0 | - | - |
| 13 | 39.5 | 1.99 (1H, dd, 9.6, 18.0); | 11, 12, 14, 15 |
| | | 2.49 (1H, dd, 5.4, 18.0) | |
| 14 | 43.3 | 3.19 (1H, br) | - |
| 15 | 40.7 | 1.63 (1H, m); 1.39 (1H, ddd, 6.0, 12.6, 12.6) | 11, 13, 14, 16, 17 |
| 16 | 26.4 | 2.89 (1H, dq, 6.0, 6.0) | 10, 11, 12, 14, 15, 17 |
| 17 | 20.4 | 0.98 (3H, d, 7.2) | 11, 15, 16 |

[a] At 600 MHz. [b] At 125 MHz. [c] In $CD_2Cl_2$.

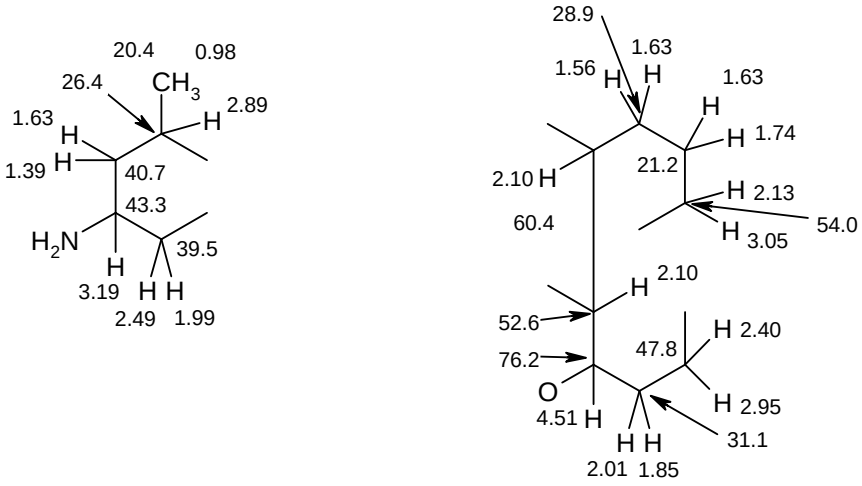


**Figure 88.** The partial structures of grandisine F (**129**) established from HSQC and COSY spectra.

The connection of the partial structures of **129** was established by an HMBC experiment (Figure 89). The structure of the 7-oxy-8-ketoindolizidine functionality was secured in an identical manner as for isoelaeocarpiline (**63**), grandisine C (**127**) and E (**128**). HMBC correlations were observed from the proton at δ 4.51 ppm (H-7) to the ketone carbonyl carbon C-10 at δ 193.1 ppm. This established the connection of C-10 to C-8. The methyl group at δ 1.00 ppm showed a correlation to the α-carbon (δ 115.6 ppm, C-11) of the α,β-unsaturated ketone, and correlations from H-16 (2.89) to this quaternary olefinic carbon and to C-12 (169.0) demonstrated that C-16 and C-10 were attached to C-11. An HMBC correlation from H-16 to C-10 provided further evidence for this structure and established a connection to the 7-oxy-8-ketoindolizidine moiety. HMBC correlations from H-13 (2.49/1.99) to the quaternary olefinic carbons C-11 and C-12, confirmed this methylene to be adjacent to C-12 and enabled the formation of a 1-methyl-5-aminocyclohex-2-ene ring. H-14 (3.19) showed no HMBC correlations. An ether bridge between C-7 (76.8) and C-12 was determined from MS evidence and the chemical shifts of these carbons. Thus the structure of grandisine F (**129**) was established.

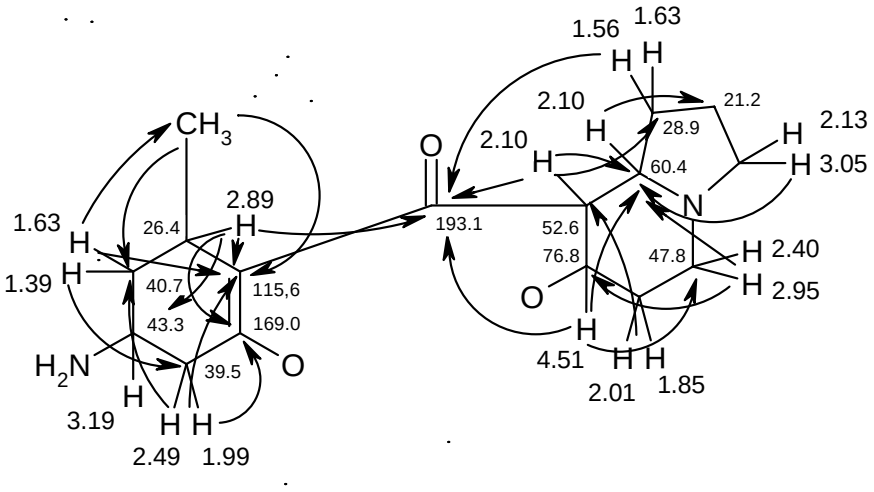


**Figure 89.** The key HMBC correlations used to establish the structure of grandisine F (**129**).

The relative stereochemistry of the indolizidine portion of **129** can be considered the same as H-7, H-8 and H-9 of isoelaeocarpiline (**63**) due to similar carbon and proton chemical shifts. The relative stereochemistry of H-14 and H-16 could not be determined from ROESY data as H-14 exhibited no correlations. H-16 exhibited two couplings of 6.0 Hz, which are typical for an equatorial proton. The methyl group is therefore axial. Inspection of the coupling constants of the methylenes adjacent to H-14 also indicate that this proton was axial. Figure 90 shows the energy minimized structure of grandisine F (**129**).

Grandisine F (**129**) is proposed to be an artifact of grandisine D (**126**). The formation of **129** from **126** is illustrated in Figure 91. Nucleophilic attack by ammonia occurs from the opposite face of the cyclohexenone ring to the methyl substitute in grandisine D (**126**). The enol form of the amino-cyclohexenone can then undergo a Michael addition onto the beta carbon C-7 of the indolizidine to form **129**.

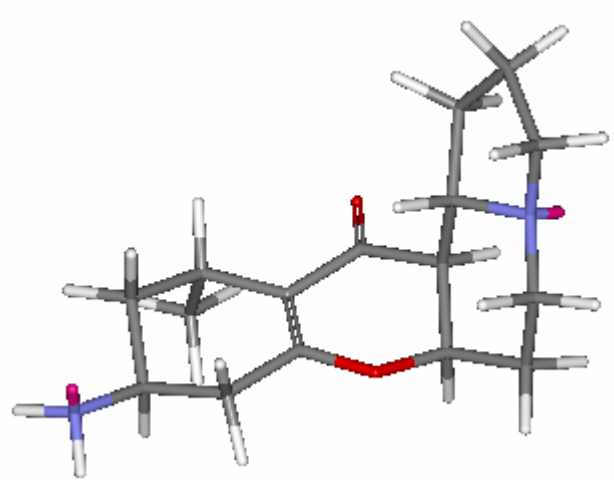

**Figure 90.** The energy minimized structure of grandisine F (**129**).

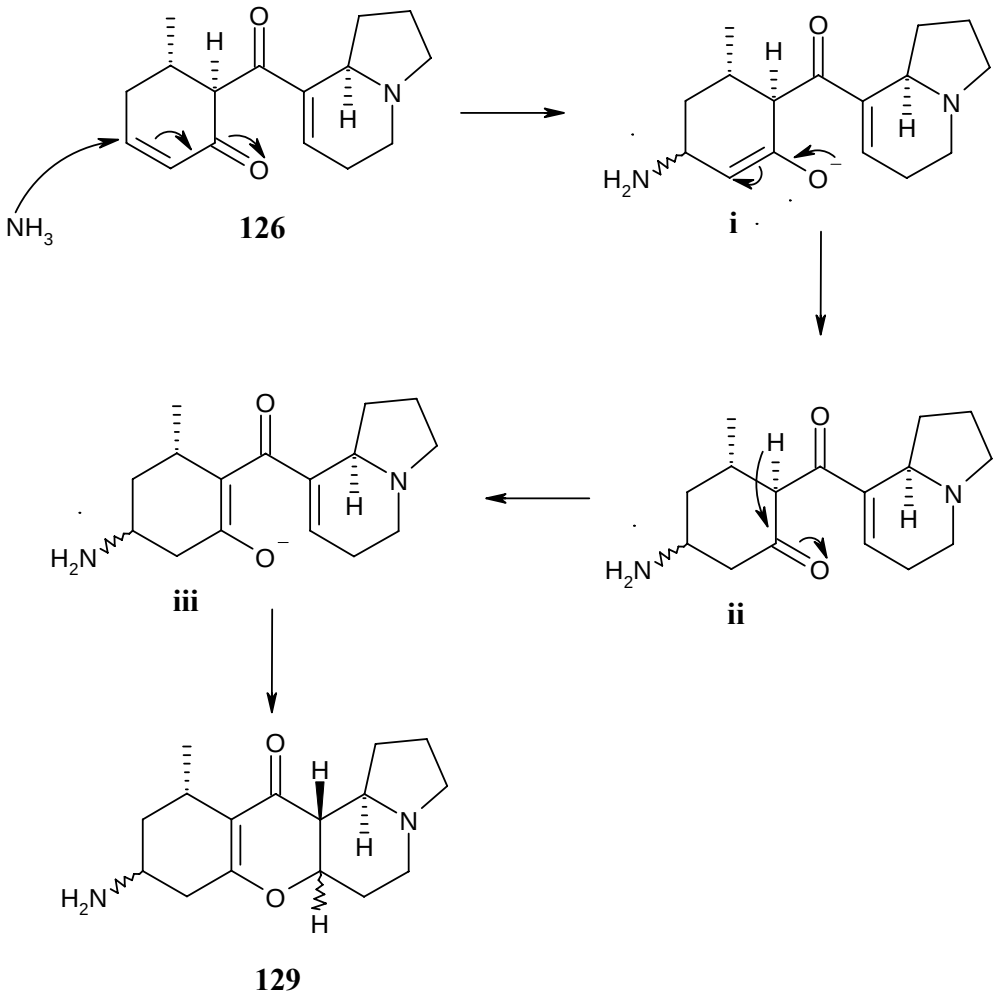


**Figure 91.** The proposed formation of grandisine F (**129**) by Michael addition of ammonia to grandisine D (**126**).

## 6.9 Structure Elucidation of Grandisine G (130)

The $^{1}$H NMR spectrum of grandisine G (**130**) (Figure 92) displayed features which made grandisine G unique among the *E. grandis* alkaloids. One olefinic proton was found at δ 6.55 ppm, which was observed as a broad singlet. A methyl doublet was found at δ 0.94 and a methoxy at 3.61 ppm. Other protons were found at δ 0.79, 2.55, 2.37, 2.65, 3.07, 3.83 and 4.32 ppm. A group of five protons were found between between 1.5 - 2.0 ppm. A total of 19 protons were observed. The water peak at δ 3.30 and DMSO peak at 2.49 ppm obscured some protons. A broad exchangeable proton was found at 10.01 ppm. The positive LRESIMS of **130** revealed a mass ion peak at *m/z* 291, however attempts to obtain a positive HRESIMS for this compound were unsuccessful, as the compound was unstable and decomposed.

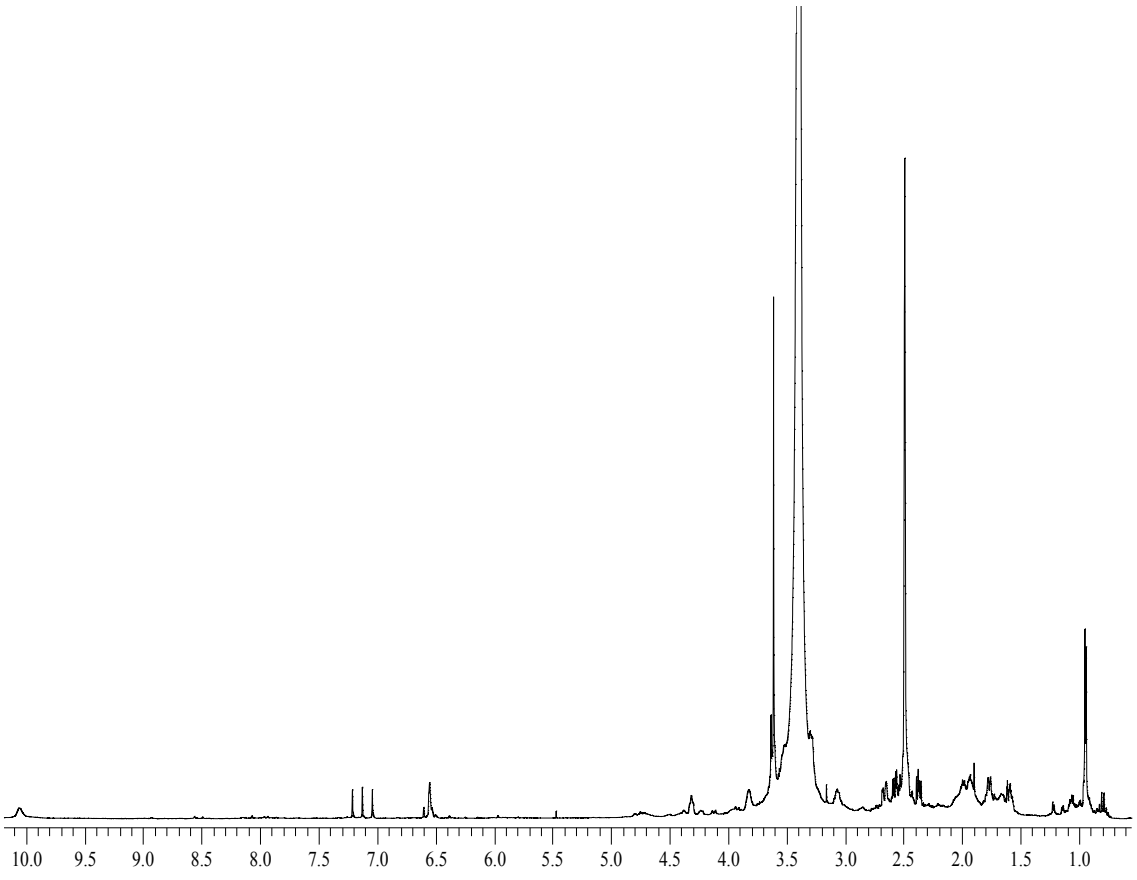


**Figure 92.** The $^{1}$H NMR spectrum of grandisine G (**130**) at 600 MHz in $d_6$-DMSO.

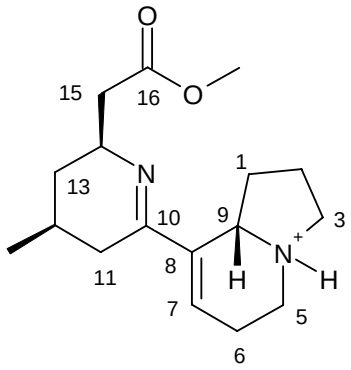


**Table 19.** $^{1}$H,[a] $^{13}$C[b] and HMBC NMR spectral data of grandisine G (**130**)[c]

| position | $\delta_C$ | $\delta_H$ (mult; *J* in Hz) | HMBC ($^{2,3}J_{CH}$) |
|---|---|---|---|
| 1 | 28.5 | 1.59 (1H, m); 2.49 (1H, m) | 3, 9 |
| 2 | 20.1 | 1.95 (1H, ddd, 3.0, 9.6, 10.2); | 1, 9 |
| | | 2.00 (1H, ddd, 4.2, 3.0, 10.2) | 1, 9 |
| 3 | 52.9 | 3.30 (1H, m); 3.52 (1H, dd, m) | 1, 9 |
| 4 | - | 10.01 (1H, br) | - |
| 5 | 43.6 | 3.07 (1H, ddd, 5.0, 5.0, 12.0); | 6, 9 |
| | | 3.30 (1H, m) | |
| 6 | 22.3 | 2.49 (2H, m) | - |
| 7 | 127.0 | 6.55 (1H, dd, 4.2, 4.2) | 5, 6, 9, 10 |
| 8 | 135.2 | - | - |
| 9 | 59.5 | 4.32 (1H, dd, 10.8, 10.8) | - |
| 10 | 163.0 | - | - |
| 11 | 32.7 | 1.61 (1H, dd, 2.4, 14.6); | 10, 12, 13, 12-Me |
| | | 2.65 (1H, dd, 6.0, 14.6) | |
| 12 | 25.6 | 1.67 (1H, m) | 11 |
| 13 | 35.4 | 1.76 (1H, m); 0.79 (1H, ddd, 11.4, 11.4, 11.4) | 11, 12, 14, 15 |
| 14 | 56.7 | 3.83 (1H, 4.0, 6.6, 9.0, 11.4) | - |
| 15 | 41.8 | 2.37 (1H, dd, 9.0, 15.0); | 13, 14, 16 |
| | | 2.55 (1H, dd, 6.6, 15.0) | 13, 14, 16 |
| 16 | 172.0 | - | - |
| 12-Me | 21.8 | 0.94 (3H, d, 6.6) | 11, 12, 13 |
| 16-OMe | 51.2 | 3.61 (3H, s) | 16 |

[a] At 600 MHz. [b] At 125 MHz. [c] In $d_6$-DMSO.

The $^{13}$C NMR spectrum of **130** revealed a total of 17 carbons including three olefinic carbons at δ 127.0, 135.2 and 163.0 ppm. The carbon at δ 163 ppm may indicate a carbonyl or imine carbon. A carbonyl carbon was found at δ 172.0 ppm, indicating an ester or amide group was present. In the upfield region of the spectrum, carbons at δ 28.5, 20.1, 52.9, 43.6 and 22.3 ppm were almost identical to the chemical shifts of C-1 to C-6

of grandisine D (**126**). Three carbons were found between 50 and 60 ppm suggesting methines bound to heteroatoms. Four aliphatic carbons were found between 20 and 40 ppm. The $^{1}H$ and $^{13}C$ NMR spectral data for grandisine G (**130**) is represented in Table 19.

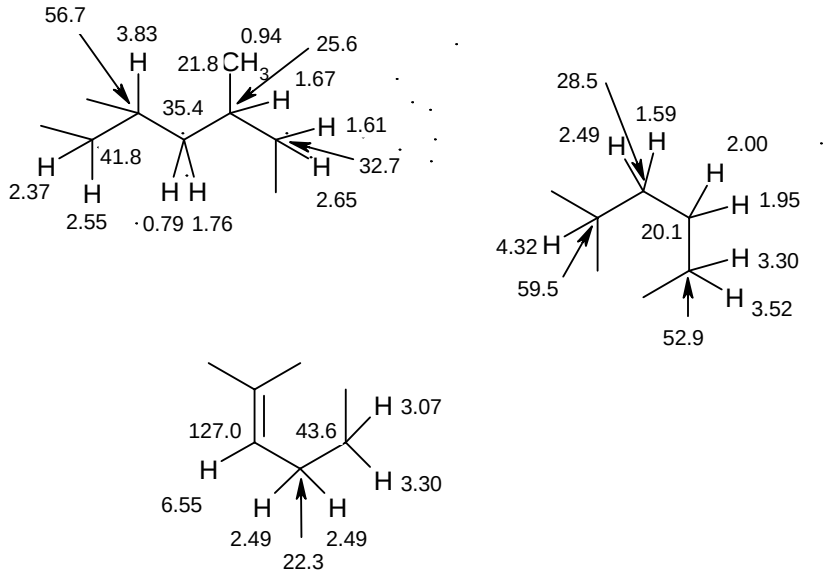


**Figure 93.** The partial structures of grandisine G (**130**) established from HSQC and COSY spectra.

The partial structures of **130** (Figure 93) were established from correlations observed in HSQC and COSY spectra. The HSQC spectrum established the presence of eight methylenes, three methines, one methoxy, one methyl and one olefinic proton. The carbon chemical shift of the methoxy group was found to be 51.2 ppm. A partial structure containing three methylenes (C-1 to C-3) and a methine (C-9) was established by COSY correlations from δ 2.00/1.95 (H-2) to 3.30/3.52 (H-3) and 2.49/1.59 (H-1), and from 4.32 ppm (H-9) to H-1. COSY correlations were observed from the olefinic proton at δ 6.55 ppm (H-7) to the methylene at δ 2.49 ppm (H-6), and this enabled the connection of C-6 and C-7. The methylene H-5 (δ 3.07/3.30 ppm) was determined to be adjacent to H-6 from COSY correlations. Another partial structure was assembled by COSY correlations from the methine proton at δ 1.67 ppm (H-12) to two methylenes at δ 1.61/2.65 (H-11) and 0.79/1.76 (H-13), and to a methyl group at 0.94 ppm (H-$12_{Me}$). The methine proton at

δ 3.83 ppm (H-14) was determined to be adjacent to H-13 from COSY correlations between H-14 and H-13, and additional correlations from H-14 to H-15 (δ 2.37/2.55 ppm) indicated that this methine was attached to another methylene.

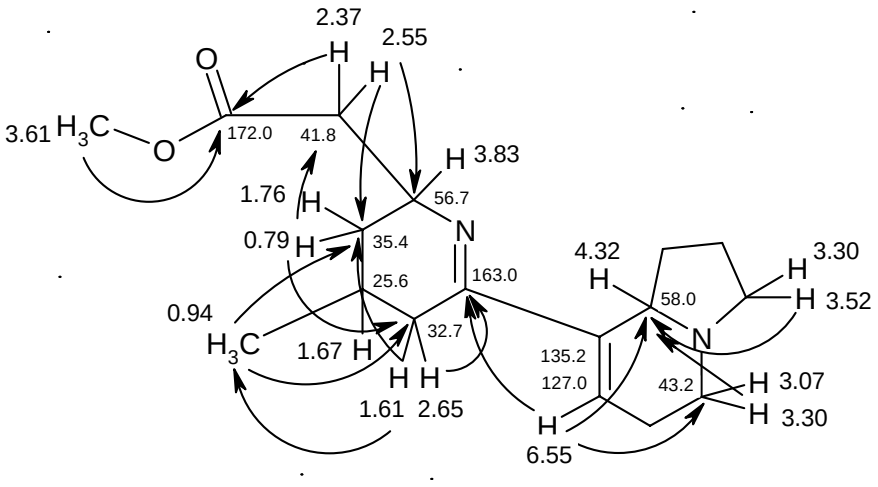


**Figure 94.** The key HMBC correlations used to establish the structure of grandisine G (**130**).

The connection of the partial structures of **130** was established from correlations observed in the HMBC spectrum (Figure 94). A single HMBC correlation from the methoxy group at δ 3.61 ppm to the carbonyl carbon C-16 (δ 172.0 ppm) indicated an ester group was present. The methylene H-15 (2.37/2.55) also showed correlations to the ester carbonyl, in addition to correlations to C-14 (56.7) and C-13 (35.4). This allowed the attachment of the ester group to H-15. The proton at δ 0.79 ppm (H-13$_{\alpha}$) showed a correlation to C-15 (41.8), supporting the position of the H-15 methylene. HMBC correlations were observed from the methylene at δ 1.61/2.65 ppm (H-11) to C-10 (163.0), C-12 (25.6), C-12$_{Me}$ (21.8) and C-13 (35.4). This indicated that the carbonyl or imine carbon C-10 was attached to C-11 (32.7). Carbon and proton chemical shifts of 56.7 and 3.83 ppm respectively, were consistent for a methine (H-14) bound to a heteroatom. A 7,8-dehydroindolizidine moiety was secured from the remaining partial structures by HMBC correlations from H-3 (3.30/3.52), H-5 (3.07/3.30) and H-7 (6.55) to C-9 (59.5). HMBC correlations were observed from H-7 to the imine/carbonyl carbon C-10 enabling the connection of C-8 and C-10. As a result, the structure established from

COSY, HSQC and HMBC spectra assigned all the protons and carbons of **130**. However, this accounted for only 276 Da. of the molecular weight of **130** (290 Da.). This indicated that grandisine G contained a second nitrogen. Therefore MS evidence concluded that **130** contained an imine. The connection of C-14 and C-11 to this nitrogen created a 1,2-dehydropiperidine ring. Thus the structure of grandisine G (**130**) was established.

The chemical shifts of the protons and carbons of the indolizidine portion of **130** were similar to those of grandisine D (**126**). The only major difference was found to be the carbon and proton chemical shift at position 7. H-7 (6.55) and C-7 (127.0) in **130** were significantly shifted upfield due to the presence of the imine, compared to the α,β-unstaturated ketone in grandisine D (**126**). A ROESY correlation between H-12 and H-14 indicated that these protons were 1,3-diaxial. This was supported by a ROESY correlation between C-$12_{Me}$ and H-$13_{ax}$ (0.79), which indicated this proton and the methyl group were *cis* to each other. The protons at δ 0.79 and 3.83 ppm exhibited large couplings of 11.4, 11.4 Hz and 12.0, 12.0 Hz respectively. This indicated that both protons were axial, therefore confirming C-$12_{Me}$ as equatorial. The stereochemistry of H-12 and H-14 relative to H-9 could not be established from ROESY correlations. The energy minimized structure of grandisine G (**130**) is shown in Figure 95.

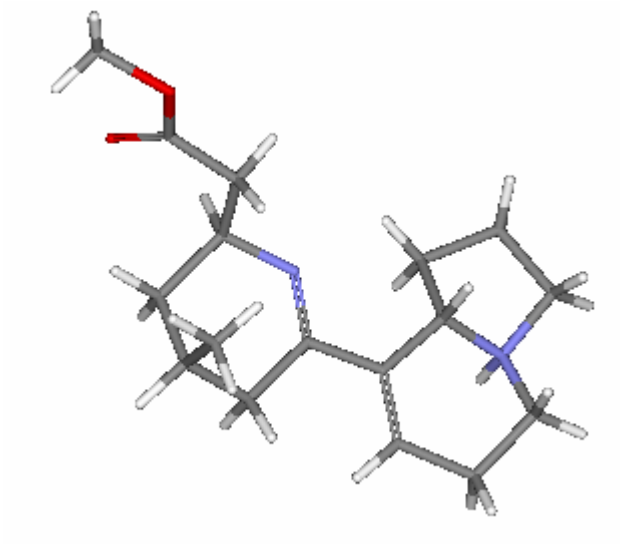

**Figure 95.** The energy minimized structure of grandisine G (**130**).

Grandisine G (**130**) is proposed to be a methanol adduct of grandisine B (**74**). Grandisine B was originally an artifact of grandisine D (**126**). The formation of **130** by the nucleophilic attack of methanol to the carbonyl carbon of the isoquinuclidinone moiety is illustrated in Figure 96.

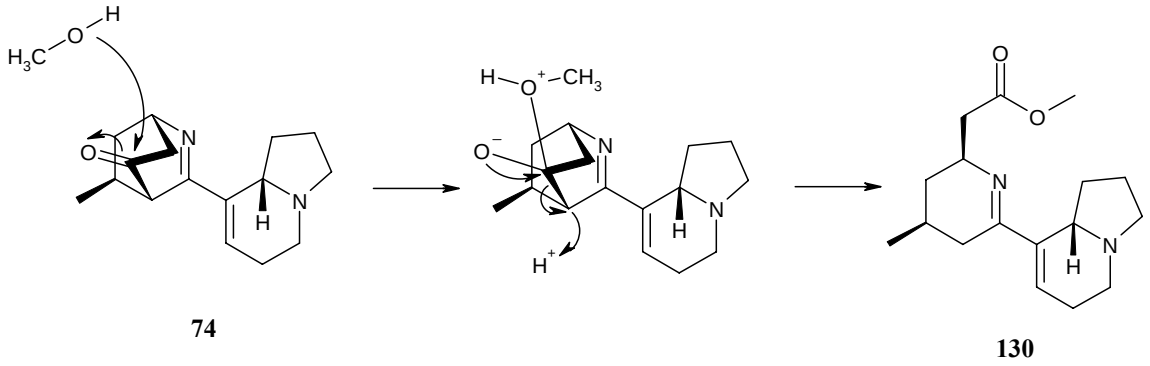


**Figure 96.** The proposed addition of a methoxide ion to grandisine B (**74**) to yield grandisine G (**130**).

## 6.10 The Proposed Structures of the Diastereomers of Compound 131

The $^{1}H$ NMR spectrum of the mixture of diastereomers is shown in Figure 97. The isomers occur in a ratio of approximately 3:2. The mixture was analysed by positive HRESIMS of the molecular ion $[M + H]^{+}$ 296.183698 (calculated for 296.185635) and the molecular formula of $C_{16}H_{26}NO_4$ was determined. This indicated that these diastereomers were 18 Da. heavier than grandisine C (**127**), suggesting that **131** contained an extra $H_2O$. Figure 97 shows the absence of olefinic protons.

The $^{13}C$ NMR spectrum of **131** revealed a carbon at δ 100 ppm, which is typical for a doubly oxygenated carbon. An absence of olefinic carbons was also noted. This suggests that the double bond of the α,β-unsaturated ketone in grandisine C (**127**) had been

hydrated at C-12 to yield two diastereomeric compounds. This was supported by the observation of two ketone carbonyl carbons at δ 207 and 208 ppm, which is characteristic of a fully saturated ketone. The presence of four exchangeable protons was established in the $^1$H NMR spectrum of the TFA salt (Figure 97), including two doublets at δ 4.57 and 4.61, and two singlets at 5.86 and 6.16 ppm. These protons were not observed in the $^1$H NMR spectrum of the free base in $CD_2Cl_2$, indicating these protons are exchangeables. The splitting of the signals at δ 4.57 and 4.61 ppm indicated that these protons were adjacent to another proton, suggesting a potential HO-CH- system.

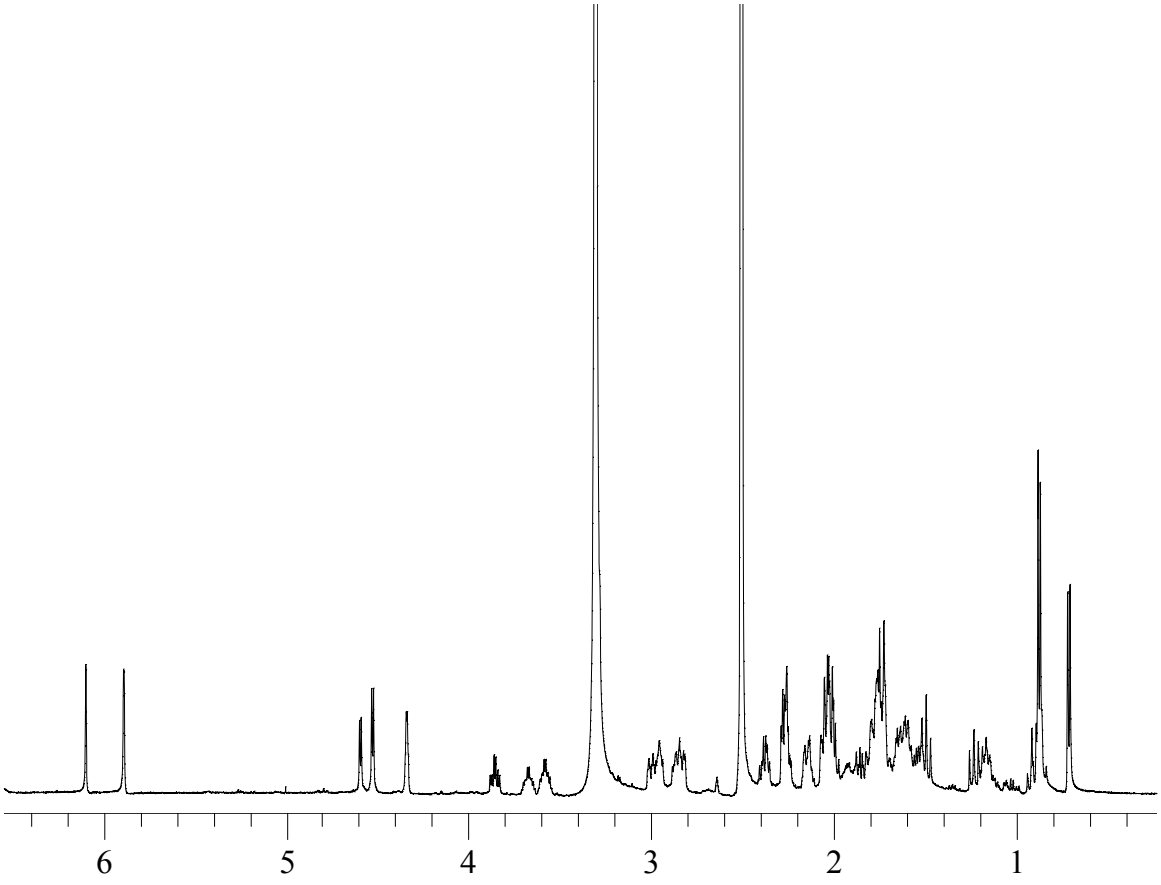


**Figure 97.** The $^1$H NMR spectrum of a pure mixture of two diastereomers of compound **131** at 500 MHz in $d_6$-DMSO.

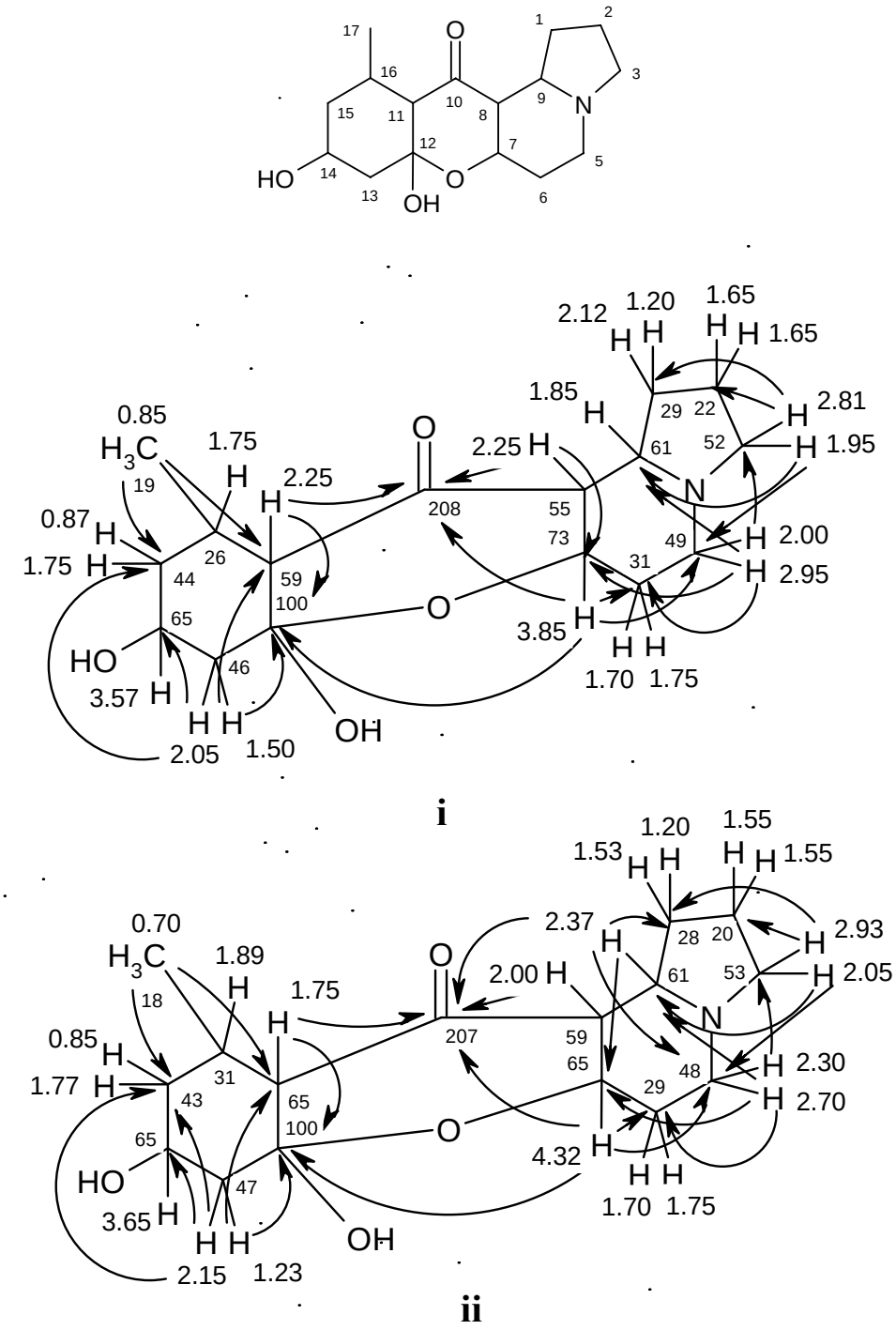


**Figure 98.** The proposed structures of the isomers of compound **131** established from $^{1}H$, $^{13}C$, COSY, HSQC and HMBC spectral data.

**Table 20.** $^{1}H$,[a] and $^{13}C$[b] NMR spectral data of **131a**[c], structure (**i**) in Figure 98.

| position | $\delta_C$ | $\delta_H$ (mult; *J* in Hz) |
|---|---|---|
| 1 | 28.7 | 2.12 (1H, brdd, 6.6, 11.4); 1.20 (1H, m) |
| 2 | 21.8 | 1.65 (1H, m); 1.65 (1H, m) |
| 3 | 52.1 | 2.81 (1H, ddd, 4.8, 6.6, 13.2); 1.95 (1H, m) |
| 5 | 48.9 | 2.00 (1H, m) |
| | | 2.95 (1H, ddd, 3.6, 6.0, 10.8) |
| 6 | 31.1 | 1.75 (1H, m ); 1.70 (1H, m) |
| 7 | 72.8 | 3.85 (1H, ddd, 4.8, 10.8, 10.8) |
| 8 | 54.7 | 2.25 (1H, dd, 9.6, 9.6) |
| 9 | 61.1 | 1.85 (1H, ddd, 6.0, 9.6, 9.6) |
| 10 | 208.6 | - |
| 11 | 59.0 | 2.25 (1H, d, 10.8) |
| 12 | 100.6 | - |
| 13 | 46.3 | 1.50 (1H, dd, 12.0, 12.0); 2.05 (1H, m) |
| 14 | 65.0 | 3.57 (1H, ddd, 4.2, 10.8, 10.8) |
| 15 | 43.8 | 1.75 (1H, m); 0.87 (1H, m) |
| 16 | 25.7 | 1.75 (1H, m) |
| 17 | 19.6 | 0.85 (3H, d, 6.6) |

[a] At 600 MHz. [b] At 125 MHz. [c] In $d_6$-DMSO.

**Table 21.** $^{1}H$,[a] and $^{13}C$[b] NMR spectral data of **131b**[c], structure (**ii**) in Figure 98.

| position | $\delta_C$ | $\delta_H$ (mult; *J* in Hz) |
|---|---|---|
| 1 | 27.8 | 1.53 (1H, dd, 6.0, 13.2); 1.20 (1H, m) |
| 2 | 20.2 | 1.55 (1H, m); 1.55 (1H, m) |
| 3 | 53.3 | 2.05 (1H, m); 2.93 (1H, brdd, 3.6, 9.0) |
| 5 | 47.7 | 2.30 (1H, m) |
| | | 2.86 (1H, ddd, 3.0, 3.0, 8.4) |
| 6 | 29.2 | 1.70 (1H, m ); 1.75 (1H, m) |
| 7 | 65.6 | 4.32 (1H, ddd, 3.0, 3.0, 5.4) |
| 8 | 59.6 | 2.00 (1H, m) |
| 9 | 60.7 | 2.37 (1H, ddd, 6.6, 10.8, 10.8) |
| 10 | 207.1 | - |
| 11 | 65.8 | 1.72 (1H, m) |
| 12 | 100.3 | - |
| 13 | 47.3 | 2.15 (1H, m); 1.23 (1H, dd, 12.0, 12.0) |
| 14 | 64.7 | 3.65 (1H, ddd, 4.8, 10.8, 10.8) |
| 15 | 42.7 | 1.77 (1H, m); 0.87 (1H, m) |
| 16 | 31.3 | 1.89 (1H, m) |
| 17 | 18.7 | 0.70 (3H, d, 6.6) |

[a] At 600 MHz. [b] At 125 MHz. [c] In $d_6$-DMSO.

Analysis of the $^{1}H$, $^{13}C$, COSY, HSQC and HMBC spectral data of **131** established the proposed two dimensional structures of the diastereomers (Figure 98). The structures of both the indolizidine moieties were established in a similar manner as for the other *E. grandis* alkaloids. The structures of the 1-methyl-3,5-dihydroxycyclohexane rings in both isomers was established by HMBC correlations from H-11 and H-13 to the di-oxygenated carbon C-12 at δ 100 ppm. The remaining segment of the 1-methyl-3,5-dihydroxycyclohexane ring was secured in an identical manner as for grandisine C (**127**).

The connection of the cyclohexane ring to the indolizidine moiety was established by correlations from H-7, H-8 and H-11 to the ketone carbonyl carbon C-10. An HMBC correlation from H-7 to C-12 was observed for each isomer, establishing the presence of the ether link. These compounds are the only tetracyclic *Elaeocarpus* alkaloids to display an HMBC correlation from H-7 to C-12. This suggested a change in the conformation of the pyran ring to allow a dihedral angle of less than 90$^{o}$ between H-7 and C-12. The $^{1}H$ and $^{13}C$ NMR spectral data of both diastereomers is presented in Tables 20 and 21.

There are seven chiral centres each in the structures (**i**) and (**ii**) in Figure 98. The presence of only two isomers suggested that only one chiral centre may be epimeric. The resonances of H-14 at δ 3.65 and 3.57 ppm for (**ii**) and (**i**) respectively were identical in multiplicity. Therefore, it is unlikely that this centre is isomeric. This confirmed that H-16 was also not isomeric. The isomerization of H-8 and H-9 would also seem unlikely, as the *trans*-diaxial relationship between these protons has been consistently observed for the *E. grandis* alkaloids. This was supported by large couplings from the H-9 protons in both diastereomers, indicating this proton as axial. The chiral centres most likely to be affected would be H-12, H-11 and H-7. The protons H-12 or H-11 could isomerise depending on the side of attack of the hydroxyl group. Under basic conditions elaeocarpenine (**122**) has previously been demonstrated to yield isoelaeocarpine (**61**) and elaeocarpine (**60**), which are isomers at H-7. The H-7 protons were found at δ 4.32 and 3.85 ppm in (**ii**) and (**i**), respectively. These protons showed different multiplicity, the resonance at δ 4.32 ppm was a narrow ddd ($J$ = 3.0, 3.0, 5.4) and the proton at δ 3.85 ppm

was a ddd ($J$ = 4.8, 10.8, 10.8). This difference in multiplicity demonstrates the proton at δ 4.32 was equatorial and the proton at δ 3.85 ppm was axial. Therefore, the diastereomers were isomers at H-7. This coupling information relates directly with the couplings of H-7 for isoelaeocarpine (**61**) and elaeocarpine (**60**), respectively. The chemical shifts of H-1 also supported this. The chemical shifts of the H-1 methylenes in **61** and **60** were δ 1.78/1.90 and 1.77/2.68 ppm, respectively. The isomer (**ii**) containing the same equatorial configuration of H-7 as **61**, the protons of H-1 were observed at δ 1.53 and 1.20 ppm, whereas the isomer (**i**) possessing the same axial configuration of H-7 as **60**, the protons of H-1 were observed at δ 2.12 and 1.20 ppm. This indicated that the configurations of H-11 and H-12 were the same in both diastereomers.

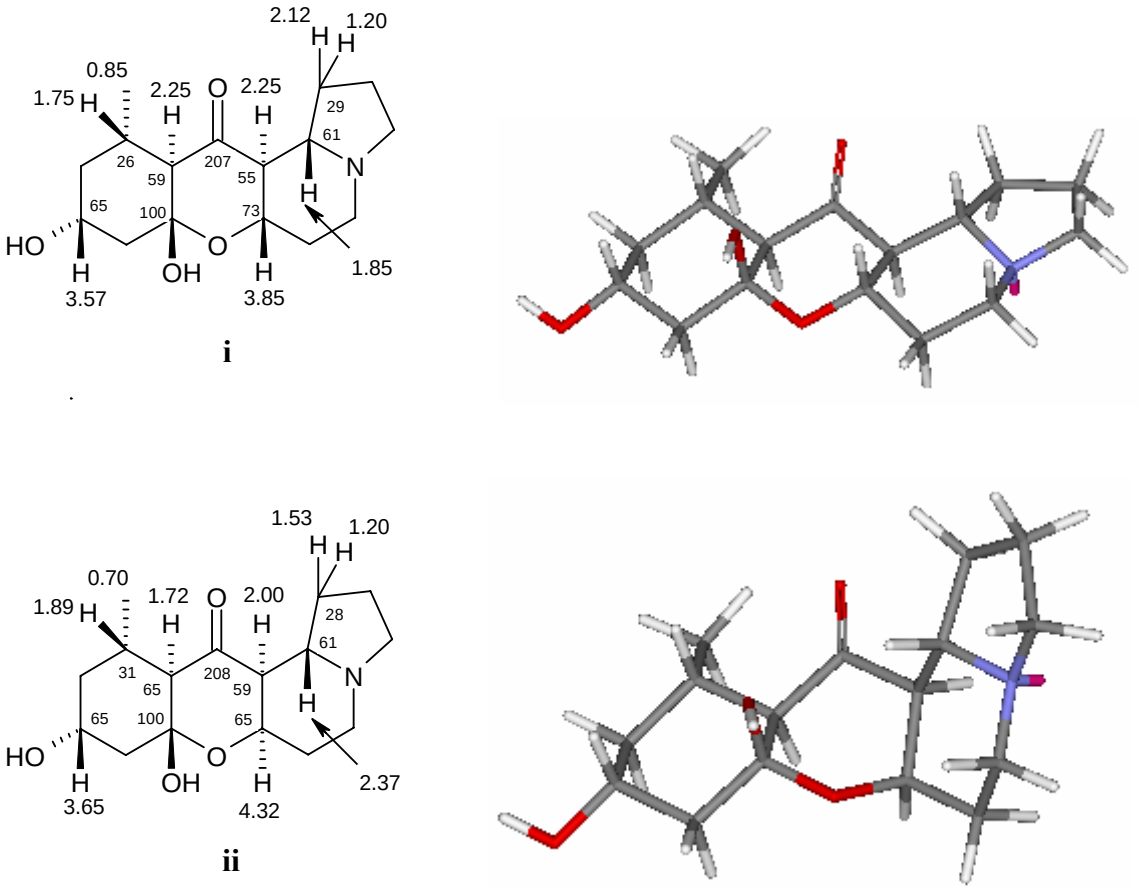


**Figure 99.** The structures and energy minimized conformations of the diastereomers of **131**.

The relative stereochemistry of H-11 in both diastereomers was axial, which was demonstrated by large couplings of 10.8 and 12.0 Hz to H-16 in (**i**) and (**ii**) respectively, thus indicating that the C-17 methyl groups are equatorial. The relative stereochemistry of H-12 could not be deduced by NMR techniques, however the coupling constants of the cyclohexyl ring indicated that it possessed a chair conformation. Figure 99 shows the relative stereochemistry of the diastereomers. Molecular modeling studies were performed on each isomer, where the stereochemistry at C-12 was inverted. Compounds (**i**) and (**ii**) of Figure 99 both displayed significantly lower energy minimized structures when the hydroxyl at C-12 was in an axial position. The C-12-OH axial energy minimized structures of these compounds are displayed in Figure 99.

## 6.11 Proposed Biogenesis of the *E. grandis* Alkaloids and Chemotaxonomic Considerations

The polyketide biosynthesis of the *E. grandis* alkaloids is proposed to occur in a similar manner to that previously described. The *E. grandis* alkaloids are chemotaxonomically related to the *E. sphaericus* alkaloids. Both species produced tetracyclic indolizidine alkaloids which did not contain a C-15-16 double bond. The cyclohexadiene ring of isoelaeocarpiline (**63**) has not been fully reduced to an aromatic rings, unlike the tetracyclic indolizidine alkaloids such as those purified from *E. fuscoides.* Figure 100 illustrates the proposed biogenesis of grandisine D (**126**), C (**127**) and isoelaeocarpiline (**63**). This biogenesis can be considered an extension of Figure 7. The polyketide condensation product (**i**) (Figure 100) serves as the precursor for **63**, **126**, **127** and grandisine E (**128**). This precursor can undergo a retroaldol reaction to create (**viii**), which is the tetra-keto precursor of **128**. Alternatively, the precursor (**i**) can be reduced to (**ii**), the tricyclic precursor of **63**, **126** and **127**. A reduction of the C-14 ketone of (**ii**) yields grandisine D (**126**). The conversion of (**ii**) into its enol tautomer at C-12 (**iii**) leads to the formation of (**iv**), a tetracyclic precursor of grandisine C (**127**) and isoelaeocarpiline (**63**). Grandisine C (**127**) is formed from the reduction of the C-14

ketone in (**iii**) to yield an alcohol. Reduction of the C-14 ketone of (**iii**) to a double bond results in the formation of isoelaeocarpiline (**63**).

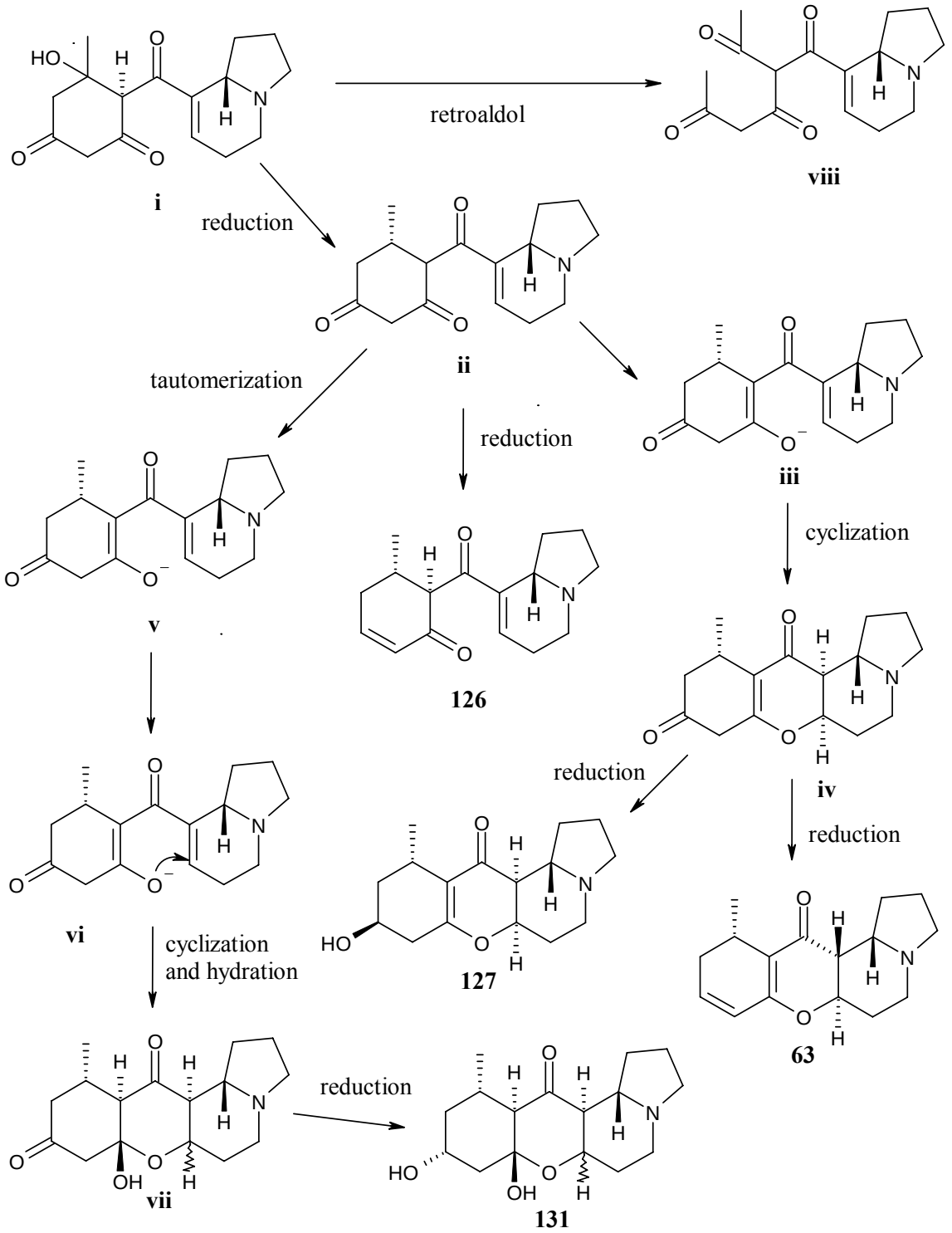


**Figure 100.** The proposed biogenesis of grandisine C (**127**), D (**126**), isoelaeocarpiline (**63**) and compound **131**.

I propose the formation of the diastereomers of **131** occurs via the attack of a hydroxide ion to the C-12 ketone of (**ii**), which is represented as (**v**). Following the addition of –OH to C-12, the epimerization at H-7 is proposed to occur during the cyclization of (**vi**) to (**vii**), due to the attack of the oxygen anion from either face of the 7,8-dihydroindolizidine ring. The addition of a second hydroxide anion to the ketone in (**vii**) yields **131a** and **131b**.

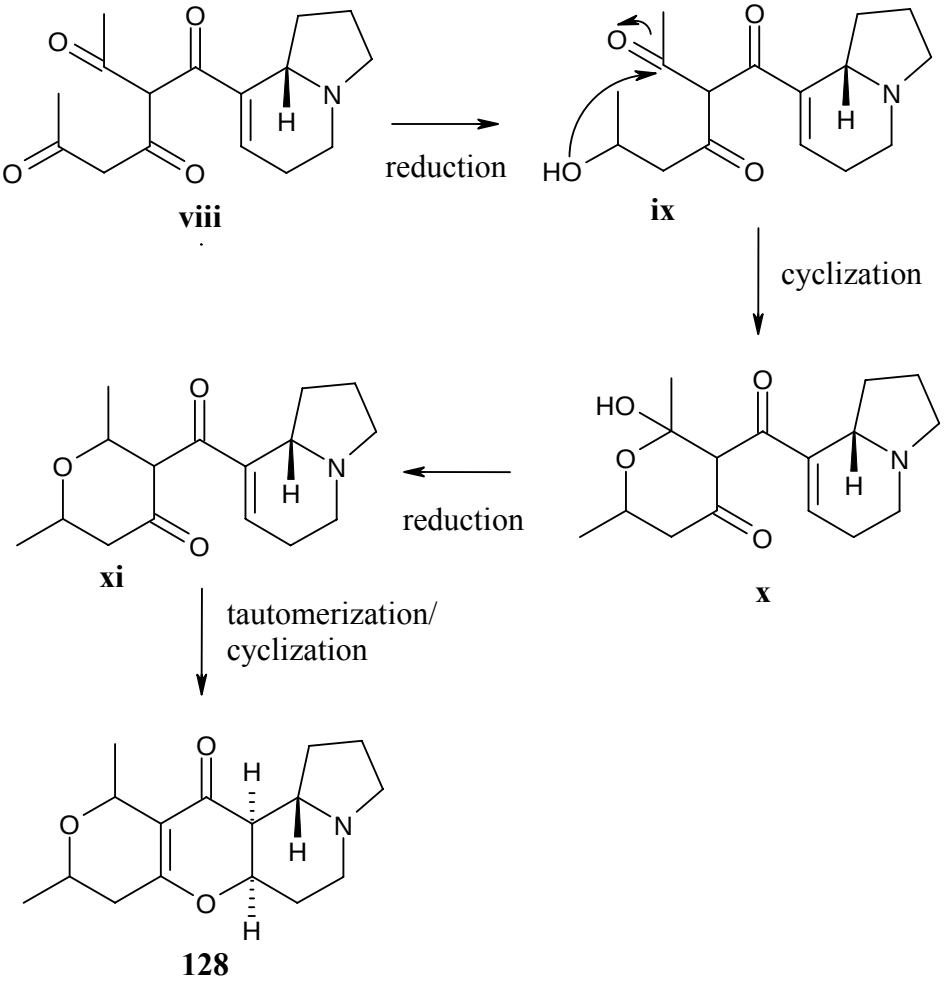


**Figure 101.** The proposed biogenesis of grandisine E (**128**).

The formation of grandisine E (**128**) (Figure 101) is proposed to occur in a similar manner as detailed for grandisine A (**73**). A ketone of the retroaldol product (**viii**) in Figure 101 is proposed to be reduced to an alcohol in (**ix**). This alcohol yields a re-

cyclised product (**x**) following nucleophilic addition to the ketone illustrated in (**ix**) to form a pyran ring. Reduction of (**x**) yields (**xi**), which can tautomerize to its enol form at C-12. A subsequent cyclization results in formation of the tetracyclic indolizidine alkaloid **128**.

## 6.12 References


1. Bartholomew, B. http://www.brisrain.webcentral.com.au/database/Elaeo_grandis.htm
2. Carroll, A. R., Arumugan, G., Quinn, R. J., Redburn, J., Guymer, G., Grimshaw, P., *J Org Chem* **2005,** 70, 1889 - 1892.
3. Johns, S. R., Lamberton, J. A., Sioumis, A. A., Suares, H., *Aust J Chem* **1971,** 24, 1679 - 1694.
4. Ray, A. B., Chand, L., Pandey, V. B., *Phytochemistry* **1979,** 18, 700 - 701.

# CHAPTER 7 – Biological Screening of the Elaeocarpaceae Alkaloids Against the Human δ Opioid Receptor.

## 7.1 Introduction to Opioid Analgesics: A Brief History

Agonists acting at the opioid receptors have become synomynous with the management of pain and are often called analgesics or antinociceptives.[1] The opioid receptors are contained within the CNS and opioid analgesics comprise an important group of substances prescribed to alleviate pain. These drugs present an alternative to the NSAIDs, such as aspirin (**132**), which are the most commonly prescribed drugs for pain management.[2, 3] Aspirin (**132**) acts as a regulator of immune response by inhibiton of cyclooxygenase, an enzyme involved in the biosynthesis of prostaglandins.[4] However, the side effects of NSAIDs make this form of pain control incompatible for a significant number of patients, particularly the elderly.[3] It has been estimated that 75 million US citizens are debilitated by chronic pain,[3] therefore propelling the management of pain as a major issue for human health.

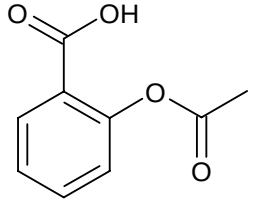


**132**

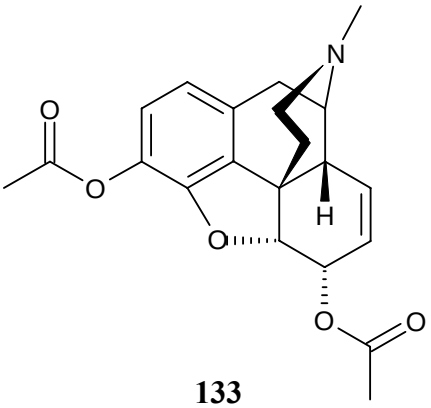


**133**

Certain opioid analgesics are known to provoke narcotic effects in combination with pain relief.[1] The addictive properties of compounds such as heroin (diacetylmorphine) (**133**)

are well known. However, not all opiates possess narcotic properties, therefore opioid analgesics constitute immense therapeutic value.[1] The importance of opioid analgesics is exemplified by investments in excess of $US 2.5 billion into opiate research by the pharmaceutical industry from 1980 to 2000.[5]

The name opioid was derived from the Greek word for "juice". The juice of the seed pods of the poppy *Papaver somniferum* was frequently employed in tonics during ancient times and was one of the oldest recorded medications for the treatment of pain.[1] This medication was called opium and was also consumed for its narcotic and euphoric affects.[1, 6, 7] Opium was speculated to be the first medicinally active tonic, which was utilized before the discovery of the fermentation process required to produce alcohol.[7] The earliest sample of opium was found in the temple of Cha in Egypt from the 15th century BC,[7] and was first introduced to Britain in the 17th century.[2]

Morphine (**1**), the first alkaloid isolated from the opium poppy, was named after Morpheus the Greek god of dreams. Isolation of other analgesic alkaloids from the opium poppy followed, such as codeine (**134**), and thebaine (**135**).[1] Heroin was originally sold in 1898 as a substitute to morphine, however it rapidly became a drug of abuse as heroin penetrates the brain faster then morphine when administered intravenously.[1] It was deemed to be a safer alternative to morphine and was named a "heroic drug" by Bayer.[8] Heroin's use was restricted by law four years following its launch.[8]

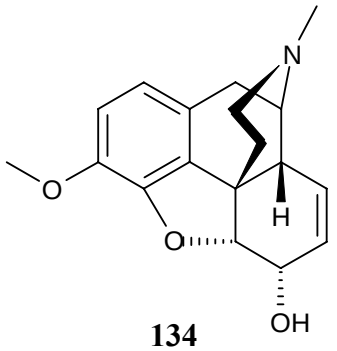


**134**

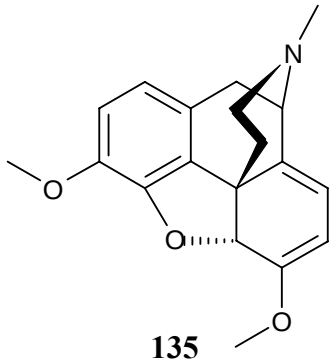


**135**

## 7.2 Opioid Receptors and Pharmacology

### *7.2.1 Opioid Receptors and Endogenous Ligands*

Evidence for the existence of opioid receptors was first discovered via binding studies in 1973.[2] However, it wasn't until 1996 that complete characterization studies of the opioid receptors were completed and three main types of receptor were identified.[9, 10] The opioid receptors are divided into three major types: mu (μ), kappa (κ) and delta (δ).[1] Pharmacological evidence exists for subtypes of each receptor but they have not been established by receptor cloning and their impact remains undefined.[2] Opioid receptors have been identified within the mammalian brain and spinal cord.[1, 11-13] The opioid receptors are concentrated in the arcuate nucleus (cortex), periaqueductal gray (located in the brain stem) and thalamic areas of the brain and in the dorsal horn of the spinal cord. These regions of the brain and spinal cord have been identified as the areas where opioid active molecules exert their actions.[1]

The opioid receptors belong to the family of G-protein coupled receptors, that inhibit adenylate cyclase and control ion channels by G-protein coupling.[9] The activation of these ion channels results in the opening of $K^+$ channels, causing an influx of ions in tandem with the inhibition of $Ca^{2+}$ channels, which ultimately prevents transmitter release.[9] The G-protein coupled receptors contain seven membrane spanning helicies and are the largest of four superfamilies of receptors, which are encoded in an estimated 600 human receptor genes. The mode of action of approximately half of all marketed drugs is against G-protein coupled receptors. Therefore this group of receptors are significant targets for pharmaceutical research.[14, 15]

Many years of research has culminated in the isolation and identification of endogenous opioid peptide ligands from mammalian brains.[1] These include Met- and Leu-enkephalins,[16] the endorphins,[17] dynorphins[18] and endomorphins.[19] The enkephalins are pentapeptides, while the others are larger peptides. The largest is β-endorphin with 31

amino acid residues.[17] One common feature of the enkephalins, endorphins and dynorphins, is the sequence of the first four amino acids in each of the peptides. That conserved sequence was found to be Tyr-Gly-Gly-Phe. An opioid active peptide has been isolated from cow's milk,[20] that being a hexapeptide called β-casomorphin. The skin of a South American frog has also proved to be a source of an opioid, the peptide dermorphin.[21] Both β-casomorphin and dermorphin are reported to be selective for the mu receptor with dermorphin found to be 100 times more potent than morphine.[21] β-endorphin was reported as an endogenous ligand for all receptor types.[1] The endomorphins, are the natural ligands for the mu receptor,[19] the dynorphins for the κ receptor[1] and the enkephalins for the δ receptor.[16]

### *7.2.2 μ Receptor Pharmacology*

Experiments with transgenic mice which had a deficiency of mu receptors, identified the mu receptor as the site where morphine (**1**) exerts its effects.[22] Morphine (**1**), an agonist of the μ receptor, was found to be selective for μ over κ and δ by a factor of 20.[1] Other agonists of the μ receptor include sufentanil (**136**) and DAMGO (**137**), which are 100 time more selective for μ.[1] Agonists of the μ receptor show a number of effects including analgesia, euphoria, immune suppression, physical addiction, respiratory depression (volume),[1] emetic effects,[23] and pupil constriction.[2] One of the characteristic symptoms of a heroin overdose is constricted pupils. Studies have shown that morphine reduces the production of phagocytic and lymphoid cells, which are generated during an immune reaction.[24] These studies concluded that patients treated with morphine were more likely to succumb to infectious diseases. The μ receptor is the principal opioid receptor in the regulation of severe pain.[2] Naloxone (**138**) and naltrexone (**139**), antagonists that bind to the mu receptor, are effective during the recuperation of heroin (**133**) overdose patients.[2]

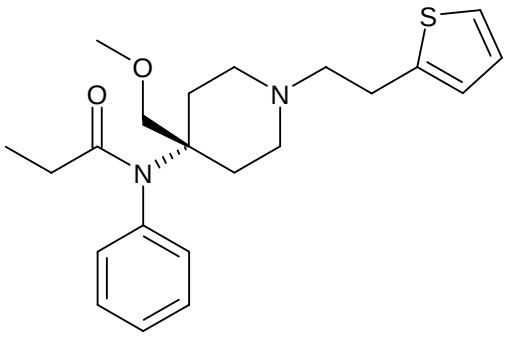


**136**

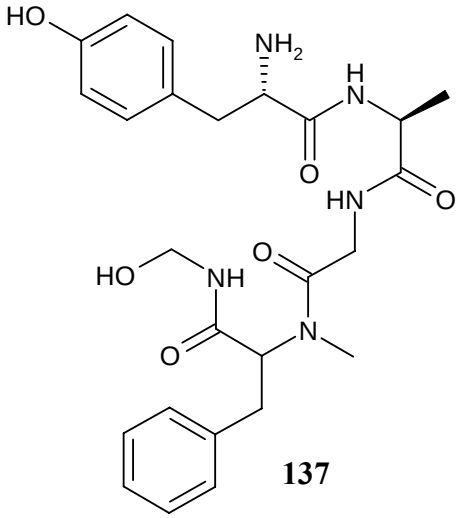


**137**

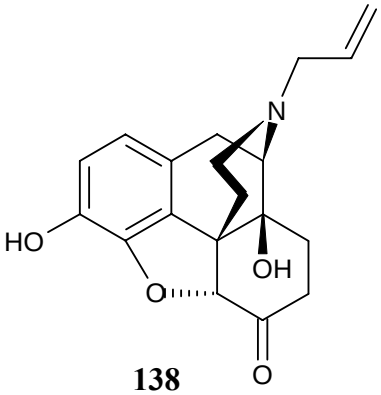


**138**

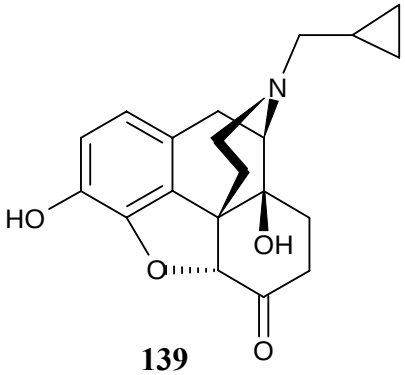


**139**

### *7.2.3 κ Receptor Pharmacology*

Selective agonists of the κ receptor include (±)-U 50488 (**140**)[25] and (±)-PD117302 (**141**).[26] The effects of a κ opioid receptor agonist include analgesia, sedation, diuresis and dysphoria.[2] The distinct advantage of a κ agonist over a μ agonist is analgesia without addictive properties. However, the clinical trials of several selective κ agonists were abandoned due to side effects of sedation and dysphoria.[1] There is one report of a κ receptor antagonist, (±)-nor-binaltorphimine (**142**),[27] however no medical benefits of a κ antagonist have been reported.[1]

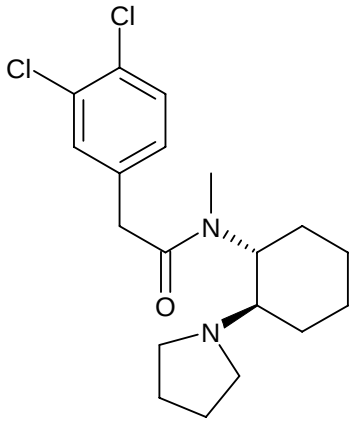


**140**

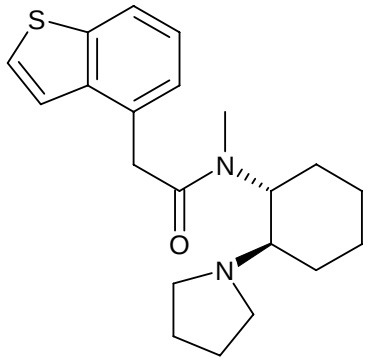


**141**

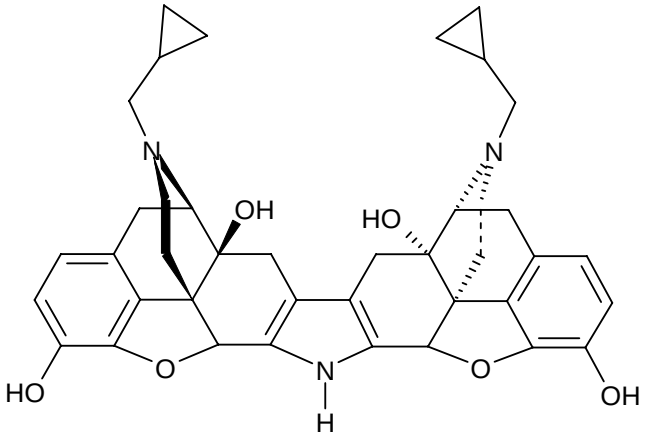


**142**

### *7.2.4 δ Receptor Pharmacology*

The enkephalin derivatives, DADLE (**143**)[28] {[D-Ser$^2$, Leu$^5$]enkephalin-Thr}, and DPDPE (**144**)[29] {[D-Pen$^2$, D-Pen$^5$]enkephalin} are δ receptor selective synthetic peptide agonists used in *in vivo* studies. Nonpeptide agonists include nor-OMI (**145**)[30] and SNC-80 (**146**).[31] Effects of a δ specific agonist include analgesia, immune stimulation and respiratory depression (rate).[1]

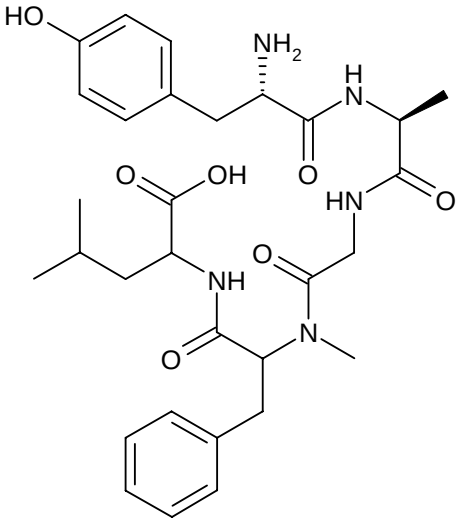

**143**

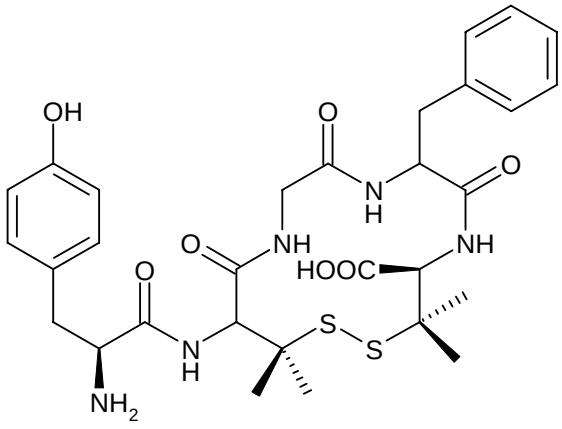

**144**

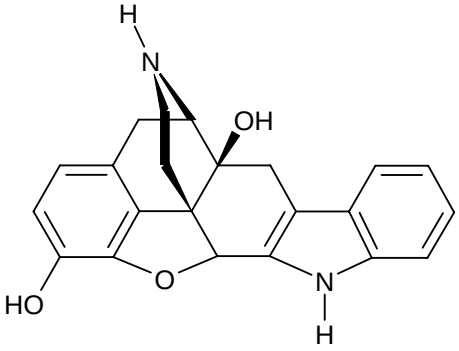

**145**

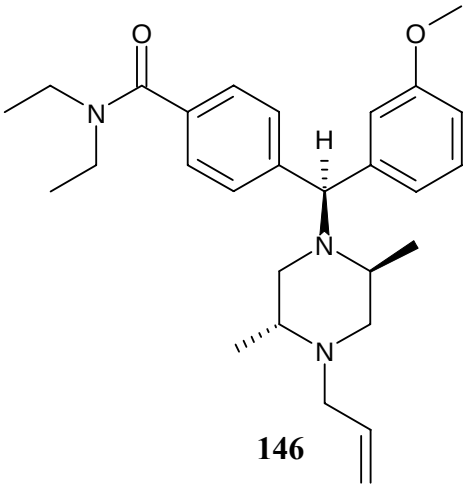

**146**

Interestingly, in comparison with agonists that bind to the μ receptor, agonists that bind to the δ receptor have the opposite effect in terms of immune response, and cause a slowing of breathing rather than a shortness of breath. Coupling of this observation with the unwanted side effects witnessed in the clinical trials of κ opioid agonists, the design of drugs acting as δ opioid agonists appears to be an attractive option. Antagonists at the δ receptor may also be of therapeutic value as immunosuppressants and in the treatment

of cocaine abuse.[1] Compounds which are δ selective antagonists include naltindole (**147**)[32] and naltriben (**148**).[33]

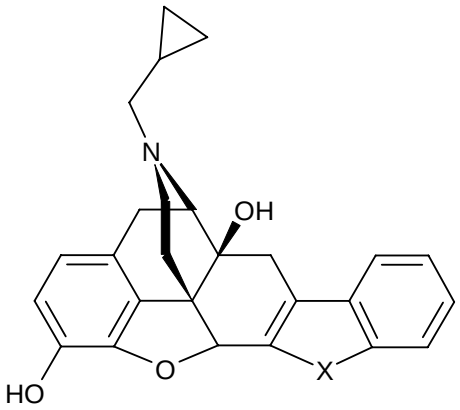


X = NH **147**
X= O **148**

## 7.3 An Overview of Clinically Available Opioid Agents

The group of μ agonists represents the largest number of clinically available opioid analgesic agents.[1] Many of these drugs are derivates of morphine. Morphine is typically used for the treatment of severe, acute and chronic pain. Drugs such as codeine are used to treat mild pain. Methadone (**149**) is another μ agonist with the same potency as morphine. It is particularly useful as a result of its greater oral potency and longer duration of action compared to other μ agonists. Doses of 20 mg are commonly used in the treatment of cancer related pain and 40 mg doses are supplied to subdue the withdrawal symptoms experienced by heroin addicts.[1] Sufentanil (**136**) is more potent than morphine (**1**) and was used as an anaesthetic due to its sedative effects and reduced respiratory depression.[1] Pethidine (**150**) has found a particular use in childbirth as it also exhibits less respiratory depression. Interestingly, only the (-)-enantiomers of $\mu$-agonists are responsible for analgesic activity against the receptor. There are particular examples where different enantiomers result in different pharmacological responses.[34] Dextromethorphan (**151**) displays antitussive (cough suppression) properties whereas

levomethorphan (**152**) produces narcotic effects. The μ antagonist naloxone (**138**) is used as a remedy for morphine and heroin overdoses, as it rapidly overturns respiratory depression.[2]

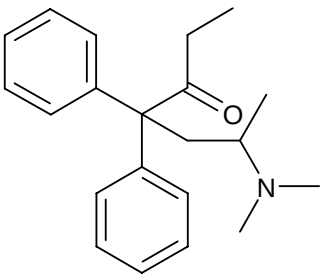


**149**

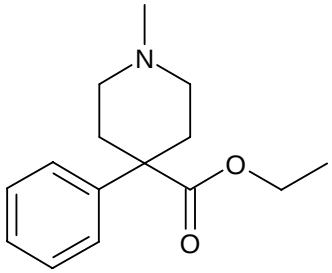


**150**

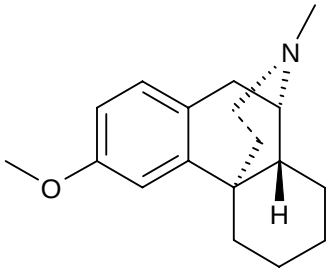


**151**

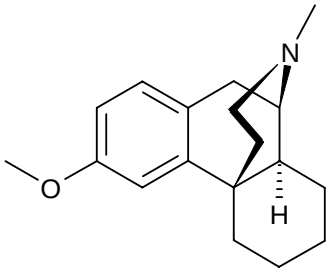


**152**

Clinically available κ agonists include (-)-butorphanol (**153**), nalbuphine (**154**), and (-)-pentazocine (**155**). All three of these drugs are also weak antagonists at the μ receptor.[1] However, these pharmaceutical agents are somewhat overshadowed by the therapeutic potential of μ agonists. The ability of these κ agonists to alleviate pain is greatly reduced compared to μ agonists, in particular for the management of severe pain. Nalbuphine (**154**) and pentazocine (**155**) are examples that are less potent than morphine.[1] Also, there are side effects associated with these drugs. These include sedative, hallucinogenic (dysphoric) effects and in particular, butorphanol (**153**) and pentazocine (**155**) increase blood pressure and heart rate.[1] This form of treatment would be unsuitable for patients with heart complications.

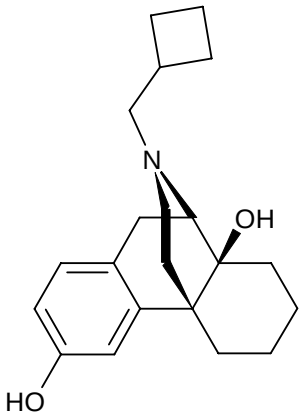


**153**

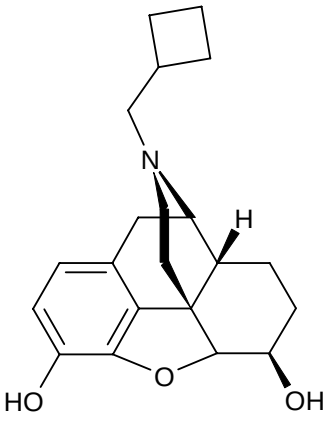


**154**

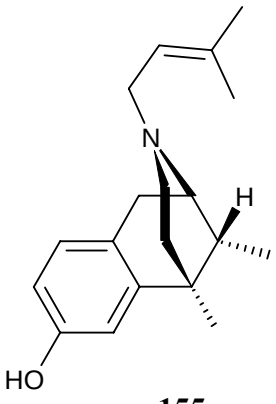


**155**

Clinically available opioid agents have not only found a use in the treatment of pain but also in the treatment of diarrhea. Agonists at the μ receptor are known to cause constipation as a side effect. However, most μ agonists would not be appropriate for use as an antidiarrheal, due to their potential for abuse and addiction.[1] Agonists at the receptor have been developed that limit the bioavailablity, dosage and penetration of blood brain barrier, thereby greatly reducing addictive properties. Examples include diphenoxylate (**156**) and loperamide (**157**), which is marketed as Imodium.[1] Agonists have also found medicinal value as cough suppressants or antitussive agents. This is due to respiratory depression effects. Codeine is the main prescribed antitussive μ agonist, and is prescribed in reduced doses to prevent analgesia.[2]

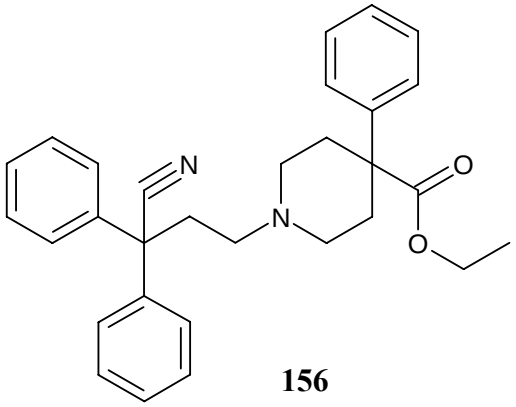


**156**

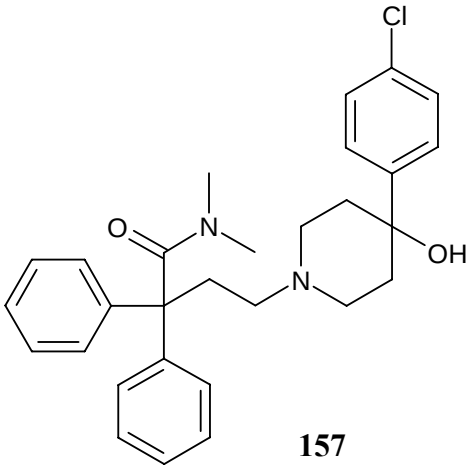


**157**

Currently there are no δ specific agonists available for the treatment of pain. However, SNC 80 (**146**) was in clinical trials as of 2002 with few side effects.[1]

## 7.4 Advantages of Drug Discovery Targeted at the δ Opioid Receptor

The development of pharmaceutical agents that are specific for the δ opioid receptor would have advantages over μ and κ specific agents. Compounds that are agonists at the κ receptor all exhibit unwanted side effects at varying levels. Compounds that are μ agonists have the sinister potential to be abused as illicit drugs. However, μ agonists are particularly useful for treatment of severe pain.

Fifty years of medicinal chemistry research into μ agonists, in particular the SAR of morphine (**1**), has resulted in extensive studies of the pharmacology of the μ receptor.[35] SAR of agonists which bind to the δ receptor are yet to be comprehensively studied. Therefore, a great potential exists for the investigation of δ opioid specific agents, as no clinical agents are currently available. There exists the potential to relieve pain without the issue of physical dependence and other complications associated with μ agonists.

## 7.5 Opioid Bioassays

Bioassays are essential for the development of new drugs. The biological activity of a new compound must be determined and compared to that of known compound.[2] In general, there are two types of bioassays, binding studies and functional assays. Only the potency or binding affinity of a compound can be calculated from a binding assay. The observation of the biological response that a compound produces can be gained from functional assays. Opioid receptor bioassays include radioligand binding assays on brain tissues. Functional assays comprise experiments on electrical stimulation of smooth muscle preparations.[1]

### *7.5.1 Opioid Receptor Competitive Binding Assays*

The three opioid receptor types are found in the brain tissues of rodents,[1] which has made this the tissue of choice in opioid bioassays. Initial experiments performed by Chang and Cautrecasas[36, 37] showed that rat brain synaptosomes (P2 fraction) proved to be useful in binding affinity experiments. This procedure has been duplicated many times.[29, 36-42] The synaptosomes used in these experiments required preincubation to remove endogenous ligands. The most commonly used radioligands in these studies were tritiated δ opioid active peptides. These included [$^3$H]DPDPE, [$^3$H]enkephalin, and [$^3$H]DADLE. [$^3$H]Naloxone has also been used.

### *7.5.2 Opioid Functional Assays*

The inhibition of smooth muscle contraction by opioid agonists has lead to the development of functional assays, utilizing ileum and vas differentia (VD) tissue. The myenteric plexus longitudinal muscle of guinea pig ileum contains μ and κ receptors.[1] Particular VD preparations were found to contain different populations of opioid receptors. For example, the VD of rats contained high concentrations of the μ receptor, mouse VD contained greater proportions of $\delta$ receptor and the VD of rabbits was high in the κ receptor.[1, 16] The contraction of these smooth muscle preparations was initiated by electrical stimulation and was inhibited by opioids.[1, 16, 29, 38, 40, 43, 44] The biological response of an unknown compound was compared with the response of a known agonist to determine its potency and agonist/antagonist properties.

### *7.5.3 Receptor Pharmacology: Considerations*

With the development of modern science, in particular receptor cloning techniques, binding studies can now be performed on a discrete receptor in a recombinant assay. This is in contrast to the assortment of receptors found in tissue preparations.[14] This can be important in regard to the development of specific medicines with reduced side effects.

Another distinct advantage is the opportunity to conduct binding affinity experiments on cloned human receptors.[14]

Another important consideration is the contrasting value of binding and functional assays. Binding assays are generally the easiest method for biological evaluation of compounds, and are typically applied to the evaluation of unknown compounds. Functional assays are most often utilized to determine whether a compound is an agonist or antagonist and are more detailed.[14] Considering the biological activities of the alkaloids isolated from the family Elaeocarpaceae against the $\delta$ opioid receptor are largely unknown, a competitive binding assay would be the best approach.

## 7.6 Protocol of the δ Opioid Bioassay to Evaluate the Natural Product Library

An opioid receptor competitive binding assay was performed on a natural product library consisting of indolizidine and pyrrolidine alkaloids isolated from *E. habbeniensis, E. fuscoides, E. grandis* and *Peripentadenia* sp. Recombinant human δ opioid receptor expressed in HEK cell membranes was employed in this study, using [$^{125}$I]-deltorphin as the radioactive ligand. HEK cell membranes expressing human μ and/or κ opioid receptors were not available from the supplier, AstraZeneca Montreal. Alkaloids were subsequently not evaluated against μ or κ opioid receptors.

The natural product library was evaluated in triplicate 11-point CRC in 96 well format. [D-pen,$^2$ D-pen$^5$]enkephalin (DPDPE) (**144**) and naloxone (**138**) were used as positive controls, and were screened in duplicate. Assay protocol involved the addition of 40 μL of $H_2O$ (10% DMSO) containing variable concentration of compound, followed by addition of 80 μL of [$^{125}$I]-Deltorphin (56 pM, binding buffer) and finally 80 μL of HEK cell membranes were added. Final concentration of DMSO in the well (screening concentration) was 2%. Radioactivity of each well was counted per minute to ascertain the displacement of the radioligand. The raw counts per minute data were tabulated and

manipulated using Prism 4 to create concentration response curves to obtain the $IC_{50}$ values relative to each compound.

## 7.7 δ Opioid Receptor Bioassay Results of Elaeocarpaceae Alkaloids

**Table 22.** Results of screening the natural product library against the δ opioid receptor.

| **Species** | **Compound** | **Exp. 1** ($IC_{50}$) | **Exp. 2** ($IC_{50}$) | **Average** ($IC_{50}$) |
|---|---|---|---|---|
| Control | DPDPE (**144**) | 0.80 nM | 1.44 nM | 1.12 nM |
| | Naloxone (**138**) | 122 nM | 154 nM | 138 nM |
| *E. fuscoides* | Elaeocarpenine (**122**) | 3.59 $\mu$M | 1.88 $\mu$M | 2.74 $\mu$M |
| | Isoelaeocarpicine (**62**) | 34.9 $\mu$M | 35.2 $\mu$M | 35.1 $\mu$M |
| | Isoelaeocarpine (**61**) | 13.5 $\mu$M | 13.7 $\mu$M | 13.6 $\mu$M |
| | Elaeocarpine (**60**) | 88.4 $\mu$M | 84.4 $\mu$M | 86.4 $\mu$M |
| *P. mearsii* | Peripentadenine (**81**) | 7.82 $\mu$M | 14.9 $\mu$M | 11.4 $\mu$M |
| | Peripentonine (**123**) | 70.3 $\mu$M | 68.0 $\mu$M | 69.2 $\mu$M |
| | Mearsamine 1 (**124**) | 21.5 $\mu$M | 40.3 $\mu$M | 30.9 $\mu$M |
| | Mearsamine 2 (**125**) | - | - | - |
| *E. grandis* | Isoelaeocarpiline (**63**) | 13.0 $\mu$M | 6.72 $\mu$M | 9.86 $\mu$M |
| | Grandisine C (**127**) | 15.6 $\mu$M | 13.5 $\mu$M | 14.6 $\mu$M |
| | Grandisine D (**126**) | 1.63 $\mu$M | 1.66 $\mu$M | 1.65 $\mu$M |
| | Grandisine F (**129**) | 1.23 $\mu$M | 1.87 $\mu$M | 1.55 $\mu$M |
| | Grandisine G (**130**) | 85.3 $\mu$M | 65.6 $\mu$M | 75.4 $\mu$M |
| *E. habbeniensis* | Habbenine (**114**) | 25.5 $\mu$M | 38.7 $\mu$M | 32.1 $\mu$M |

The results of the bioassay are summarized in Table 22. The assay was performed twice to gain reproducible and consistent results. Good consistency was observed between the

$IC_{50}$ values in both experiments. Table 20 lists the compounds tested, the species from which the compounds were isolated from, the $IC_{50}$ value from each experiment and the average $IC_{50}$ from both experiments.

A total of 14 alkaloids were assayed and revealed some interesting results. All compounds except mearsamine 2 exhibited an $IC_{50}$ less than 100 $\mu$M and exactly half of the total number of alkaloids exhibited $IC_{50}$ values less than 20 $\mu$M.

The results were determined from a CRC where $n_H = 1$. The plant *E. grandis* produced the most active series of indolizidine alkaloids. Interestingly, the most active compound in the bioassay was grandisine F, closely followed by grandisine D. The most active alkaloids with an $IC_{50}$ below 20 $\mu$M are listed in Table 23.

**Table 23.** The most active Elaeocarpaceae alkaloids with an $IC_{50}$ below 20 $\mu$M.

| **Compound** | **$IC_{50}$ ($\mu$M)** |
|---|---|
| Grandisine F | 1.55 |
| Grandisine D | 1.65 |
| Elaeocarpenine | 2.74 |
| Isoelaeocarpiline | 9.86 |
| Peripentadenine | 11.4 |
| Isoelaeocarpine | 13.6 |
| Grandisine C | 14.6 |

## 7.8 SAR, Molecular Modeling and Pharmacophoric Pattern of Known δ Opioid Analgesics

The screening of a library of compounds with unknown biological activity against a particular target is valuable for the development of structure-activity relationships. The

screening of the Elaeocarpaceae alkaloids has provided some important structure-activity considerations. A pharmacophoric model can be developed from these results with the aid of molecular modeling studies. Comparison with known models can provide valuable insight for potential synthetic modifications to enhance the potency and/or selectivity of a target compound.

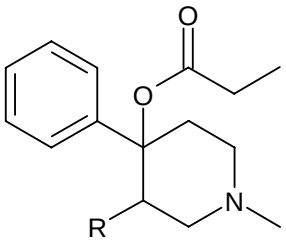


**158**

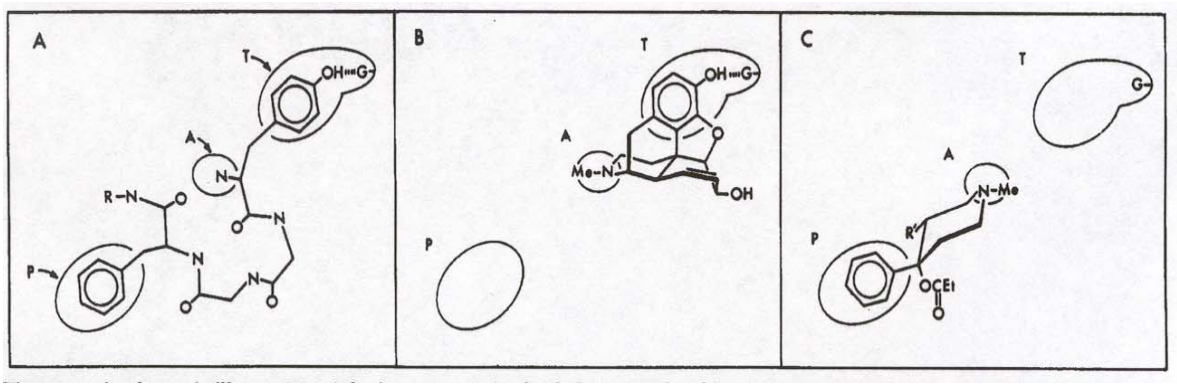


**Figure 102.** "An illustration of the interaction of enkephalins or endorphins (A), morphine (B), and allylprodine (C) with the opioid receptor subsites (T and P) which recognize the aromatic residues of 1-Tyr and 4-Phe of the opioid peptides. The anionic site A was ion paired with the protonated nitrogen of the opioids in all three cases. Group G located on the subsite T represents a hydrogen-bonding acceptor dipole."[43]

From early studies conducted by Portoghese[43, 45] a proposed receptor model was constructed for the opioid receptors based on SAR studies on endorphins, enkephalins, morphine (**1**) and allylprodine (α-1) analogues (**158**). The model highlights three important binding sites within the opioid receptors (Figure 102).[43] These include an anionic site, which binds to the charged nitrogen atom of an opioid active molecule, and

two subsites (T and P) which interact with the aromatic tyrosine and phenylalanine residues, respectively, of enkephalin and endormorphin. Morphine (**1**) was proposed to interact with the T and A subsites and allylprodine (α-1) analogues (**158**) with the P and A subsites. There was also evidence of a H-bond acceptor in the T subsite, (labeled G) which interacted with the phenolic proton of morphine. Evidence for the H-acceptor was derived from the weaker binding affinities of morphine analogues where the phenolic functional group was absent or in a different position. Further evidence suggested that the P subsite was more hydrophobic than T.

Computational studies probing the structure of the opioid receptors and active sites were conducted during the mid 1990's.[6, 46-49] A model of the most structurally stable form of the δ opioid receptor was constructed.[6] By computational studies of the modeled receptor with peptide and nonpeptide δ agonists and antagonists, a three dimensional pharmacophore was identified for the δ receptor.[6] This pharmacophore is represented in Figure 103. The pharmacophore consists of a protonated amine binding site (**A**), aromatic ring (**B**) and hydrophobic interaction sites (**C**).[6]

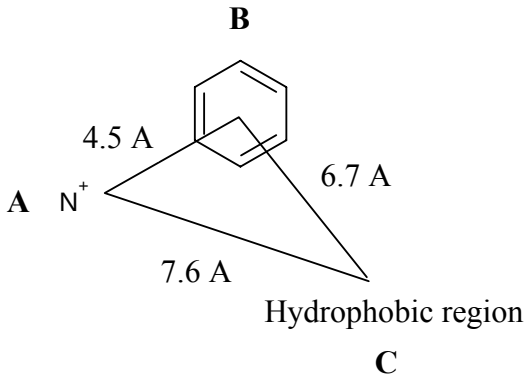


**Figure 103.** "Common pharmacophore for recognition of the δ opioid receptor by peptides and nonpeptides. The pharmacophore components consist of a protonated amine (**A**), an aromatic ring (**B**), and a hydrophobic region (**C**)."[6]

The model proposed by Portoghese bears good overlap when compared to the computational study. Both models are consistent in that three binding areas are important for biological activity. One feature that the computational study does not acknowledge is

the presence of the hydrogen-bond acceptor (G) in the T subsite of the Portoghese model. The T subsite is presumably analogous with the aromatic ring binding domain (B) in the computational study.

## 7.9 SAR, Molecular Modeling and Pharmacophore Identification of the Eleocarpaceae Alkaloids

In this study, SAR data from the screening of the natural product library against the human δ opioid receptor was compared with the pharmacophoric pattern of the δ opioid receptor. The compounds were analyzed discretely depending on structure class, indolizidine or pyrrolidine, and binding affinity. The aim of the study was to gain a better understanding of biological activities observed.

### *7.9.1 Molecular modeling studies of the* E. fuscoides *series of indolizidine alkaloids*

The first series of alkaloids to be assessed was the aromatic indolizidine alkaloids isolated from the New Guinean species *E. fuscoides*. This series provided some interesting results, producing one of the most active alkaloids from the natural product library, elaeocarpenine (**122**), as well as the least active, elaeocarpine (**60**). The variation in biological activity of this series can be explained by the overlay of the energy minimized structures (Figure 104). The modeled structures of the four *E. fuscoides* compounds isoelaeocarpicine (**62**), elaeocarpenine (**122**), isoelaeocarpine (**61**) and elaeocarpine (**60**), shared a common feature in a planar aromatic group. This unifying feature was used as a platform to "tether" the molecules together to observe the differences in orientation of the indolizidine moiety in relation to the aromatic group.

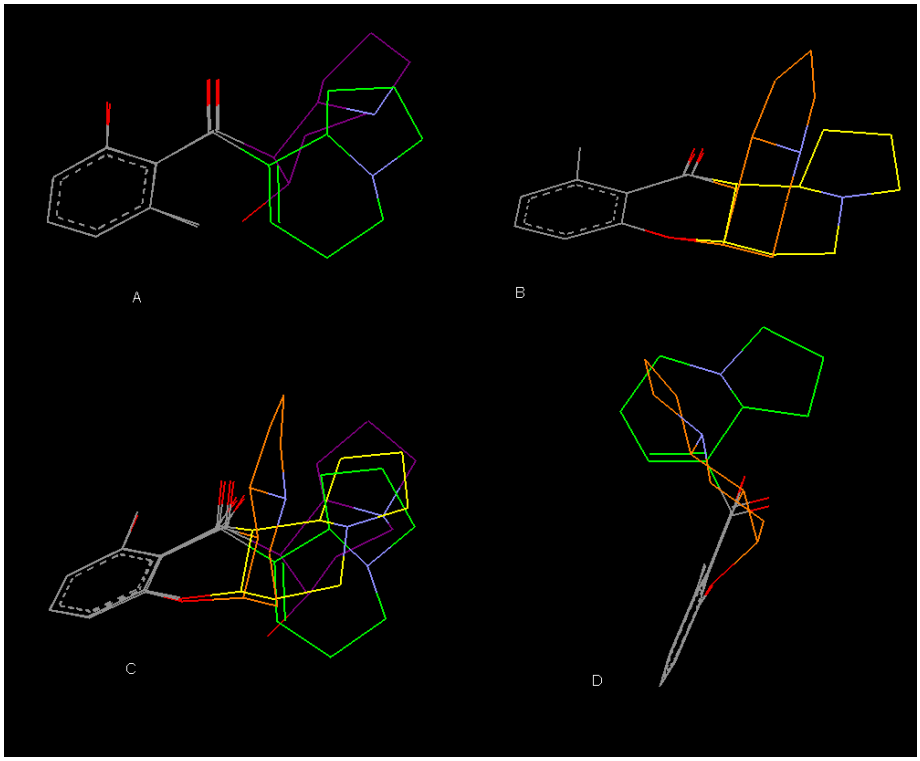


**Figure 104.** Molecular overlays of elaeocarpenine (**122**) and isoelaeocarpicine (**62**) in A; isoelaeocarpine (**61**) and elaeocarpine (**60**) in B; elaeocarpenine, isoelaeocarpicine, isoelaeocarpine and elaeocarpine in C; and an overlay of elaeocarpenine and isoelaeocarpine in D.

A comparison of elaeocarpenine (**122**) and isoelaeocarpicine (**62**), illustrated in overlay A in Figure 104, shows the indolizidine functional group in different conformations in relation to the aromatic ring. This is due to hydrogen bonding from the C-7 hydroxyl to the carbonyl of C-10 in isoelaeocarpicine (**62**). This results in a significant loss of potency. A dramatic loss of activity was witnessed between the diastereomers isoelaeocarpine (**61**) and elaeocarpine (**60**). The molecular overlay of these two compounds, as depicted in B of Figure 104, demonstrates the planar or "flat" elaeocarpine (**60**), which was in contrast to the "bent" energy minimized structure of isoelaeocarpine (**61**). An overlay of all four molecules in this series is shown in C. Overlay D provides a different view of an overlay of **122** and **61**. These compounds, which possess the greatest binding affinities in the *E. fuscoides* series of alkaloids, both

have a similar orientation of the indolizidine functionality in relation to the aromatic ring. The indolizidine moiety is in an orthogonal direction above the plane of the aromatic ring. As a result, this type of spacial arrangement appears important for biological activity against the δ opioid receptor for the *E. fuscoides* alkaloids.

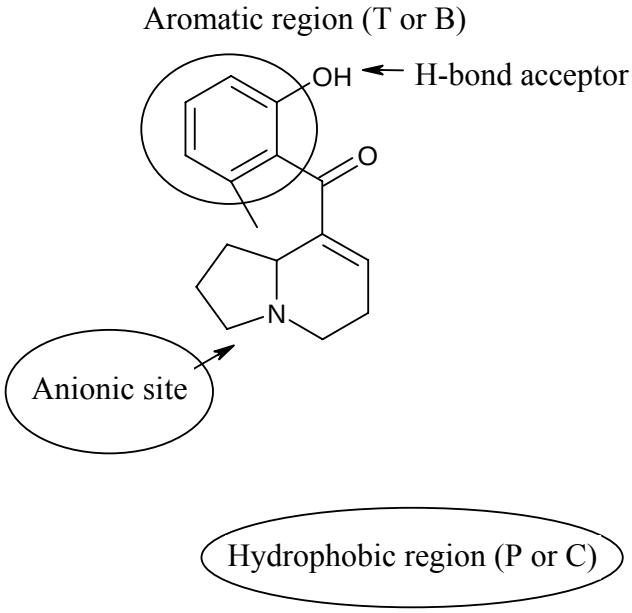


**Figure 105.** Proposed interactions of elaeocarpenine (**122**) with the anionic site and H-bond acceptor of the aromatic region of the pharmacophoric pattern of the $\delta$ opioid receptor.

In an attempt to incorporate the pharmacophore of the δ opioid receptor into this study, a plausible depiction of the interaction of elaeocarpenine (**122**) is shown in Figure 105. The free phenolic group potentially interacts with the hydrogen bond acceptor in the aromatic region (shown as T in the Portoghese model and B in the computational model). Due to the orthogonal direction of the indolizidine group in the energy minimized structure, the nitrogen may be available to interact with the anionic site. This may infer that elaeocarpenine (**122**) interacts with two of the three binding domains in the receptor model. Isoelaeocarpine (**61**) may also interact with two binding domains, one of which would be the anionic site, and the other may be the aromatic region. As isoelaeocarpine

contains no free phenolic group, no interactions with the hydrogen bond acceptor are possible. This could account for the reduced activity of isoelaeocarpine (**61**) when compared with elaeocarpenine (**122**). It is hypothesized that isoelaeocarpicine (**62**) interacts with only the aromatic domain, including the H-bond acceptor. The nitrogen of **62** may not bind to the anionic site, as its energy minimized conformation is different to that of elaeocarpenine (**122**).

### *7.9.2 Molecular modeling studies of the* E. grandis *series of indolizidine alkaloids*

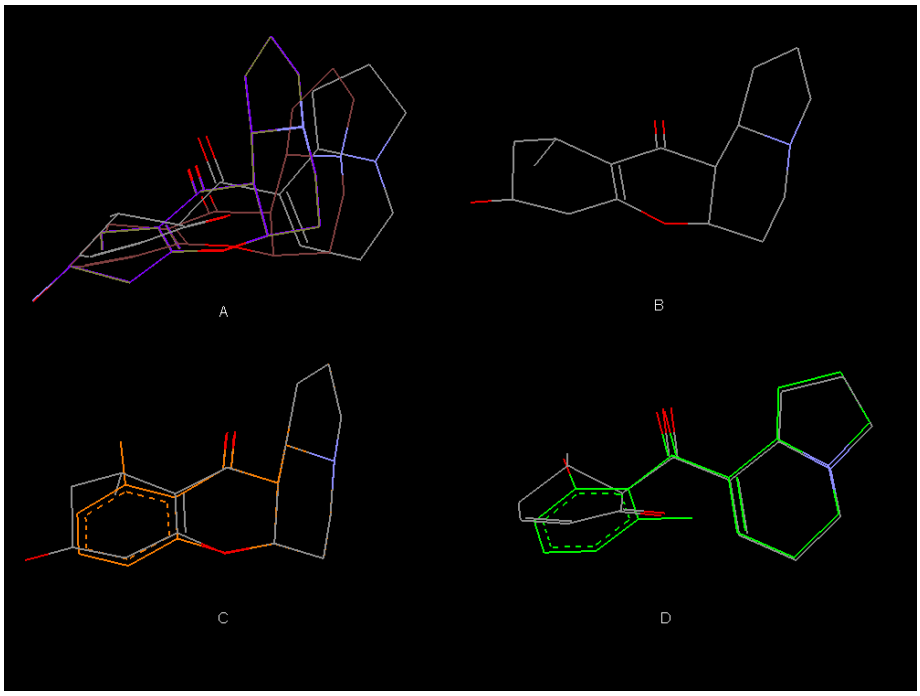


**Figure 106.** Molecular overlays of grandisine C, (**127**) D (**126**) and F (**129**), and isoelaeocarpiline (**63**) in A; grandisine C and F in B; grandisine C and F and isoelaeocarpine (**61**) in C; and grandisine D and elaeocarpenine (**122**) shown in D.

The series of non-aromatic indolizidine alkaloids isolated from the Queensland plant *E. grandis* showed the most promising biological activities of the Elaeocarpaceae alkaloids

against the δ opioid receptor. The $IC_{50}$ determined for isoelaeocarpiline (**63**), 9.86 $\mu$M, compares very well with the published value of 11.0 $\mu$M.[50] Grandisine F (**129**) exhibited the greatest binding affinity of the entire natural product library. The energy minimized structures of grandisine C (**127**), D (**126**), F (**129**) and isoelaeocarpiline (**63**) were analyzed in a molecular overlay (Figure 106).

An overlay of all four structures, illustrated in A of Figure 106, shows the minimized structures in reasonable comparison to each other. This can account for the similar binding affinities of these alkaloids. Overlay B shows the identical alignment of the minimized structures of grandisine C (**127**) and F (**129**). However, grandisine F (**129**) demonstrates significantly more activity with its C-14 amino group in contrast to the hydroxyl group in the same position for grandisine C (**127**). Grandisine C and F also possess similar minimized conformations to isoelaeocarpiline (**63**), as depicted in C. The molecular overlay of elaeocarpenine (**122**) and grandisine D (**126**), represented as D in Figure 106, demonstrated that both minimized structures are almost identical in the orientation of the indolizidine moiety to the six-membered ring. Therefore it is proposed that grandisine D (**126**) has the same mode of interaction as elaeocarpenine (**122**). The reduction in binding affinity of the tetracyclic indolizidines isoelaeocarpine (**61**) and isoelaeocarpiline (**63**) indicated that a C-12 ketone in **126** or C-12 phenol in **122** is important for activity. The diketo system found in grandisine D (**126**) may tautomerise to its enol form at C-12 to result in a conjugated system and a free alcohol. The alcohol is then proposed to interact with the H-bond acceptor.

Grandisine F (**129**) may have a different mode of interaction. The amino group is hypothesized to preferentially bind to the anionic site instead of the indolizidine nitrogen. This is proposed to mimic the actions of the amino group in endogenous opioid peptides such as enkephalin and other peptides like DPDPE (**144**). This amino group binds to the anionic site. The lower binding affinity of this compound suggested that a primary amine interacts more strongly with the anionic site than a more hindered tertiary amine.

### *7.9.3 Molecular modeling studies of the* E. habbeniensis *and* P. mearsii *series of pyrrolidine alkaloids*

The series of pyrrolidine alkaloids isolated from *P. mearsii* and *E. habbeniensis* consisted of peripentadenine (**81**), peripentonine (**123**), mearsamine 1 (**124**) and habbenine (**114**). The alkaloid mearsamine 2 (**125**), which was not active in the binding study, possesses the same bicyclic dipyrano system found in grandisine A (**73**), an indolizidine alkaloid with an $IC_{50}$ of 2.7 $\mu$M.[50] This demonstrates a large difference in the δ opioid binding affinities of these two compounds. This indicated that the indolizidine moiety of grandisine A (**73**) contributes significantly to binding affinity.

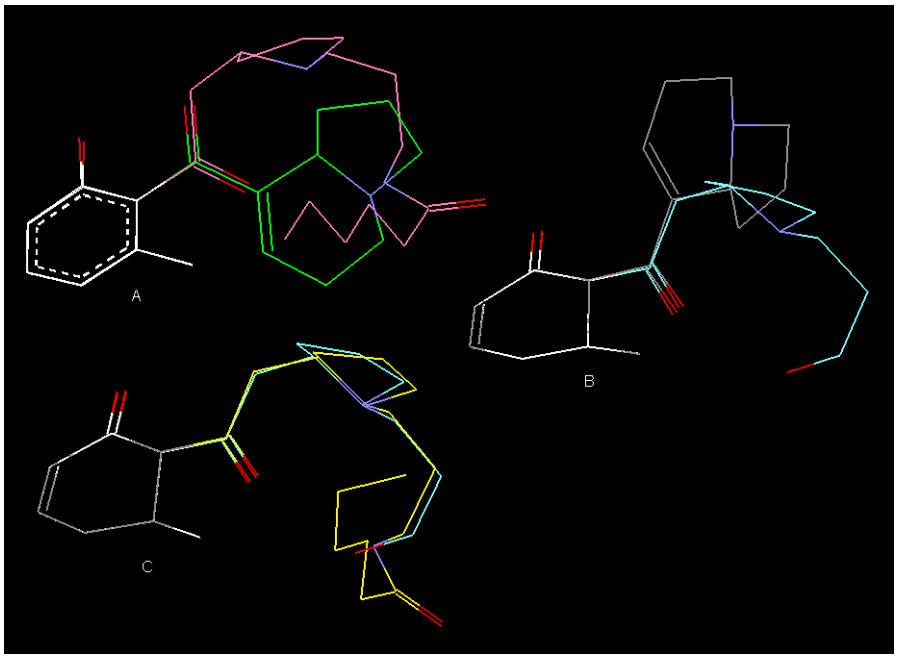


**Figure 107.** Molecular overlays of elaeocarpenine (**122**) and peripentadenine (**81**) in A; grandisine D (**126**) and habbenine (**114**) in B; and habbenine and peripentonine (**123**) in C.

The series of pyrrolidine alkaloids showed the least biological appeal when compared to the *E. fuscoides* and *E. grandis* alkaloids. Peripentadenine (**81**) was the most potent of the pyrrolidine alkaloids, with an $IC_{50}$ of 11.4 $\mu$M. The phenolic group in **81** was also

encountered in elaeocarpenine (**122**), however **81** demonstrates a four fold decrease in activity in comparison to **122**. This supports the hypothesis that an indolizidine functionality rather than pyrrolidine is important for δ opioid activity. The presence of the long propylhexanamide chain in peripentadenine (**81**) may inhibit the binding of the nitrogen to the anionic site. An overlay of peripentadenine and elaeocarpenine is shown as A in Figure 107.

Further evidence for the increased δ opioid activity of an indolizidine in preference to a pyrrolidine can be seen with the comparison of the $IC_{50}$ values of 1.65 and 32.1 $\mu$M for grandisine D (**126**) and habbenine (**114**), respectively. Both molecules, seen as overlay B in Figure 107, possess methylcyclohexenone moieties, however the indolizidine alkaloid grandisine D is approximately 20 times more potent than the pyrrolidine alkaloid habbenine (**114**). The same trend was observed with peripentonine (**123**), also possessing pyrrolidine and methylcyclohexenone moieties. Peripentonine demonstrated an $IC_{50}$ of 69.2 $\mu$M, which is 42 times less potent than grandisine D. A comparison of habbenine (**114**) and peripentonine (**123**), illustrated in C of Figure 107, suggested the presence of the propylhexanamide chain in **123** significantly reduces activity. The activity of mearsamine 1 (**124**) ($IC_{50}$ = 30.9 $\mu$M) when compared to **123** ($IC_{50}$ = 69.2 $\mu$M), suggests the carboxylic acid functional group contributes some biological value. This may be explained by an H-bond interaction of the acidic proton of the carboxylic acid with the hydrogen bond acceptor located within the aromatic binding region.

## 7.10 Conclusion

The biological evaluation of the natural product library of indolizidine and pyrrolidine alkaloids against the human δ opioid receptor has highlighted the pharmacological potential of these compounds and provided some interesting structure-activity considerations. The most outstanding structural features contributing to bioactivity were a ketone or alcohol at C-12 of grandisine D (**126**) and elaeocarpenine (**122**), respectively. Tetracyclic alkaloids which possessed an ether linkage between C-12 and C-7, such as

isoelaeocarpine (**61**) and isoelaeocarpiline (**63**), demonstrated weaker bind affinities. The difference in binding affinity between indolizidine and pyrrolidine alkaloids was also discussed. Direct comparison of **122** with peripentadenine (**81**), and **126** with habbenine (**114**) and peripentonine (**123**) indicated that an indolizidine alkaloid exhibited lower binding affinities than a pyrrolidine alkaloid. A comparison of **114** with **123** indicates that the propylhexanamide group of **123** significantly reduces interactions with the δ opioid receptor. The tetracyclic indolizidine alkaloid grandisine F (**129**) was proposed to have a different binding mode to the other alkaloids. The C-14 amino group of **129** was speculated to mimic the amino group of opioid active peptides.

Compounds such as elaeocarpenine (**122**) were proposed to interact with two of three binding sub-domains of the δ opioid receptor pharmacophore. Synthetic embellishments of such compounds to introduce further aromaticity, which may improve the binding affinities to the receptor, would be an interesting study.

## 7.11 References


1. Fries, D. S., *Opioid Analgesics*. In *Foye's Principles of Medicinal Chemistry*, 5th ed.; Williams, D. A., Lemke, T. L., Eds. Lippincott Williams and Wilkins: Philadelphia, **2002**; pp. 453 - 475.
2. Rang, H. P., Dale, M. M., Ritter, J. M., *Analgesic Drugs*. In *Pharmacology*, 4th ed.; Eds. Churchill Livingstone: **1999**; pp. 589 - 603.
3. Schnitzer, T. J., *Am J Med* **1998,** 105, 45S - 52S.
4. Borne, R. F., *Nonsteroidal Anti-Inflammatory Agents*. In *Foye's Principles of Medicinal Chemistry*, 5th ed.; Williams, D. A., Lemke, T. L., Eds. Lippincott Williams and Wilkins: Philadelphia, **2002**; pp. 751 - 793.
5. Williams, M., Kowaluk, E. A., Arneric, S. P., *J Med Chem* **1999,** 42, 1481 - 1500.
6. Loew, G. H., *Modern Drug Discovery* **1999,** 2, 24 - 26.

**7.** Booth, M., *Opium, a history*. ed.; Simon & Schuster Ltd: London, **1996**.

**8.** Foye, W. O., *Origins of Medicinal Chemistry*. In *Foye's Principles of Medicinal Chemistry*, 5th ed.; Williams, D. A., Lemke, T. L., Eds. Lippincott Williams and Wilkins: Philadelphia, **2002**; pp. 1 - 10.

**9.** Dhawan, B. N., Cesselin, F., Raghubir, R., Reisine, T., Bradley, P. B., Portoghese, P. S., Hamon, M., *Pharmacol Rev* **1996,** 48, 567 - 592.

**10.** Satoh, M., Minami, M., *Pharmacol Ther* **1995,** 68, 343 - 364.

**11.** Terenius, L., *Acta Pharmacol Toxicol* **1973,** 32, 317 - 320.

**12.** Pert, C. B., Snyder, S. H., *Science* **1973,** 70, 2243 - 2247.

**13.** Simon, E. J., Hiller, J. M., Edelman I., *PNAS* **1973,** 70, 1947 - 1949.

**14.** Brauner-Osborne, H., *Receptors: Structure, function and pharmacology*. In *Textbook of Drug Design and Discovery*, 3rd ed.; Krogsgaard-Larsen, P., Liljefors, T., Madsen, U., Eds. Taylor and Francis: **2002**; pp. 156 - 172.

**15.** Triggle, D. J., *Drug Receptors: A Perspective*. In *Foye's Principles of Medicinal Chemistry*, 5th ed.; Williams, D. A., Lemke, T., L., Eds. Lippincott Williams and Wilkins: Philadelphia, **2002**; pp. 248.

**16.** Hughes, J., Smith, T. W., Kosterlitz, H. W., *Nature (Lond)* **1975,** 258, 577 - 579.

**17.** Li, C. H., Lemaire, S., Yamashiro, D., Doneen, B. A., *Biochem Biophys Res Comm* **1976,** 71, 19 - 25.

**18.** Goldstein, A., Tachibana, S., Lowney, L. I., Hunkapiller, M., Hood, L., *PNAS* **1979,** 76, 6666 - 6670.

**19.** Zadina, J. E., Hackler, L., Ge, L-J., Kastin, A. J., *Nature* **1997,** 386, 499 - 502.

**20.** Brantl, V., Teshemacher, H., *Naunyn Schmiedebergs Arch Pharmacol* **1979,** 306, 301 - 304.

**21.** Montecucchi, P. C., de Castiglioni, R., Piani, S., Gozzini, L., Erspamer, V., *Int J Pept Protein Res* **1981,** 17, 275 - 283.

**22.** Childers, S. R., *Curr Biol* **1997,** 7, R695 - R697.

**23.** Kieffer, B. L., *Trends Pharmacol Sci* **1999,** 20, 19 - 25.

**24.** Eisenstein, T. K., Hilburger, M. E., *J Neuroimmunol* **1998,** 83, 36 - 44.

**25.** Szmuszkovicz, J., von Voigtlander, P. F., *J Med Chem* **1982,** 25, 1125 - 1126.

**26.** Clark, C. R., Halfpenny, P. R., Hill, R. G., Horwell, D. C., Hughes, J., Jarvis, T. C., Rees, D. C., Schofield, D., *J Med Chem* **1988,** 31, 831 - 836.

**27.** Choi H, M., T. F., DeLander, G. E., Caldwell, V., Aldrich, J. V., *J Med Chem* **1992,** 35, 4638 - 4639.

**28.** James, I. F., Goldstein A., *Mol Pharmacol* **1984,** 25, 337 - 342.

**29.** Mosberg, H. I., Hurst, R., Hruby, V. J., Gee, K., Yamamura, H. I., Galligan, J. J., Burks, T. F., *PNAS* **1983,** 80, 5871 - 5874.

**30.** Portoghese, P. S., Larson, D. L., Sultana, M., Takemori, A. E., *J Med Chem* **1992,** 35, 4325 - 4329.

**31.** Bilsky, E. J., Calderon, S. N., Wang, T., Bernstein, R. N., Davis, P., Hruby, V. J., McNutt, R. W., Rothman, R. B., Rice, K. C., Porreca, F., *J Pharmacol Exp Ther* **1995,** 273, 359 - 366.

**32.** Portoghese, P. S., Sultana, M., Takemori, A. E., *Eur J Pharmacol* **1988,** 146, 185 - 186.

**33.** Takemori, A. E., Sultana, M., Nagase, H., Portoghese, P. S., *Life Sciences* **1992,** 149, 1491 - 1495.

**34.** Kennedy, I. J., Jane, D. E., *Stereochemistry in drug design*. In *Textbook of Drug Design and Discovery*, 3rd ed.; Krogsgaard-Larsen, P., Liljefors, T., Madsen, U., Eds. Taylor and Francis: **2002**; pp. 65.

**35.** May, E. L., *J Med Chem* **1992,** 35, 3586 - 3594.

**36.** Salvadori, S., Bianchi, C., Lazarus, L. H., Scaranari, V., Attila, M., Tomatis, R., *J Med Chem* **1992,** 35, 4651 - 4657.

**37.** Chang, K.-J., Cuatrecasas, P., *J Biol Chem* **1979,** 254, 2610 - 2618.

**38.** Balboni, G., Salvadori, S., Guerrini, R., Negra, L., Giannini, E., Bryant, S. D., Jinsmaa, Y., Lazarus, L. H., *J Med Chem* **2004,** 47, 4066 - 4071.

**39.** Balboni, G., Salvadori, S., Guerrini, R., Negri, L., Giannini, E., Jinsmaa, Y., Bryant, S. D., Lazarus, L. H., *J Med Chem* **2002,** 45, 5556 - 5563.

**40.** Schmidhammer, H., Burkard. W. P., Eggstein-Aeppli, L., Smith, C. F. C., *J Med Chem* **1989,** 32, 418 - 421.

**41.** Jinsmaa, Y., Miyazaki, A., Fujita, Y., Li, T., Fujisawa, Y., Shiotani, K., Tsuda, Y., Yokoi, T., Ambo, A., Sasaki, Y., Bryant, S. D., Lazarus, L. H., Okada, Y., *J Med Chem* **2004,** 47, 2599 - 2610.

**42.** Okada, Y., Tsuda, Y., Fujita, Y., Yokoi, T., Sasaki, Y., Ambo, A., Konishi, R., Nagata, M., Salvadori, S., Jinsmaa, Y., Bryant, S. D., Lazarus, L. H., *J Med Chem* **2003,** 46, 3201 - 3209.

**43.** Portoghese, P. S., Alreja, B. D., Larson, D. L., *J Med Chem* **1981,** 24, 782 - 787.

**44.** Snyder, K. R., Murray, T. F., DeLander, G. E., Aldrich, J. V., *J Med Chem* **1993,** 36, 1100 - 1103.

**45.** Portoghese, P. S., *J Med Chem* **1965,** 8, 609 - 616.

**46.** Strahs, D., Weinstein, H., *Protein Eng* **1997,** 10, 1019 - 1038.

**47.** Alkorta, I., Loew, G. H., *Protein Eng* **1996,** 9, 573 - 583.

**48.** Filizola, M., Carteni-Farina, M., Perez, J. J., *J Comp Aid Mol Des* **1999,** 13, 397 - 407.

**49.** Filizola, M., Villar, H. O., Loew, G. H., *J Comp Aid Mol Des* **2001,** 15, 297 - 307.

**50.** Carroll, A. R., Arumugan, G., Quinn, R. J., Redburn, J., Guymer, G., Grimshaw, P., *J Org Chem* **2005,** 70, 1889 - 1892.

# CHAPTER 8 – Synthetic Studies on Isoelaeocarpine (61) and Peripentadenine (81)

## 8.1 Natural Products as Combinatorial Templates

In the past ten years, there has been increasing interest in the synthesis of small molecule libraries based on natural product templates.[1] Studies have focused on improving the potency of bioactive natural products as a means to increase their therapeutic potential. Natural product based combinatorial libraries have the potential to provide more structural diversity than pure synthetic libraries, which primarily concentrate on small heterocycles.[1] However, molecular complexity of natural products may also hinder synthetic studies. This may result in simple functional groups such as esters, amines, amides, and hydroxyls as the only routes of combinatorial diversification.[1]

Natural products have been incorporated into combinatorial chemistry by two techniques.[2] The first and most common technique is the total synthesis of a natural product based combinatorial library. Examples of this method include the synthesis of libraries of the anticancer compound curacin A (**159**),[3] the synthesis of a pharmacophore library based on the cyclic depsipeptide HUN-7293,[4] the synthesis of analogues based on the spiroketal scaffold found in macrolide antibiotics,[5] combinatorial synthesis of dolastatin E analogues,[6] the synthesis of demethoxyfumitremorgin C (**160**) analogues,[7] the synthesis of sarcodictyin libraries,[8] and the synthesis of analogues of the bradykinin B1 receptor antagonist martinellic acid (**161**).[9]

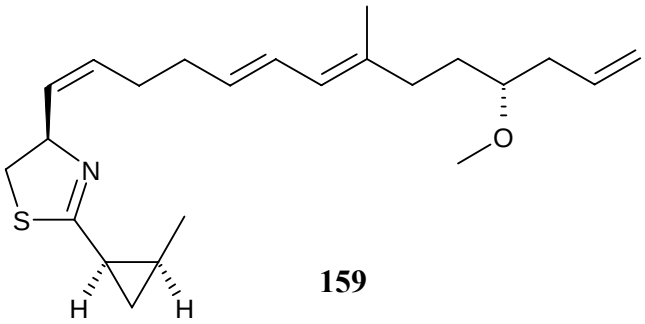

**159**

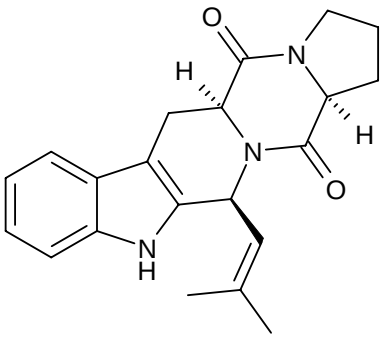

**160**

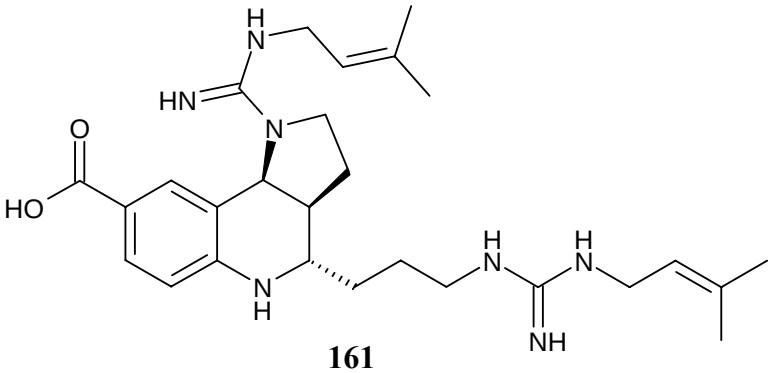

**161**

The second technique for incorporating natural products into combinatorial chemistry libraries involves the use of an isolated natural product as a template for synthetic modification.[2] Examples of this technique are limited, however it has been applied to the synthesis of teicoplanin aglycone (**162**),[10] rauwolscinic acid (**163**),[11] and tambjamine (**164**) analogues.[2]

Combinatorial structural diversification of an isolated natural product is therefore a much understudied technique. Natural products with low molecular weight would be of particular interest as small templates for chemical elaboration.

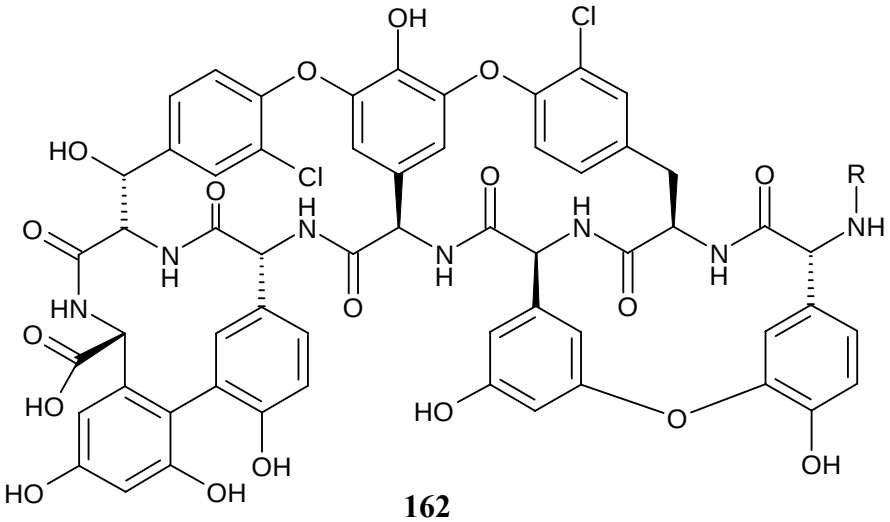

**162**

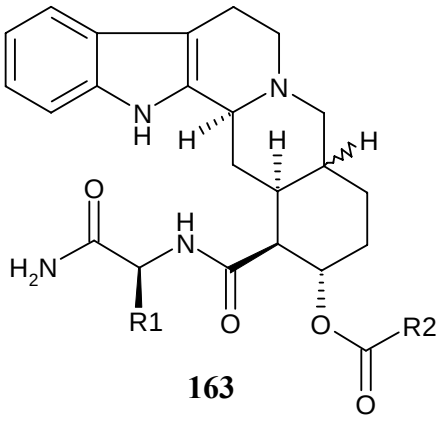

**163**

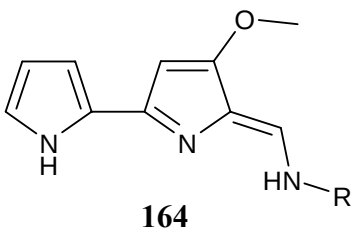

**164**

## 8.2 Elaeocarpenine (122), Isoelaeocarpine (61) and Peripentadenine (81) as Potential Templates for Combinatorial Diversification

Elaeocarpenine (**122**), isoelaeocarpine (**61**) and peripentadenine (**81**) were selected as templates for synthetic studies. All three compounds were potentially available in large amounts and displayed reasonably low binding affinity for the δ opioid receptor relative to other Elaeocarpaceae alkaloids. The goal of this study was to investigate the potential of elaeocarpenine (**122**), isoelaeocarpine (**61**) and peripentadenine (**81**) as templates for combinatorial diversification. The introduction of additional aromatic functionality to **122**, **61** and **81** may increase the binding affinities of these natural products. An

additional aromatic functionality has the potential to provide a third group which could interact with the third binding domain of the δ opioid receptor. Such analogues of **122**, **61** and **81** may produce a mimic of the potent δ opioid agonist SNC 80 (**146**). The proposed chemical elaborations of elaeocarpenine (**122**), isoelaeocarpine (**61**) and peripentadenine (**81**) are illustrated in Figure 108. Elaeocarpenine contains a Michael acceptor which can undergo an addition reaction, and isoelaeocarpine and peripentadenine both contain ketones which could be used to introduce aromatic amines via reductive amination reactions.

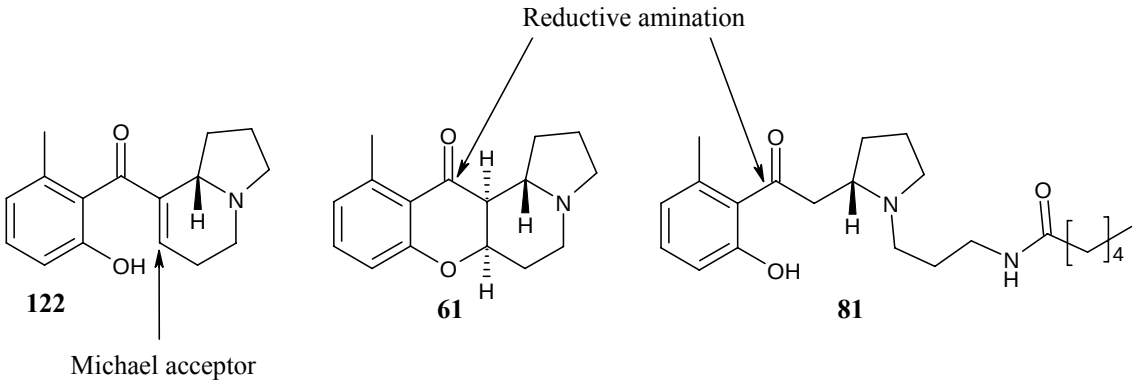


**Figure 108.** The proposed avenues for the chemical elaboration of elaeocarpenine (**122**), isoelaeocarpine (**61**) and peripentadenine (**81**).

The initial efforts of this investigation were focused on the isolation of isoelaeocarpiline (**63**) and peripentonine (**123**). Both of these compounds could be purified in amounts of up to several hundred milligrams and both compounds had been demonstrated to yield isoelaeocarpine (**61**) and peripentadenine (**81**) following reduction with Pd/C of **63** and **123**, respectively. It was postulated that elaeocarpenine (**122**) could be obtained following an ether cleavage reaction of isoelaeocarpine (**61**).

## 8.3 The Re-isolation of Isoelaeocarpiline (63) and Subsequent Reduction of 63 to Isoelaeocarpine (61)

Johns *et al.* demonstrated that isoelaeocarpiline (**63**) could be readily reduced by Pd/C under reflux to isoelaeocarpine (**61**).[12] Isoelaeocarpiline (**63**) (148 mg), purified from the leaves of *E. grandis* by the acid/base procedure (Scheme 10), was dehydrogenated in the presence of Pd/C (77 mg) to yield isoelaeocarpine (**61**) (81.6 mg, 66%) (Scheme 12).

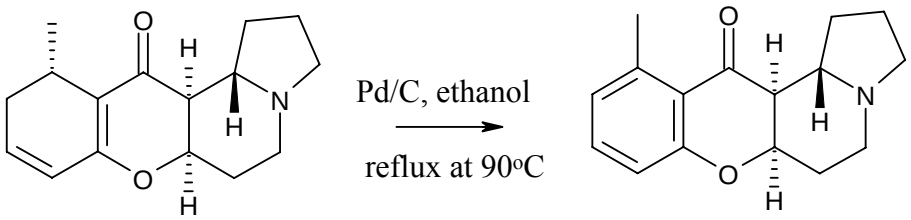


**63** **61**

**Scheme 12.** The dehydrogenation of isoelaeocarpiline (**63**) to isoelaeocarpine (**61**) in the presence of Pd/C.

A further 93.5 mg of **63** was obtained from another extraction of the leaves of *E. grandis* (Scheme 13). Dried and ground leaves of *E. grandis* were extracted with DCM. The DCM extract was evaporated and partitioned between hexane and methanol. The hexane layer was discarded and the methanol was evaporated. The residue was further partitioned between 1% TFA/$H_2O$ and DCM. The aqueous layer was evaporated and separated into 100 fractions by C18 RP-MPLC using a gradient of $H_2O$ to 1% TFA/MeOH over 200 minutes. Fractions 20 to 22 were found to be grandisine C (**127**) and were not purified further. The combined fractions of interest were 29-37 and 40-48 which were shown to be grandisine D (**126**) and isoelaeocarpiline (**63**) by $^1$H NMR, respectively. Grandisine D (83.8 mg, 0.0062%) was purified by semi-preparative C18 RP-HPLC using a gradient of 7:3 to 3:7 $H_2O$:1%TFA/MeOH over 15 minutes.

Isoelaeocarpiline (93.5 mg, 0.0069%) was purified by the same conditions on preparative C18 RP-HPLC.

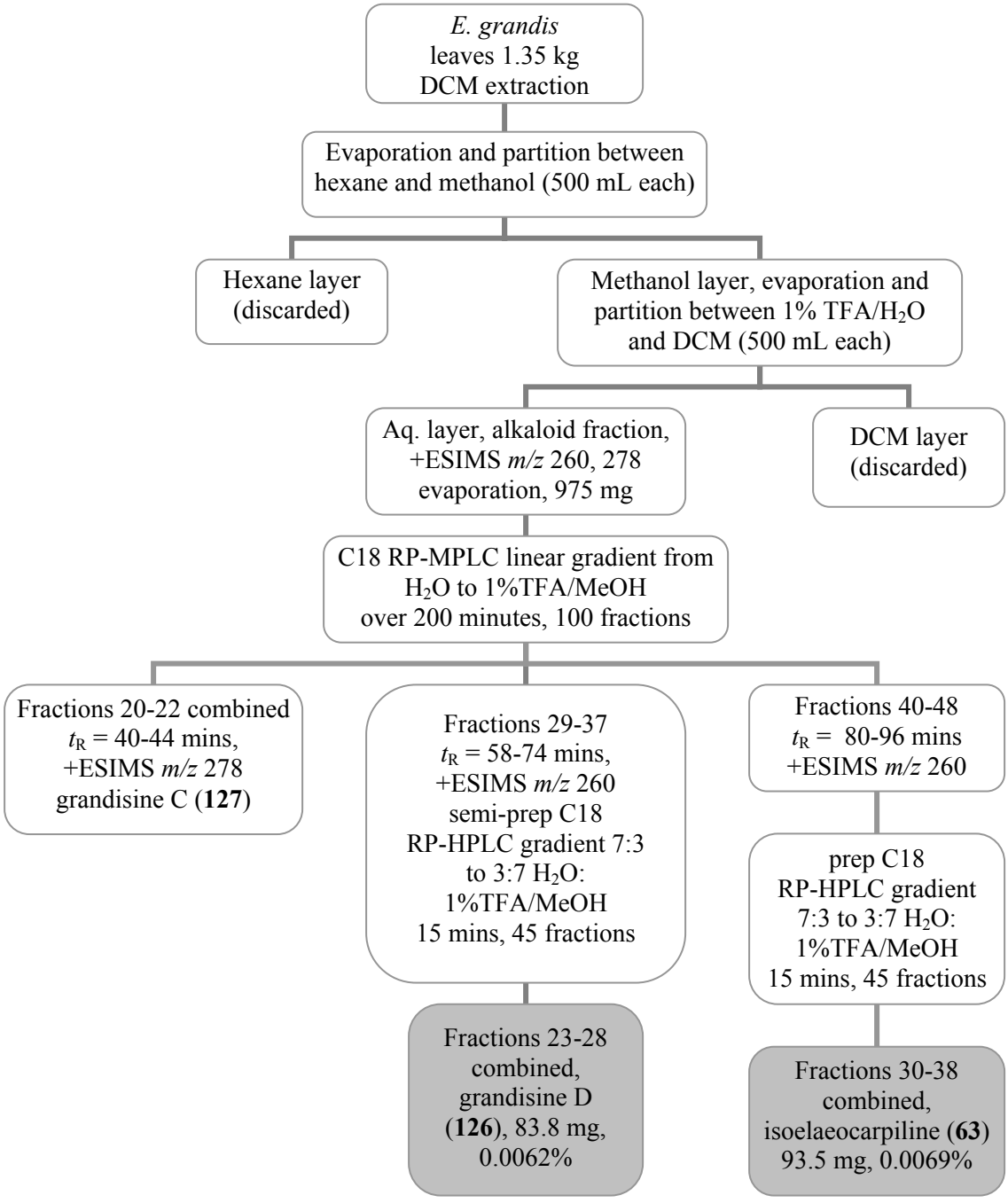


**Scheme 13.** The re-isolation of isoelaeocarpiline (**63**) from the leaves of *E. grandis*.

A further 65.6 mg of isoelaeocarpine (**61**) was obtained from the dehydrogenation of 93.5 mg of isoelaeocarpiline (**63**). Grandisine D (**126**) (83.8 mg) was also reduced with Pd/C (Scheme 14), and purification by C18 RP-HPLC yielded isoelaeocarpine (**61**) (23.4 mg, 27.9%) and elaeocarpine (**60**) (23.8 mg, 28.4%), respectively.

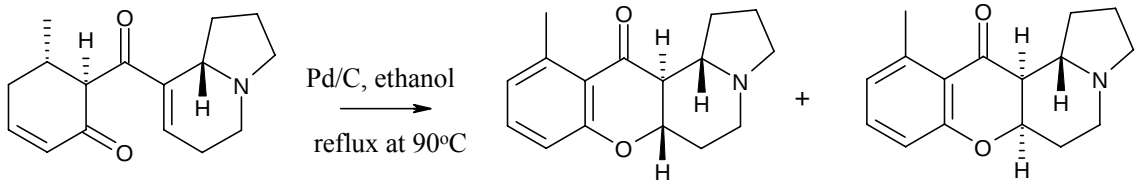


**126** **60** **61**

**Scheme 14.** The dehydrogenation of grandisne D (**126**) in the presence of Pd/C to yield elaeocarpine (**60**) and isoelaeocarpine (**61**).

## 8.4 The Re-isolation of Peripentonine (123) and Subsequent Reduction of 123 to Peripentadenine (81)

Peripentonine (**123**) was also demonstrated to be readily reduced to peripentadenine (**81**) (Figure 55). The reduction of **123** was initially attempted with two equivalents of the oxidizing agent DDQ[13] under refluxing conditions in ethanol. Analysis of the product mixture after 16 hours by $^{1}$H NMR indicated that the majority of peripentonine was unreacted. A small amount of the desired product, peripentadenine (**81**), was detected. The success of Johns *et al.*[12] in the reduction of isoelaeocarpiline (**63**) with Pd/C supported the use of Pd/C rather than DDQ. A further 1.12 g of **123** was purified from the leaves of *P. mearsii* (Scheme 15). Dried and ground leaves of *P. mearsii* were extracted with methanol and the extract was subjected to the same SCX/C18 procedure as described in chapter 5. Peripentonine (**123**) was purified from the alkaloid fraction by C18 RP-MPLC. Peripentonine (**123**) (332 mg) was reduced with Pd/C (182 mg) and separated by C18 RP-HPLC to yield peripentadenine (**81**) (213 mg, 64%).

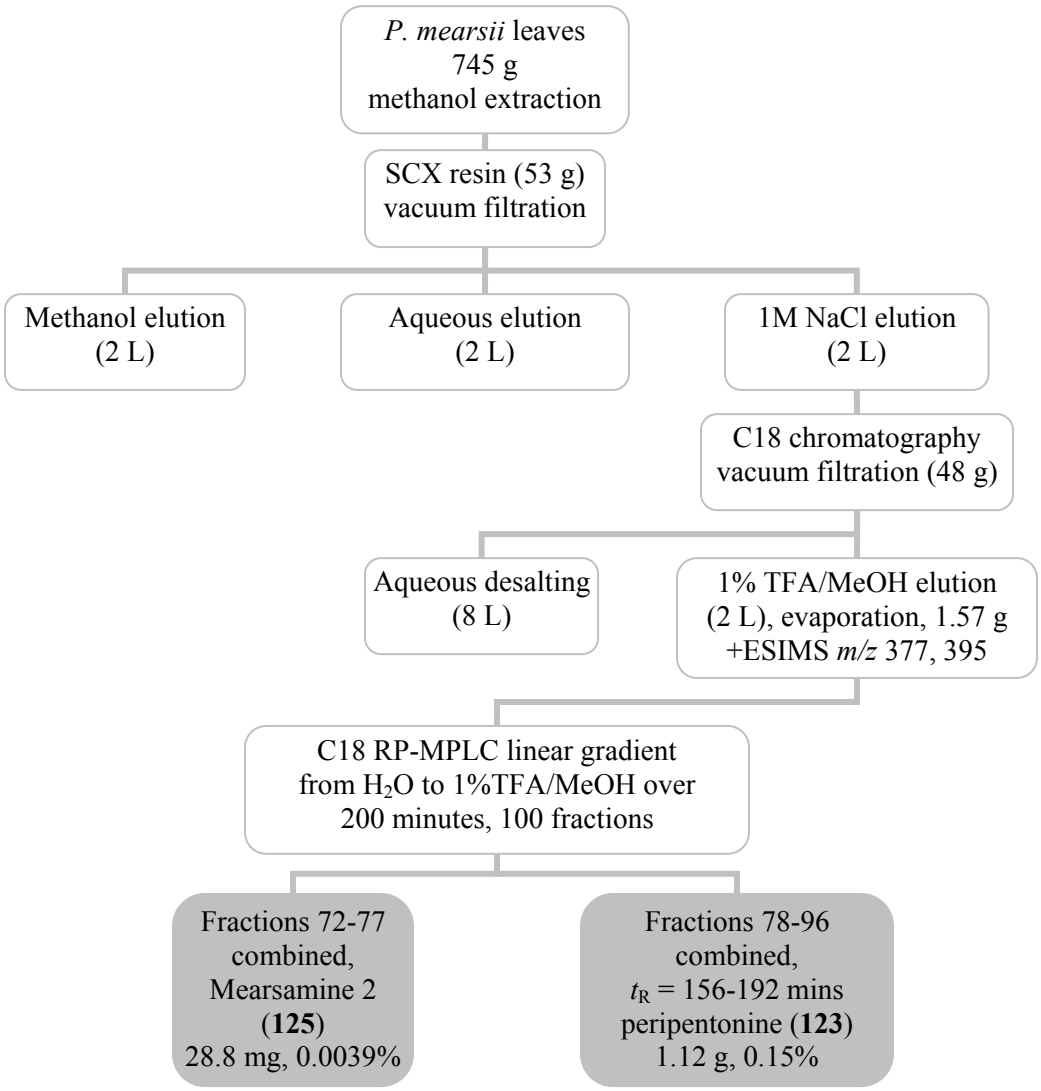


**Scheme 15.** The re-isolation of peripentonine (**123**) from the leaves of *P. mearsii*.

## 8.5 The Attempted Acid Catalyzed Ether Cleavage of Isoelaeocarpine (61)

Hydrogen bromide under refluxing conditions is a typical reagent for the acidic cleavage of aromatic ethers.[13, 14] It was postulated that elaeocarpenine (**122**) would be formed from cleavage of the aromatic ether in isoelaeocarpine (**61**). During the acid promoted cleavage of ethers the oxygen atom becomes protonated and a subsequent nucleophilic

substitution reaction occurs.[14] Isoelaeocarpine (**61**) was dissolved in AcOH/$H_2O$, HBr was added, and the reaction was allowed to stir at 100°C for 16 hours. Following evaporation, the residue was dissolved in methanol and filtered. Analysis of the filtrate by $^1$H NMR indicated that the reaction was unsuccessful. It was speculated that the nitrogen was selectively protonated over the oxygen atom of the ether, and the formation of the doubly charged species **165** would seem highly unlikely.

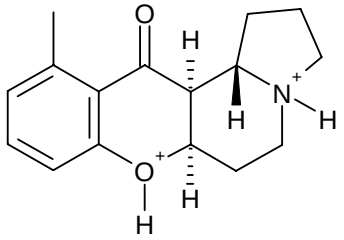


**165**

## 8.6 The Base Catalysed Ether Cleavage of Isoelaeocarpine (61)

Literature examples exist for the cleavage of aromatic ethers contained in flavanoids with the use of $K_2CO_3$ and benzyl bromide.[15] This reaction is generalized in Scheme 16. The base removes an acidic proton alpha to the ketone to generate a carbanion. A thermodynamically stable α,β-unsaturated ketone is formed following the movement of electrons from the carbanion and ring opening at the oxygen. As a result, ether cleavage occurs when the oxygen is eliminated from the carbon beta to the ketone. The electron rich oxygen anion then undergoes nucleophilic attack of the brominated carbon of benzyl bromide to yield a benzyl ether.

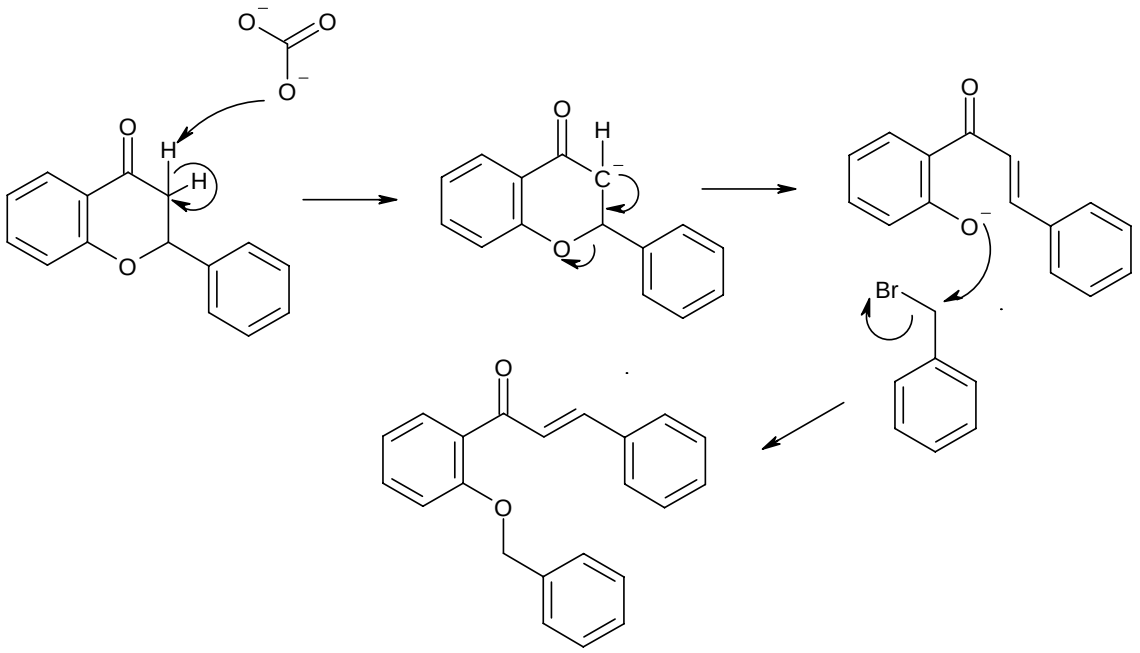

**Scheme 16.** The mechanism for the cleavage of aromatic ethers contained in flavanoids with potassium carbonate and benzyl bromide.

Isoelaeocarpine (**61**) contains the same aromatic-pyran bicyclic system as illustrated in Scheme 16. However, **61** contains a methine alpha to the ketone, as opposed to the alpha methylene illustrated in Scheme 16. The base catalysed reaction of isoelaeocarpine (**61**) was attempted with sodium methoxide and benzyl bromide. Isoelaeocarpine (9.6 mg) was dissolved in methanol, 1.5 equivalents of 0.5 M sodium methoxide and two equivalents of benzyl bromide were added. The reaction was monitored after four hours by positive ESIMS. Three major mass ion peaks were observed at *m/z* 348, 438 and 528, in a ratio of 10:6:2. Compound **166** was speculated to be responsible for the mass ion peak at *m/z* 348, as the nitrogen lone pair could readily react with benzyl bromide. A further three equivalents of benzyl bromide was added and the reaction was allowed to stir at room temperature for 16 hours, to increase the ratio of the unknown minor mass ion peaks at *m/z* 438 and 528. After 16 hours the reaction was again monitored by positive ESIMS and indicated that the major product was the mass ion peak at *m/z* 528 (relative intensity 50%), with two minor peaks at *m/z* 438 (25%) and 348 (25%). The reaction mixture was evaporated and separated by C18 RP-HPLC using a gradient of 100% $H_2O$ to 3:7

$H_2O$:1% TFA/MeOH. One major peak was observed, which corresponded to mass ion peak at *m/z* 528. The mass ion peaks at *m/z* 438 and 348 were detected in the fractions, however significant amounts for structure elucidation could not be obtained. The structure of compound **168** (1.2 mg, 6.11%) was determined by $^1$H and 2D NMR experiments from the fractions containing the mass ion peak of *m/z* 528.

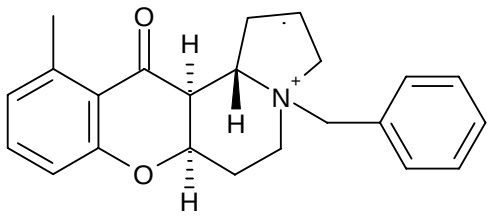

**166**

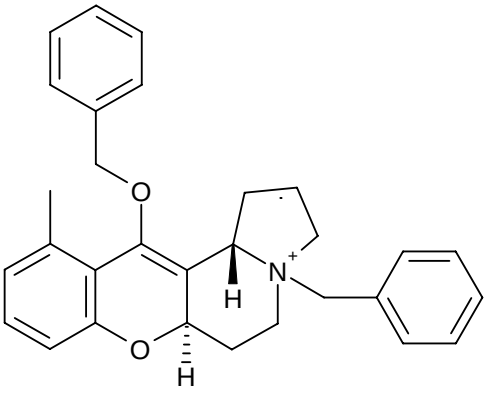

**167**

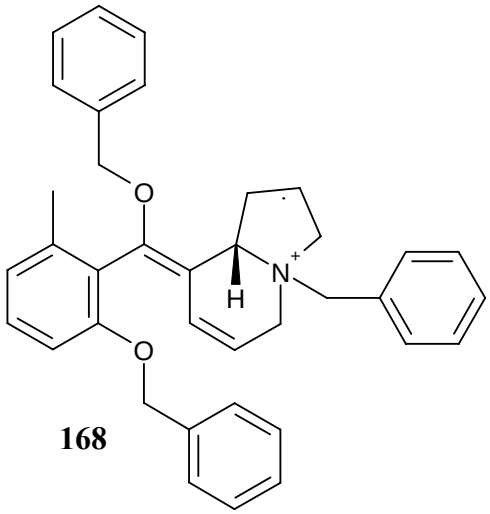

**168**

Figure 109 illustrates the key HMBC correlations from the benzylic methylenes at δ 4.11/4.20, 4.59/4.64 and 5.11/5.14 ppm. These correlations secured the structure of compound **168**. The protons at δ 4.11/4.20 ppm displayed HMBC correlations to two aliphatic carbons at δ 59 and 52 ppm, and to three aromatic carbons to confirm this benzyl group as attached to the nitrogen of isoelaeocarpine (**61**). The other two benzylic methylenes, at δ 4.59/4.64 and 5.11/5.14 ppm, both showed a single HMBC correlation each to oxygenated quaternary carbons at δ 152 and 156 ppm, respectively. An HMBC correlation from the aromatic proton at δ 7.45 to the carbon at 156 ppm was part of the methylated aromatic ring of isoelaeocarpine (**61**). This confirmed the attachment of the benzylic methylene (5.11/5.14) to the oxygen substituent of the quaternary carbon at δ

156 ppm. The position of the second oxygenated quaternary carbon at δ 152 ppm was confirmed by a $^{3}J_{CH}$ correlation from the proton at δ 4.34 ppm, which was attached to the carbon alpha to the nitrogen. The third benzylic methylene (4.59/4.64) was therefore attached to an oxygen substituting an olefinic carbon. This indicated that an enol ether was formed during the reaction, in addition to the cleavage of the aromatic ether and the benzylation of the indolizidine nitrogen. The $^{1}$H chemical shifts of the aromatic protons of the benzyl groups could not be accurately assigned as they were coincident.

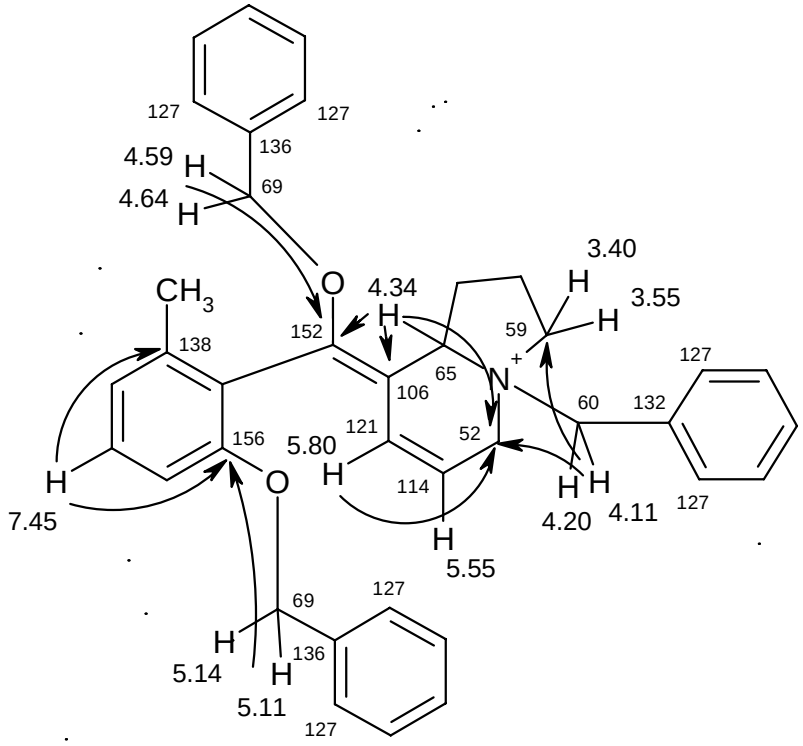


**Figure 109.** The key HMBC correlations observed for compound **168**.

Two additional olefinic protons were also observed in the $^{1}$H NMR spectrum of compound **168**. These protons resonated at δ 5.80 and 5.55 ppm and correlations from the HSQC spectrum demonstrated that they were attached to carbons at δ 121 and 114 ppm, respectively. COSY correlations were observed from the proton at δ 5.55 ppm to the protons at δ 3.64 and 3.97 ppm. HSQC correlations indicated that these two protons were attached to the carbon at δ 52 ppm. HMBC correlations ($^{3}J_{CH}$) were observed from the

benzylic methylene protons at 4.11/4.20, from the olefinic proton at δ 5.80, and from the proton at 4.34 ppm. This indicated that the 3.97/3.64 methylene was attached to the nitrogen, and the olefinic carbons at δ 121 and 114 ppm were part of the indolizidine functionality. Thus the structure of **168** was established.

The structure of the compound responsible for the mass ion peak at *m/z* 438 could therefore be proposed as **167**. The presence of a methine alpha to the ketone in isoelaeocarpine (**61**) is speculated to have an effect in promoting the formation of the enol ether.

This indicated that the base catalysed ether cleavage of isoelaeocarpine (**61**) was successful. However, cleavage failed to yield the benzylated derivative of elaeocarpenine (**122**). This was evident with the formation of the enol ether and dehydroindolizidine functionalities in **168**. Hydrogenation to remove the benzyl groups of **168** would yield **169**. Compound **169** no longer possesses a Michael acceptor, therefore the proposed chemical elaborations could not be attempted.

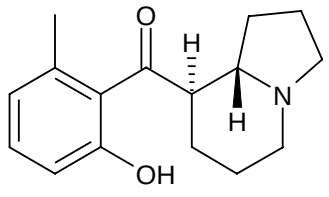


**169**

## 8.7 Reductive Amination Reactions: An Overview

The ketone functional groups in both isoelaeocarpine (**61**) and peripentadenine (**81**) became the focus of synthetic modifications as efforts to obtain elaeocarpenine (**122**) from **61** failed.

A reductive amination reaction (Scheme 17) involves the addition of an amine to an aldehyde or ketone, followed by the elimination of $H_2O$ to yield an enamine which is then

reduced to yield an amine.[16, 17] Reductive aminations are among the most versatile routes for the synthesis of amines.[16, 18] Amines and their derivatives are the most commonly encountered functional groups in medicinal chemistry.[19] Secondary amines in particular are widely recognized as elements of pharmacophores, indicating the importance of synthetically prepared amines.[18, 19]

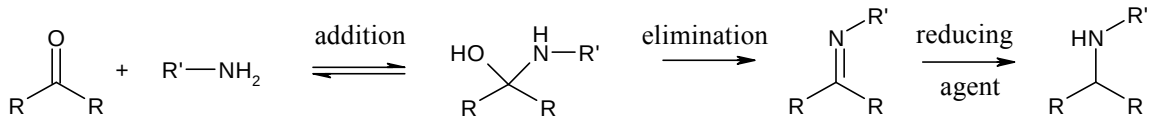


**Scheme 17.** A general reductive amination reaction.

Studies have shown that the selection of the reducing agent in reductive aminations is vital to the reactions, as the reducing agent must selectively reduce imines over aldehydes or ketones.[16] Reducing agents mostly commonly used include $H_2$/Pd-C, $NaBH_4$, $NaBH_3CN$ and $LiAlH_4$.[13] Reductive amination reactions have been used to prepare combinatorial libraries in solution.[20] Specific cases are highlighted by reacting primary ethanolamines and aliphatic ketones using $NaBH_3CN$,[21] aromatic aldehydes and amino acid esters utilizing $NaBH(OAc)_3$.[22, 23]

The use of sodium triacetoxyborohydride in reductions with a range of aldehydes, ketones and amines have been studied.[16] This reducing agent is reported to be mild and selective against a wide variety of enamine substrates, with fewer side products compared to other reducing agents. The scope of this reaction includes aliphatic, acyclic and cyclic ketones, aliphatic and aromatic aldehydes, and primary and secondary amines including a variety of weakly basic and nonbasic amines.[16] Limitations include reaction with aromatic ketones and unsaturated ketones, and some sterically hindered ketones and amines.[16, 24] DCE is reported to be the best solvent, however reactions can also be performed in THF.[16] Acetic acid may be used as a catalyst with ketone reactions, with reactions being generally faster in DCE.[16] The steric and electron-withdrawing effects of the three acetoxy groups of sodium triacetoxyborohydride stabilize the boron-hydrogen bond and are responsible for its mild reducing properties.[16] Sterically hindered ketones are even less reactive than aromatic and α,β-unsaturated ketones.[16] The stereoselective

effect of different reducing agents has also been reported. Reductions of cyclohexyl imines with small reagents such as $NaBH_4$ and $NaBH_3CN$ were shown to favour an axial approach, whereas bulkier reagents such as triacetoxyborohydrides favour an equatorial approach (Figure 110).[25]

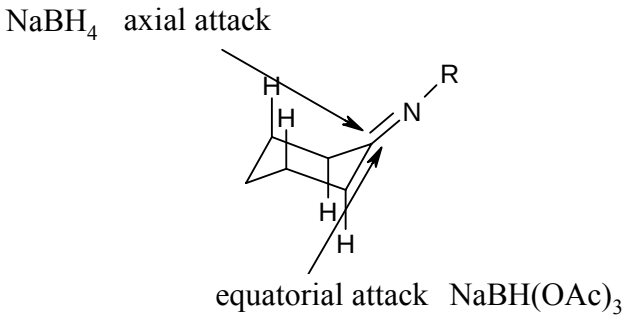


**Figure 110.** Illustration of the axial and equatorial attack of different reducing agents.

As isoelaeocarpine (**61**) and peripentadenine (**81**) both contain aromatic ketones, issues with the unreactivity of the ketones may be encountered. The reductive amination of aromatic ketones has been successfully reported in the presence of a titanium tetraisopropyloxide catalyst, $Ti(O^iPr)_4$.[17-19, 24] This catalyst has been used successfully for aromatic and sterically hindered ketones. $Ti(O^iPr)_4$ acts as a mild Lewis acid and is hypothesized to transform the hydroxyl group, formed by attack of the amine on a carbonyl, into a better leaving group (Scheme 18).[18]

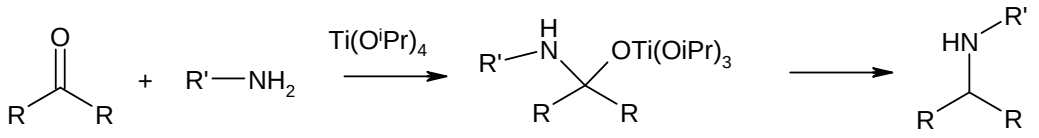


**Scheme 18.** The proposed role of titanium isopropyloxide during a reductive amination reaction.[18]

## 8.8 Preliminary Reductive Amination Reactions of Peripentadenine (81) and Acetophenone (170)

The reductive amination of peripentadenine (**81**) was initially attempted using AcOH as a catalyst, with 1.5 equivalents of 4-methoxyphenethyl amine in DCE, as detailed by literature examples.[16] Analysis of the reaction, following purification by HPLC, indicated that peripentadenine had not reacted. A series of test reactions were subsequently performed using the aromatic ketone acetophenone (**170**) and titanium (IV) isopropyl oxide. Acetophenone (50 mg), three equivalents of amine, 0.2 equivalents of $Ti(O^iPr)_4$ and three equivalents of $NaBH(OAc)_3$ were added sequentially to a stirred solution of DCE. After stirring for 16 hours (rt), water was added to the product mixture and partitioned with DCE. The DCE layer was separated by semi-preparative C18 RP-HPLC using a gradient from $H_2O$ to 1%TFA/MeOH over 15 minutes. Two different aromatic amines, 4-methoxyphenethyl amine and 2-chlorobenzyl amine, were used in this preliminary study. The reductive amination of acetophenone with these amines yielded *N*-[2-(4-methoxyphenyl)ethyl]-1-phenylethanamine (**171**) (25.6 mg, TFA salt, 23.9%) and *N*-(2-chlorobenzyl)-1-phenylethanamine (**172**) (27.7 mg, TFA salt, 27.0%), respectively.

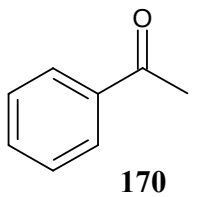


**170**

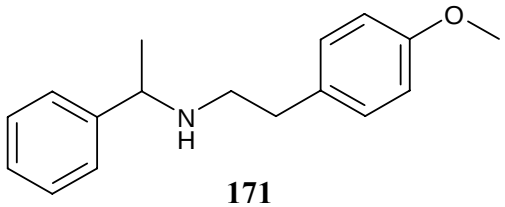


**171**

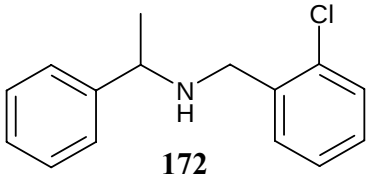


**172**

The reductive amination of aromatic ketones and aldehydes in the presence of one or more equivalents of $Ti(O^iPr)_4$ has also been reported.[18,19] In a comparative reaction using 2-chlorobenzyl amine and one equivalent of $Ti(O^iPr)_4$, the yield of **172** (5.5 mg) was reduced dramatically to 5.37%. This indicated that catalytic amounts of $Ti(O^iPr)_4$ produce a much higher yield.

## 8.9 The Reductive Amination of Peripentadenine (81)

Peripentadenine (**81**) was subjected to a series of reductive aminations using three equivalents of different amines, a catalytic amount of $Ti(O^iPr)_4$ and three equivalents of $NaBH(OAc)_3$. Purification of the reaction mixtures was achieved by an acid-base extraction, followed by C18 RP-HPLC using a gradient from $H_2O$ to 1%TFA/MeOH over 15 minutes. The amines used were 4-methoxyphenethyl amine, 2-chlorobenzyl amine, benzyl amine, *N*-methylphenethyl amine and α-aminotoluic acid. The reaction of **81** with α-aminotoluic acid was performed in EtOH. These amines were selected to investigate the effects of various substituents on the aromatic ring and nitrogen. Phenethyl and benzyl amines were also chosen to observe the effect on the reaction of the number of carbons between the amine and aromatic functionalities. 4-methoxyphenethyl amine was selected as the δ opioid agonist SNC 80 (**146**) contains a methoxyphenyl group. The carboxylic acid functionality of α-aminotoluic acid could be converted to an *N,N*-diethyl amide derivative, which is also present in **146**.

The reductive aminations of peripentadenine (**81**) with 2-chlorobenzyl amine, *N*-methylphenethyl amine and α-amino toluic acid were all unsuccessful. The work up of each of these reactions by HPLC yielded peripentadenine and the amine. The chlorine group of 2-chlorobenzyl amine was speculated to create too much steric hindrance with the aromatic methyl group or phenol of **81**. The *N*-methyl group of *N*-methylphenethyl amine was also suggested to create steric hindrance. Alpha-aminotoluic acid was found to be insoluble in DCE or THF, thus the reaction was performed in EtOH. Literature evidence indicates that reductive aminations with $NaBH(OAc)_3$ were only successful in DCE or THF,[16, 18] however some reductive aminations with $Ti(O^iPr)_4$ and $NaBH_4$ were performed in EtOH.[19]

The reactions of **81** with 4-methoxyphenethyl amine and benzyl amine were successful. These reductive aminations yielded the compounds **173** (3.7 mg, 27.4%) and **174** (3.1 mg, 25.1%). These products were purified as a mixture of diastereromers and the $^1H$ NMR spectra of **173** and **174** are illustrated in Figures 111 and 112, respectively. There

was an excess of one of the diastereomers of both **173** and **174**, indicating that $NaBH(OAc)_3$ was slightly stereoselective. The $^{1}H$ and $^{13}C$ NMR spectral data of the major diastereomers of these compounds is presented in Tables 24 and 25, respectively. The key HMBC correlations of H-16, H-17, and H-26 (Figure 113) enabled the structures of **173** and **174** to be proven unambiguously. No attempt was made to separate the diastereomers due to the small amount of material obtained.

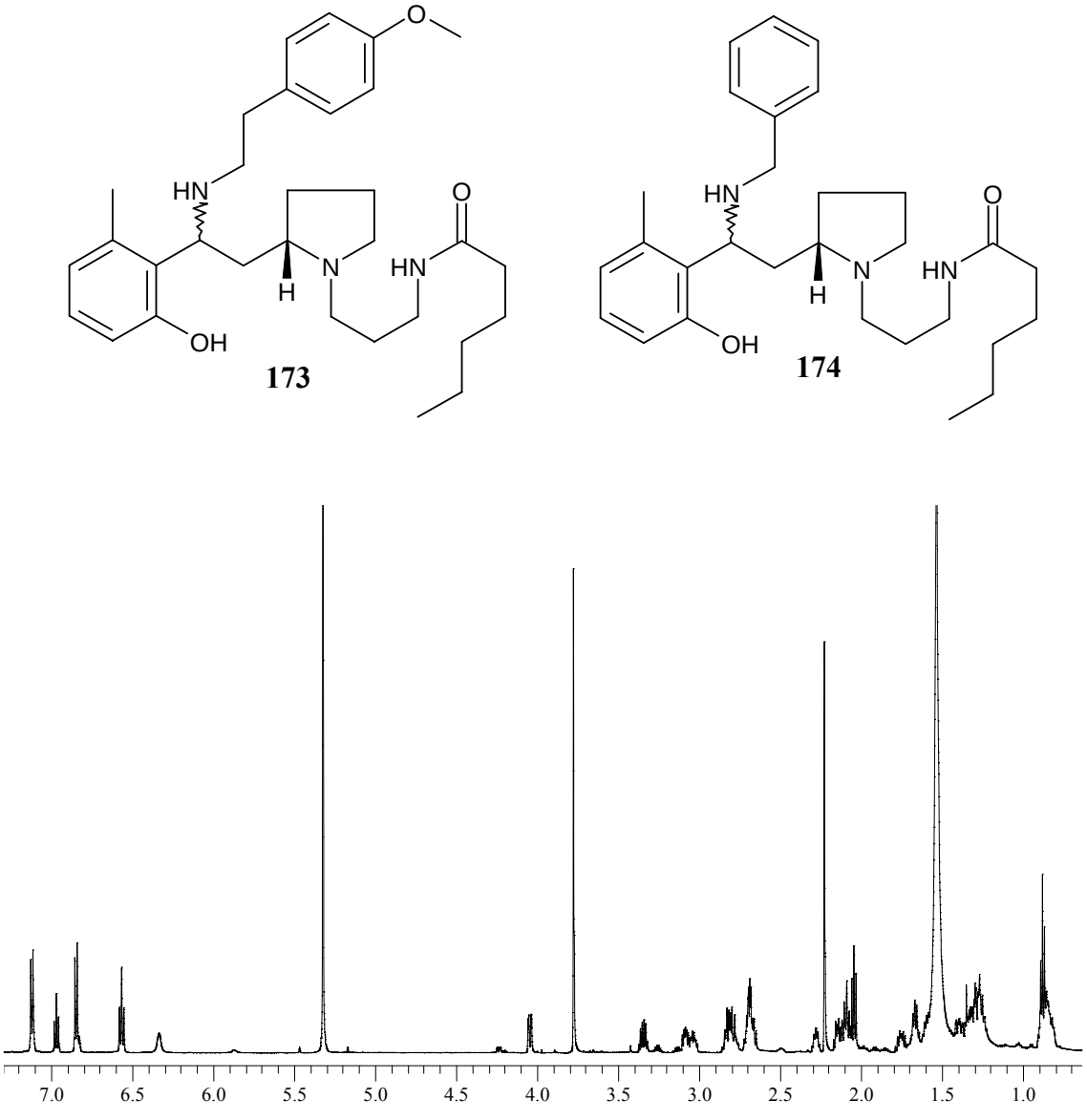


**Figure 111.** The $^{1}H$ NMR spectrum (600 MHz, $CD_2Cl_2$) of compound **173**, the product of the reductive amination of peripentadenine (**81**) with 4-methoxyphenethyl amine.

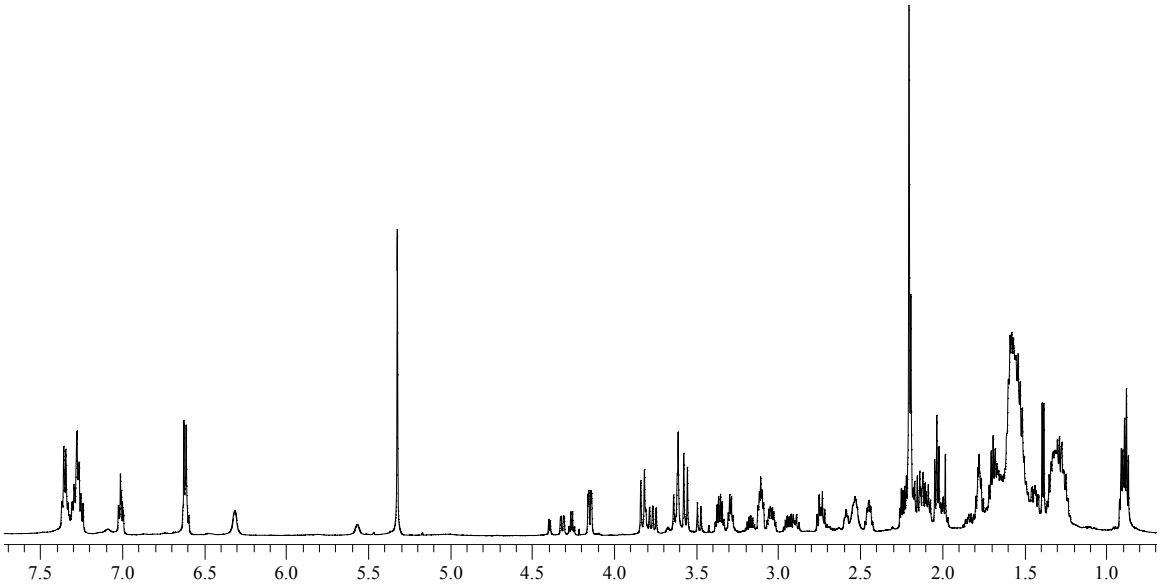


**Figure 112.** The $^{1}H$ NMR spectrum (600 MHz, $CD_2Cl_2$) of compound **174**, the product of the reductive amination of peripentadenine (**81**) with benzyl amine.

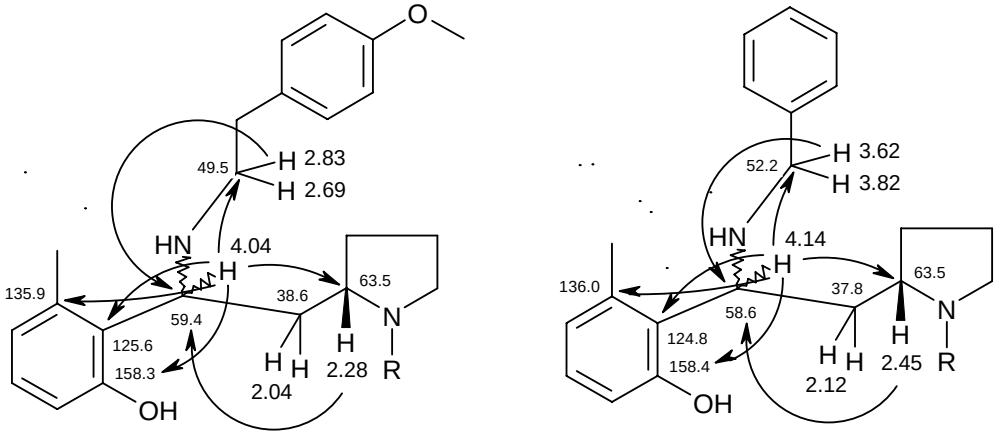


**Figure 113.** The key HMBC correlations observed for H-16, H-17 and H-26 for **173** and **174**.

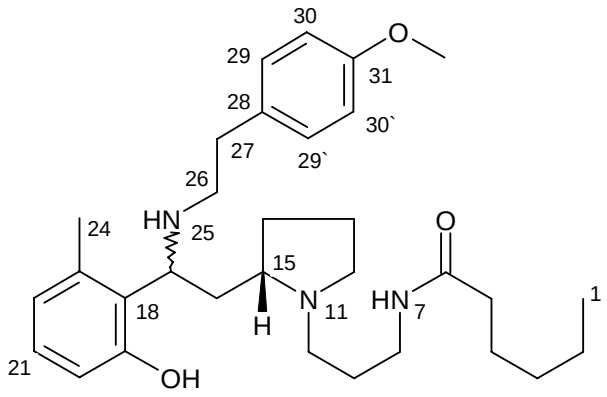


**Table 24.** $^{13}C^{a}$ and $^{1}H^{b}$ NMR spectral data for **173**[c].

| position | $^{13}C$, δ | $^{1}H$, δ, mult, *J* (Hz) |
|---|---|---|
| 1 | 13.4 | 0.83 (3H, t, 7.2) |
| 2 | 21.6 | 1.33 (2H, m) |
| 3 | 32.0 | 1.29 (2H, m) |
| 4 | 28.8 | 1.53 (2H, m) |
| 5 | 38.7 | 2.12 (2H, m) |
| 6 | 172.1 | - |
| 7 | - | 6.33 (1H, br) |
| 8 | 39.1 | 3.04 (1H, ddd, 6.6, 6.6, 15.6); 3.34 (1H, ddd, 6.6, 6.6, 12.6) |
| 9 | 26.3 | 1.53 (2H, m) |
| 10 | 53.5 | 2.09 (1H, m); 2.66 (1H, m) |
| 12 | 53.2 | 2.07 (1H, m); 3.08 (1H, ddd, 4.8, 4.8, 10.2) |
| 13 | 22.9 | 1.31 (1H, m); 1.65 (1H, m) |
| 14 | 31.9 | 1.34 (1H, m); 1.76 (1H, m) |
| 15 | 63.5 | 2.28 (1H, ddd, 7.2, 7.2, 13.8) |
| 16 | 38.6 | 2.04 (1H, t, 7.8) |
| 17 | 59.4 | 4.04 (1H, dd, 3.0, 10.2) |
| 18 | 125.6 | - |
| 19 | 158.3 | - |
| 20 | 115.6 | 6.57 (1H, d, 8.4) |
| 21 | 128.5 | 7.13 (1H, dd, 7.8, 7.8) |
| 22 | 121.6 | 6.57 (1H, d, 8.4) |
| 23 | 135.9 | - |
| 24 | 20.1 | 2.23 (3H, s) |
| 26 | 49.5 | 2.69 (1H, m); 2.83 (1H, m) |
| 27 | 35.6 | 2.68 (1H, m); 2.78 (1H, m) |
| 28 | 131.7 | - |
| 29/29` | 130.3 | 7.11 (2H, d, 8.4) |
| 30/30` | 114.6 | 6.84 (2H, d, 8.4) |
| 31 | 158.8 | - |
| 31-OMe | 56.2 | 3.78 (3H, s) |

[a]At 125 MHz. [b]At 600 MHz. [c]In $CD_2Cl_2$.

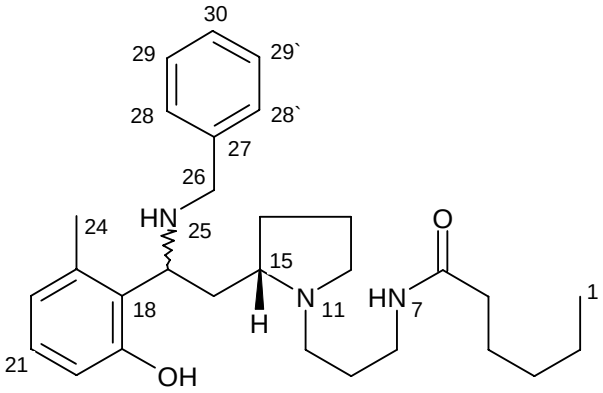


**Table 25.** $^{13}C^{a}$ and $^{1}H^{b}$ NMR spectral data for **174**[c].

| position | $^{13}C$, δ | $^{1}H$, δ, mult, *J* (Hz) |
|---|---|---|
| 1 | 13.4 | 0.88 (3H, t, 7.2) |
| 2 | 21.6 | 1.33 (2H, m) |
| 3 | 32.1 | 1.30 (2H, m) |
| 4 | 29.3 | 1.54 (2H, m) |
| 5 | 38.6 | 2.03 (2H, t, 7.8) |
| 6 | 172.2 | - |
| 7 | - | 6.31 (1H, br) |
| 8 | 39.2 | 3.04 (1H, ddd, 7.2, 7.2, 11.4); 3.35 (1H, ddd, 6.0, 6.0, 12.6) |
| 9 | 26.3 | 1.53 (2H, m) |
| 10 | 53.5 | 2.09 (1H, m); 2.66 (1H, m) |
| 12 | 53.1 | 2.07 (1H, m); 3.08 (1H, ddd, 4.8, 4.8, 10.2) |
| 13 | 23.3 | 1.35 (1H, m); 1.62 (1H, m) |
| 14 | 32.2 | 1.35 (1H, m); 1.76 (1H, m) |
| 15 | 63.5 | 2.45 (1H, ddd, 7.2, 7.2, 14.4) |
| 16 | 37.8 | 2.12 (1H, m) |
| 17 | 58.6 | 4.14 (1H, dd, 2.4, 10.2) |
| 18 | 124.8 | - |
| 19 | 158.4 | - |
| 20 | 115.6 | 6.23 (1H, d, 7.8) |
| 21 | 128.4 | 7.01 (1H, dd, 7.8, 7.8) |
| 22 | 121.5 | 6.23 (1H, d, 7.8) |
| 23 | 136.0 | - |
| 24 | 20.2 | 2.20 (3H, s) |
| 26 | 52.2 | 3.62 (1H, d, 13.2); 3.82 (1H, d, 13.2) |
| 27 | 139.4 | - |
| 28/28` | 129.6 | 7.31 (2H, m) |
| 29/29` | 129.4 | 7.36 (2H, dd, 7.2, 7.2) |
| 30 | 128.7 | 7.31 (1H, m) |

[a]At 125 MHz. [b]At 600 MHz. [c]In $CD_2Cl_2$.

## 8.10 The Attempted Reductive Amination of Isoelaeocarpine (61)

All attempts to reductively aminate the ketone in isoelaeocarpine (**61**) were unsuccessful. The reactions were tried in an identical manner as for the reductive amination of peripentadenine (**81**) using $NaBH(OAc)_3$ and the amines 4-methoxyphenethyl amine and ethanolamine. The unsuccessful reaction of **61** with 4-methoxyphenethyl amine suggested that the aromatic group of this amine may be creating steric interferences with the aromatic or indolizidine groups in isoelaeocarpine (**61**). However, the second unsuccessful reaction with ethanolamine, an amine not containing an aromatic group, indicated that steric hindrance of a bulky aromatic amine was not preventing the reaction from occurring. Analysis of the mixtures by positive ESIMS and $^1H$ NMR indicated that the starting materials were present for both mixtures, therefore indicating the reactions were unsuccessful.

Considering the equatorial attack of triacetoxyborohydrides (Figure 102), it was speculated that the indolizidine group, orthogonal to the aromatic ring, may have prevented the approach of $NaBH(OAc)_3$. The reaction of **61** with 4-methoxyphenethyl amine was attempted again with $NaBH_4$. This reaction was also unsuccessful, indicating that a less bulky reducing agent attacking from the axial side of the cyclohexyl ring had no effect.

The chemical shift of the carbonyl carbon in isoelaeocarpine (**61**), δ 194.6 ppm, alludes to the unreactivity of the ketone to a reductive amination. The chemical shift of the carbonyl carbon in peripentadenine (**81**) was δ 203.4 ppm. This is a significant difference between the two molecules, suggesting that the carbonyl carbon in **61** is more shielded by the aromatic group compared to the carbonyl carbon in **81**. This therefore suggests that the ketone in isoelaeocarpine (**61**) may be part of a conjugated system and is therefore unreactive. Peripentadenine contained an acyclic ketone, whereas isoelaeocarpine possesses a cyclic ketone, another factor that may contribute to the unreactivity of the ketone in **61**. Inspection of the energy minimized structure of isoelaeocarpine suggests

that the ketone is in the same plane as the aromatic ring, which may provide steric hindrance.

## 8.11 Conclusion

Synthetic studies of peripentadenine (**81**) indicated that aromatic functionality could be introduced via reductive amination reactions. Evidence indicates that sterically hindered amines do not react with **81** and the methyl or phenol of **81** may inhibit some reactions. Isoelaeocarpine (**61**) did not react with aromatic and non-aromatic amines via reductive amination reactions. As a result, isoelaeocarpine (**61**) may not be suitable as a template for combinatorial diversification via reductive amination due to the unreactivity of the ketone.

Elaeocarpenine (**122**) offers potential as a natural product template for combinatorial libraries. This molecule contains a Michael acceptor, however the synthesis of analogues of **122** by Michael addition reactions was not explored. Attempts to obtain elaeocarpenine (**122**) from isoelaeocarpine (**61**) via ether cleavage reactions proved unsuccessful, suggesting that **122** itself needs to be synthesized or purified from *E. fuscoides* in large amounts. Compound **169** could also be used as a template for reductive amination or esterification.

## 8.12 References


1. Hall, D. G., Manku, S., Wang, F., *J Comb Chem* **2001,** 3, 125 - 150.
2. Davis, R. A., Carroll, A. R., Quinn, R. J., *Aust J Chem* **2001,** 54, 355 - 359.
3. Wipf, P., Reeves, J. T., Balachandran, R., Giuliano, K. A., Hamel, E., Day, B. W., *J Am Chem Soc* **2000,** 122, 9391 - 9395.

**4.** Chen, Y., Bilban, M., Foster, C. A., Boger, D. L., *J Am Chem Soc* **2002,** 124, 5431 - 5440.

**5.** Kulkarni, B. A., Roth, G. P., Lobkovsky, E., Porco, J. A., *J Comb Chem* **2002,** 4, 56 - 72.

**6.** Mink, D., Mecozzi, S., Rebek, L., *Tetrahedron Lett* **1998,** 39, 5709 - 5712.

**7.** Wang, H., Ganesan, A., *Org Lett* **1999,** 1, 1647 - 1649.

**8.** Nicolaou, K. C., Winssinger, N., Vourloumis, P., Ohshima, T., Kim, S., Pfefferkorn, J., Xu, J-Y., Li, T., *J Am Chem Soc* **1998,** 120, 10814 - 10826.

**9.** Batey, R. A., Simoncic, P. D., Lin, D., Smyj, R. P., Lough, A. J., *Chem Comm* **1999**, 651 - 652.

**10.** Seneci, P., Sizemore, C., Islam, K., Kocis, P., *Tetrahedron Lett* **1996,** 37, (35), 6319 - 6322.

**11.** Atuegbu, A., Maclean, D., Nguyen, C., Gordon, E. M., Jacobs, J. W., *Bioorg Med Chem* **1996,** 4, 1097 - 1106.

**12.** Johns, S. R., Lamberton, J. A., Sioumis, A. A., Suares, H., *Aust J Chem* **1971,** 24, 1679 - 1694.

**13.** LaRock, R. C., *Comprehensive Organic Transformations: A Guide to Functional Group Preparations*. 2nd ed.; VCH Publishers: New York, **1989**.

**14.** McMurry, J., *Organic Chemistry*. 3rd ed.; Brooks/Cole: Belmont, **1992**.

**15.** Nanayakkara, N. P. D., Hussain, R. A., Pezzuto, J. M., Soejarto, D. D., Kinghorn, A. D., *J Med Chem* **1988,** 31, 1250 - 1253.

**16.** Abdel-Magid, A. F., Carson, K. G., Harris, B. D., Maryanoff, C. A., Shah, R. D., *J Org Chem* **1996,** 61, 3849 - 3862.

**17.** Mattson, R. J., Pham, K. M., Lueck, D. J., Cowen, K. A., *J Org Chem* **1990,** 55, 2552 - 2554.

**18.** Neidigh, K. A., Avery, M. A., Williamson, J. S., Bhattacharyya, S., *J Chem Soc Perkin Trans 1* **1998**, 2527 - 2731.

**19.** Kumpaty, H., Bhattacharyya, S., Rehr, E. W., Gonzalez, A. M., *Synthesis* **2003,** 14, 2206 - 2210.

**20.** Austel, V., *Solution-Phase Combinatorial Chemistry*. In *Combinatorial Chemistry: Synthesis, Analysis and Screening*, 1st ed.; Jung, G., Eds. Wiley-VCH: Weinheim, **1999**; pp. 77 - 89.

**21.** Siegel, M. G., Shuker, A. J., Droste, C. A., Hahn, P. J., Jesudason, C. D., McDonald, J. H., Matthews, D. P., Rito, C. J., Thorpe, A. J., *Molecular Diversity* **1998,** 3, 113 - 116.

**22.** Sim, M. M., Lee, C. L., Ganesan, A., *J Org Chem* **1997,** 62, 9358 - 9360.

**23.** Sim, M. M., Ganesan, A., *J Org Chem* **1997,** 62, 3230 - 3235.

**24.** Chandrasekhar, S., Reddy, C. R., Ahmed, M., *Synlett* **2000,** 11, 1655 - 1657.

**25.** Hutchins, R. O., Su, W-Y., Sivakumar, R., Cistone, F., Stercho, Y. P., *J Org Chem* **1983,** 48, 3412 - 3422.

# CHAPTER 9 – Experimental

## 9.1 General Experimental Procedures

All solvents used were HPLC grade. Milli-Q PF filtered water was used. $H_2SO_4$, $NH_3$ and NaCl were BDH analytic grade purchased from Merck. TFA was purchased from Fluka. Analytical grade glacial AcOH was used (Ajax). KI, bismuth (III) subcarbonate and Pd/C (10%) were purchased from Aldrich.

Optical rotations were measured on a JASCO P-1020 polarimeter (23 °C, 10 cm cell). The UV and IR spectra of habbenine (**114**), elaeocarpenine (**122**), peripentonine (**123**), mearsamine 1 (**124**) and 2 (**125**), grandisine D (**126**) and grandisine E (**128**) were recorded on a GBC 916 UV/Vis spectrophotometer and a Thermo Nicolet NEXUS FT-IR spectrometer, respectively. The UV and IR spectra of grandisine C (**127**), F (**129**), G (**130**) and compound **131** were recorded on a CAMSPEC M501 single beam scanning UV/Vis spectrophotometer and a Perkin Elmer 16 PC FT-IR spectrometer, respectively.

NMR spectra were recorded on a Varian Unity Inova 600 MHz and 500 MHz NMR spectrometers. The 500 MHz spectrometer was fitted with a SMS autosampler. $^1$H, $^{13}$C, COSY, ROESY, HSQC and HMBC spectra were acquired using standard Varian parameters. Proton coupling constants were calculated from $^1$H NMR spectra which had been transformed and processed with a sine-bell weighting. $^1$H NMR spectra in each structure elucidation chapter were processed with Mest-Rec-23 software. Samples were dissolved in either $d_6$-DMSO, $CD_3OD$, $CD_2Cl_2$, $CD_3CN$, $CDCl_3$ or $d_5$-pyridine. Chemical shifts were calculated relative to the dimethylsulfoxide solvent peak ($^1$H δ 2.49 and $^{13}$C δ 39.5 ppm), methanol solvent peak ($^1$H δ 3.31 ppm), methylene chloride solvent peak ($^1$H δ 5.32 and $^{13}$C δ 54.0 ppm), acetonitrile solvent peak ($^1$H δ 1.94 and $^{13}$C δ 118.7 ppm), chloroform solvent peak ($^1$H δ 7.26 and $^{13}$C δ 77.0 ppm) or pyridine solvent peak ($^1$H δ 8.74 ppm).

(+)-LRESI mass spectra were measured on a Mariner Biospectrometry TOF workstation using positive electrospray ionization, mobile phase 1:1 MeOH:$H_2O$ containing 0.1% formic acid or a Fisons VG platform quadruple mass spectrometer. (+)-HRESI mass spectra of habbenine (**114**), elaeocarpenine (**122**), grandisine D (**126**), and E (**128**) were also measured on the Mariner workstation. (+)-HRESI mass spectra of peripentonine (**123**), mearsamine 1 (**124**) and 2 (**125**), grandisine C (**127**), F (**129**), G (**130**) and compound **131** were mearsured on a Bruker Daltonics Apex III 4.7e FT-MS fitted with an Apollo API ionization source.

Molecular modeling was performed on a Silicon Graphics OCTANE workstation. An MM2 forcefield was implemented in the molecular modeling program Macromodel®, version 6.0. Energy minimized structures were determined from a MonteCarlo conformational search in vacuum. The manipulation and overlay of energy minimized structures was achieved by use of WebLab Viewer software.

Dowex 50WX8-400 strongly acidic ion exchange resin, 200-400 μm mesh (Aldrich), Alltech Davisil bonded C18 silica gel (endcapped, 35-70 μm), polyamide gel, particle size 0.05-0.16mm (Polyamid CC6 Macherey-Nagel), and Sephadex LH-20 (Amersham Pharmacia Biotech AB) were used during separation and purification. HPLC purifications were achieved using Hypersil BDS C18 preparative (150 x 21.2 mm, 5μm) and semi-preparative (250 x 10 mm, 5μm), and BETASIL C18 semi-preparative (100 x 10 mm, 5μm) columns on a Waters HPLC system containing a 600 pump, 996 PDA detector, and 717 autosampler, which was connected to a Gilson 204 or Waters fraction collector. The Waters system was controlled with Millennium software. Extractions of plant material was achieved by loading the sample into a custom made metal column (30 x 3.5 cm), which was connected to an Alltech 301 isocratic HPLC pump.

## 9.2 Chapter 2 Experimental

**Dragendorff's reagent:** Bismuth (III) subcarbonate was dissolved in 20 mL of water, and 5 mL of glacial AcOH was added to make solution A. 10 g of KI was dissolved in 25 mL of water to make solution B. Solutions A and B were mixed, and allowed to stand in darkness for 2 hours at 5$^{o}$C. The reagent was stored at 5$^{o}$C in a foil-lined bottle.

**Procedure of the phytochemical survey.** Individual plant parts (400 mg) were loaded into an SPE cartridge and extracted with methanol (5 mL). The extracts were evaporated to dryness and re-dissolved in 1.5 mL of 1M $H_2SO_4$ and partitioned twice with 3mL of DCM. The organic layer was removed each time and the pH of the aqueous layer was adjusted to pH 10 with 32% $NH_3$ solution and allowed to stand for 30 minutes. The basified aqueous layer was partitioned twice with 3 mL of DCM. The organic phase was removed and evaporated. The residue was dissolved in methanol (1 mL) and 200 µL was transferred to a 96-well microtitre plate. The methanol in the microtitre plate was reduced to 50 µL and 150 µL of Dragendorff's reagent was added.

**The extraction of *Sloanea tieghemii.*** Plant material was collected by Topul Rali in PNG. Leaves of *S. tieghemii* (80 g) were extracted with methanol (3 L). The extract was filtered through PAG and the filtrate was evaporated. The residue (8.4 g) was partitioned between DCM and $H_2O$. The aqueous layer was found to give a positive Dragendorff test and was filtered through SCX resin (50 g). A load fraction was obtained (500 mL), which produced a positive result in a Dragendorff test. The SCX resin was washed with $H_2O$ before elution with $CaCl_2$ (1 L). The SCX load fraction was evaporated and the residue (1.3 g) was absorbed onto C18 silica gel (1.2 g) and transferred into a small metal HPLC column (10 x 15 mm). This column was connected to a C18 RP-MPLC column (22 x 2.5 cm) and separated into 70 fractions by a gradient of $H_2O$ to MeOH over 120 minutes at 5 mL/minute. Fractions 37 to 47 were found to produce a positive Dragendorff test and were combined (74 mg). Mass ion peaks of *m/z* 689 and 691 were observed following analysis by –ESIMS. This combined fraction was separated into 50 fractions by isocratic semi-preparative C18 RP-HPLC with conditions of 1:4 $H_2O$:MeOH. Fractions 33 and 34

were combined to yield compound **112** (30.6 mg, 0.038%), and fractions 39 and 40 were combined to yield compound **113** (28.6 mg, 0.036%).

**Compound (112):** yellow gum; $[\alpha]_D^{23}$ +16.01° (*c* 0.067, MeOH), +12.43° (*c* 0.1334, MeOH); UV (MeOH) $\lambda_{max}$ (log ε) 225 (3.94) 281 (3.81) nm; IR (KBr) $\upsilon_{max}$ 3404 br, 1746, 1640, 1347, 1172, 1021 $cm^{-1}$; $^1H$ NMR (600 MHz, $d_6$-DMSO) and $^{13}C$ NMR (125 MHz, $d_6$-DMSO) Table 3; (-)-LRESIMS *m/z* (rel. int.): 689 (100%) $[MH^-, C_{34}H_{25}O_{16}]^-$; (+)-HRESIMS *m/z* 689.115273 $[M + H]^+$ (calcd for $C_{34}H_{25}O_{16}$, 689.114808); CD (MeOH) 232 nm, + 42, 265 nm, -18, 285 nm, +5.

**Compound (113):** yellow gum; $[\alpha]_D^{23}$ +22.19° (*c* 0.067, MeOH), +12.74° (*c* 0.1334, MeOH); UV (MeOH) $\lambda_{max}$ (log ε) 227 (3.95) 279 (3.90) nm; IR (KBr) $\upsilon_{max}$ 3374 br, 1745, 1621, 1356, 1172, 1022 $cm^{-1}$; $^1H$ NMR (600 MHz, $d_6$-DMSO) and $^{13}C$ NMR (125 MHz, $d_6$-DMSO) Table 4; (-)-LRESIMS *m/z* (rel. int.): 691 (100%) $[MH^-, C_{34}H_{27}O_{16}]^-$; (+)-HRESIMS *m/z* 691.132501 $[M + H]^+$ (calcd for $C_{34}H_{27}O_{16}$, 691.130458); CD (MeOH) 232 nm, + 52, 265 nm, -18, 285 nm, +5.

**The extraction of the leaves of *E. sphaericus*, *E. polydactylus*, and *E. densiflorus*:** Ground and dried leaf material of *E. sphaericus* (130 g), *E. polydactylus* (140 g) and *E. densiflorus* (139 g) were extracted in series by an identical procedure. A methanol extract of each species (5 L) was evaporated to 250 mL and filtered through PAG (~50 g). The filtrate was loaded onto SCX resin (50 g) and a methanol load fraction was obtained. The SCX resin was washed sequentially with methanol (1 L) and water (1 L), before alkaloid fractions were eluted with 1M NaCl (500 mL). The alkaloid/salt solution was filtered through C18 silica gel under vacuum, and the C18 (30 g) was washed with water (5 L). Alkaloid fractions were eluted with 1%TFA/MeOH (500 mL). The alkaloid fractions were evaporated and absorbed onto C18 silica gel (1.2 g). The C18/alkaloid was transferred into a small metal HPLC column (10 x 15 mm), and the column was connected in-line to a preparative C18 RP-HPLC column. Alkaloids were eluted into 60 fractions with a gradient from $H_2O$ to 1%TFA/MeOH over 180 minutes (flow rate 2 mL/min). Analysis of the fractions 16 – 29 by +ESIMS (m/z 258), and $^1H$ NMR of each

fractionation demonstrated that the same compounds were present in each species. The fractions from the separation of the *E. polydactylus* and *E. densiflorus* extracts revealed small quantities of alkaloids present and further attempts at purification were abandoned. Fractions 16 – 29 from the separation of the *E. sphaericus* extract were combined and purification was achieved by semi-preparative C18 RP-HPLC using isocratic conditions of 4:1 $H_2O$:1%TFA/ACN. Isoelaeocarpine (**61**) (0.8 mg, 0.00062%) was obtained by comparison with $^1$H NMR spectra of **61** purified from *E. fuscoides.*

**The extraction of *E. dolichostylus* and *E. kaniensis*:** The leaves of *E. dolichostylus* (120 g) and *E. kaniensis* (120 g) were extracted in an identical procedure. Voucher specimens for *E. dolichostylus* (1468) and *E. kaniensis* (909) are deposited at Biodiversity Ltd, at the University of Papua New Guinea, Port Moresby. The leaves of *E. dolichostylus* were collected from Wain, past Bumbu river, 50 km from Lae in the Morobe province of PNG. The leaves of *E. kaniensis* were collected from the Manegilli village swamp forest near Ialibu in the southern highlands province of PNG. A methanol extract of each species (5 L) was loaded onto SCX resin (50 g) and a methanol load fraction was obtained. The SCX resin was washed sequentially with methanol (1 L) and water (1 L), before alkaloid fractions were eluted with 1M NaCl (500 mL). The alkaloid/salt solution was filtered through C18 silica gel under vacuum, and the C18 (30 g) was washed with water (5 L). Alkaloid fractions were eluted with 1%TFA/MeOH (500 mL). The alkaloid fractions were evaporated (106.1 mg for *E. dolichostylus*, 108.5 mg for *E. kaniensis*) and absorbed onto C18 silica gel (1.2 g). The C18/alkaloid was transferred into a small metal HPLC column (10 x 15 mm), and the column was connected to a preparative C18 RP-HPLC column. Alkaloids were eluted into 100 fractions with a gradient from $H_2O$ to 1%TFA/MeOH over 100 minutes (flow rate 5 mL/min).

Fractions 24-33 from the fractionation of the *E. dolichostylus* extract were combined (+ESIMS *m/z* 258, 68.7 mg) and $^1$H NMR revealed the same compounds were present as purified from *E. fuscoides*. This mixture of compounds, elaeocarpine (**60**), isoelaeocarpine (**61**) and elaeocarpenine (**122**), was dissolved in methanol and filtered through SCX resin (15 g) and eluted with a solution of 3:2 ammonia:methanol (500 mL).

This alkaloid fraction was evaporated and the residue (65.3 mg) was absorbed onto C18 silica gel (1.2 g), which was transferred into an empty metal HPLC column (10 x 15 mm). This column was connected to semi-preparative C18 HPLC column, and the alkaloids were separated using a gradient from 3:1 to 1:3 $H_2O$:MeOH over 10 minutes. This afforded isoelaeocarpine (**61**) (6.1 mg), a 1:1 mixture of compounds **61** and **60** (32.7 mg) and elaeocarpine (**60**) (6.0 mg).

Fractions 33-35 and 36-38 from the fractionation of the *E. kaniensis* extract were purified by semi-preparative C18 RP-HPLC gradients of 3:2 to 1:4 $H_2O$:1% TFA/MeOH and 4:1 to 1:9 $H_2O$:1% TFA/MeOH, respectively. Sixty fractions were collected over 15 minutes for both separations. Impure compounds were detected in fractions 8-12 (+ESIMS *m/z* 191, 4.9 mg) from the separation of fractions 33-35, and in fractions 22-25 (+ESIMS *m/z* 194/196, 3.9 mg) from the separation of fractions 36-38. Both mixtures were subjected to normal phase DIOL isocratic HPLC (1:19 MeOH:DCM), however compounds were lost during separation.

## 9.3 Chapter 3 Experimental

**Plant Material.** Leaves of *E. habbeniensis* were collected by Topul Rali in January 1999 from the Manegilli village swamp forest, near Ialibu, in the southern highlands province of PNG. A voucher specimen, 910, is deposited at Biodiversity Ltd, at the University of Papua New Guinea, Port Moresby.

**The isolation of habbenine (114) from *E. habbeniensis*.** The air-dried leaves of *E. habbeniensis* (80.5 g) were ground and extracted with methanol at room temperature. The MeOH extract was filtered through polyamide gel (50 g) under vacuum and the filtrate was evaporated. The resulting residue (6.28 g) was dissolved in $H_2O$ (500 ml) and partitioned with DCM (500 mL). The aqueous layer gave a positive result in an alkaloid test. The aqueous layer was filtered through SCX resin and a 500 mL load fraction was

obtained. The SCX resin was washed with $H_2O$ (500 mL) before an alkaloid fraction was eluted with 1M NaCl solution (500 mL). The alkaloid fraction was evaporated under vacuum and the salt residue was suspended in a 1:1 $CHCl_3$:MeOH mixture (100 mL), which was filtered to remove NaCl. The filtrate (22.9 mg) was separated by Sephadex LH-20 column chromatography (60 x 2.5 cm). One hundred fractions were eluted with 100% MeOH. Fractions 33 and 34 were combined and re-chromatographed on LH-20 to afford habbenine (**114**) (7.7 mg, 0.0096%). Attempts to separate the diastereomers of **114** by analytical C18 RP-HPLC, using isocratic conditions of 84:15:1 $H_2O$:MeOH:TFA, 89:10:1 $H_2O$:ACN:TFA and 85:7:7:1 $H_2O$:MeOH:ACN:TFA, were unsuccessful. An attempted separation using normal phase HPLC on phenyl bonded silica, and isocratic elution with 94:5:1 $H_2O$:MeOH:TFA also proved unsuccessful. The PDA spectra of the attempted C18 RP-HPLC revealed one peak, however splitting of two peaks in a ratio of 1:1 was observed in the PDA spectra of the normal phase HPLC on phenyl bonded silica. These peaks could not be separated to baseline resolution.

**Habbenine trifluoroacetate (114):** yellow gum; $[\alpha]_D^{23}$ +13.73° (*c* 0.1334, MeOH), +11.55° (*c* 0.067, MeOH); UV (MeOH) $\lambda_{max}$ (log ε) 227 (3.35), 270 (2.85), 339 (2.70) nm; IR (KBr) $\upsilon_{max}$ 3400 br, 1712, 1674, 1201, 1127 $cm^{-1}$; $^1H$ (600 MHz, $d_6$-DMSO) and $^{13}C$ NMR (125 MHz, $d_6$-DMSO) Table 5; (+)-LRESIMS *m/z* (rel. int.): 280 (100%) $[MH^+, C_{16}H_{26}NO_3]^+$; (+)-HRESIMS *m/z* 280.18939 $[M + H]^+$ (calcd for $C_{16}H_{26}NO_3$, 280.19072).

## 9.4 Chapter 4 Experimental

**Plant Material.** Leaves of *E. fuscoides* Knuth., were collected and identified by Topul Rali (Biodiversity Ltd) on 14/08/99 from Kirene forest, Ialibu, Southern Highlands Province, Papua New Guniea. A voucher specimen, 1277, is deposited at Biodiversity Ltd, at the University of Papua New Guinea, Port Moresby.

**The isolation of isoelaeocarpicine (62), eleaocarpenine (122), isoelaeocarpine (61) and elaeocarpine (60) from *E. fuscoides*.** The dried and ground leaves of *E. fuscoides* (120 g) were extracted with methanol (3 L). The methanol extract was filtered through SCX resin (50 g). The resin was washed sequentially with 1 L each of methanol and water, prior to elution of an alkaloid fraction with 1M NaCl (1 L). The salt was removed from the alkaloid fraction by vacuum filtration through C18 RP silica gel chromatography. NaCl was removed by washing with copious amounts of $H_2O$ (5 L) prior to elution of the alkaloids with 1%TFA/MeOH (500 mL). The alkaloid fraction was evaporated and the residue (402.4 mg) was absorbed onto C18 silica gel (1.2 g) which was transferred into a metal HPLC column (10 x 15 mm). This column was connected to a preparative C18 RP-HPLC column and the alkaloids were separated into 50 fractions using a linear gradient from $H_2O$ to 1%TFA/MeOH over 100 minutes. Mass ion peaks of *m/z* 276 in fractions 13 – 20, and *m/z* 258 in fractions 21 - 24 and 26 – 31, were observed following analysis by +ESIMS. Semi-pure isoelaeocarpicine (**62**) was detected in fractions 13 - 20, pure elaeocarpenine (**122**) in fractions 21 - 24, and a mixture of two compounds in 26 - 31. Fractions 21 - 24 were combined to yield elaeocarpenine (**122**) (94.7 mg, 0.079%). Fractions 13 - 20 were combined and separated by semi-preparative C18 RP-HPLC employing a gradient of 3:1 $H_2O$:MeOH to 1%TFA/MeOH over 15 minutes. Fractions 29 to 31 were combined to yield isoelaeocarpicine (**62**) (4.0 mg, 0.0033%). Purification of the two compounds detected in fractions 26 - 31 (*m/z* 260) was performed by C18 RP-HPLC, with a gradient of 1:1 $H_2O$:MeOH to 1%TFA/MeOH over 15 minutes. Analysis of the fractions afforded isoelaeocarpine (**61**) (38.7 mg, 0.032%) in fractions 22 – 24, and elaeocarpine (**60**) (17.6 mg, 0.011%) in fractions 27- 31.

**Isoelaeocarpicine trifluoroacetate (62):** yellow gum; $[\alpha]_D^{23}$ +6.19º (*c* 0.067, MeOH), +9.25º (*c* 0.1334, MeOH) (lit. +29º, *c* 0.30, $CHCl_3$); $^1H$ (600 MHz, $d_6$-DMSO) and $^{13}C$ NMR (125 MHz, $d_6$-DMSO) Table 7; (+)-LRESIMS *m/z* (rel. int.): 276 (75%) $[MH^+, C_{16}H_{22}NO_3]^+$, 258 (25%) $[MH^+ - H_2O]^+$.

**Elaeocarpenine trifluoroacetate (122):** yellow gum; $[\alpha]_D^{23}$ 0º (*c* 0.067 and 0.1334, MeOH); UV (MeOH) $\lambda_{max}$ (log ε) 223 (3.29) nm; IR (KBr) $\upsilon_{max}$ 3404 br, 1683, 1461,

1281, 1199, 1123, 720 $cm^{-1}$; $^1H$ (600 MHz, $d_6$-DMSO) and $^{13}C$ NMR (125 MHz, $d_6$-DMSO) Table 6; (+)-LRESIMS *m/z* (rel. int.): 258 (100%) $[MH^+, C_{16}H_{20}NO_2]^+$; (+)-HRESIMS *m/z* 258.1490 $[M + H]^+$ (calcd for $C_{16}H_{20}NO_2$, 258.14886).

**Isoelaeocarpine (61):** yellow gum; $[\alpha]_D^{23}$ +14.49º (*c* 0.067, MeOH) (lit. +0.15º, *c* 3.41, $CHCl_3$); $^1H$ NMR (600 MHz, $d_6$-DMSO) see Table 8; $^1H$ NMR (500 MHz, $CD_2Cl_2$) δ 1.68 (1H, m, H-2a), 1.70 (2H, m, $H_2$-1), 1.79 (1H, ddd, *J* = 3.0, 10.0, 15.0 Hz, H-2b), 2.03 (1H, ddd, *J* = 3.1, 5.0, 14.5 Hz, H-6a), 2.12 (1H, dd, *J* = 2.0, 14.5 Hz, H-6b), 2.23 (1H, dd, *J* = 9.5, 18.0 Hz, H-3a), 2.37 (1H, ddd, *J* = 3.8, 9.0, 9.0 Hz, H-9), 2.49 (1H, brd, *J* = 11.5 Hz, H-8), 2.60 (3H, s, $H_3$-17), 2.63 (1H, m, H-5a), 3.08 (1H, dd, *J* = 5.0, 11.5 Hz, H-5b), 3.16 (1H, brdd, *J* = 8.5, 8.5 Hz, H-3b), 4.65 (1H, brdd, *J* = 3.0, 3.0 Hz, H-7), 6.79 (1H, d, *J* = 7.0 Hz, H-15), 6.84 (1H, d, *J* = 8.5 Hz, H-13), 7.32 (1H, dd, *J* = 8.0, 8.0 Hz, H-14); $^{13}C$ NMR (125 MHz, $CD_2Cl_2$) Table 6; (+)-LRESIMS *m/z* (rel. int.): 258 (100%) $[MH^+, C_{16}H_{20}NO_2]^+$.

**Elaeocarpine (60):** yellow gum; $[\alpha]_D^{23}$ +12.36º (*c* 0.067, MeOH) (lit. +0.4º, *c* 1.91, $CHCl_3$); $^1H$ NMR (600 MHz, $d_6$-DMSO) see Table 9; $^1H$ NMR (500 MHz, $CD_2Cl_2$) 1.82 (1H, ddd, *J* = 3.0, 10.5, 18.0 Hz, H-1a), 1.98 (2H, m, $H_2$-2), 2.31 (2H, brt, *J* = 5.5 Hz, $H_2$-6), 2.47 (2H, m, H-3a, H-5a), 2.57 (3H, s, $H_3$-16-Me), 2.61 (1H, br, H-9), 2.69 (1H, ddd, *J* = 5.0, 5.0, 10.0 Hz, H-1b), 2.96 (1H, brdd, *J* = 11.0, 11.0 Hz, H-8), 3.36 (1H, brdd, *J* = 10.5, 10.5 Hz, H-3b), 3.45 (1H, brd, *J* = 12.0 Hz, H-5b), 4.26 (1H, ddd, *J* = 6.5, 9.5, 12.5 Hz, H-7), 6.82 (2H, dd, *J* = 8.5, 8.5 Hz, H-13, H-15), 7.32 (1H, dd, *J* = 8.0, 8.0 Hz, H-14); $^{13}C$ NMR (125 MHz, $CD_2Cl_2$) Table 7; (+)-LRESIMS *m/z* (rel. int.): 258 (100%) [M, $C_{16}H_{20}NO_2]^+$.

**The conversion of 122 to 60 and 61:** The conversion of elaeocarpenine (**122**) to isoelaeocarpine (**61**) and elaeocarpine (**60**) was observed upon reacting **122** (5.2 mg) with an excess of ammonia in methanol (2 mL). The reaction mixture was evaporated and separated by reversed phase semi-preparative HPLC, employing a gradient from 3:1 to 1:3 $H_2O$:MeOH over 10 minutes. This afforded isoelaeocarpine (**61**) (1.2 mg), and

elaeocarpine (**60**) (1.2 mg). The optical rotations of **61** and **60** purified from this reaction were +11.43 and +9.66 (c 0.067, MeOH), respectively.

## 9.5 Chapter 5 Experimental

**Plant material.** The leaves, bark and seeds of *P. mearsii* were collected in north Queensland by Paul Forster. Voucher specimens, for the leaves (0324119804023959, 0.14100004026336) and bark (0424119204023959) are located at the Queensland Herbarium.

**The isolation of peripentonine (123), peripentadenine (81), mearsamine 1 (124) and 2 (125).** The dried and ground leaves of *P. mearsii* (42.18 g) were extracted with methanol (3 L) and the extract was evaporated. The resulting residue (4.79 g) was dissolved in $H_2O$ (500 mL) and partitioned three times with DCM (500 mL). The organic layer was discarded. The alkaloid containing aqueous layer was filtered through SCX resin (36 g) and peripentonine (**123**) was eluted with 1M NaCl (700 mL). Evaporation of this salt solution, followed by re-suspension of the residue in 1:1 $CHCl_3$:MeOH (100 mL) and filtration yielded pure peripentonine (**123**) (45.5 mg, 0.108 %).

The dried and ground leaves of *P. mearsii* (50.79 g) were extracted with methanol (3 L). The extract was filtered through SCX resin under vacuum and washed sequentially with MeOH (1 L) and $H_2O$ (1 L). Alkaloids were eluted from the SCX resin with 1M NaCl (1 L). The alkaloid/NaCl solution was filtered through C18 (27 g) silica gel under vacuum. The NaCl was separated from the alkaloids by extensive washing of the C18 with $H_2O$ (5 L) and an alkaloid fraction was eluted with 1% TFA/MeOH (500 mL). This alkaloid fraction was evaporated and the residue (108.7 mg) was absorbed onto C18 silica gel (1.2 g). The alkaloid impregnated C18 was loaded into a metal HPLC column (10 x 15 mm), which was connected in-line to a preparative C18 RP-HPLC column. The alkaloids were separated into 50 fractions with a gradient from $H_2O$ to 1% TFA/MeOH over 100

minutes. Fractions 22 and 23 were found to be pure mearsamine 1 (**124**) (11.2 mg, 0.0221%), fraction 25 yielded pure mearsamine 2 (**125**) (13.2 mg, 0.0260%) and fractions 28 – 32 yielded pure peripentonine (**123**) (33.2 mg, 0.636%).

Purification of the bark of *P. mearsii* was achieved by the same methanol extraction, SCX/C18 filtration and preparative C18 gradient HPLC protocol as discussed for the leaves of *P. mearsii*. The bark of *P. mearsii* yielded peripentadenine (**81**) (19.0 mg, 0.0127%) in fractions 34 - 36 of the preparative C18 HPLC separation.

Extraction of the seeds of *P. mearsii* was achieved by the same methanol extraction, SCX/C18 filtration and preparative C18 gradient HPLC protocol as described for the leaves of *P. mearsii*. The bark of *P. mearsii* (150 g) yielded peripentadenine (**81**) (19.0 mg, 0.0127 %) from fractions 34 - 36 of the preparative C18 HPLC separation. The extraction of the bark of *P. mearsii* (50 g) was performed in an identical manner. The extract of the bark of *P. mearsii* yielded peripentadenine (**81**) (3.2 mg, 0.0064%). Peripentonine (**123**) (18.7 mg, 0.0468%) was purified from the seeds of *P. mearsii,* and was obtained from fractions 34 - 36 of the preparative C18 HPLC separation.

**Peripentonine trifluoroacetate (123):** yellow gum; $[\alpha]_D^{23}$ +18.97$^o$ (*c* 0.1334, MeOH), +15.06$^o$ (*c* 0.067, MeOH); UV (MeOH) $\lambda_{max}$ (log ε) 226 (3.45), 339 (2.81) nm; IR (KBr) $\upsilon_{max}$ 3410, 3294 br, 2967, 2926, 1667, 1543, 1415, 1193, 1123, 715 cm$^{-1}$; $^1$H (600 MHz, $CD_3CN$) and $^{13}$C NMR (125 MHz, $CD_3CN$) Table 10; (+)-LRESIMS *m/z* (rel. int.): 377 (75%) $[MH^+, C_{22}H_{37}N_2O_3]^+$, 225 (25%) (+)-HRESIMS *m/z* 377.279196 $[M + H]^+$ (calcd for $C_{22}H_{37}N_2O_3$, 377.279869).

**Peripentadenine trifluoroacetate (81):** yellow gum; $[\alpha]_D^{23}$ 0$^o$ (*c* 0.067 and 0.1334, MeOH); $^1$H (600 MHz, $d_6$-DMSO) and $^{13}$C NMR (125 MHz, $d_6$-DMSO) Table 11; (+)-LRESIMS *m/z* (rel. int.): 375 (100%) $[MH^+, C_{22}H_{35}N_2O_3]^+$.

**Mearsamine 1 trifluoroacetate (124):** yellow gum; $[\alpha]_D^{23}$ -5.81$^o$ (*c* 0.067, MeOH), -5.99$^o$ (*c* 0.1334, MeOH); UV (MeOH) $\lambda_{max}$ (log ε) 204 (2.62), 269 (2.05), 339 (1.73) nm;

IR (KBr) $\upsilon_{max}$ 3404 br, 2955, 2920, 1683, 1438, 1199, 1152 $cm^{-1}$; $^{1}H$ (600 MHz, $d_6$-DMSO) and $^{13}C$ NMR (125 MHz, $d_6$-DMSO) Table 12; (+)-LRESMS *m/z* (rel. int.): 285 (100%) $[MH^+, C_{15}H_{29}N_2O_3]^+$; (+)-HRESIMS *m/z* 285.215921 $[M + H]^+$ (calcd for $C_{15}H_{29}N_2O_3$, 285.217269).

**Mearsamine 2 trifluoroacetate (125):** yellow gum; $[\alpha]_D^{23}$ -1.54° (*c* 0.067, MeOH); UV (MeOH) $\lambda_{max}$ (log ε) 202 (3.14), 265 (3.38) nm; IR (KBr) $\upsilon_{max}$ 3457 br, 3288 br, 2973, 2932, 2873, 1677, 1555, 1426, 1187, 1123 $cm^{-1}$; $^{1}H$ (600 MHz, $d_6$-DMSO) and $^{13}C$ NMR (125 MHz, $d_6$-DMSO) Table 13; (+)-LRESIMS *m/z* (rel. int.): 395 (100%) $[MH^+, C_{22}H_{39}N_2O_4]^+$; (+)-HRESIMS *m/z* 395.290601 $[M + H]^+$ (calcd for $C_{22}H_{39}N_2O_4$, 395.290434).

**The dehydration of peripentonine (123):** Peripentonine (**123**) (44.0 mg) was dissolved in 5 mL of ethanol. Pd/C (23.2 mg) was added and was allowed to stir under reflux for 16 hours at 90ºC. The reaction mixture was filtered through celite with methanol (250 mL) to remove the Pd/C. The filtrate was separated by semi-preparative C18 RP-HPLC using a gradient from 7:3 to 1:4 $H_2O$:1%TFA/MeOH to yield peripentadenine (**81**) (25.5 mg, 63%). The optical rotation of **81** from this reaction was 0°.

## 9.6 Chapter 6 Experimental

**Plant Material.** Leaves of *E. grandis* were collected in December 2001 from Mt. Tamborine in south east Queensland, by Anthony Carroll. A voucher specimen, 0328119704021918, is located at the Queensland Herbarium. A second collection of the leaves of *E. grandis* was undertaken in January 2004 by Paul Forster (Queensland Herbarium) in north Queensland.

**The isolation of isoelaeocarpiline (63), grandisine C (127), D (126) and E (128) from *E. grandis* by an SCX extraction procedure.** The dried and ground leaves (293.7 g) of *E. grandis* were extracted exhaustively with MeOH (3.0 L). The MeOH extract was

filtered through 50g of SCX resin under vacuum. The SCX resin was washed several times with MeOH (1.0 L), and then with water (1.0 L) before the alkaloids were eluted using 1M NaCl (500 mL). The eluant was filtered through C18, the C18 was washed with copious amounts of water (5 L) and the alkaloids eluted with 1%TFA/MeOH (500 mL). The alkaloid fraction was evaporated to yield a residue (180.3 mg) which was absorbed onto C18 (1.2 g). The C18 silica gel containing the alkaloids was transferred into a small metal HPLC column (10 x 15 mm) and connected to a preparative C18 RP-HPLC column. The alkaloids were separated by a linear gradient from $H_2O$ to 1%TFA/MeOH over 100 minutes. Fifty fractions were collected and analysed by +ESIMS. Mass ion peaks of *m/z* 278 in fractions 14 and 18, and *m/z* 260 in fractions 19 - 24, were observed. The $^1$H NMR spectra of individual fractions showed semi-pure grandisine C (**127**) and E (**128**) in fractions 14 and 18, respectively. Fractions 19 and 20, and 22 - 24 were combined to yield semi-pure grandisine D (**126**) and isoelaeocarpiline (**63**), respectively. Isoelaeocarpiline (**63**), grandisine C (**127**), D (**126**) and E (**128**) were purified by isocratic C18 RP-HPLC. Conditions of 17:3 $H_2O$:1%TFA/MeOH were used to purify grandisine C (**127**) (2.7 mg, 0.00092%) and E (**128**) (0.8mg, 0.00027%). Grandisine D (**126**) (3.3 mg, 0.0011%) was purified from fractions 19 – 20 by conditions of 4:1 $H_2O$:1%TFA/MeOH. Isoelaeocarpiline (**63**) (3.4 mg, 0.0012%) was purified from fractions 22 – 24 by isocratic C18 HPLC conditions of 3:1 $H_2O$:1%TFA/MeOH.

**Isoelaeocarpiline (63)**: yellow gum (3.4 mg, 0.00092%); $[\alpha]_D^{23}$ +112.10$^o$ (c 0.067, MeOH), +77.34$^o$ (c 0.1334, MeOH); $^1$H (600 MHz, $CDCl_3$) and $^{13}$C NMR (125 MHz, $CDCl_3$) Table 14; (+)-LRESIMS *m/z* (rel. int.): 260 (100%) $[MH^+, C_{16}H_{22}NO_2]^+$.

**Grandisine C** (**127**): yellow gum (2.7 mg, 0.00092%); $[\alpha]_D^{23}$ –2.79$^o$ (c 0.067, MeOH), –9.66$^o$ (c 0.1334, MeOH); UV (MeOH) $\lambda_{max}$ (log ε) 204 (3.39), 273 (3.56) nm; IR (NaCl) $\nu_{max}$ 3367, 2956, 1664, 1604, 1406, 1182, 1056, 754 cm$^{-1}$; $^1$H (600 MHz, $CDCl_3$) and $^{13}$C NMR (125 MHz, $CDCl_3$) Table 16; (+)-LRESIMS *m/z* (rel. int.): 278 (100%) $[MH^+, C_{16}H_{24}NO_3]^+$; (+)-HRESIMS *m/z* 278.14709 $[M + H]^+$ (calcd for $C_{16}H_{24}NO_3$, 278.17507).

**Grandisine D trifluoroacetate** (**126**): yellow gum (3.3 mg, 0.0011%); $[\alpha]_D^{23}$ +10.24° (c 0.0067, MeOH), +18.34° (c 0.1334, MeOH); UV (MeOH) $\lambda_{max}$ (log ε) 222 (3.28), 267 (2.80), 325 (2.43) nm; IR (KBr) $\nu_{max}$ 3419, 1652, 1208, 1125 $cm^{-1}$; $^1H$ NMR (600 MHz, $d_6$-DMSO) Table 15, and $^{13}C$ NMR (125 MHz, $d_6$-DMSO) Table 13; (+)-LRESIMS *m/z* (rel. int.): 260 (100%) $[MH^+, C_{16}H_{22}NO_2]^+$. (+)-HRESIMS *m/z* 260.16502 $[M + H]^+$ (calcd for $C_{16}H_{22}NO_2$, 260.16451).

**Grandisine E** (**128**): unstable colorless gum (0.8 mg, 0.00027%); $[\alpha]_D$ was not measured; UV (MeOH) $\lambda_{max}$ (log ε) 272 (1.14) nm; IR (NaCl) $\nu_{max}$ 3419, 1646, 1318, 1318, 1203, 1134$cm^{-1}$; $^1H$ (600 MHz, $CDCl_3$) and $^{13}C$ NMR (125 MHz, $CDCl_3$) Table 17; (+)-LRESIMS *m/z* (rel. int.): 278 (100%) $[MH^+, C_{16}H_{24}NO_3]^+$. (+)-HRESIMS *m/z* 278.17578 $[M + H]^+$ (calcd for $C_{16}H_{24}NO_3$, 278.17507).

**The isolation of isoelaeocarpiline (63), grandisine C (127), D (126), F (129), G (130) and 131 from *E. grandis* by an acid/base extraction procedure.** The ground dried leaves of *E. grandis* (1.73 kg) were initially extracted with 32% $NH_3$ solution (500 mL) followed by an exhaustive extraction with DCM (10 L). The extraction of the ground leaves was carried out in 500 g batches, with 500 g of leaf material placed in a large scintered funnel lined with filter paper. DCM was filtered through the ground leaves under vacuum. The DCM extract was separated from the aqueous ammonia. The volume of the organic extract was reduced under vacuum, and was subsequently partitioned with aq. $H_2SO_4$ (1.5 L, pH 1). The organic layer of this partition was discarded (2 L). The aqueous layer was then basified with $NH_3$ to pH 10 and partitioned three times with DCM (2 L). The presence of alkaloids in this organic layer was determined by +ESIMS. This alkaloid fraction was evaporated to dryness. The residue (1.69 g) was absorbed onto 2 g of C18 silica gel which was transferred into an empty metal HPLC column (5 x 1.5 cm). This column was connected to a large metal MPLC column (30 x 3.5 cm) containing C18 silica gel. The alkaloids were separated into 100 fractions using a gradient of $H_2O$ to 1%TFA/MeOH over 200 minutes. Two sets of pooled fractions were obtained from this separation. Fractions 27 to 43 and 44 to 48 were combined on the basis of similar $^1H$

NMR spectra and mass ion peaks in the +ESIMS. The combined fraction of 27 - 43 contained mass ion peaks of *m/z* 277, 278, 291 and 296. A mass ion peak of *m/z* 260 was detected for the combined fractions of 44-48. Analysis of this fraction by $^{1}$H NMR demonstrated a mixture of grandisine D (**126**) and isoelaeocarpiline (**63**) was present. A C18 RP-HPLC gradient of 3:2 to 9:11 $H_2O$:1%TFA/MeOH over 15 minutes was used to separate the combined fractions of 44 – 48. A total of 45 fractions were collected, which yielded **126** (63.3 mg, 0.0037%) in fractions 10 to 18, and **63** (148 mg, 0.0086%) in fractions 19-30. The pooled fraction of 27 to 43 was separated into 50 fractions by preparative C18 RP-HPLC using a gradient of $H_2O$ to 1:4 $H_2O$/1%TFA over 100 minutes. Pure grandisine C (**127**) (6.8 mg, 0.00039%) was detected in fractions 10 to 17. The mass ion peak of *m/z* 296 was observed in fractions 18 to 25 by +ESIMS. Purification of these combined fractions was achieved by a C18 RP-HPLC gradient of 4:1 to 3:2 $H_2O$:1%TFA/MeOH. A pure mixture of two diastereomeric compounds **131** (2.1 mg) was obtained from the early eluting fractions 2-7. An attempt was made to separate this mixture by semi-preparative C18 RP-HPLC isocratic conditions of 4:1 $H_2O$:1%TFA/MeOH, however the separation was not successful.

Mass ion peaks of *m/z* 277 and 260 were detected in fractions 27 to 30 from the preparative C18 RP-HPLC separation. These fractions were combined and separated into 50 fractions by semi-preparative C18 RP-HPLC using a gradient of 4:1 to 2:3 $H_2O$:1%TFA/MeOH over 25 minutes. The mass ion peaks of *m/z* 277 and 260 were observed in fractions 14 – 24 and 32 – 34, respectively. Analysis by $^{1}$H NMR revealed fractions 32 to 34 to be grandisine D (**126**) (5.3 mg, 0.00031%). A mixture of diastereomers of grandisine F (**129**) (21.1 mg, 0.0012%) was detected in fractions 18 – 24. Fractions 14 – 17 yielded grandisine F (**129**) (5.1 mg, 0.00029%).

The mass ion peak of m/z 291 was detected by +ESIMS in fractions 31 to 36 from the preparative C18 RP-HPLC separation. These fractions were combined and purification of grandisine G (**130**) was achieved by a semi-preparative C18 RP-HPLC gradient of 7:3 to 2:3 $H_2O$:1%TFA/MeOH. Sixty fractions were collected over 20 minutes. Grandisine G (**130**) was detected in fractions 22 – 24 (3.8 mg, 0.00022%)

**Grandisine F (129):** yellow gum (5.1 mg, 0.0011%); $[\alpha]_D^{23}$ +5.52$^o$ (*c* 0.067, MeOH); UV (MeOH) $\lambda_{max}$ (log ε) 202 (3.20), 274 (3.50) nm; IR (NaCl) $\nu_{max}$ 3292, 2929, 2800, 1654, 1608, 1406, 1181, 752 cm$^{-1}$; $^1$H (600 MHz, $d_6$-DMSO) and $^{13}$C NMR (125 MHz, $d_6$-DMSO) Table 18; (+)-LRESIMS *m/z* (rel. int.): 277 (100%) [MH$^+$, $C_{16}H_{25}N_2O_2]^+$. (+)-HRESIMS *m/z* 277.190345 [M + H]$^+$ (calcd for $C_{16}H_{25}N_2O_2$, 277.191054).

**Grandisine G trifluoroacetate** (**130**): unstable yellow gum (3.8 mg, 0.0011%); UV (MeOH) $\lambda_{max}$ (log ε) 209 (3.39), 271 (3.08), 308 (3.00) nm; IR (NaCl) $\nu_{max}$ 3400, 2957, 1681, 1415, 1200, 1130, 830, 799, 754, 720 cm$^{-1}$; $^1$H (600 MHz, $d_6$-DMSO) and $^{13}$C NMR (125 MHz, $d_6$-DMSO) Table 19; (+)-LRESIMS *m/z* (rel. int.): 291 (100%) [MH$^+$, $C_{17}H_{27}N_2O_2]^+$; (+)-HRESIMS not measured as the compound was unstable.

**Compounds 131a and b**: unstable colourless gum (2.1 mg, 0.0011%); UV (MeOH) $\lambda_{max}$ (log ε) 205 (3.40), 273 (3.04) nm; IR (NaCl) $\nu_{max}$ 3305, 2930, 2817, 1713, 1650, 1600, 1461, 1371, 1309, 1161, 1104, 1009, 753 cm$^{-1}$; $^1$H (600 MHz, $d_6$-DMSO) and $^{13}$C NMR (125 MHz, $d_6$-DMSO) Tables 20 and 21; (+)-LRESIMS *m/z* (rel. int.): 296 (100%) [MH$^+$, $C_{16}H_{26}NO_4]^+$. (+)-HRESIMS *m/z* 296.183698 [M + H]$^+$ (calcd for $C_{16}H_{26}NO_4$, 296.185635).

## 9.7 Chapter 7 Experimental

Compounds were screened in triplicate 11-point CRC in a 96-well format. DPDPE (**144**) and naloxone (**138**) were used as positive controls and were screened in duplicate. Assay protocol involved the addition of 40 µL of $H_2O$ (10% DMSO) containing variable concentration of compound, followed by subsequent addition of 80 µL of [$^{125}$I]-Deltorphin (56 pM, binding buffer) and finally 80 µL of membrane (0.047 mg/mL, binding buffer). Final concentration of DMSO was 2%. Plates were sealed and shaken at room temperature for 1 hour. Plates were harvested using a Brandel harvester with wash buffer. Filtermats used for harvesting were pre-soaked in 0.1% PEI and were allowed to

dry at 50°C for 30 minutes after harvest. Filtermats were sealed in plastic with scintillant (BetaScint) which were counted for one minute per well by a Wallac Microbeta Trilux. Binding buffer contained 50 mM Tris (Sigma), 3mM $MgCl_2$ (Sigma) at pH 7.1 with 1 mg/mL of BSA (Sigma) added. Wash buffer contained 50 mM Tris, 3 mM $MgCl_2$ at pH 7.1 which was stored at 4°C. [$^{125}$I]-Deltorphin II radioactive ligand, code IMQ1595, pack size 100 μCi, was purchased from Amersham Biosciences as a lyophilized solid. HEK cell membranes expressing recombinant human δ opioid receptors were obtained from AstraZeneca Montreal. Data analysis of radioactive counts per minute was achieved by GraphPad Prism 4, CA., USA, to determine potency ($IC_{50}$) and hill slope ($n_H$).

## 9.8 Chapter 8 Experimental

**The re-isolation of isoelaeocarpiline (63) from the leaves of *E. grandis*:** Dried and ground leaves of *E. grandis* (1.35 kg) were extracted with DCM (10 L). The DCM extract was evaporated and partitioned between hexane (500 mL) and methanol (500 mL). The hexane layer was discarded and the methanol was evaporated. The residue was partitioned between 1%TFA/$H_2O$ (500 mL) and DCM (500 mL). The aqueous layer was evaporated and separated into 100 fractions by C18 RP-MPLC (22 x 2.5 cm) using a gradient of $H_2O$ to 1%TFA/MeOH over 200 minutes. Fractions 20 to 22 were found to be grandisine C (**127**) (5.8 mg, 0.0004%) and were not purified further. The combined fractions of 29-37 and 40-48 were shown by $^1$H NMR to be grandisine D (**126**) and isoelaeocarpiline (**63**), respectively. Grandisine D (83.8 mg, 0.0062%) was purified by semi-preparative C18 RP-HPLC using a gradient from 7:3 to 3:7 $H_2O$:1%TFA/MeOH over 15 minutes. Isoelaeocarpiline (93.5 mg, 0.0069%) was purified by the same conditions on preparative C18 RP-HPLC.

**The dehydrogenation of isoelaeocarpiline (63) to isoelaeocarpine (61):** Isoelaeocarpiline (**63**) (148 mg) was dissolved in 5 mL of ethanol. Pd/C (77 mg) was added and the mixture was stirred under reflux for 16 hours at 90ºC. The reaction mixture

was filtered through celite (20 g) to remove the Pd/C and washed with methanol (250 mL). The filtrate was separated by semi-preparative C18 RP-HPLC using a gradient from 7:3 to 1:4 $H_2O$:1%TFA/MeOH, to yield isoelaeocarpine (**61**) (81.6 mg, 55%). The optical rotation of **61** produced from this reaction was +25.22$^o$ (*c* 0.067, MeOH), +20.27$^o$ (*c* 0.1334, MeOH). A further 65.6 mg of isoelaeocarpine (**61**) was obtained from the dehydrogenation of 93.5 mg of isoelaeocarpiline (**63**).

**The dehydrogenation of grandisine D (126) to elaeocarpine (60) and isoelaeocarpiline (61):** Grandisine D (**126**) (83.8 mg) was dissolved in ethanol (5 mL), Pd/C (50.2 mg) was added and the mixture was stirred for 16 hours under refluxing conditions. The reaction mixture was filtered through celite (20 g) to remove the Pd/C and washed with methanol (250 mL). The filtrate was separated by C18 RP-HPLC using a gradient from 3:1 to 1:3 $H_2O$:MeOH over 10 minutes to yield isoelaeocarpine (**61**) (23.4 mg, 27.9%) and elaeocarpine (**60**) (23.8 mg, 28.4%).

**The attempted reaction of isoelaeocarpine (61) with hydrogen bromide:** Isoelaeocarpine (**61**) (12.6 mg) was dissolved in 1% AcOH/$H_2O$ (3 mL) and HBr (100 µL) was added. The reaction was stirred under reflux at 100$^o$C for 16 hours. The reaction mixture was cooled to room temperuature and the mixture was evaporated yielding a residue (14.3 mg). The residue was dissolved in methanol and filtered. The filtrate was evaporated to yield a residue (12.2 mg), and the $^1$H NMR spectrum of the residue was acquired in $d_6$-DMSO at 500 MHz. The $^1$H NMR spectrum revealed unreacted isoelaeocarpine (**61**).

**The reaction of isoelaeocarpine (61) with sodium methoxide and benzyl bromide to afford 186:** Isoelaeocarpine (9.6 mg) was dissolved in methanol (2.5 mL), 1.5 equivalents of 0.5 M sodium methoxide (20 µL) and two equivalents of benzyl bromide (15 µL) were added. The reaction was monitored by +ESIMS after four hours of stirring at room temperature. Three major mass ion peaks were observed at *m/z* 348, 438 and 528 in a ratio of 10:6:2. A further three equivalents of benzyl bromide (20 µL) was added and the reaction mixture was stirred at room temperature for a further 16 hours. The reaction

was again monitored by +ESIMS and this indicated that the major product was a compound with a mass ion peak at *m/z* 528 (relative intensity 65%), followed by two minor peaks at *m/z* 438 (23%) and 348 (12%). The reaction mixture was evaporated and separated into 40 fractions by C18 RP-HPLC using a gradient of 100 % $H_2O$ to 3:7 $H_2O$:1% TFA/MeOH. Fraction 29 yielded **168** (1.2 mg, 6.11%, *m/z* 528). The mass ion peaks at *m/z* 438 and 348 were detected in the fraction 24 and 18 respectively, however insufficient amounts were obtained for structure elucidation.

**Compound 168:** $^1$H (600 MHz, $d_6$-DMSO) δ 1.82 (1H, dddd, *J* = 6.6, 11.4, 11.4, 11.8 Hz), 2.05 (1H, m), 2.06 (3H, s), 2.18 (1H, m), 2.37 (1H, ddd, *J* = 3.0, 3.0, 14.4 Hz), 3.41 (1H, ddd, *J* = 2.4, 2.4, 9.0 Hz), 3.54 (1H, brdd, *J* = 10.2, 18.0 Hz), 3.64 (1H, dd, *J* = 6.0, 12.0 Hz), 3.97 (1H, ddd, *J* = 2.6, 3.6, 18.0 Hz), 4.11 (1H, d, 7.8), 4.20 (1H, d, 7.8), 4.50 (1H, m), 4.59 (1H, d, 12.0), 4.64 (1H, 12.0), 5.11 (1H, d, 12.0), 5.14 (1H, d, 12.0), 5.53 (1H, ddd, *J* = 1.8, 5.2, 10.2 Hz), 5.80 (1H, dd, *J* = 2.8, 10.8 Hz), 6.98 (1H, d, 7.8), 7.13 (2H, m), 7.16 (3H, d, 7.8), 7.29 (6H, m), 7.35 (3H, m), 7.43 (2H, m), 7.45 (1H, m); (+)-LRESIMS *m/z* (rel. int.): 528 (100%) $[M^+, C_{37}H_{38}NO_2]^+$.

**The re-isolation of peripentonine (123) from the leaves of *P. mearsii*:** Dried and ground leaves of *P. mearsii* (745 g) were extracted with methanol (6.5 L). The extract was filtered through SCX resin (53 g). A methanol load fraction was collected, and the SCX resin was washed sequentially with methanol (2 L) and water (2 L) before an alkaloid fraction was eluted with 1M NaCl (2 L). The alkaloid fraction was filtered through C18 silica gel (48 g) under vacuum. The C18 was washed with water (8 L) and the alkaloids were eluted with 1% TFA/MeOH (2 L). The eluant was evaporated (1.57 g) and absorbed onto C18 (2.6 g). The alkaloid/C18 was placed on top of a large metal MPLC column (22 x 2.5 cm) packed with C18 silica gel. Alkaloids were eluted into 100 fractions from the column by a gradient of $H_2O$ to 1% TFA/MeOH over 200 minutes. Mearsamine 2 (**125**) (28.8 mg, 0.0039%) was detected in fractions 72 to 77 and peripentonine (**123**) (1.12 g, 0.15%) was obtained from the pooling of fractions 78 to 96.

**The dehydration of peripentonine (123) to peripentadenine (81):** Peripentonine (**123**) (332 mg) was dissolved in 15 mL of ethanol. Pd/C (182 mg) was added and was allowed to stir under reflux for 16 hours at 90ºC. The reaction mixture was filtered through celite (20 g) to remove the Pd/C and washed with methanol (250 mL). The filtrate was evaporated and separated by semi-preparative C18 RP-HPLC using a gradient from 7:3 to 1:4 $H_2O$:1%TFA/MeOH to yield peripentadenine (**81**) (213 mg, 64%).

**The reaction of peripentonine (123) and DDQ:** Peripentonine (**123**) (14.7 mg) was dissolved in ethanol (5 mL) and two equivalents of DDQ (17.6 mg) was added. The reaction was allowed to stir at 90$^o$C for 16 hours. The reaction mixture was evaporated and analyzed by $^1$H NMR. Analysis of the product mixture by $^1$H NMR indicated that the majority of peripentonine was unreacted. A small amount of the desired product, peripentadenine (**81**), was detected. This small quantity of **81** was not separated by HPLC.

**The reductive amination of acetophenone (170) with 4-methoxyphenethylamine using a catalytic amount of titantium isopropyloxide to afford 171:** Acetophenone (50 mg) was added to DCE (1 mL) followed by the addition of 1.3:0.2:3 equivalents of 4-methoxyphenethylamine (85 μL), $Ti(O^iPr)_4$ (5 μL) and $NaBH(OAc)_3$ (250 mg), respectively. After stirring for 16 hours at room temperature, water (1 mL) was added to the product mixture and partitioned with DCE. The DCE layer was separated from the aq. layer and purified by semi-preparative C18 RP-HPLC using a gradient from $H_2O$ to 1%TFA/MeOH over 15 minutes which yielded *N*-[2-(4-methoxyphenyl)ethyl]-1-phenylethylamine (**171**) (25.6 mg, 23.9%).

***N*-[2-(4-methoxyphenyl)ethyl]-1-phenylethylamine (171):** $^1$H (600 MHz, $d_6$-DMSO) δ 1.56 (3H, d, $J$ = 7.8 Hz), 2.80 (2H, m), 2.83 (1H, m), 3.01 (1H, dd, $J$ = 5.4, 9.6 Hz), 3.70 (3H, s), 4.41 (1H, dd, $J$ = 7.8, 7.8 Hz), 6.84 (2H, d, $J$ = 10.2 Hz), 7.07 (2H, d, $J$ = 10.2 Hz), 7.41 (1H, dd, $J$ = 9.0, 9.0 Hz), 7.45 (2H, dd, $J$ = 9.0, 9.0 Hz), 7.52 (2H, d, $J$ = 9.0 Hz), 9.05 (1H, br), 9.30 (1H, br); $^{13}$C NMR (125 MHz, $d_6$-DMSO) δ 19.0 (1C), 30.7 (1C), 46.3 (1C), 55.0 (1C), 57.0 (1C), 114.0 (2C), 127.6 (2C), 128.7 (1C), 129.0 (2C), 129.5

(2C), 137.1 (1C), 158.1 (1C); (+)-LRESIMS *m/z* (rel. int.): 256 (100%) [$MH^+$, $C_{17}H_{22}NO]^+$.

**The reductive amination of acetophenone (170) with 2-chlorobenzyl amine using a catalytic amount of titantium isopropyloxide to afford 172:** Acetophenone (50 mg) was added to DCE (1 mL) followed by the addition of 1.3:0.2:3 equivalents of 2-chlorobenzyl amine (80 µL), $Ti(O^iPr)_4$ (5 µL) and $NaBH(OAc)_3$ (250 mg), respectively. After stirring for 16 hours at room temperature, water (1 mL) was added to the product mixture and partitioned with DCE. The DCE layer was separated from the aq. layer and purified by semi-preparative C18 RP-HPLC using a gradient from $H_2O$ to 1%TFA/MeOH over 15 minutes which yielded *N*-(2-chlorobenzyl)-1-phenylethylamine (**172**) (27.7 mg, 27.0%).

***N*-(2-chlorobenzyl)-1-phenylethylamine (172):** $^1H$ (600 MHz, $d_6$-DMSO) δ 1.62 (3H, d, *J* = 7.2 Hz), 3.93 (1H, dd, *J* = 10.2, 10.2 Hz), 4.52 (1H, dd, *J* = 6.6, 6.6 Hz), 7.44 (3H, m), 7.49 (2H, dd, *J* = 7.2, 7.2 Hz), 7.52 (1H, d, *J* = 7.2 Hz), 7.56 (2H, d, *J* = 7.2 Hz), 9.17 (1H, br), 9.45 (1H, br); $^{13}C$ NMR (125 MHz, $d_6$-DMSO) δ 19.3 (1C), 45.7 (1C), 57.9 (1C), 127.5 (1C), 127.8 (2C), 129.0 (2C), 129.2 (1C), 129.6 (1C), 129.7 (1C), 131.1 (1C), 132.2 (1C), 133.7 (1C), 136.6 (1C); (+)-LRESIMS *m/z* (rel. int.): 246 (67%), 248 (33%) [$MH^+$, $C_{15}H_{17}NCl]^+$.

**The reductive amination of acetophenone (170) with 2-chlorobenzyl amine to afford 172:** Acetophenone (50 mg) was added to DCE (1 mL) followed by the addition of 1.3:1:3 equivalents of 2-chlorobenzyl amine (80 µL), $Ti(O^iPr)_4$ (120 µL) and $NaBH(OAc)_3$ (250 mg), respectively. After stirring for 16 hours at room temperature, water (1 mL) was added to the product mixture and partitioned with DCE. The DCE layer was separated from the aq. layer and purified by semi-preparative C18 RP-HPLC using a gradient from $H_2O$ to 1%TFA/MeOH over 15 minutes which yielded *N*-(2-chlorobenzyl)-1-phenylethylamine (**172**) (5.5 mg, 5.37%).

**The reductive amination of peripentadenine (81) with 4-methoxyphenethyl amine to afford 173:** Peripentadenine (10.4 mg) was dissolved in DCE (1 mL) and 1.3:0.2:3 equivalents of 4-methoxyphenethyl amine (5.5 mg), $Ti(O^iPr)_4$ (3 μL) and $NaBH(OAc)_3$ (17.0 mg) were added sequentially. After stirring for 16 hours room temperature, water (1 mL) was added to the product mixture and partitioned with DCE. The DCE layer was separated from the aq. layer and purified by semi-preparative C18 RP-HPLC using a gradient from $H_2O$ to 1%TFA/MeOH over 15 minutes, which yielded compound **173** (3.7 mg, 27.4%).

**Compound 173:** $^1H$ (600 MHz, $CD_2Cl_2$) and $^{13}C$ NMR (125 MHz, $CD_2Cl_2$) Table 24; (+)-LRESIMS *m/z* (rel. int.): 510 (100%) $[MH^+, C_{31}H_{48}N_3O_3]^+$.

**The attempted reductive amination of peripentadenine (81) with 2-chlorobenzyl amine:** Peripentadenine (9.6 mg) was dissolved in DCE (1 mL) and 1.3:0.2:3 equivalents of 2-chlorobenzyl amine (4.7 mg), $Ti(O^iPr)_4$ (3 μL) and $NaBH(OAc)_3$ (15.7 mg) were added sequentially. After stirring for 16 hours at room temperature, water (1 mL) was added to the product mixture and partitioned with DCE. The DCE layer was separated from the aq. layer and purified by semi-preparative C18 RP-HPLC using a gradient from $H_2O$ to 1%TFA/MeOH over 15 minutes. This yielded peripentadenine (**81**) (4.6 mg), therefore indicating the reaction was unsuccessful.

**The reductive amination of peripentadenine (81) with benzyl amine to afford 174:** Peripentadenine (10.1 mg) was dissolved in DCE (1 mL) and 1.3:0.2:3 equivalents of benzyl amine (3.2 mg), $Ti(O^iPr)_4$ (3 μL) and $NaBH(OAc)_3$ (16.5 mg) were added sequentially. After stirring for 16 hours at room temperature, water (1 mL) was added to the product mixture and partitioned with DCE. The DCE layer was separated from the aq. layer and purified by semi-preparative C18 RP-HPLC using a gradient from $H_2O$ to 1%TFA/MeOH over 15 minutes which yielded compound **174** (3.1 mg, 25.1%).

**Compound 174:** $^1H$ (600 MHz, $CD_2Cl_2$) and $^{13}C$ NMR (125 MHz, $CD_2Cl_2$) Table 25; (+)-LRESIMS *m/z* (rel. int.): 466 (100%) $[MH^+, C_{29}H_{44}N_3O_2]^+$.

**The attempted reductive amination of peripentadenine (81) with *N*-methylphenethyl amine:** Peripentadenine (10.5 mg) was dissolved in DCE (1 mL) and 1.3:0.2:3 equivalents of *N*-methylphenethyl amine (4.9 mg), $Ti(O^iPr)_4$ (3 μL) and $NaBH(OAc)_3$ (17.2 mg) were added sequentially. After stirring for 16 hours at room temperature, water (1 mL) was added to the product mixture and partitioned with DCE. The DCE layer was separated from the aq. layer. The organic layer was analyzed by positive ESIMS, which revealed the mass ion peaks of **81** (*m/z* 375) and *N*-methylphenethyl amine (*m/z* 136). The $^1H$ NMR spectrum of the product mixture confirmed both starting materials were present, therefore indicating the reaction was unsuccessful.

**The reaction of α-bromotoluic acid with excess ammonia:** α-bromotoluic acid (48.6 mg) was dissolved in DMF (500 μL), and this solution was added drop wise over 1 minute to a stirring solution of 32% ammonia (2 mL). The reaction mixture was allowed to stir at room temperature for 5 minutes. The positive ESIMS revealed three mass ion peaks at 152 (80%), 286 (15%) and 421 (5%) *m/z*. The aqueous ammonia was evaporated, and the resulting DMF solution was purified by purified by semi-preparative C18 RP-HPLC using a gradient from $H_2O$ to 1%TFA/MeOH over 15 minutes which yielded α-aminotoluic acid (*m/z* 152) (28.1 mg, 81.8%).

**α-aminotoluic acid:** white gum; $^1H$ (500 MHz, $d_6$-DMSO) δ 4.11 (2H, s), 7.57 (2H, d, $J$ = 8.5 Hz), 7.97 (2H, d, $J$ = 8.0 Hz); $^{13}C$ NMR (125 MHz, $d_6$-DMSO) δ 41.9 (1C), 128.9 (2C), 129.4 (2C), 130.8 (1C), 138.7 (1C), 166.9 (1C); (+)-LRESIMS *m/z* (rel. int.): 152 (100%) $[MH^+, C_8H_{10}NO_2]^+$.

**The attempted reductive amination of peripentadenine (81) with α-aminotoluic acid:** Peripentadenine (11.2 mg) was dissolved in EtOH (1 mL) and 1.3:0.2:3 equivalents of α-aminotoluic acid (5.8 mg), $Ti(O^iPr)_4$ (3 μL) and $NaBH(OAc)_3$ (18.4 mg) were added sequentially. After stirring for 16 hours at room temperature, the EtOH was evaporated and water (1 mL) and DCM (1 mL) were added to the product residue. The product residue was partitioned between DCM and $H_2O$. The organic layer was separated from

the aq. layer. The organic layer was analyzed by positive ESIMS, which revealed the mass ion peaks of **81** (*m/z* 375) and α-aminotoluic acid (*m/z* 152). The $^1$H NMR spectrum of the product mixture confirmed both starting materials were present, therefore indicating the reaction was unsuccessful.

**The attempted reductive amination of isoelaeocarpine (61) with 4-methoxyphenethyl amine:** Isoelaeocarpine (13.6 mg) was dissolved in DCE (1 mL) and 1.3:0.2:3 equivalents of 4-methoxyphenethyl amine (10.3 mg), $Ti(O^iPr)_4$ (3 μL) and $NaBH(OAc)_3$ (32.6 mg) were added sequentially. After stirring for 16 hours at room temperature, water (1 mL) was added to the product mixture. The product mixture was partitioned between DCE and $H_2O$. The organic layer was separated from the aq. layer. The organic layer was analyzed by positive ESIMS, which revealed the mass ion peaks of **61** (*m/z* 258) and 4-methoxyphenethyl amine (*m/z* 152). The $^1$H NMR spectrum of the product mixture confirmed both starting materials were present, therefore indicating the reaction was unsuccessful.

**The attempted reductive amination of isoelaeocarpine (61) with ethanolamine:** Isoelaeocarpine (11.9 mg) was dissolved in DCE (1 mL) and 1.3:0.2:3 equivalents of ethanolamine (3.7 mg), $Ti(O^iPr)_4$ (3 μL) and $NaBH(OAc)_3$ (28.5 mg) were added sequentially. After stirring for 16 hours at room temperature, water (1 mL) was added to the product mixture. The product mixture was partitioned between DCE and $H_2O$. The organic layer was separated from the aq. layer. The organic layer was analyzed by positive ESIMS (acquired from *m/z* 100 to 1500), which revealed the mass ion peak of **61** (*m/z* 258). The $^1$H NMR spectrum of the product mixture confirmed both starting materials were present, therefore indicating the reaction was unsuccessful.

**The attempted reductive amination of isoelaeocarpine (61) with 4-methoxyphenethyl amine and $NaBH_4$:** Isoelaeocarpine (10.7 mg) was dissolved in EtOH (1 mL) and 1.3:0.2:3 equivalents of 4-methoxyphenethyl amine (8.1 mg), $Ti(O^iPr)_4$ (3 μL) and $NaBH(OAc)_3$ (25.6 mg) were added sequentially. After stirring for 16 hours at room temperature, the EtOH was evaporated and water (1 mL) and DCM (1 mL) were added to

the product residue. The product residue was partitioned between DCM and $H_2O$. The organic layer was separated from the aq. layer. The organic layer was analyzed by positive ESIMS, which revealed the mass ion peaks of **61** (*m/z* 258) and 4-methoxyphenethyl amine (*m/z* 152). The $^1H$ NMR spectrum of the product mixture confirmed both starting materials were present, therefore indicating the reaction was unsuccessful.

# APPENDIX I – Complete List of Species of Elaeocarpaceae Evaluated in the Phytochemical Survey

The complete list of Elaeocarpaceae in Queensland and Plant Parts of each Species tested. (F = flower, Se = seeds, L = leaves, B = bark, Fr = fruit, R = root, St = stem, HW = heartwood, M = mix of leaves, bark and stem, Sb = stem bark). The five-digit number is a species-location code provided by the Queensland Herbarium.

| **Genus** | **Species** | **Plant parts** | **Alkaloid +** |
|---|---|---|---|
| *Aceratium* | *concinnum* | 21272: Se, L, B, St, HW | |
| | *doggrellii* | 25871: L, B, St | |
| | *ferrugineum* | 16760: Se, L, St | |
| | | 22965: L, B, R, St, HW | |
| | *megalospermum* | 15560: St, M | M |
| | | 23963: B, R, St, HW | |
| | *sericoleopsis* | 23956: L, B, St | |
| *Dubouzetia* | *saxatilis* | N/A | |
| *Elaeocarpus* | *arnhemicus* | 15321: St, M | |
| | | 23097: Se, B, R, St, HW, M | |
| | *bancroftii* | N/A | |
| | *carolinae* | 00889: L, St, B, M | |
| | *coorangooloo* | N/A | |
| | *elliffii* | 21996: L, B, St, HW, M | |
| | | 00936: L, B, R, St, HW, M | |
| | *eumundi* | 14281: F, St, M | |
| | | 16874: St, M | |
| | | 21935: F, L, B, St, HW, M | |
| | *ferruginiflorus* | 17317: L, St | |
| | | 25780: L, B, St, M | |
| | *foveolatus* | 21949: L, B, St, HW, M | |
| | | 21839: L, B, St, HW, M | |
| | | 25563: Se, L, B, St | |
| | *grahamii* | 21847: L, B, St, HW, M | M |
| | *grandis* | 02031: Se, L, St | L |
| | | 21918: Se, L, B, St, HW, M | St , M |
| | | 25523: L, B, St, HW | L, St |
| | *johnsonii* | 19294: L, R, St | |
| | | 21800: L, B, R, St, HW | |

| | | | |
|---|---|---|---|
| | *kirtonii* | 02049: Se, L, St | |
| | | 25505: B, St, HW, M | |
| | | 25450: L, B, St, HW, M | |
| | *largiflorens* | 14317: St, M | |
| | | 18453: F | |
| | | 17176: Se, L, St | |
| | | 21855: Se, L, B, St, HW, M | |
| | | 25826: Se, L, B, St | |
| | *linsmithii* | N/A | |
| | *michaelii* | N/A | |
| | *obovatus* | 02025: F, St | |
| | | 18119: L, B, St | |
| | *reticulatus* | 01795: Se, L | |
| | | 00192: F, St | |
| | | 18248: B | |
| | *ruminatus* | 18113: Se, L, B, St | Se |
| | | 22932: L, St | |
| | *sericopetalus* | 21909: Se, L, B, St, HW | Se |
| | | 21871: B, St, M | |
| | sp.[1] | N/A | |
| | sp.[2] | 00929: F, B, St, HW | |
| | sp.[3] | 17264: L, St | |
| | | 22897: Se, L, B, St, HW, M | L |
| | sp.[4] | N/A | |
| | sp.[5] | N/A | |
| | *stellaris* | 00946: Se, L, B, Fr, St, HW | |
| | *thelmae* | N/A | |
| *Peripentadenia* | *mearsii* | 26336: L, B, St | L, B |
| | | 23959: L, Se, B, St | L, B, Se |
| *Sloanea* | *australis* | 00076: F, L, St | L, St |
| | | 25905: L, B | |
| | | 25732: B, St | |
| | *langii* | 25822: L, B, St | |
| | *macbrydei* | 18116: L, B, St | |
| | | 24058: L, Se, R, St, HW | Se, St |
| | *woollsii* | 00224: Se | Se |
| | | 00048: F, L, St | |

1. Mossman Bluff D.G.Fell DF1666
2. Mt. Bellenden Ker L.J.Brass 18336
3. Mt. Lewis B.P.Hyland 2907
4. Mt. Misery L.J.Webb+ 10905
5. Yeti Ridge P.I.Forster+ PIF17330

Species tested in the Phytochemical Survey from PNG.

| **Genus** | **Species** | **Plant part** | **Alkaloid +** |
|---|---|---|---|
| | | | |
| *Aceratium* | *brassii* | L, B | |
| | *oppositifolia* | L | |
| | *parvifolium* | L | |
| | *sphaerocarpum* | L | |
| | sp. (1729) | L, B, St, HW | |
| | sp. (1728) | L, R, St, HW | |
| | | | |
| *Dubouzetia* | *galorii* | L, B | L |
| | | | |
| *Elaeocarpus* | *amplifolia* | L | |
| | *branderhorstii* | L, B, R, St, HW | |
| | *culminicola* | L, R, St, Sb, HW | |
| | *culminicola warb.* | L, B, St | L |
| | *densiflorus* | L, B, R, Se | L, Se |
| | *dolichostylus* | R, St | |
| | *floridenos* | L, R, HW | |
| | *fuscoides* | L, B, R | L |
| | *habbeniensis* | L, B | L |
| | *kaniensis* | L, B | L, B |
| | *ledermannii* | L, B | |
| | *leucanthus* | L, B, R, St | |
| | *lingualis* | L, B, Se | Se |
| | *nouhuysii* | L, B, R, St, HW | |
| | *poculiferus* | L, B, R, Se | Se |
| | *polydactylus* | L, B, R, St | L |
| | *ptilanthus* | L | L |
| | *pycanthus* | L, B, R, St | |
| | sp. | R | |
| | *dolichostlyus* | L | L |
| | *sphaericus* | L, B, R, HW | L |
| | *trichophyllus* | L, B, St | |
| | *womersleyii* | L, B, | |
| | *calophylla* | L, R, B | |
| | *gaultheria* | L, B, R | |
| | | | |
| *Sloanea* | *arberrans* | L, R, B, St | L |
| | *forbesii* | L, B | |
| | *nymanii* | L, R, B | |
| | *pulleniana* | L, B | |
| | *tieghemii* | L, R | L |

| | | | |
|---|---|---|---|
| | sp. (1688) | L, B, St, HW | |

Species tested in the Phytochemical Survey from China.

| **Genus** | **Species** | **Plant part** | **Alkaloid +** |
|---|---|---|---|
| | | | |
| *Elaeocarpus* | *assimilis* | R | |
| | *chiangiana* | B | B |
| | *dubia* | L, Fr | Fr |
| | *duclouxii* | L, R, St | |
| | *lanceaefolius* | L | |
| | *nitentifolius* | L, R, St | |
| | *nitentifolius* | L, B, R, St | |
| | *sylvestris* | B, R | R |
| | *tsiangiana* | B | |

# APPENDIX I I – The Energy Minimised Structures of Diphenyl Enantiomers of 113

The energy minimized structures of hexahydroxydiphenyl (HHDP) enantiomers of **113**.

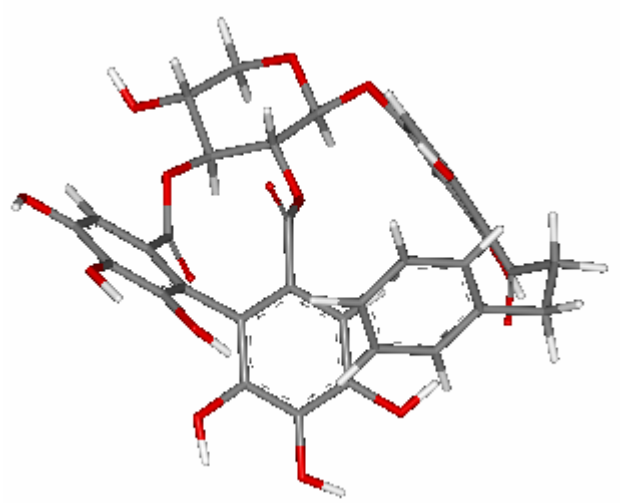

*S*-HHDP enantiomer

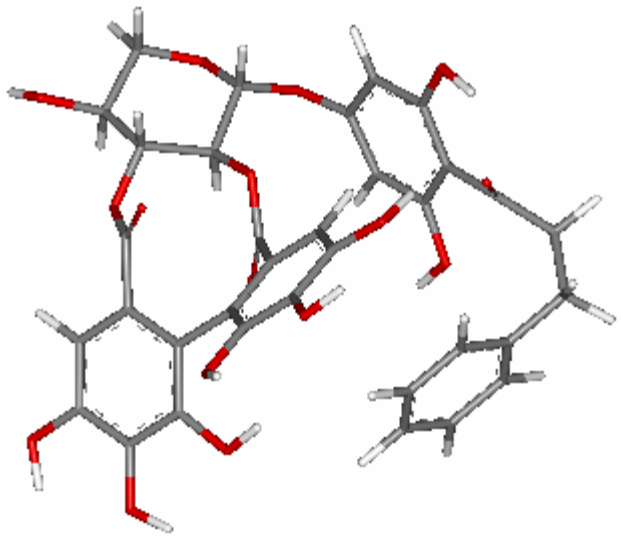

*R*-HHDP enantiomer

The determination of the xylopyranoside configuration in each enantiomer.

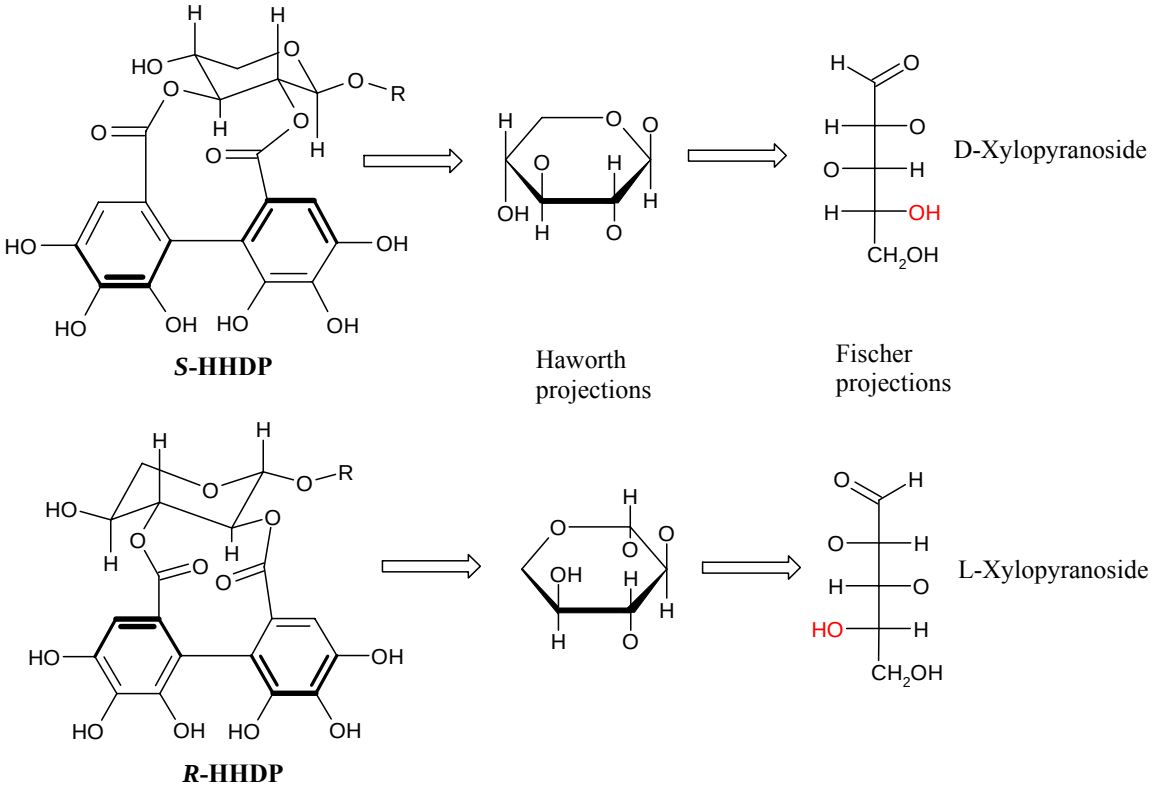

# APPENDIX I I I – Photographs of *Elaeocarpus grandis*